

In vitro and *in vivo* models of renal ischemia reperfusion
injury

Thesis submitted for the degree of
Doctor of Philosophy
at the University of Leicester

by

Zinah Dheyaa Zwaini

Department of Infection, Immunity and Inflammation
University of Leicester

2017

Dedication

To the soul of whom I shall never forget

.....

.....

My father

Dheyaa

Abstract

In vitro and *in vivo* models of renal ischemia reperfusion injury

Zinah Dheyaa Zwaini

Successful kidney transplantation is a life-saving procedure to patients with irreversible chronic renal failure. Despite the presence of various obstacles facing this surgery, preserving donor kidney and consequent ischemia reperfusion injury (IRI) are still major challenges affecting renal function as well as prognosis of transplant surgery.

This study pursued two main aims: firstly, characterising changes in damage associated inflammatory gene expressions through developing, and analysis of an *in vitro* model of proximal tubular epithelial cells (PTEC) of normal human kidney mimicking renal IRI *in vivo*. The second aim was to simulate the concurrence of factors relevant to human intervention (renoprotective anaesthesia, peri- and postoperative analgesia, volume substitution) in mice deficient of properdin and congenic controls and to allow long-term observation of renal outcome after IRI.

In this study, a reproducible and standardisable *in vitro* model was developed. It demonstrated the complexity of signalling where a multitude of factors affects the target cells. Secondly, the use of congenic properdin deficient mice showed that properdin has a significant role to play in renal injury (and recovery). There was significant impairment in renal function (and structure) compared to wildtype mice after IRI.

Acknowledgement

At the beginning, I would like to express my deepest respect and gratitude to Dr Cordula M. Stover, my supervisor, for giving me the opportunity to undertake this higher research degree and for her invaluable advice, guidance and patience during this research period. Without her, this study would never happen.

In addition, I would like to present my thanks to Dr Bin Yang, my second supervisor, for her encouragement and support. Her knowledge and expertise were vital particularly throughout the months of mice work.

I would like to thank the Higher Committee for Education Development in Iraq (HCED) for offering the fund for the study. Without their financial support, this research would not have been possible.

I would like to thank the head, academic and administrative members as well as colleagues of my department, Infection, Immunity and Inflammation, particularly those in 211b (and Dr Simon Byrne).

I would like to thank the Division of Biomedical Services, University of Leicester for their expert animal care and colleagues in the Renal Transplant Research Unit, General Hospital, University of Leicester.

I would like to thank my mum (Suad), my sister (Dina) and my brothers (Zaid, Mustafa, and Amjed) as well as my aunt (Widad) for unforgatable support and encouragement during the period of my study.

Lastly, I must thank my family, particularly my husband (Wadhah) as well as my sons (Hassan, Hussain and Hayder) for being so understanding in my commitment and pursuit of success in my career.

List of contents

Dedication.....	1
Abstract.....	2
Acknowledgement	3
List of contents.....	4
List of tables.....	8
List of figures.....	9
List of abbreviations	12
1 Chapter one (introduction).....	15
1.1 Anatomy of kidney.....	16
1.1.1 Histology.....	17
1.1.2 Proximal convoluted tubule (PCT).....	17
1.1.3 Function of proximal convoluted tubule (PCT).....	18
1.2 Kidney transplantation	19
1.2.1 End stage renal diseases (ESRD).....	19
1.2.2 Complication of Kidney transplantation.....	20
1.2.3 Ischemic injury	21
1.2.4 Ischemia reperfusion injury (IRI)	23
1.2.5 Renal IRI.....	24
1.3 Complement system (CS)	27
1.3.1 History of complement system	27
1.3.2 Activation of complement system	28
1.3.3 Functions of complement system	31
1.3.4 Regulation of complement activation	34
2 Chapter two (aims and objectives).....	35
2.1 Aims	36
2.1.1 Hypoxia/ nutrient starvation – replenishment (HNSR) model (<i>in vitro</i>) of PTEC of human kidney (HK-2).....	36
2.1.2 Surgical induction of renal IRI in mice (<i>in vivo</i>)	36
2.2 Objectives.....	36
2.2.1 HNSR model (<i>in vitro</i>) of PTEC of human kidney (HK-2)	36
2.2.2 Surgical induction of renal IRI in mice (<i>in vivo</i>)	37
3 Chapter three (establishing an <i>in vitro</i> renal hypoxia- nutrient starvation/ replenishment model)	38
3.1 Introduction.....	39
3.2 Materials and methods	40

3.2.1	Tissue culture	40
3.2.2	Characterisation of PTEC	41
3.2.3	Establishing an <i>in-vitro</i> model simulating <i>in-vivo</i> renal ischemia reperfusion injury	41
3.2.4	Lactate dehydrogenase (LDH) assay	44
3.2.5	MTT cell viability assay	46
3.2.6	Hydrogen peroxide detection (H ₂ O ₂) test	46
3.2.7	Statistics	48
3.3	Results	49
3.3.1	Optimisation of <i>in vitro</i> renal HNSR model	49
3.3.2	Assessing degree of PTEC damage in <i>in vitro</i> renal HNSR model via measuring LDH release.....	51
3.3.3	Cell viability across <i>in vitro</i> renal HNSR model	52
3.3.4	Calculation of reactive oxygen species (ROS) release from HK-2 cells..	53
3.4	Discussion	54
4	Chapter four (characterisation of the inflammatory response of human PTEC (HK-2) to <i>in vitro</i> HNSR)	58
4.1	Introduction	59
4.2	Materials and methods	60
4.2.1	Extraction of ribonucleic acids from HK-2 cells	60
4.2.2	Formation of complementary DNA (cDNA).....	61
4.2.3	Polymerase chain reaction (PCR)	62
4.2.4	Enzyme Linked Immunosorbent Assay (ELISA).....	66
4.2.5	Transmission electron microscopy (TEM)	67
4.2.6	Statistics	69
4.3	Results	70
4.3.1	Effect of HNSR on HK-2 cell mRNA expression of cytokines and inflammatory markers.....	70
4.3.2	Effect of HNSR on HK-2 cell expression of cytokines and inflammatory markers proteins.....	75
4.3.3	Effect of HNSR on auto-phagosome formation in HK-2 cells.....	76
4.4	Discussion	78
4.4.1	HK-2 response to injury.....	78
4.4.2	Autophagosome	79
5	Chapter five (mouse model of renal IRI and the role of complement properdin) ..	81
5.1	Introduction	82
5.1.1	Discovery and structure of properdin	82
5.1.2	Properdin function	83

5.2	Materials and methods	84
5.2.1	Experimental design	84
5.2.2	Induction of renal IRI	85
5.2.3	Harvesting kidneys and tissue collection.....	87
5.2.4	Tissue homogenisation	88
5.2.5	Total protein quantification	88
5.2.6	Evaluating renal function.....	89
5.2.7	Microscopic features.....	90
5.2.8	Investigating the underlying mechanism of injury during renal IRI	92
5.2.9	Statistics	103
5.3	Results	104
5.3.1	Renal function.....	104
5.3.2	Microscopic feature	105
5.3.3	The underlying mechanism.....	109
5.4	Discussion	118
5.4.1	Specifications of our renal IRI model.....	118
5.4.2	Properdin deficiency impaired renal function	119
5.4.3	Inflammatory mediators circulating in P ^{KO} mouse after 72 h from IRI .	119
5.4.4	Activation of complement system	122
5.4.5	Aftermath repair.....	123
6	Chapter six (conclusions).....	125
6.1	Conclusions	126
6.2	Strengths and limitation	127
6.3	Future work	127
7	Chapter seven (appendix)	129
7.1	Human proximal tubular epithelial cells (HK-2)	130
7.1.1	Simulation of ischemia by mineral oil immersion.....	130
7.1.2	Simulation of ischemia by Locke's buffer and / or hypoxia.....	131
7.1.3	Effect of HNSR model on TNF- α production by renal PTEC (HK2)	133
7.1.4	Western blotting.....	136
7.1.5	Microarray proteome profiler	141
7.1.6	Induction of HK-2 cells injury by LPS stimulation	148
7.1.7	Treatment with human erythropoietin recombinant protein	150
7.1.8	Immunohistochemistry (IHC) for examining C5-9 in HNSR model	152
7.1.9	Fluorescence-activated cell sorting (FACS)	152
7.2	Human podocyte	155
7.3	Primary mouse renal tubular cells (RTC)	157
7.3.1	Mouse renal tubular cell (RTC) culture	157

7.3.2	Testing the sensitivity of mouse RTC to HNSR model.....	158
7.3.3	Properdin knockout mouse	158
7.4	Cadaveric kidneys	159
7.4.1	Introduction.....	159
7.4.2	Materials and methods	164
7.4.3	Results.....	167
7.4.4	Discussion.....	185
7.4.5	Conclusion	192
7.5	Participations, presentations and publications	194
	Bibliography	200

List of tables

TABLE 4-1 LIST OF PRIMERS AND THEIR SPECIFICATIONS (HUMAN SPECIFIC)	63
TABLE 4-2: CONTENTS OF 5X TBE (TRIS/BORATE/EDTA)	64
TABLE 4-3: A TEMPLATE FOR CALCULATING THE NORMALISATION OF TARGET GENES TO HOUSEKEEPING ONES.....	65
TABLE 4-4: SHOWS EXPRESSION OF B2M FROM EXPERIMENTAL GROUPS OF HNSR <i>IN VITRO</i> MODEL (A) AND QUANTIFICATION REPORT (B). EXPRESSION WAS PRESENTED AS CYCLE THRESHOLD (CT). ...	65
TABLE 5-1 REAGENTS AND QUANTITIES WERE USED TO PREPARE DIFFERENT PERCENTAGES OF RESOLVING GEL (10 ML).....	93
TABLE 5-2 A REGENTS AND QUANTITIES USED TO PREPARE 5M OF 5% STACKING GEL	93
TABLE 5-3 REAGENTS AND QUANTITIES WERE USED TO PREPARE 10 X OF SDS RUNNING BUFFER.....	93
TABLE 5-4 REAGENTS AND QUANTITIES WERE USED TO PREPARE 10 X OF TRANSFER (BLOTTING) BUFFER.	94
TABLE 5-5 PRIMARY AND SECONDARY ANTIBODIES WERE USED IN WESTERN BLOT.....	95
TABLE 7-1 INGREDIENTS REQUIRED TO PREPARE 10 ML OF LYSIS BUFFER.....	137
TABLE 7-2 PRIMARY AND SECONDARY ANTIBODIES WERE USED DURING WESTERN BLOT.	138
TABLE 7-3 FACS FOR HK-2 CELLS EXPOSED TO HNSR INJURY	154
TABLE 7-4 COMPONENTS OF COLD STATIC SOLUTIONS.....	159

List of figures

FIGURE 1-1: A DIAGRAM ILLUSTRATING THE RELATION BETWEEN HIF-1A AND ERYTHROPOIETIN (EPO)	23
FIGURE 1-2 A DIAGRAM ILLUSTRATES THE COMPLEMENT CASCADE.	31
FIGURE 3-1: CONFLUENT PROXIMAL TUBULAR EPITHELIAL CELLS (PTEC) OF HUMAN KIDNEY (HK-2) UNDER LIGHT MICROSCOPE.....	40
FIGURE 3-2: EXPERIMENTAL DESIGN OF <i>IN-VITRO</i> RENAL HNSR MODEL.....	42
FIGURE 3-3: HYPOXIC CHAMBER.	44
FIGURE 3-4: CARTOON ILLUSTRATES PRINCIPLES OF LDH CYTOTOXICITY ASSAY.....	45
FIGURE 3-5 STANDARD CURVE OF HYDROGEN PEROXIDE ASSAY.	48
FIGURE 3-6: QUANTITATIVE ASSESSMENT OF LACTATE DEHYDROGENASE (LDH) RELEASE FROM <i>IN VITRO</i> RENAL HNSR MODEL.	51
FIGURE 3-7: CELL VIABILITY OF HUMAN PTEC (HK-2).	52
FIGURE 3-8 A QUANTITATIVE ASSESSMENT OF ROS RELEASE FROM HK-2 CELLS IN <i>IN VITRO</i> HNSR MODEL.....	53
FIGURE 4-1 A CARTOON SHOWING THE MAIN PARTS OF TRANSMISSION ELECTRON MICROSCOPE (TEM).	67
FIGURE 4-2: QUANTITATIVE MEASURING OF MRNA EXPRESSION OF AP MARKERS FROM <i>IN VITRO</i> RENAL HNSR MODEL.....	71
FIGURE 4-3: QUANTITATIVE CALCULATION OF MRNA EXPRESSION OF INFLAMMATORY MARKERS FROM <i>IN VITRO</i> RENAL HNSR MODEL.....	73
FIGURE 4-4: QUANTITATIVE CALCULATION OF MRNA EXPRESSION OF HYPOXIA MARKERS FROM <i>IN</i> <i>VITRO</i> RENAL IRI MODEL.	74
FIGURE 4-5: REPRESENTATIVE TRANSMISSION ELECTRON MICROGRAPHS ANALYSIS (TEM) OF HK-2 CELLS EXPOSED TO IRI MODEL.	77
FIGURE 5-1: EXPERIMENTAL DESIGN OF IN-VIVO MURINE RENAL IRI.....	84
FIGURE 5-2 DETERIORATION RATE OF MICE BEFORE CULLING USING KAPLAN–MEIER.....	85
FIGURE 5-3 SURGICAL OPERATION FOR RENAL IRI INDUCTION IN MOUSE.....	87
FIGURE 5-4 WESTERN BLOT FROM (BIO-RAD).	94
FIGURE 5-5 METHOD ILLUSTRATION OF SEMI QUANTITATIVE CALCULATION OF PROTEIN EXPRESSION	97
FIGURE 5-6: MACROSCOPIC PICTURES OF NORMAL AND DAMAGED KIDNEY.	104
FIGURE 5-7 RENAL FUNCTION OF THE FOUR EXPERIMENTAL GROUPS.	105
FIGURE 5-8: H AND E STAIN OF RENAL TISSUE OF MICE.....	106
FIGURE 5-9: PAS STAIN OF KIDNEY.	107
FIGURE 5-10: MITOTIC FIGURE.	108
FIGURE 5-11 TRANSMISSION ELECTRON MICROSCOPE (TEM).	108
FIGURE 5-12 DENSITOMETRY (A) AND WESTERN BLOT (B) OF NF-KB AGAINST B-ACTIN.....	109

FIGURE 5-13 DENSITOMETRY (A) AND WESTERN BLOT (B) OF HMGB-1 AGAINST B-ACTIN.....	110
FIGURE 5-14 DENSITOMETRY (A) AND WESTERN BLOT (B) OF CASPASE-3 AGAINST B-ACTIN.....	111
FIGURE 5-15 DENSITOMETRY AND WESTERN BLOT OF PCNA AGAINST B-ACTIN.	111
FIGURE 5-16 IL-6 IN SERUM OF MICE.	112
FIGURE 5-17 CXCL-16 IN SERUM OF MICE.	113
FIGURE 5-18 COMPLEMENT PROTEINS IN SERUM OF MICE.....	114
FIGURE 5-19 MCP-1 IN SERUM AND RENAL TISSUE HOMOGENATE OF MICE.....	115
FIGURE 5-20 APOPTOTIC BODIES IN DIFFERENT PARTS OF MURINE KIDNEY.....	116
FIGURE 5-21 APOPTOTIC CELLS IN MURINE RENAL TISSUE.	117
FIGURE 5-22 ROLE OF PROPERDIN AS A PATTERN RECOGNITION MOLECULES IN RENAL IRI.	124
FIGURE 7-1 STIMULATION OF RENAL IRI BY OIL IMMERSION	131
FIGURE 7-2 THE INITIAL EXPERIMENTAL DESIGN OF IN-VITRO RENAL HNSR MODEL.	132
FIGURE 7-3 QUANTITATIVE ASSESSMENT OF LACTATE DEHYDROGENASE (LDH) CELL CYTOTOXICITY FROM IN VITRO INITIAL RENAL HNSR MODELS.....	133
FIGURE 7-4 STANDARD CURVE OF TNF-A.	134
FIGURE 7-5 ELISA FOR TNF-A PROTEIN.	135
FIGURE 7-6: SEMI-QUANTITATIVE CALCULATION OF PROTEIN EXPRESSION OF AP MARKERS FROM IN VITRO RENAL IRI MODEL.	139
FIGURE 7-7: SEMI-QUANTITATIVE CALCULATION OF PROTEIN EXPRESSION OF INFLAMMATORY MARKERS FROM IN VITRO RENAL IRI MODEL.	140
FIGURE 7-8: PROTEOME PROFILER OF HK-2 CELLS SHOWED DOWNREGULATION IN PROTEIN SYNTHESIS.	143
FIGURE 7-9: PROTEOME PROFILER OF HK-2 CELLS SHOWED LOWEST PROTEIN SYNTHESIS AT HNSR 48H.	144
FIGURE 7-10: PROTEOME PROFILER OF HK-2 CELLS SHOWED LOWER PROTEIN SYNTHESIS FROM HNS 6H THAN CONTROL GROUP.....	145
FIGURE 7-11 MICROARRAY PROTEIN PROTEOME PROFILER OF HK-2 CELLS WERE EXPOSED TO HNSR INJURY.	147
FIGURE 7-12 EFFECT OF LPS ON RENAL PTEC.	148
FIGURE 7-13 EXPRESSION OF TNF-A PROTEIN FROM PTEC OF HUMAN KIDNEY AFTER STIMULATION WITH LPS	149
FIGURE 7-14 LIGHT SCATTERING AND FLUORESCENCE EMISSION FROM SINGLE CELL.....	153
FIGURE 7-15 CONFLUENT HUMAN PODOCYTES UNDER LIGHT MICROSCOPE	156
FIGURE 7-16PTEC CELLS OF WT (A) AND P ^{KO} MOUSE (B). NUMEROUS DOME FORMATIONS DUE TO THE EXISTENCE OF TIGHT JUNCTIONS AND AN INTACT TRANSCELLULAR TRANSPORT PROCESS ARE CHARACTERISTIC MANIFESTATIONS OF CONFLUENT CULTURES.....	158
FIGURE 7-17 C4D FORMATION AND ITS RELATION TO COMPLEMENTS PATHWAYS.	162

FIGURE 7-18 VWF SYNTHESIS AND REGULATION DURING ENDOTHELIAL INJURY.	163
FIGURE 7-19: STANDARD CURVE OF TOTAL PROTEIN ASSAY OF TISSUE HOMOGENATE FROM DECEASED KIDNEYS.....	166
FIGURE 7-20 IMMUNOHISTOCHEMICAL ANALYSIS OF C4D DEPOSITION IN TUBULAR EPITHELIUM	169
FIGURE 7-21 SEMIQUANTITATIVE ANALYSIS OF C4D DEPOSITION IN RENAL TUBULAR EPITHELIUM.....	171
FIGURE 7-22 SEMI-QUANTITATIVE ANALYSIS OF C4D DEPOSITION IN RENAL TUBULAR EPITHELIUM PLOTTED AGAINST SUM SCORE	172
FIGURE 7-23 SEMI-QUANTITATIVE ANALYSIS OF C4D DEPOSITION IN RENAL TUBULAR EPITHELIUM PLOTTED AGAINST COLD ISCHEMIC TIME IN DBD AND DCD.....	173
FIGURE 7-24: IMMUNOHISTOCHEMICALANALYSIS OF VWF REACTIVITY IN GLOMERULI.	174
FIGURE 7-25 SEMI-QUANTITATIVE ANALYSIS OF VWF REACTIVITY BLOTTED AGAINST HISTOPATHOLOGICAL DAMAGE.....	175
FIGURE 7-26 SEMIQUANTITATIVE ANALYSIS OF VWF REACTIVITY PLOTTED AGAINST SUM SCORE	176
FIGURE 7-27 SEMIQUANTITATIVE ANALYSIS OF VWF REACTIVITY PLOTTED AGAINST COLD ISCHEMIC TIME	177
FIGURE 7-28 SEMIQUANTITATIVE ANALYSIS OF C3 FRAGMENT	178
FIGURE 7-29 SEMIQUANTITATIVE ANALYSIS OF C3 AND B-ACTIN EXPRESSION USING WESTERN BLOT.	180
FIGURE 7-30 SEMIQUANTITATIVE ANALYSIS OF C3 AND B-ACTIN EXPRESSION USING WESTERN BLOT.	181
FIGURE 7-31 SEMIQUANTITATIVE ANALYSIS OF C3 FRAGMENT AND B-ACTIN EXPRESSION USING WESTERN BLOT.	182
FIGURE 7-32: HISTOPATHOLOGICAL SCORING GRADES IN DBD AND DCD KIDNEY BEFORE EXPOSING TO NP	183
FIGURE 7-33 EFFECT OF NORMOTHERMIC PERFUSION ON VWF REACTIVITY AND C4D EXPRESSION.	185

List of abbreviations

ADP	Adenosine diphosphate
AKI	Acute kidney injury
AMP	Adenosine monophosphate
ARNT	Aryl hydrocarbon nuclear receptor translocator
ATG5	Autophagy related 5
ATN	Acute tubular necrosis
ATP	Adenosine triphosphate
bHLH	Double basic Helix- Loop- Helix proteins
CI	Cold ischaemia
CIT	Cold ischemic time
CKD	Chronic kidney diseases
COPD	Chronic obstructive pulmonary disease
Cr	Creatinine
CrCl	Creatinine clearance
CS	Cold storage
CXCL-16	Chemokine (C-X-C motif) ligand 16
DCD	Donation after circulatory death
DBD	Donation after brain death
DGF	Delayed graft function
EC	Endothelial cell
ECD	Extended criteria donor
ELISA	Enzyme linked immunosorbant assay

EPO	Erythropoietin
ER	Endoplasmic reticulum
ESRD	End stage renal diseases
ESRF	End stage renal failure
FABP1	Fatty acid-binding protein 1
GFR	Glomerular filtration rate
H	Hour/s
HBSS	Hank's balanced salt solution
HD	Haemodialysis
HIF-1 α	Hypoxia inducible factor 1 α
HIF-2 α	Hypoxia inducible factor 2 α
HIF-3 α	Hypoxia inducible factor 3 α
HNS	Hypoxia/ nutrient starvation
HNSR	Hypoxia/ nutrient starvation- replenishment
HRP	Horseradish peroxidase
ICAM-1	Intercellular adhesion molecule-1
IL-1	Interleukin-1
IL-2	Interleukin-2
IL-6	Interleukin-6
IL-8	Interleukin-8
IR	Ischaemia reperfusion
IRI	Ischemia reperfusion injury
KIM-1	Kidney injury molecule 1
LDH	Lactate dehydrogenase

MAC-1	Macrophage-1 antigen
MMP	Matrix metalloproteinases
MPO	Myeloperoxidase
NADPH	Nicotinamide adenine dinucleotide phosphate
NF κ B	Nuclear factor-kappa B
NP	Normothermic perfusion
PAS	Periodic acid Schiff
PCNA	Proliferating cell nuclear antigen
PBS	Phosphate buffered saline
pVHL	Hippel-Lindau tumor suppressor
RBF	Renal blood flow
ROS	Reactive oxygen species
RRT	Renal replacement therapy
TFF3	Trefoil factor 3
TLR	Toll-like receptor
TNF- α	Tumour necrosis factor alpha
TUNEL	Terminal deoxynucleotidyl transferase dUTP nick end labeling
VCAM-1	Vascular adhesion molecule-1
VEGF	Vascular endothelial growth factor
vWF	Von Willebrand factor
WI	Warm ischaemia
WIT	Warm ischemic time

1 Chapter one (introduction)

1.1 Anatomy of kidney

Grossly, kidneys are pair of bean-shaped organs that rest over the posterior abdominal wall on both sides of the vertebral column and behind the peritoneum (retroperitoneal structure) which envelopes the abdominal organs. In adults, their measurements are about 10 cm x 5 cm x 2.5 cm. The weight of each kidney is about 150 g and equals to about 0.2% of total body weight. They are protected posteriorly by the lower part of the thoracic cage and anteriorly by the abdominal viscera and are enclosed by the renal fascia (Nielsen *et al*, 2012; Fogo *et al*, 2014).

The cortex, medulla and collecting system are the main parts of each kidney and can be identified macroscopically. A section through the kidney shows an external thin membrane called renal capsule. Next, the cortex, which is a pale granulated area of 15 mm thickness where glomeruli and convoluted tubules can be localised. Deeper to the cortex is a reddish- brown area, the medulla, consisting of 8-18 triangular shape structures named pyramids. Strips of connective tissue (the columns of Bertin) separate these pyramids where their bases face the cortex while apices direct toward collecting system forming medullary papilla. The renal lobe represents the area between two adjacent Bertin columns and including one medullary pyramid and the related cortex. Thirdly, a pool for collecting the produced urine with its extensions is called the renal pelvis, a funnel dilation at the beginning of the ureter, and these extensions are termed major (2-3) and minor (3-4) calyces (Fogo *et al*, 2014). This macroscopic distinction is necessary to prepare mouse renal tubular epithelial cells.

Each kidney receives its blood supply (20% of cardiac output to both kidneys) directly from aorta through a single renal artery where it gives posterior and anterior branches at the hilum before they enter kidney and subdivide into inter-lobar arteries where they run between lobes. At the cortico-medullary area, arcuate branches are formed from inter-lobar arteries where they divide further into multiple intralobular arteries. The latter direct toward the renal capsule forming afferent arterioles that end with sac-like assembly of capillaries (glomerulus). Efferent tubules are developed from glomerular capillaries before branching again developing new glomerulus, giving rise to interstitial capillaries around tubules, or emerging medulla and supply it through vasa recta. The last two forms of capillaries merge forming interlobular veins where renal venous system starts. Renal

venous vasculature chases the arterial one in size and distribution and ends with formation of several renal veins that extend out of the kidney, and drains to the inferior vena cava (Nielsen *et al*, 2012).

1.1.1 Histology

Microscopically, the uriniferous tubule is the functional unit of the kidney; it constitutes a nephron and a collecting tubule. The nephron, which number about 1 million in each kidney, forms from the capillary bed (glomerulus) and tubular system. A distended end of the tubular system is fashioned to a cup shape that encases the capillary knot. This tubular cup is called Bowman's capsule and together with the enveloped capillaries is named the renal corpuscle. Bowman's capsule is connected to about 3 cm looped tubules (proximal convoluted tubule, loop of Henle, and distal convoluted tubule). Although some nephrons are found in the medulla, the majority are located in the cortex. However, the medulla contains the collecting ducts that divert urine from the nephrons on its way to the calyces (Nielsen *et al*, 2012; Fogo *et al*, 2014).

Histologically, the inner surface of Bowman's capsule that faces the glomerulus (visceral layer) is composed of podocytes, the key in the glomerulus filtration barrier through their unique features and complicated architecture. They are responsible for the selective permeability of the barrier. This gives them the importance in sustaining kidney function and preserving the integrity of the kidney (Pavenstadt, Kriz and Kretzler, 2003).

1.1.2 Proximal convoluted tubule (PCT)

Bowman's capsule is drained to the proximal tubule, which denotes the first part of the renal tubule. It is divided into convoluted and straight regions that are named the proximal convoluted tubule and pars recta respectively. Both are structured from single layer of cuboidal cells with microvilli cover the apex of the cells and line the lumen (simple cuboidal epithelial tissue). Although the brush border is not visualised routinely under microscope, it gives an indistinct border that characterises the proximal tubule from the rest of renal tubules (loop of Henle and distal tubule). Another microscopic feature for the PCT is that cells look like a sheet of cytoplasm studded irregularly with nuclei as a

consequence to inter-digitation of plasma membrane of neighbouring cells (Fogo *et al*, 2014).

1.1.3 Function of proximal convoluted tubule (PCT)

Urine production passes through three main processes (filtration, reabsorption and secretion respectively). The PCT have a noticeable role in reabsorption where they are responsible for reabsorption of approximately 2/3 of filtrates entering the renal system. Actively, sodium is transferred from the lumen of the PCT to the blood while chloride ions and PO_4^{3-} move out passively under the influence of their electrical charge. Eventually, an osmosis imbalance from sodium and chloride transportation will oblige the water to leave the PCT lumen to the blood vessel. Consequently, the lack of water and electrolyte will increase the concentration of the filtrate (especially urea) in the PCT leading it to diffuse passively to the blood vessel. Lastly, glucose and amino acids are passively moved out using sodium co-transport mechanism (Bakris *et al*, 2009)

Wilkinson *et al.*, (2011) emphasised that autologous immune reaction is controlled by human PTEC through its effect on T and B lymphocyte responses. In the same manner, Kassianos *et al*, (2013) suggested that the immune modulatory function of human PTEC is through an interaction between the dendritic cells, which have major impact on the immune system, and the activated PTEC in the context of inflammation. This may inhibit the pro-inflammatory reaction inside kidney tissue in many renal diseases of immune-related pathology, which may place tremendous impact on treatment of renal diseases (Wilkinson *et al*, 2011; Kassianos *et al*, 2013).

1.2 Kidney transplantation

1.2.1 End stage renal diseases (ESRD)

Kidneys may suffer from insults due to either unknown cause (primary) or secondary to various causes (such as diabetes mellitus, hypertension and infection). These may result in: (i) acute kidney injury where a sudden deterioration in renal function (within 48 h) is noticed with decrease urine output to 0.5 ml/kg/h (oliguria) for 6 hours or elevation of serum creatinine above normal with equal or more than 50%. (ii) Chronic kidney disease (CKD), which refers to kidneys that suffer from abnormal function and/ or structure. CKD is classified into 5 stages according to the level of glomerular filtration rate (GFR) and presence of protein in urine (proteinuria). Lastly, CKD may ends with (iii) end stage renal disease, an irreversible persistent decline in renal function, when kidneys cannot meet the body's requirements and necessitate renal replacement therapy (RRT) (Gilg *et al*, 2011).

Several reports have stated that numbers of patients with end stage renal disease (ESRD) have dramatically increased all over the world during the last twenty years. While 6-8.5% of adults in UK have stages 3-5 CKD (Kerr *et al*, 2012), in India, about 80.000 new patients are diagnosed with ESRD each year (Gopalakrishnan and Gourabathini, 2007). In 2009, an annual report from the United State renal data system stated that numbers of ESRD patients in the United State were increased by 20% during the ten years till 2008 (Binnani, Gandhi and Bahadur, 2012).

Renal replacement therapy (RRT) is the only choice for patients with ESRD where patient cannot survive without it (Gilg *et al*, 2011). It could be either by dialysis (both peritoneal and haemodialysis) or through implanting a new kidney donated from another human (allograft kidney transplantation). Kidney transplantation is beyond dispute superior to both types of dialysis because of the lower morbidity and long-term mortality, better life style and less financial burdening (De Rosa, Muscogiuri and Sarno, 2013).

1.2.2 Complication of Kidney transplantation

1.2.2.1 Infection

The mortality and morbidity rates due to infection within one year after transplant surgery have declined significantly from 50% before 1980 compared to less than 5% in 2006. However, various infections still have a major impact on surgical success rate. Wound of surgery, skin and soft tissue, urinary tract, central venous line infection, and respiratory tract (mainly pneumonia) infections as well as bacteraemia are recorded after transplant surgery. Additionally, opportunistic infections such as cytomegalovirus and herpes zoster are frequently noticed that may end with Kaposi's sarcoma (due to herpes type 8 infection). Nevertheless, the revolution in immunosuppressant drugs and new antimicrobial protocols lead to substantial decline in infection rates in recent years (Alangaden *et al*, 2006; Hosseini-Moghaddam *et al*, 2012).

1.2.2.2 Vascular complications

These are usually related to both renal artery and vein thrombosis that occur earlier and may result in renal transplant failure. Another frequently noticed complication is renal artery stenosis, which could be repaired via endovascular intervention. Other late complication such as biopsy-induced vascular injuries, pseudo-aneurysm formation, and hematomas are infrequent (Ojo, 2006).

1.2.2.3 Cardiovascular complications

Patients who undertake kidney transplant surgery are 50 times more likely to develop cardiovascular diseases (CVD) than healthy people. Anaemia, elevated serum C-reactive protein, proteinuria, renal dysfunction and immune suppressant drugs are risk factors that increase morbidity and mortality from CVD. These complications, which are mainly due to atheroma development, are of four categories (according to ERA-EDTA records). The most common and fatal groups are coronary artery diseases (CAD) and left ventricular hypertrophy (LVH) in addition to cerebrovascular and peripheral vascular diseases (Briggs, 2001; Ojo, 2006).

1.2.2.4 Gastrointestinal Complications

It has been reported that gastro-intestinal intolerance (diarrhoea is a common symptom mainly during the first year post-transplant). This is usually a side effect of the immune-suppressant drugs such as mycophenolate mofetil (MMF) (Vanhove *et al*, 2013).

1.2.2.5 Urological complications

These are mainly ureteral- related such as urinary leaking, ureteral stenosis and vesico-ureteral reflux (VUR). It occurs after transplant surgery in 2.5% to 14.1% of patients. Excessive dissection, which results in ureteral necrosis, may be one of the most common causes of such complication (Slagt *et al*, 2014).

1.2.3 Ischemic injury

In 1975, Jennings *et al.*, defined ischemia in tissue as reduction in blood supply to that tissue due to arterial stenosis or obstruction resulting in depression in perfusion pressure as well as insufficient oxygen supply (Jennings, Ganote and Reimer, 1975). Ischemia can affect various body tissues or organs participating in fatal diseases such as coronary artery diseases (CAD), cerebrovascular accidents (CVA), renal failure as well as its potential role in pathogenesis of malignancy (Eickelberg *et al*, 2002). Hypoxia (low oxygen supply), nutrient depletion (starvation), hypercapnia (high level of CO₂) and accumulation of waste products are the main cause of ischemic injury (Eickelberg *et al*, 2002; Russ, Haberstroh and Rundell, 2007).

1.2.3.1 Hypoxia

The production of adenosine triphosphate (ATP) in mitochondria depends on molecular oxygen. It is provided during normoxia when oxygen concentration is around 20% in the cellular environment. Hypoxia arises when oxygen supply falls below tissue requirements with oxygen concentrations range between 0.1% and 10% (Kumar and Choi, 2015). Hypoxia obliges cells to get energy from breaking down glucose (glycolysis) via anaerobic pathway. As the generated energy from this glycolysis is enormously less than

that of aerobic pathway (2 vs around 32 mol ATP/ mol glucose), persistent hypoxia will damage cells (Russ, Haberstroh and Rundell, 2007). Injured cell responds to acute hypoxia via serial changes in protein production while chronic ischemia results in alterations in gene expression. However, hypoxia does not only compromise metabolic activity but also oxygen-sensitive gene transcription (Semenza, 2000; Ziello, Jovin and Huang, 2007). Of these, HIF-1 is a heterodimeric DNA binding transcription factor that is classically called ARNT (Aryl hydrocarbon nuclear receptor translocator). It presents in two forms (alpha and beta) and both these subunit proteins have PerARNT – Sim and double basic Helix- Loop- Helix proteins (bHLH) which are responsible for dimerization through DNA binding. More recently, another two subtypes of HIF have been added to the bHLH-PAS family, these are HIF-2 α and HIF-3 α (Semenza, 2000; Kumar and Choi, 2015).

Fundamentally, oxygen tension in tissues steers the HIF-1 α pathway. Therefore, in normal oxygen level HIF-1 α is eliminated via direct binding to a protein named von Hippel-Lindau tumor suppressor (pVHL). Meanwhile, hypoxia precludes the above binding process leading to HIF-1 α assembly. HIF-1 α is an organizer to many O₂ sensitive gene targets. Hence, its relationship to erythropoietin production has been identified in addition to other regulatory functions (Ziello, Jovin and Huang, 2007; Ke and Costa, 2006).

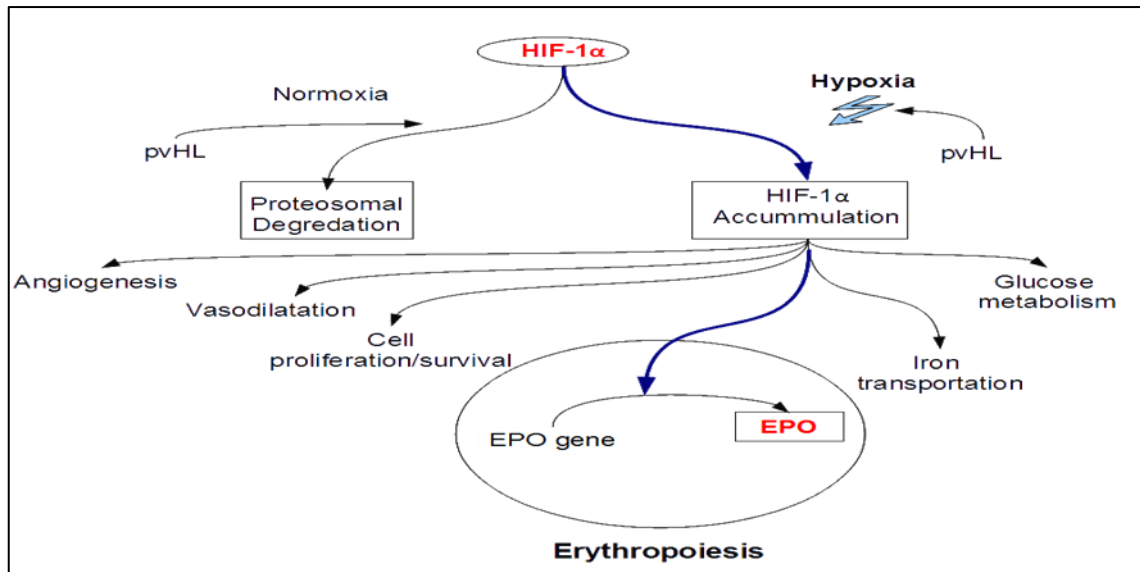


Figure 1-1: A diagram illustrating the relation between HIF-1 α and erythropoietin (EPO)

1.2.3.2 Nutrient depletion

Additionally, lack of blood supply will lead to decrease substrates delivery (such as glucose) to affected tissues resulting in starvation (Russ, Haberstroh and Rundell, 2007). This was proved by a study on murine cardiac cells that showed a reduction in blood flow reduces nutrient delivery by about 50 fold (Lloyd *et al*, 2004).

1.2.4 Ischemia reperfusion injury (IRI)

A state of ischemia/ reperfusion refers a situation in which the blood supply to tissues or organs is restored after a previous reduction in blood flow reaching those tissues or organs (Eltzschig and Eckle, 2011; Gorsuch *et al*, 2012). Although ischemia elicits sequences of damages due to tissue hypoxia because the supplements do not meet the metabolic requirements of that tissue, unexpectedly, reperfusion may lead to *more* tissue damage and often enhances the inflammatory reaction in the reperfused tissue producing what is called ischemia/ reperfusion injury (IRI) (Eltzschig and Eckle, 2011). IRI could be the result for a variety of clinical problems like sepsis, infarction and graft rejection (van der Pol *et al*, 2012). It may affect one organ (bowels and kidneys), lead to multiple organ failure (after trauma) or occur after surgery (compartment syndrome of limbs) (Eltzschig and Eckle, 2011; Gorsuch *et al*, 2012) with a very high morbidity and mortality.

1.2.5 Renal IRI

Renal ischemia reperfusion injury is an inevitable event during kidney transplantation that occurs during the period from harvesting the donated kidney until connecting renal vessels to recipient's (artery and vein). Thereafter, studies were directed toward understanding the molecular signalling behind the various injurious mechanisms.

PTEC are more liable to ischemia because of the diversity in renal functions including active ion transportation as well as presence of mitochondria abundantly inside PTEC converted kidneys to a highly demanding organs that deplete 7% of total daily generated energy in order to perform their functions normally (Lin, Wang and Hill, 2014).

Combinatorial effects of renal IRI, which are oxygen/ nutrient deprivation and accumulation of waste products, result in acute kidney injury (AKI) as well as launch a defensive repair mechanism simultaneously. To start with, disproportional reduction of renal blood flow with more in medulla than other kidney parts beside hypoxia and lack of nutrient results in vascular endothelial damages: cellular swelling, actin cytoskeleton changes, glycocalyx destruction and cell-cell contact loss. This is associated with stimulation of ICAMs, VCAMs, selectins and other adhesion molecules causing leukocyte adhesion, trans-endothelial leukocytes infiltration, coagulating system activation, fluid accumulation in interstitial compartment and upregulation of vaso-active cytokines. Subsequently, vascular occlusion due to micro thrombi formation and vasoconstriction leading to local ischemia, particularly at medulla, affecting tubular epithelial cells which could be injured, becoming apoptotic and necrotic as well as brush border shedding and luminal obstruction by sloughed cells. A compensatory repair process attempts to replace lost cells via migration and differentiation of viable cells to the damaged area (restitution) as well as autophagy for cleaning up (Bonventre and Yang, 2011).

1.2.5.1 Inflammatory cascade

Activation of inflammatory cascades is augmented during renal IRI and is considered as a pivotal player in recruiting cells (such as macrophage and neutrophils); upregulating various pro-inflammatory cytokines (see chapter 4); releasing chemokines such as intracellular adhesion molecule-1 (ICAM-1) and liberating reactive oxygen species

(ROS). In addition, inhibiting inflammatory cascades through delivering anti-inflammatory agents (such as nicotin) ameliorate renal IRI via impeding neutrophil gathering (Malek and Nematbakhsh, 2015).

1.2.5.2 Oxidative stress synthesis and mitochondrial dysfunction

The release of ROS from damaged cells during ischemic phase of renal IRI results in oxidative stress affecting both mitochondria and endoplasmic reticulum, depletion in ATP, decrease calcium efflux and protease enzyme activation (Malek and Nematbakhsh, 2015). These insults are aggravated during reperfusion phase due to oxygen free radicle production leading to cellular injury, apoptosis and cell death secondary to DNA and protein oxidation as well as lipid (including membranous) peroxidation (Shingu *et al*, 2010; Malek and Nematbakhsh, 2015). Moreover, anti-oxidant agents such hydrogen rich saline and berberine, an alkaloid extract from herbs, attenuate the deleterious effect of IRI on rodent and on human PTEC (HK-2 cells) respectively via reducing oxidative stress-induced cell apoptosis by inhibiting reactive oxygen species (ROS) release (Shingu *et al*, 2010; Yu *et al*, 2013).

1.2.5.3 Nitrite and nitric oxide

Nitric oxide synthase (NOS) is activated from kidney during IRI causing nitric oxide release. While the inducible isoform of NOS (iNOS) is toxic to the kidney and increases renal damage after IRI, the endothelial isoform (eNOS) was found to have a protective role; however NO synthesis from PTEC during IRI is mediated via iNOS (Milsom *et al*, 2010; Malek and Nematbakhsh, 2015).

1.2.5.4 Renin-angiotensin system

The renin-angiotensin system (RAS) is activated during renal IRI with two opposite roles. The renal vessel vasoconstrictor (angiotensin II) exacerbates renal injury while angiotensin 1-7 reduces IRI (Santos *et al*, 2013).

Usually, angiotensin II works through activating two surface receptors, type 1 receptor (AT1) and type 2 receptor (AT2) launching various physiological changes such as vascular smooth muscle cells constriction, aldosterone synthesis, sodium and water retention, as well as increases cardiac contractility. Additionally, promoting pro-inflammatory mediators is one of the roles that are reported for angiotensin II (Ni *et al*, 2013).

1.3 Complement system (CS)

Complement is a non-cellular enzymatic complex, mostly of hepatic origin, of around 30 proteins localised in blood (20 plasma proteins) and on surfaces of normal cells (9 membrane proteins) in an inert (named zymogens) status (Nesargikar, Spiller and Chavez, 2012; Sarma and Ward, 2011; Ross, 1986). Complement can respond to pathogens either naturally (innate pathway) without participation of leukocytes or antibodies; or via binding to antibody-antigen complex on the surface of pathogens (adaptive pathway) (Sarma and Ward, 2011). Activation of complement system runs in serial interaction of its tightly controlled components resulting in end products have the ability to promote inflammation, endorse pathogen clearance and kill microbes. It is composed from three main cascades; classical, lectin and alternative pathway in addition to a non-enzymatic assembly of the membrane attack complex (MAC) which is also called lytic pathway (Ricklin *et al*, 2010).

1.3.1 History of complement system

Before more than a century, 1890s, researchers were discussing the Metchnikoff theory about the bactericidal role of plasma phagocytes, which was supported by the discovery of a heat-sensitive plasma protein can kill bacteria named alexin by Buchner and his colleagues. Later, Jules Bordet proposed the presence of a heat-stable substances which are circulating in plasma helping the alexin in their bactericidal effect called them sensitizer (Nesargikar, Spiller and Chavez, 2012). In 1899, Paul Ehrlich emphasised the side-chain theory when he considered the sensitizers as amboceptors (the former name of antibodies) which are produced secondary to the activation of specific receptors on the surface of bacteria or pathogens and shed in plasma. He suggested that the defensive capability of amboceptor is generated via formation of a complex with their plasma heat-sensitive mate (alexin) and he called the latter 'complement' accordingly (Nesargikar, Spiller and Chavez, 2012; Ehrnthaller *et al*, 2011).

Ferrata and Brand described C1 and C2 while C3 was named by Cocca which followed by the discovery of C4 by 1920. In 1966, Robert Nelson and his colleagues succeeded in isolating C3 into 6 separated proteins sharing the ability to destroy erythrocytes;

thereafter, their characterisation were completed by Muller-Eberhard and his colleagues over 2 decades and called them C5-9. However, It looks that the nomenclature of the first four complement substances were based on history of discovery while the rest depended on their sequence of action in the complement activation scheme (Ehrnthaller *et al*, 2011; Nesargikar, Spiller and Chavez, 2012; Ross, 1986). The above antibody- dependent complement responses in addition to several supplementary regulators were defined as 'classical pathway (CP)'. In 1913, different route for complement activation without antibody reaction was emphasised by Brorwning and Mackie, which later named as 'alternative' or properdin pathway after the discovery of properdin by Louis Pillemer in 1954 and his successor Irwin Lepow (Ehrnthaller *et al*, 2011; Ross, 1986). After huge debate among scientists about properdin pathway, they finally agreed on the presence of this pathway as well as its regulatory proteins, which termed as factor B (fB), factor D (fD), and factor H (fH). In 1978, Kawasaki and his colleagues described the 'mannose-binding lectin (MBL)' or lectin pathway to be added to the previous two pathways (Ehrnthaller *et al*, 2011; Ross, 1986).

1.3.2 Activation of complement system

1.3.2.1 Classical pathway

The first part of CS (C1) is the key complement in activation CP. It is a multi-molecular protein composing from a single, recognition, (C1q) molecule with six terminal heads and two C1r and C1s fragments (the latter two are also known as catalytic proteases). The initiator of this cascade stimulation is the binding of C1q to either apoptotic or any injured cells (through C-reactive protein on their surfaces) or immune (Ag-Ab) complex assembled by IgM or IgG. This complement-target conjugation causes for activation of C1r that will split and stimulate C1s molecule. Thereafter, the active form of C1s will split another complement, C4, into big C4b and small C4a fragments. C4b will conjugate with C2 complement results in C2 cleavage producing free C2b and cell-bound C4b2a complex (also known as C3 convertase) (Carroll and Georgiou, 2013; Rossi *et al*, 2014). It seems that the CP has only one complement component (C1) and participates in the complement cascade through C3 convertase assembly.

1.3.2.2 Lectin pathway (LP)

Mannose-binding Lectin (MBL) is an oligomeric protein of mainly hepatic origin (although synthesised minimally by intestine and testis) containing a C1q-like part. It assembles from three 32 kDa subunits with 4 parts for each of them; carbohydrate-recognition domain (CRD) also is called lectin, is responsible for non- classical pathway complement stimulation via direct targeting the oligosaccharide (sugar) molecules on surfaces of injured cells or on micro-organisms. A hydrophobic neck region, a collagenous region and a cysteine-rich N-terminal region are the remaining parts. MBL is a member of collectins (protein family contains lung surfactant A and D) which works as pattern-recognition molecules in the LP and plays a crucial role in innate immunity. In addition to complement stimulation and its consequences, MBL can regulate inflammatory responses, facilitate phagocytosis directly without complement intervening and enhance apoptosis (Osthoff *et al*, 2014; Turner, 2003).

Similar to MBL, ficoin, a lectin protein that has both fibrinogen and collagen- like domains, has the ability to activate LP too through binding to the carbohydrate motifs (Matsushita and Fujita, 2001). On the other hand, several proteins, MBL-associated serine proteases (MASP) 1-3, mainly MASP-2 bind to MBL forming a complex initiates serial complement activation that ends with splitting C4 and C2 as well as formation of C3 convertase (C4b2a) (Turner, 2003). However, it appears that both LP and CP activation result in C3 convertase synthesis.

1.3.2.3 Alternative pathway (AP)

The alternative pathway (AP) contributes significantly to the activation level of complement triggered by either the classical pathway or lectin pathway (Thurman *et al.*, 2006). In fact, the alternative pathway functions are to amplify the activity of the complement system (Hourcade, 2006; Laarman *et al.*, 2010). The characteristic features of this pathway are the ability to form a positive feedback loop that is responsible for production of an amplified response; and the presence of factor B, factor D and properdin, which are only found in the alternative pathway (Gaarkeuken *et al.*, 2008). The main complement in alternative cascade is C3. It is a 185-kDa protein, which consists from α

(110 kDa) and β (75 kDa) chains whom join each other by disulphide bond (Ekdahl *et al*, 1992).

Alternative pathway passes through two phases, the fluid phase in the serum and solid phase on the surface of the cells (Banda *et al*, 2011). It is thought to be stimulated continuously (although in low steady pace) without the need for immune complex (unlike CP) or pattern recognition molecules (as in LP) by spontaneous hydrolysis of C3 thioester bond developing C3(H₂O) (Sweigard *et al*, 2014). C3(H₂O) is supposed to bind to the surface directly functioning like C3b. C3b or its functional analogue, C3(H₂O), is bound to factor B in presence of magnesium (Mg²⁺) producing C3bB. This binding will aid factor D to cleave factor B into Ba and Bb. Ba is released while C3bBb denotes the active phase of C3 (C3 convertase) (Hourcade, 2006; Laarman *et al.*, 2010; Iwaki *et al.*, 2011).

Properdin, the sole positive regulator of the AP, is a positive promoter to C3, i.e. through binding to C3bBb, and stabilizing C3bBb. This will raise the half-life of C3 convertase from 90 second to longer (5- 10 folds). This persistence of C3 convertase is vital for the positive feedback and alternative pathway activation (Harboe and Mollnes, 2008). Accumulation of C3b around foreign or targeted surface enhancing the phagocytic action of the PML (opsonisation) and production of C3bBbC3b, which acts as C5 convertase (Roumenina *et al*, 2011; Hoffman *et al*, 2014)

1.3.2.4 Membrane attack complex (MAC)

Interestingly, all the three complement cascades (CP, LP and AP) end with production of C5 convertase (either C4bC2aC3b or C3bBbC3b) which cleaves C5 into C5a and C5b (Hourcade, 2006; Laarman *et al.*, 2010). C5a as well as C3a (from the alternative pathway) have the ability to attract leukocytes to the infected area (chemotaxis) while C5b acts as stimulator to the fourth pathway (lytic) pathway through serial activation of complements C6, C7, C8, and C9 (Laarman *et al.*, 2010). To start with, the active form (C5b) binds to C6 then C7 forming C5bC6C7 that is capable to attach weakly to the cell surface. Then, C8, a trimer composed of α , β and γ domains, is added to the complex enabling it to anchoring to the cell membrane via C8 α molecule insertion inside the cell membrane and constructing a foundation to recruit 12-18 C9 complements. The final MAC or C5b-9 construction pattern forms a hole in the cellular membrane resulting in

lytic process of target cell ends with cell necrosis (Kondos *et al*, 2010; Murphy, Travers and Walport, 2007). Hence, MAC represents the final outcomes of all the complement cascades causing cell necrosis and death.

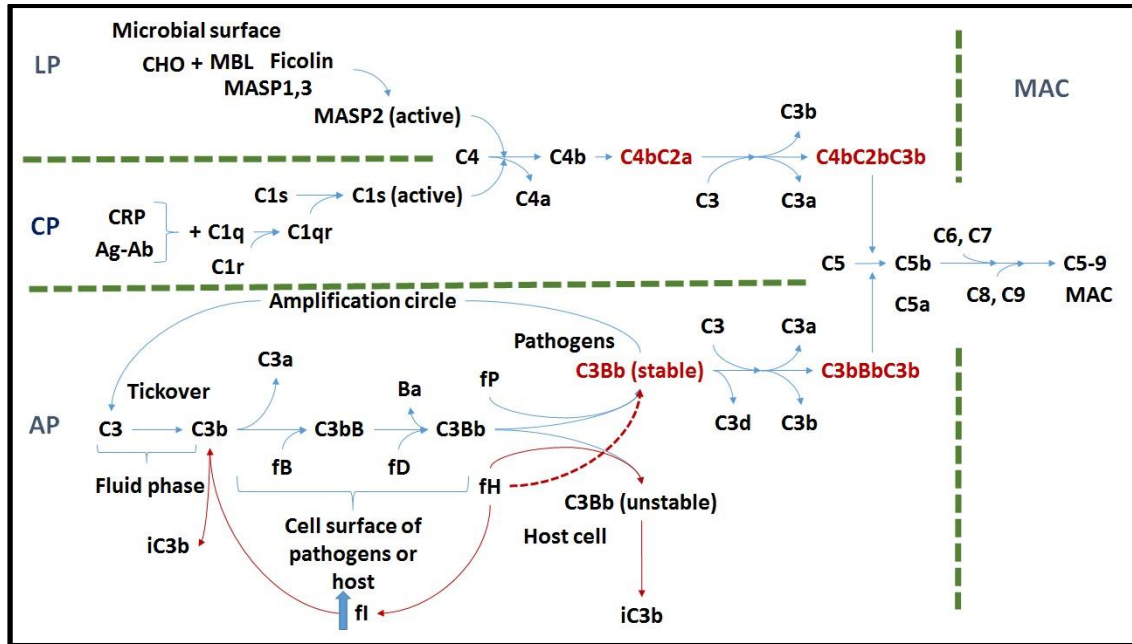


Figure 1-2 A diagram illustrates the complement cascade. Ab: antibody, Ag: antigen, Ap: alternative pathway, C: complement, CHO: oligosaccharide (sugar) molecules, CP classical pathway, CRP: C reactive protein, fB: factor B, fD: factor D, fH: factor H, fI: factor I, fP: factor properdin, iC: inactive complement molecule, LP: lectin pathway, MAC: membrane attack complex, MASP: MBL-associated serine proteases, MBL: Mannose binding lectin.

1.3.3 Functions of complement system

1.3.3.1 Opsonisation

The process of covering pathogens with recognising, opsonin, protein in order to facilitate its discovery by phagocytic cells is called opsonisation (Owens and Peppas, 2006). C3b, C4b and C5b, resulting from cleavage of C3-5 due to activation of any of the three complement pathways, can act as opsonin proteins via binding to their relevant receptor on surface of pathogenic cells via their thioester bond (Ehrnthaller *et al*, 2011). Secondly, opsonin proteins have the ability to bind to immune complexes enabling their elimination. The opsonin complements bind to erythrocytes via complement receptor 1 (CR1; CD35)

thereby anchoring immune complex to red blood cells (RBCs), which trap and disintegrate inside liver and spleen. Thirdly, innate and adaptive immunity are linked through C3 products-B lymphocytes interaction. Both CR1, CR2 (CD21) exist on the cell surface of B cells and have the ability to conjugate to C3b and C3d respectively resulting in increased immunogenicity of B leukocytes (Ehrnthaller *et al*, 2011; Lindorfer *et al*, 2003; Boackle *et al*, 1998).

1.3.3.2 Chemotaxis

It is a process of moving biological molecules or cells (e.g. phagocytes) toward inflammatory or injured site under the influence of chemical gradients produced from chemotactic proteins (chemoattractant) (Isfort *et al*, 2011; Hillen and Painter, 2009). Studies revealed that stimulation of complement pathways results in generation of C3a and C5a fragments, which have the capability to attract various leukocyte cells (such as monocytes) and neutrophils and mesenchymal human cells to inflammatory (complement activation) area (Schraufstatter *et al*, 2009; Ricklin *et al*, 2010). On contrary, Ward, 2010 found that C5a binds to C5aR on phagocytic cell surfaces resulting in inhibition of chemotaxis during sepsis (Ward, 2010). Factor H, regulator of AP, has chemotactic role as well. Ohtsuka *et al*, 1993 and Nabil *et al*, 1997 in separate studies suggested the ability of fH to attract monocytes during delayed type hypersensitivity reaction (Ohtsuka *et al*, 1993; NABIL *et al*, 1997).

1.3.3.3 Cell and immune complex clearance

Pathogenic cells could be targeted directly by MAC resulting in pore formation and cell lysis (see above) or via phagocytosis, which is the first defence line of innate immune system as well as the initiator for adaptive immunity. Phagocytic mechanism is a cellular event where cells can engulf and ingest large molecules ($\geq 0.5 \mu\text{m}$) after recognising them via surface receptors. Neutrophil and macrophage are common examples of phagocytic cells while bacteria, fungi, and apoptotic cells are the usual targets (Flannagan, Jaumouillé and Grinstein, 2012).

Phagocytosis is mediated by complement cascade and its receptors where they are working as opsonin and chemoattractant molecules (C3b, C4b and C5b) on the surface of target cells (Ehrnthaller *et al*, 2011). Moreover, phagocytosis can be promoted by a phagocytic receptor (C3R) where C3b and iC3b are deposited on the surface of bacteria enabling them to be recognised by antibodies (Hyams *et al*, 2010).

In addition, molecules modulation on cellular membrane of apoptotic cells releases CD46 and CD59, which activate complement pathway and bind to C3b and C4b as well in order to promote phagocytosis to eliminate apoptotic cells (Ricklin *et al*, 2010). Furthermore, antigen-antibody (immune) complexes are also targeted by complement components where they are opsonised by binding C3b and C4b to them, which they interact with CR1 (on erythrocytes). The above molecular trafficking will help in transferring immune complexes to both spleen and liver where they engulfed by Kupffer, macrophage and dendritic cells (Noris and Remuzzi, 2013).

It seems that all three processes, opsonisation, chemotaxis and phagocytosis, are working in harmony to eradicate pathogens and complement cascades play pivotal role in initiating them.

1.3.3.4 Anaphylaxis and inflammation

C3a, C4a, and C5a (the small fragments of complement) are also called anaphylatoxins as they induce confined inflammatory reaction through binding to their specific receptors. This reaction could be life threatening when becomes general (i.e. when injected systemically) resulting in anaphylactic shock. The three molecules can act on smooth muscle cells causing contraction and increase vascular wall permeability. Both C3a and C5a can promote endothelial and mast cells to release adhesion molecules and histamine (and TNF- α) respectively (Janeway *et al*, 1997; Dunkelberger and Song, 2010). Additionally, upregulation of CR1 with its ligands leads to pro-inflammatory molecules release, such as interleukin (IL)-1 α , IL-1 β (Dunkelberger and Song, 2010). However, the fact that complement activation can reduce inflammation by regulating apoptotic cell eradication highlights the dual effect of complement system on target organs.

1.3.4 Regulation of complement activation

A strict control over the activation of the complement system is mandatory to avoid the harmful effect of over production of C3 convertase and C5 convertase as well as hampering the self-damage (Laarman *et al*, 2010). These effects are observed in ischemia reperfusion injury and they are detrimental (Leshner and Song, 2009). There are specific regulators for each pathway but some of these proteins work on more than one pathway (Westra *et al*, 2012). In the fluid phase, factor H, factor I, C4 binding protein and C1 inhibitor are immune-regulatory proteins that responsible for controlling the undesirable over activation of the complement system, while membrane cofactor protein (MCP/CD46), decay-accelerating factor (DAF/CD55), complement receptor 1 (CR1/CD35), and CD59 are inhibitory regulators in the solid phase (Leshner and Song, 2009)

Factor H, MCP/CD46 and CR1 play a substantial role in monitoring the amplification circle of alternative pathway though the exact mechanism is not clearly understood (Westra *et al*, 2012). Both the 155 KDa factor H glycoprotein and DAF can carry their action by inhibiting the cleavage of factor B into Ba and Bb through ameliorating its attachment to the hydrolysed C3 (C3b) (Leshner and Song, 2009). Another possible mode of action is facilitating the formation of inactive C3b (iC3b) via compulsory stimulation of factor I. However, both CR1 and MCP share in this mode of inactivation resulting in degradation of iC3b. Lastly, factor H, CR1 and DAF may act on destruction of C3bBb complexes (Zipfel and Skerka, 2009)

2 Chapter two (aims and objectives)

2.1 Aims

2.1.1 Hypoxia/ nutrient starvation – replenishment (HNSR) model (*in vitro*) of PTEC of human kidney (HK-2)

1. Establishing a reproducible *in vitro* model simulating renal IRI *in vivo*.
2. Investigating expression of complement components in response to HNSR.
3. Determining production of pro inflammatory cytokine in response to HNSR.
4. Assessing the presence of apoptosis in HNSR model
5. Investigating the presence of autophagy.

2.1.2 Surgical induction of renal IRI in mice (*in vivo*)

1. Simulating the concurrence of factors relevant to human intervention (renoprotective anaesthesia, peri- and postoperative analgesia, volume substitution) in mice deficient of properdin (P^{KO}) and congenic controls.
2. Observing the outcome of renal IRI after 72 h in P^{KO} and wild type mice.
3. Investigating potential mechanisms involved such as inflammation, apoptosis and complement activation.

2.2 Objectives

2.2.1 HNSR model (*in vitro*) of PTEC of human kidney (HK-2)

1. Lactate dehydrogenase (LDH), MTT cell viability assay, hydrogen peroxide detection (H₂O₂) test and tumor necrosis factor α protein quantification.
2. Gene expression analysis and protein quantification for C3, properdin factor B and factor H.
3. Conducting:
 - i. Gene expression analysis for tumor necrosis factor α , interleukin 6, kidney injury molecule-1, tissue growth factor- β , versican, and protein quantification for IL-6 and TGF- β and vascular endothelial growth factor.

- ii. Protein quantification for nuclear factor- κ B, High mobility group box 1, and proliferating cell nuclear antigen.
- iii. Proteome profiler.
- 4. Gene expression analysis for caspase -3.
- 5. Ultrastructural analysis by electron microscopy (TEM).

2.2.2 Surgical induction of renal IRI in mice (*in vivo*)

- 1. Bilateral clamping of renal vessels of properdin deficient mice and congenic wild type.
- 2. Assessing:
 - i. Renal function (blood urea nitrogen and serum creatinine).
 - ii. Histological study (haematoxylin, and eosin staining and PAS stain) of kidneys and examining ultrastructure via electron microscope.
- 3.
 - i. Protein quantification of NF- κ B, HMGB-1, PCNA, IL-6, CXCL-16, caspase-3, C5a, C5b-9, and MCP-1.
 - ii. Calculating apoptotic bodies via indirect TUNEL assay
 - iii. Assessing lectin pathway activity using ELISA.

3 Chapter three (establishing an *in vitro* renal hypoxia- nutrient starvation/ replenishment model)

3.1 Introduction

Renal ischemia reperfusion injury (IRI) can damage kidney after transplant operation resulting in patients' morbidity and mortality (van der Pol *et al*, 2012). Despite presence of many complications such as vascular thrombosis and/ or areterial twisting (Aktas *et al*, 2011), delayed wound healing and infection (Kuo *et al*, 2012) as well as renal complications (e.g. vesico-ureteral reflux and ureteric stenosis) (Khor *et al*, 2015), IRI is considered as one of the major causes that leads to failure after kidney transplantation (Meldrum *et al*, 2001).

Conducting preclinical experiments on *in vitro* models of human PTEC line are desirable for two reasons. Firstly, conducting experiments on living animals was and still is a common trend in research laboratory but big concerns have been raised about animal rights asking for using alternatives (replacement), modifying experiments to reduce animal pain and distress (refinement) as well as decreasing number of used animals (reduction). At the time being, the 3Rs principles were included as part of Animal (Scientific) Procedures Act, 1986 (Flecknell, 2002).

Secondly, this is attributed to the fact that the influence of ischemia on the different parts of the kidney is variable (Schumer *et al*, 1992). The complex histology of the kidney means that cells vary in their susceptibility to damage incurred during IRI. Tubular epithelial cells are highly susceptible (PTEC) and the glomerular cells (podocyte) on the other end of the spectrum represents an example of cells most resistant to ischemia (Schumer *et al*, 1992).

Accordingly, in this chapter an *in vitro* model of hypoxia and nutrient starvation with subsequent media replenishment (HNSR) has been established using human PTEC simulating *in vivo* renal IRI in an attempt to replace animals in line with 3Rs principles.

3.2 Materials and methods

3.2.1 Tissue culture

Proximal tubular epithelial cells (PTEC) of normal human kidney (HK-2) (ATCC® NO.CRL-2190™) were grown in culture medium Dulbecco's Modified Eagle Medium: Nutrient Mixture:F-12, DMEM:F-12 (Invitrogen™ from Thermo Fisher Scientific, Loughborough, UK). The media contains L- glutamine (200 mM), 10% fetal calf serum (FCS), 0.4 µg/ml recombinant human epidermal growth factor (hEGF) (Sigma-Aldrich, MO, USA), Penicillin (100 IU/ml) and Streptomycin (100 µg/ml) (Invitrogen™ from Thermo Fisher Scientific, Loughborough, UK).

To maintain the culture, the cells were split by trypsin-mediated detachment (0.25% trypsin, 0.02% EDTA) (Sigma-Aldrich, MO, USA) after formation of a confluent monolayer in 25 cm² flask and rinsing twice with phosphate-buffered saline (PBS). The cells were seen under microscope (objective X 40) as adherent polygonal cells with vacuole inclusions (Figure 3-1) and compare to the image deposited for the cell line (ATCC® NO.CRL-2190™).

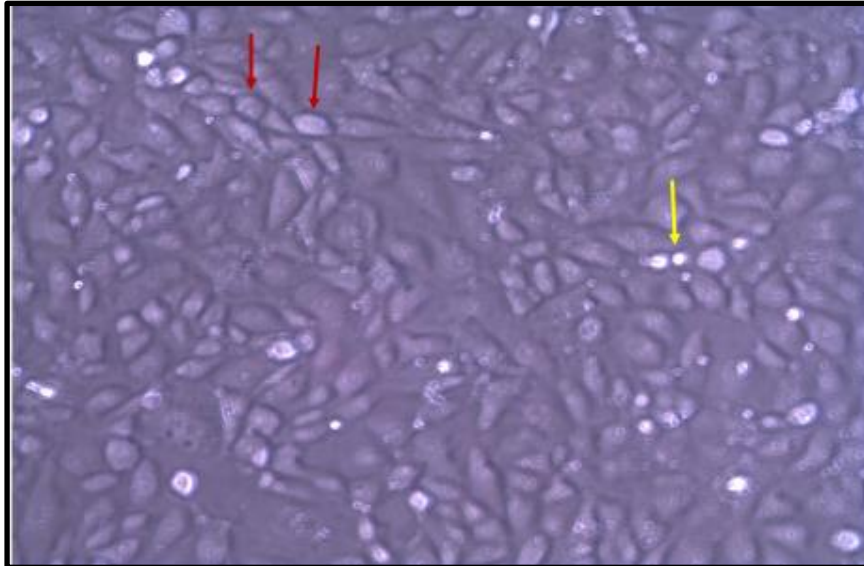


Figure 3-1: Confluent proximal tubular epithelial cells (PTEC) of human kidney (HK-2) under light microscope (X40). They look as polygonal cells (red arrows) with vacuole inclusions (yellow arrow).

3.2.2 Characterisation of PTEC

The cells were confirmed to be proximal tubular epithelial cells depending on the work of a colleague in the laboratory (Dalia Alammary) where she examined the HK-2 cells looking for brush border, a characteristic feature of PTEC. Both villin-1 protein (marker for differentiated brush border) and alkaline phosphatase (an enzyme characteristic of brush borders) were detected. In addition, ultrastructure analysis using electron microscopy showed evidence of microvilli. Meanwhile, confirming the human origin of these cells were based on the usage of human specific primers during qPCR. Moreover, it was verified to be free of mycoplasma by PCR (EZ-PCR mycoplasma test kit, Biological Industries Beit Haemek Ltd., Israel). Finally, cells were examined under microscope to confirm that they are solely PTEC and flasks contain no other cell types.

3.2.3 Establishing an *in-vitro* model simulating *in-vivo* renal ischemia reperfusion injury

3.2.3.1 Principles

The aim of this experiment was to establish an *in-vitro* model of renal hypoxia-nutrient starvation/ replenishments injury (HNSR) mimicking clinically ischemia reperfusion injury (IRI). Basically, simulating ischemia was performed by induction of hypoxia and nutrient starvation (HNS) through incubating PTEC of human kidney (HK-2) in a hypoxic chamber to eliminate oxygen (Leonard *et al*, 2003) as well as nutrient starvation using Locke's buffer to deprive cells from their nutrients and supplying them with only basic salts that keep their osmolarity (Pavlovski *et al*, 2012). Later the replenishment phase was being simulated via transferring cells to oxygen-containing incubator and replacing Locke's buffer with normal media.

3.2.3.2 Experiment design

This HNSR model was set up into three experimental groups; while the first group was exposed to combined hypoxia and nutrient starvation (HNS) for 6 hours only, groups two

and three were replenished with normal media and incubated in oxygen-containing environment for 24 and 48 hours respectively. Sequentially, three control groups (one for each experimental time point) were set up as well in order to compare the effect of HNS alone versus replenishment in relation to their controls (Figure 3-2).

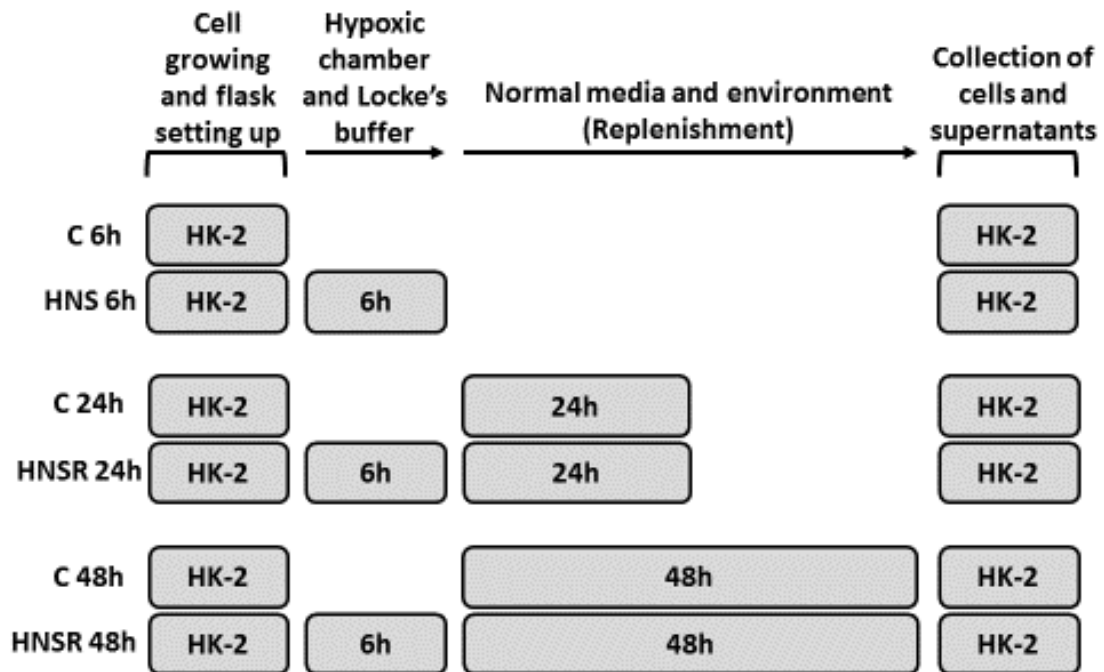


Figure 3-2: Experimental design of *in-vitro* renal HNSR model. Three pairs (control and experimental) of human renal proximal tubular epithelial (HK-2) cells were grown in 25 cm² flasks. Experimental groups were exposed to hypoxia (hypoxic chamber) and nutrient starvation (Locke's buffer) for 6 h without (group one, HNS 6h) or with replenishment for 24 h (group two, HNSR 24h) and 48 h (group three, HNSR 48h). Both cells and supernatant were collected for analysis. HNS, hypoxia and nutrient starvation; HNSR, hypoxia/ nutrient starvation- replenishment.

3.2.3.3 Technique

The hypoxic chamber used in these experiments was designed by Dr Simon Byrne from University of Leicester and was built in-house. Constructed from 10mm Perspex, it has a bottom-hinged front with an integral silicone rubber seal and top-mounted catches. The internal dimensions are 260mm (breadth), 89mm (height) and 130mm (front to rear); its volume is thus 3 litres. There are 2 perforated metal shelves, with space beneath the lower one for a shallow water tray. The gas inlet port is close to the bottom of one side, whilst the outlet port is in the middle of the top. The whole chamber sits on 4 short legs which allow the front to be opened flat. The dimensions of the chamber are such that it will accommodate a maximum of 12 small (25cm²) tissue culture flasks.

In order to decrease variability among cells' cycles, HK-2 cells were cultured initially until reaching confluence. Then an equal number of cells (0.7×10^5 cells) were seeded in 25 cm² flasks and were left for 24 hours before conducting the experiment. Then, 5ml of nutrient starvation (Locke's) buffer (154 mM NaCl, 5.6 mM KCl, 2.3 mM CaCl₂, 1 mM MgCl₂, 3.6 mM NaHCO₃ and 5 mM HEPES, pH 7.2) was added to the experimental flasks before transferring them to the especially designed enclosed (hypoxic) chamber. Initially, it was filled with atmospheric air then a customized gas mixture (0.5 % O₂, 5% CO₂, balanced % N₂; BOC. Ltd) was flushed inside the chamber from the side opening (inlet) to extrude the atmospheric air from the top opening (outlet). After isolating the chamber by closing the openings, the chamber is moved to the incubator at 37 °C for 6 hours. Sensors within the chamber monitored the concentration of oxygen showing that this method was reliable and reproducible (O₂ concentration less than 1%). This fraction of O₂ (<1% O₂, equal to pO₂ <7.6mmHg) is relevant in the context of experimental renal ischemia (Sauvant *et al*, 2009). Later, the cells were replenished with normal media and returned back to oxygen- containing incubator (21% oxygen and 5% CO₂) for the designed time points.

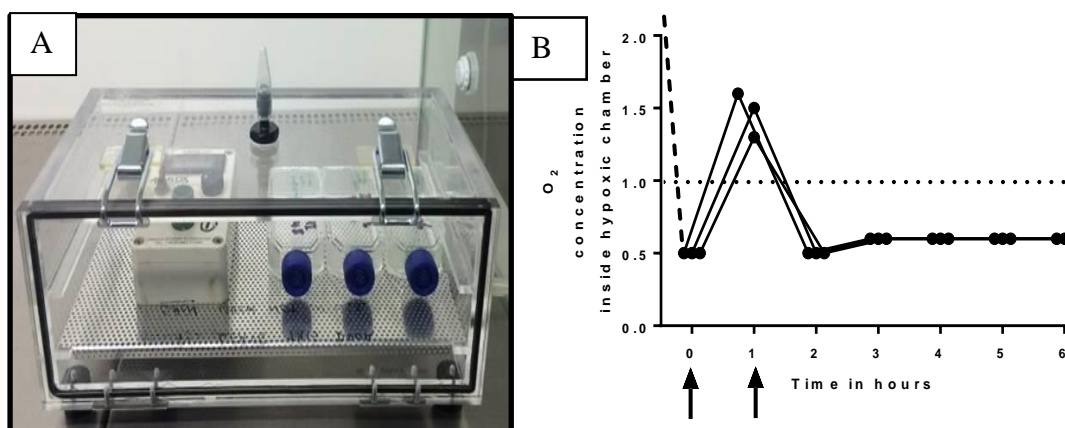


Figure 3-3: Hypoxic chamber. Frontal aspect of the hypoxic chamber with sensor (left) and three 25 cm² experimental flasks with blue, ventilated caps in a tissue culture hood (A) Curve illustrating the constancy of the oxygen concentration inside the chamber along the period of hypoxia in three separate experiments (B). Arrows indicate purges with hypoxic gas mixture. Dashed line represents reduction of O₂ concentration from atmospheric. Dotted line represents standard hypoxic conditions.

3.2.4 Lactate dehydrogenase (LDH) assay

3.2.4.1 Principle

Measuring extracellular LDH release from injured cell is a colorimetric non-radioactive technique which is developed to detect cellular toxicity particularly membrane damage. The LDH (a 140 kDa intracellular enzyme) leaks from injured cell cytoplasmic membrane catalyse serial reactions end with synthesis of red formazan from 2-(iodophenyl)-3-(p-nitrophenyl)-5-phenylterazolium chloride. The quantity of formazan production reflects the amount of LDH release, which is proportional to damaged cell (Figure 3-4) (Han *et al*, 2011; Russ, Haberstroh and Rundell, 2007).

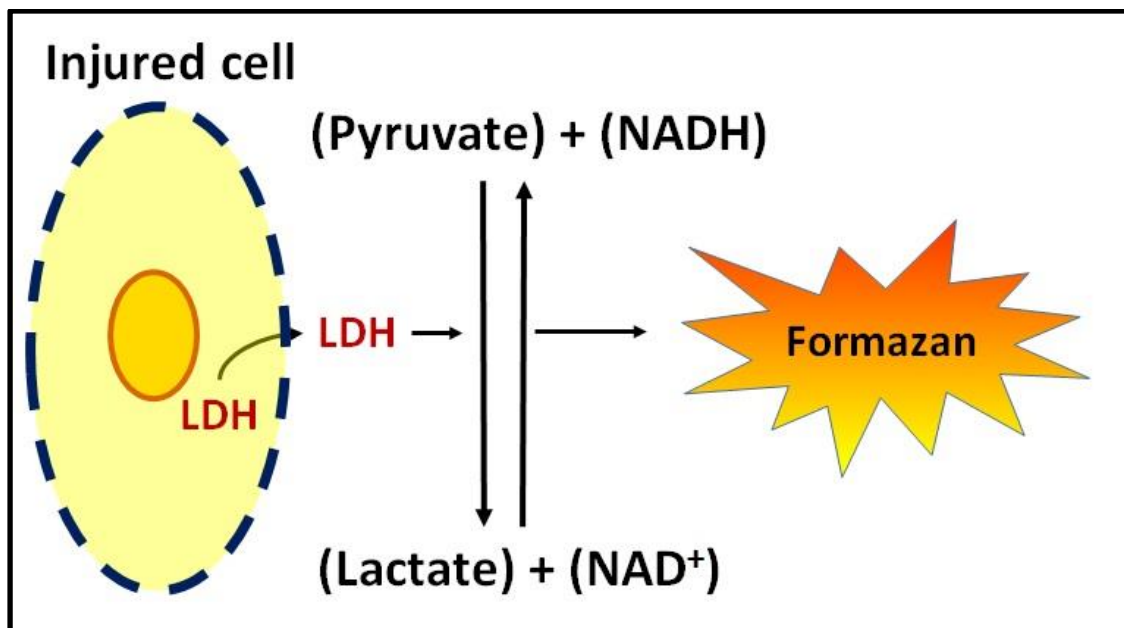


Figure 3-4: Cartoon illustrates principles of LDH cytotoxicity assay. The generating formazan is directly proportion to the amount of leaked LDH from cell lysate supernatant. LDH, Lactate dehydrogenase; NAD⁺ and NADH, oxidised and reduced nicotinamide adenine dinucleotide.

3.2.4.2 Technique

A CytoTox 96® Non-Radioactive Cytotoxicity (Promega, WI, USA) was used according to manufacturer's protocol where at the beginning, the supernatant was collected from all experimental and control groups to measure the amount of LDH release. Following the manufacturer's instructions, the stock of substrate mix was diluted by adding 12 ml of buffer solution and the positive control was prepared (had to be fresh) by adding 5 ml of fresh media to 1 µl of stock positive control. Next, from the sample that would be tested, 50 µl of supernatant was transferred to a new 96 well plate. 50 µl of substrate mix was added to all samples including positive control and was kept out from light for 30 minutes. Then, 50 µl of stop solution was added and was read out in ELISA reader (Bio-Rad, iMark) at a wavelength of 490 nm. A ratio of LDH release (represented by optical density, OD) was measured in relation to its matched time point control (Wang and Sanders, 2007).

3.2.5 MTT cell viability assay

3.2.5.1 Principle

It is one of the cell-dependant colorimetric tests, which is widely used in assessing the influence of various effectors on cell viability. Its principle of action is based on ability of reducing (3-(4,5-dimethylthiazol-2-yl)-2,5-diphenyltetrazolium bromide) tetrazolium (MTT) to formazan by living cells rather than dead ones. Although the mechanism of this conversion is not clearly understood, mitochondria may have a role. Accordingly, it is based on assessing absorbance differences due to formazan synthesis (Riss *et al*, 2004).

3.2.5.2 Technique

The protocol was adopted from Zhu and his colleague where at each time point of the experiment, 150 µl of 5 mg/ml solution of thiazolyl blue tetrazolium bromide (Sigma-Aldrich, MO, USA) in phosphate buffered saline (PBS) was incubated for 4 hours at 37 °C till insoluble violet formazan crystals formed. Thereafter, supernatant was separated and floating cells were collected in a pellet by centrifuging supernatant at 1000 rpm. Both groups of cells (at flask and pellet) were solubilised in 1 ml dimethyl sulfoxide (DMSO) (Thermo Fisher, Loughborough, UK). After gentle shaking of flasks at room temperature for 10 minutes, optical density was measured using ELISA reader (Bio-Rad, iMark) at 595 nm wave length (Zhu *et al*, 2012).

3.2.6 Hydrogen peroxide detection (H₂O₂) test

3.2.6.1 Principle

It is another colorimetric technique, which has been used to detect the release of hydrogen peroxide from cells and various specimens secondary to reactions involving peroxidase. It is a very selective and relatively easily applied assay based on detection of a red-fluorescent resorufin generating from oxidation of 10-acetyl-3, 7-dihydroxyphenoxazine by H₂O₂ where horseradish peroxidase (HRP) catalyses the reaction and the assay can be

performed spectrophotometrically as the extinction coefficient of resorufin is high (Watabe *et al*, 2011; Su, Wei and Guo, 2011).

3.2.6.2 Stock solutions

Amplex® Red Hydrogen Peroxidase / Peroxide Assay Kit (Invitrogen) which is the commercial name of 10-acetyl-3, 7-dihydroxyphenoxazine was used to detect H₂O₂ from PTEC of human kidney (HK-2 cells). The stock solutions were prepared in accordance with the manufacturer's guidance where one vial of Amplex® red reagent was dissolved in 60 µl of DMSO to get 10 mM Amplex® red reagent stock solution. Next, 4 ml of 5X reaction buffer was diluted by 16 ml H₂O to make 20 ml of 1X reaction buffer before a 10 U/ml horseradish peroxidase (HRP) stock solution was prepared by dissolving its vial in 1 ml of 1X reaction buffer. Lastly, 20 mM H₂O₂ working solution was prepared by adding 977 µl of 1X reaction buffer to 22.7 µl of 3% H₂O₂.

3.2.6.3 Assay procedure

After all stock solutions were ready, the standard curve was set up from concentration of 0-10 µM of H₂O₂ in 1X reaction buffer (total volume was 50 µl each). 50 µl of each standard as well as supernatants from experimental flasks were loaded into a 96 well-plate. This was followed by loading 50 µl of freshly made mixture of 100 µl of 10 U/ml HRP, 50 µl of 10 mM Amplex® red reagent stock solution and 4.85 ml of 1X reaction buffer). The plate was incubated for 30 minutes at room temperature in dark place before measuring optical density (OD) using ELISA reader (Bio-Rad, iMark) at 560 nm wavelength.

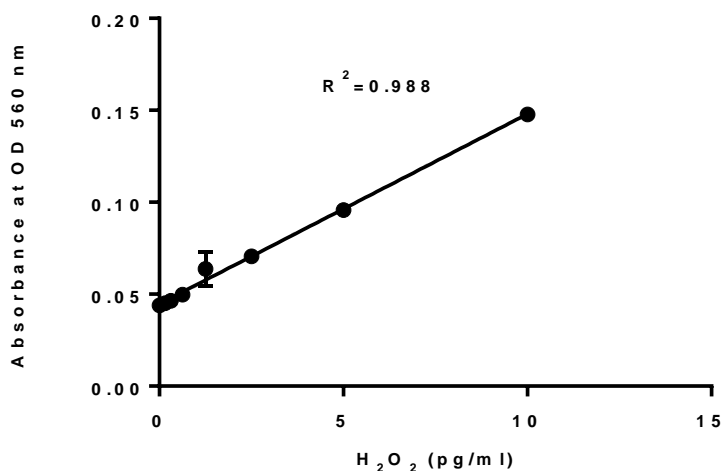


Figure 3-5 Standard curve of hydrogen peroxide assay.

3.2.7 Statistics

Experiments were repeated three times and readings were in triplicate (unless stated). Data interpretation, standard curve were calculated using Microsoft Excel ® 2010 and GraphPad Prism ® 6.07. Data were presented as mean \pm SD and ANOVA and Tukey's multiple comparison tests were used for analysing unpaired parametric data while Kruskal-Wallis and Dunn's multiple comparison tests were used for comparing nonparametric results. Data was described as significant when p value was < 0.05 .

3.3 Results

3.3.1 Optimisation of *in vitro* renal HNSR model

3.3.1.1 HNSR model by oil immersion

The purpose of our work was to establish a reproducible and easy to set up *in vitro* model of human renal PTEC (HK-2) HNSR reflecting *in vivo* IRI, which would be amenable to further analysis. Initially, mineral oil immersion with media replacement was used as method of HNSR induction. This is based on a study by Meldrum and his colleagues in 2001 when they designed an *in vitro* model evaluating cellular response to renal HNSR in isolation from systemic factors. Their model was set up through overlaying of porcine renal tubular epithelial cells (LLC-PK1) with mineral oil for various time points (0-60 minutes) to limit both oxygen and nutrient supplementation and prevent elimination of waste products followed by media replacement for 0-48h (Meldrum *et al*, 2001). Accordingly, a monolayer of HK-2 cells was overlayed with mineral oil for various time points with substrate replacement for 24 and 48h (see appendix for details). To investigate the damage resulting from the above model, cell viability was assessed by trypan blue (similar to Meldrum's article) which depends basically on staining the compromised cell with blue while the viable one remain unstained (Tran *et al*, 2011). The results showed slight differences among time points; moreover, cell numbers were small as the adherent cells only had been assessed. Nevertheless, the dead cells were most likely discarded during washing out the mineral oil and before media replacement. Therefore, measuring LDH release in supernatant was an alternative to trypan blue. The results were neither promising nor reproducible (experimental design and results were presented at appendix) as the LDH activity was greater in supernatant from cells left in their medium for 24 and 48h than supernatant from cells receiving oil immersion treatment. This could be attributed to the growth-inhibition effect of oil immersion on cells of treated groups, in contrast to the control cells were continuing growth hence becoming so dense consequently more LDH release.

3.3.1.2 Induction of HNSR model using hypoxic environment and Locke's buffer

A pilot experiment using HK-2 cell was done to induce hypoxic injury and nutrient starvation separately without substrate replacement using either hypoxic chamber or Locke's buffer. There was an increase in LDH release from supernatant of both experimental groups in comparison to their relative controls (data not shown). Then, a combination of these conditions was set up for various time points followed by media replacement for different time points as well.

The LDH release was much more when the time of ischemia was prolonged (6h) among the sets of experiment. Accordingly and as the combined effect of hypoxia and Locke's buffer exerted the most detrimental influence on HK-2 cells after 24 and 48h replenishment and it has more clinical relevance for ischemia *in vivo*, this type of hypoxia was pursued thereafter for all the experiments with three time points 6, 24 and 48h. A refinement of the experimental design was deemed necessary due to fluctuation using a conventional hypoxic chamber. Subsequently, cells were exposed to a customised gas mixture (details were mentioned in method). It is reproducible, easy to monitor, affordable and standardisable.

3.3.2 Assessing degree of PTEC damage in *in vitro* renal HNSR model via measuring LDH release

There was an increase in LDH release ratios across the experimental groups where LDH release ratio of both HNSR for 24h and HNSR for 48h were significantly higher than that of HNS for 6h ($p=0.0017$ and 0.002 respectively). The LDH release ratio of HNSR for 48h was more than that of HNSR for 24h but not significant ($p> 0.05$) (Figure 3-6).

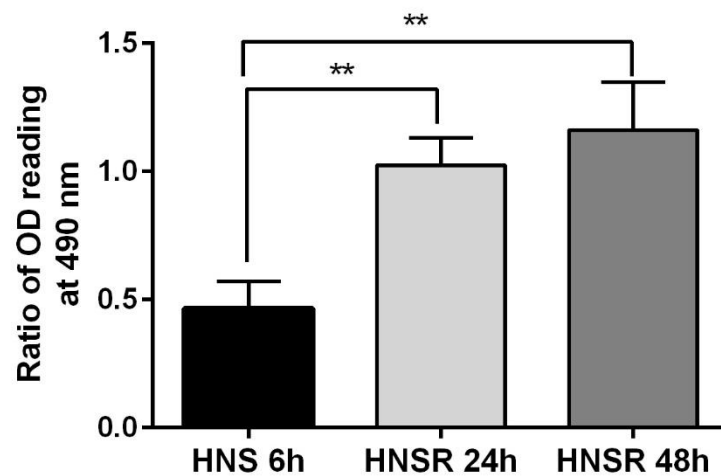


Figure 3-6: Quantitative assessment of lactate dehydrogenase (LDH) release from *in vitro* renal HNSR model. Ratio of LDH release from each experimental group to its control was measured using supernatant of human proximal tubular epithelial (HK-2) cells; $n=3$ in triplicate, $p(*) < 0.05$, data were presented as mean \pm SD; HNS, hypoxia and nutrient starvation; HNSR 24h and 48h, hypoxia and nutrient starvation followed by replenishment for 24 and 48 hours respectively.

3.3.3 Cell viability across *in vitro* renal HNSR model

Using MTT cell viability test, the effect of combined hypoxia and nutrient starvation for 6h followed by media replenishment for 24 and 48h on PTEC of human kidneys (HK-2) was assessed in comparison to their controls (Figure 3-7). There was a noticeable reduction in MTT ratio after HNS 6h to control which was followed by significant gradual rise in MTT ratios in both HNSR for 24h ($p=0.004$) and HNSR for 48h ($p < 0.0001$) in comparison to HNS for 6h group. The difference between two replenished groups (24 and 48h) was significant as well ($p= 0.029$).

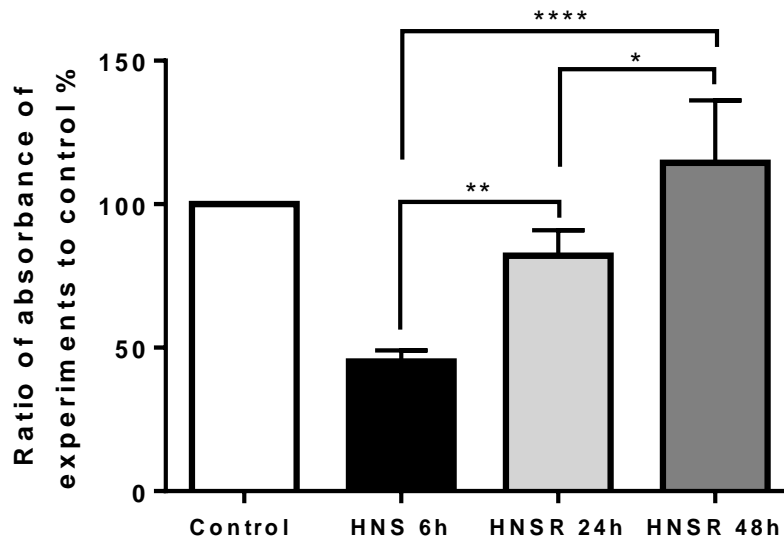


Figure 3-7: Cell viability of human PTEC (HK-2). Quantitative measurements of human renal PTEC (HK-2) proliferation over *in vitro* renal HNSR model. Using MTT cell viability test, a percentile ratio of formazan formation in each experimental groups was measured in comparison to control; n=3 each in 4 replicates, $p^{(*)} < 0.05$, $(^{**}) \leq 0.01$, $(^{***}) \leq 0.001$, $(^{****}) \leq 0.0001$ data were presented as mean \pm SD; HNS, hypoxia and nutrient starvation; HNSR 24h and 48h, hypoxia and nutrient starvation followed by replenishment for 24 and 48 hours respectively.

3.3.4 Calculation of reactive oxygen species (ROS) release from HK-2 cells

There was an increase in LDH release ratios across the experimental groups where LDH release ratio of both HNSR for 24h and HNSR for 48h were significantly higher than that of HNS for 6h ($p=0.02$ and 0.0098 respectively). The LDH release ratio of HNSR for 48h was more than that of HNSR for 24h but not significant ($p > 0.05$) (Figure 3-8).

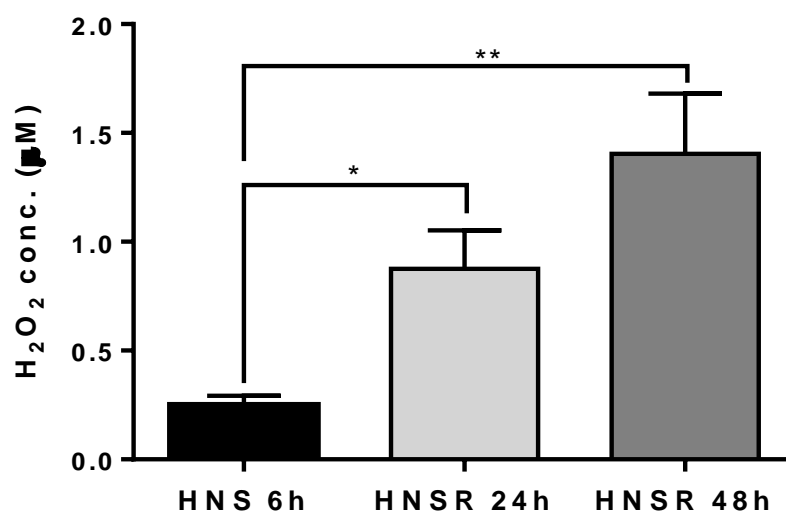


Figure 3-8 A quantitative assessment of ROS release from HK-2 cells in *in vitro* HNSR model. Concentration of hydrogen peroxide (one of ROS) release from each of the three treated groups was measured and normalised to their control mates respectively; ; n=3, in triplicates, $p(*) < 0.05$ ($** < 0.01$), data were presented as mean \pm SD; HNS, hypoxia and nutrient starvation; HNSR 24h and 48h, hypoxia and nutrient starvation followed by replenishment for 24 and 48 hours respectively.

3.4 Discussion

During kidney transplantation, impairment of renal function caused by IRI is unavoidable and may end with chronic kidney disease (CKD). The complexity of injury during IRI (ischemia as well as reperfusion) and the need for further exploration of the exact mechanisms that participate in inducing IRI are the reasons to develop various *in vitro* models mimicking the *in vivo* IRI (Kurian and Pemaih, 2014). In this study a novel *in vitro* HNSR model was established to simulate both phases of IRI (6h and 24h) and was extended to cover the healing phase as well (48h). Ischemia was simulated via combined treatment of human PTEC (HK-2) with serum- free, glucose- free Locke's buffer and incubation in hypoxic chamber while incubation with normal media inside oxygenated chamber represented the reperfusion phase. The superiority of combined over single (Locke's buffer or hypoxic chamber) treatment as well as duration of HNS (6h over 3h) were based on measuring LDH release and TNF- α protein expression. LDH release was higher (i.e. more cell damage) with HNS for 6h followed by replenishment for 24h and 48h respectively than other experimental modalities (Figure 7-3). These results were supported by TNF- α protein expression as it was higher (i.e. more inflammation) from HK-2 exposed to combined stimulation for 6h and HNSR 48h than single treatment and significantly more than control group as well (Figure 7-5).

Using LDH assay to assess cellular response is in agreement with other studies. It was used by Wang and Sanders, 2007 to assess the effect of immunoglobulin on human renal PTEC (HK-2) *in vitro* (Wang and Sanders, 2007) and Breggia and Himmelfarb in 2008 assessed the influence of hypoxia and chemically induced ischemia on murine renal PTEC using LDH release as well (Breggia and Himmelfarb, 2008). Moreover, Meldrum *et al.*, used TNF- α to monitor an *in vitro* model development similar to *in vivo* renal IRI via exposure of porcine renal PTEC to oil immersion followed by media replacement (Meldrum *et al.*, 2001). Peng *et al.*, 2012 found that TNF- α protein secretion is elevated after exposing murine renal PTEC to hypoxic/ re-oxygenation environment (Peng *et al.*, 2012). *In vivo*, TNF- α expression from renal PTEC (mice) has been used as pro-inflammatory marker in renal IRI model (Linkermann *et al.*, 2012).

Principally, ischemia can be induced *in vitro* by immersion cells either by chemical agents such as antimycin and rotenone, treating cells with enzymes (e.g. catalase and glucose

oxidase) or by incubation in hypoxic chamber (Kurian and Pemaih, 2014). Both hypoxic chamber and Locke's buffer were used together by Arumugam *et al*, 2007 to simulate ischemia in murine cortical neuronal cells to evaluate the effect of immunoglobulin administration on complement cascade during stroke (Arumugam *et al*, 2007). Similarly, Pavlovski and his colleagues adopted this method for assessing the role of CS (C5a) on apoptosis in murine cortical neuronal cells as well (Pavlovski *et al*, 2012). Locke's buffer alone has also been used in primary neuronal cell line (mice) to simulate cerebral ischemia *in vitro* (Lee *et al*, 2015). The above studies did not use this model to explore the effect of reperfusion on neurons and the model represented the ischemic phase only.

Simulation of ischemia *in vitro* via incubating cells in hypoxic environment was seen in many articles. Hotter *et al*, 2004 showed that incubating porcine PTEC in hypoxic chamber induced apoptosis as is the case for renal ischemia *in vivo* (Hotter, Palacios and Sola, 2004). Later, Basu and colleagues applied the same technique on human renal PTEC to investigate the role of hypoxia during acute kidney injury (Basu *et al*, 2011). Meanwhile, reperfusion phase was simulated by culturing hypoxic cells in standard incubator developing *in vitro* hypoxia/ reoxygenation simulator to *in vivo* IRI. This model was applied by Leonard and colleagues on human renal PTEC (HK-2) to study the molecular signalling of PTEC during acute renal failure, ARF (Leonard *et al*, 2003).

Moreover, conducting *in vitro* model instead of *in vivo* one may be of benefit in assessing the exact response of specific cells to IRI and measuring more accurately type and quantity of injurious factors and cell-surrounding environment (such as pO_2 and pCO_2) which make repetition of same experiment more reliable (Russ, Haberstroh and Rundell, 2007). Nevertheless, *in vitro* models are not without drawbacks as they are simulators rather than real IRI models, there is no assessment of the interaction between various cells/ tissues, and some cells show different behaviour *in vitro* than *in vivo* (Russ, Haberstroh and Rundell, 2007). All the same, many researchers have suggested that a well-designed *in vitro* model is crucial in understanding effectively molecular mechanisms of PTEC trafficking while studying IRI and gives foundation to subsequent *in vivo* work as well (Russ, Haberstroh and Rundell, 2007; Kurian and Pemaih, 2014).

While different renal cell lines (of human and animal origin) have been used in various *in vitro* models such as medullary cells, fibroblast, cells from distal tubule, as well as

podocytes (Russ, Haberstroh and Rundell, 2007), human PTEC have been used in the HNSR model in this thesis. This is because during IRI, PTECs are the most seriously affected cell type due to their high metabolic demands; this results in cytoskeleton impairment, and give rise to serial inflammatory and vasoactive mediators affecting other parts of the renal nephron (medulla, glomeruli and microvascular system) (Bonventre and Weinberg, 2003).

The epithelial cellular response of our HNSR model was assessed by measuring LDH release as it is commonly used to monitor HK-2 cells (Wang and Sanders, 2007). Results have so far revealed incremental LDH release from supernatant of PTEC with combined stimulation and replenishment than HNS treatment alone reflecting more cell damage (Figure 3-6). These results are in line with other studies on *in vivo* murine IRI models, which showed elevated LDH release from kidneys affected by IRI (Wang *et al*, 2015; Linkermann *et al*, 2013). *In vitro*, various cell lines have been used including rat myoblast (Joshi *et al*, 2011), porcine (LLC-PK1) and human (HK-2) renal PTEC (Kishi *et al*, 2015; Turman and Rosenfeld, 1999) where all of them showed increase of LDH release after exposing them to hypoxic environment.

Further analysis of HNSR model was performed via measuring hydrogen peroxide generation from HK-2 cells. It is the most common reactive oxygen species production during renal IRI resulting in tubular cell death (apoptosis) and renal failure (Zhuang *et al*, 2007; Lee *et al*, 2013). The current study found that maximum H₂O₂ release (i.e. more apoptosis) was after 24h replenishment although it was not significant and decreased (but significantly higher than HNS alone) after 48h replenishment (Figure 3-8). *In vitro*, studies showed that H₂O₂ causes cell apoptosis in both rabbit and human PTEC (Zhuang *et al*, 2007; Lee *et al*, 2013) while *in vivo* work showed that renal PTEC (mice) produce ROS in response to IRI and H₂O₂ assay can be used to monitor the degree of tubular damage (Kunduzova *et al*, 2002; Wang *et al*, 2011).

Finally, one unanticipated finding was that cell viability test (MTT) showed a significant decrease in cell viability after HNS which stepped up significantly after 24h and 48h of replenishment (Figure 3-7). Ma *et al.*, 2014 used MTT to assess renal PTEC (rat) viability in *in vitro* model simulating IRI (Ma *et al*, 2014) and Zhuang *et al.*, used it in evaluating

rabbit renal tubular epithelial cells viability after exposure to hydrogen peroxide (Zhuang *et al*, 2007).

These results may be explained by the fact that both cell damage (expressed by LDH release) and cell regeneration and growth (presented by MTT) are occurring simultaneously during HNSR *in vitro* model. It is obvious that various mechanisms are controlling IRI pathogenesis such as ROS pathway (Lee *et al*, 2013) and immune-inflammatory signaling (Tadagavadi, Wang and Ramesh, 2010) . However, further studies are needed to understand the underlying molecular trafficking during IRI in order to reduce mortality and morbidity after renal transplant (Lee *et al*, 2014). According to these data, we can infer that our HNSR model is a new *in vitro*, dependable and easily applicable model that can simulate and replace the *in vivo* renal IRI. This model can reliably deliver insight in IRI mechanisms via evaluating both injurious phases (ischemia and hypoxia) as well as exploring both damage and repair pathways.

4 Chapter four (characterisation of the
inflammatory response of human PTEC (HK-2) to
in vitro HNSR)

4.1 Introduction

Renal IRI is an integrated process of cellular injury, inflammatory reaction and haemodynamic changes that is followed by healing process (Bonventre and Yang, 2011). Renal tubular epithelial cells are particularly susceptible to IRI damage, which may end with apoptosis and/ or acute tubular necrosis; nevertheless, they play a part in inflammation via expression and controlling various pro-inflammatory molecules such as IL-1 and IL-6, and TNF- α (Bonventre and Yang, 2011). Furthermore, despite the debate of the exact mechanism of action, the complement system undoubtedly occupies a role in the pathology of renal IRI (de Vries *et al*, 2003). PTECs have the ability to express and activate the complement cascade particularly AP components. Peake *et al*, 1999 showed that C3, fH, fB, fI, and fD mRNA were expressed from HK-2 cells using PCR. Furthermore, C3, fH and fB proteins and their cleaved component were also produced from HK-2 cells on western blot (Kinsey, Li and Okusa, 2008; Peake *et al*, 1999). *In vivo*, immunofluorescence microscopy revealed greater C3 deposition in kidneys of wild mice exposed to IRI than control (Thurman *et al*, 2003).

Hypoxia markers particularly HIF-1 α signalling was assessed in HK-2 cells exposed to low oxygen, low glucose / reoxygenation protocol *in vitro*. It has been shown that HIF-1 α protein was expressed more after hypoxia than after media replenishment while its mRNA did not show any expression differences (Conde *et al*, 2012). On the other hand a study by Suzuki *et al*, 2008 revealed that autophagosomes are increased in PTEC (HK-2) exposed to ischemia *in vitro*. Although their exact role is not clear, it could be part of cellular injury or defensive mechanism against renal ischemia (Suzuki *et al*, 2008). In this chapter, the inflammatory response of human PTEC of HK-2 to *in vitro* HNSR was investigated in attempt to clarify the molecular signalling during both phases of IRI, which may help in finding the targets for reducing injury and improving healing.

4.2 Materials and methods

4.2.1 Extraction of ribonucleic acids from HK-2 cells

4.2.1.1 Trizol- phenol- chloroform protocol

Confluent HK-2 cells were exposed to the optimised HNSR model (details in chapter 3). In each 25 cm² flask, the medium was removed and replaced with 1 ml of Trizol-reagent (Ambion® from Thermo Fisher Scientific, Loughborough, UK) for 10 minutes at room temperature to maximise the amount of the lysed cells collected. In order to separate RNA from proteins, 200 µl of chloroform was added and the tube was shaken vigorously for 15 seconds. Next, the sample was incubated for 15 minutes at room temperature and the tubes were centrifuged at 12000 xg for 15 minutes. The upper colourless aqueous layer was moved to a new 1.5 ml tube and a 500 µl of isopropanol was added and shaken well before incubation for 10 minutes to precipitate the RNA (The RNA precipitate is often invisible at this step). Then, centrifugation at 12000 xg for 10 minutes was performed to pellet the RNA, followed by discarding the supernatant, replacing with 1 ml of 75 (v/v) % ethanol and centrifugation at 7500 xg for 5 minutes for washing. Thereafter, the supernatant was removed to leave the RNA to dry, then the pellet was dissolved in 25 µl DEPC (Diethyl pyrocarbonate) 0.02 (v/v) % treated water. Then, the sample was put in the heat block at 55⁰C for 15 minutes. Finally, RNA concentration was measured (in ng/µl) using nanodrop machine programme RNA-40 (Invitrogen™ from Thermo Fisher Scientific, Loughborough, UK) at 260nm wavelength.

4.2.1.2 Qiagen RNA extraction protocol

More sensitive protocol has been used that did not need phenol or chloroform for RNA extraction. This was conducted via using RNeasy ® Plus Mini Kit (Qiagen, Texas, USA). According to the manufacture's guide, HK-2 cells from our HNSR model were lysed with 350 µl RLT plus buffer and were centrifuged for 3 minute (maximum speed). While residues were discarded, the supernatant was transferred to a gDNA eliminator spin column after inserting it in a new 2 ml collecting tube. The tube was centrifuged at more

than 8000 xg for 30 seconds before removing the column. 350 µl of 70% ethanol were added to the tube and was mixed by frequent gentle pipetting. 700 µl of the sample were taken to an RNAeasy spin column after placing it inside 2 ml collection tube. The tube was centrifuged at more than 8000 xg for 15 seconds and flow-through was discarded. Next, 700 µl of RW1 buffer was added to the spin column after inserting it in new 2 ml collection tube before centrifugation for 15 second at more than 8000 xg and followed by discarding the flow-through. Then, 500 µl of RPE buffer were added to the spin column; centrifuged again at more than 8000 xg for 15 second; and the flow- through was discarded again. Lastly, 500 µl of RPE buffer was added to the spin column again, centrifuged again at more than 8000 xg for 2 minutes; and the flow- through was discarded again. Finally, the spin column was transferred to a new 1.5 reaction tube and 30-50 µl of RNase- free water was added before centrifuging the tube at more than 8000 xg for 1 minute. The spin column was removed and the RNA in the reaction tube was stored at -80°C or applied to the next step.

4.2.2 Formation of complementary DNA (cDNA)

Complementary DNA was prepared from the extracted RNA using Maxima™ H Minus first strand cDNA synthesis kit (Thermo Scientific) according to the manufacturer's protocol. For each sample, 5 µg from RNA (appropriately adjusted for each sample) was transferred to 0.5 ml RNase free tube (on ice) followed by addition of 1µl (100 pmol) of oligo (dT)₁₈ primer, 1µl (10 mM) dNTP mix in a final volume of 15µl . The RNA template was vortexed slightly, centrifuged, incubated at 65°C for 5 minutes and cooled by ice. Then, 4µl of 5X RT buffer [250 mM Tris-HCl (pH 8.3 at 250C), 375 mM KCl, 15 mM Mg Cl₂, 50 mM DTT)] and 1µl Maxima H Minus Enzyme mix were added.

Next, the mixture was incubated for ½ h at 50°C at first before temperature was raised to 65°C. The operation was completed by raising temperature to 85°C for 5 minutes to denature the enzyme.

4.2.3 Polymerase chain reaction (PCR)

4.2.3.1 Principle

Reverse transcription (RT) PCR is the amplification performed for a specific complementary cDNA which is assembled according to messenger mRNA extracted from certain cells. It may be set up as endpoint or quantitative PCR (Hue-Roye and Vege, 2008).

4.2.3.2 Technique

A 3 μ l from the prepared complementary DNA is transferred into 0.5 ml tube after adding 2.5 μ l 10X Reaction buffer, 1.5 μ l MgCl (25mM), 4 μ l dNTPs (1.25mM), 0.2 μ l Thermo Prime Enzyme (5 U/ μ l), 10.8 μ l PCR grade water, 2 μ l forward primer (5 μ M) and 2 μ l reverse primer (5 μ M). Primers that were used are listed in Table 4-1. The number of cycles used for amplification varied depending on the condition of individual gene by using PCR machine (TECHNE, TC-3000 from Bibby Scientific, Staffordshire, UK).

Table 4-1 List of primers and their specifications (human specific).

Primer	Forward sequence	Size	NCBI accession numbers	Annealing temperature
β-actin	CAC CAA CTG GGA CGA CAT*	1761 bp	X00351.1	55 ⁰ C
	ACAGCCTGGATAGCAAC			
β2m	GGC TAT CCA GCG CAC TCC AAA*	987 bp	NM_004048	50 ⁰ C
	CAA CTT CAA TGT CGG ATG GAT G			
18sRNA	CGG CTA CAT CCA AGG AA*	1969 bp	M10098	57 ⁰ C
	GCT GGA ATT ACC GCG GCT			
TGF-β1	CCC AGC ATC TGC AAA GCT C*	2583 bp	NM_000660	60 ⁰ C
	GTC AAT GTA CAG CTG CCG CA			
Caspase- 3	AGA ACT GGA CTG TGG CAT TGA G*	2689 bp	NM_004346	60 ⁰ C
	GCT TGT CGG CAT ACT GTT TCA G			
IL6	GCCCAGTGGACAGGTTTCT*	1201 bp	NM_000600 .3	62 ⁰ C
	TCCTGCAGAAAAAGGCAAAG			
Kim-1	CTG CAG GGA GCA ATA AGG A-G*	1713 bp	NM_001308 156	54 ⁰ C
	ACC CAA AAG AGC AAG AAG CA-AA*			
Clustrin	AAG GAA ATT CAA AAT GCT GTC AA*	1620 bp	BC013221	50 ⁰ C
	ACA GAC AAG ATC TCC CGG CAC TT			
Factor B	AAGCTGACTCGGAAGGAGGT*	2388 bp	L15702	58 ⁰ C
	TCCACTACTCCCCAGCTGAT			
Properdin	GCATCCAGCACTGCCCCTTGAAA*	1785 bp	NM_002621	60 ⁰ C
	GGCACGGGTAGGATTAGGTCCACA			
Factor H	GGAACCACCTCAATGCAAAG*	3926 bp	Y00716	55 ⁰ C
	AAGCTTCTGTTTGGCTGTCC			
C3	CTGGGTGTACCCCTTCTTGA*	5148 bp	NM_000064	58 ⁰ C
	GCTGAAGCACCTCATTG6TGA			
VEGF	TCACCGCCTCGGCTTGTCACAT	640 bp	AY047581	60 ⁰ C
	GAGATGAGCTTCCTACAGCAC			
VCAN	CAAGCATCCTGTCTCACGAA	1925 bp	BC050524	55 ⁰ C
	CAACGGAAGTCATGCTCAAA			

*: sequence of forward primer

4.2.3.3 Agarose gel electrophoresis

1% (w/v) agarose gel was prepared in 0.5X TBE gel (Table 4-2). Ethidium bromide (0.5 µg/ml) was used to visualise the bands. DNA ladder was from Thermo Scientific (GeneRuler 1 kb Plus DNA ladder). DNA gel loading dye (10X) was 15% (w/v) bromophenol blue, 50% (v/v) glycerol and 0.5 mM EDTA pH8.0), and gels are run at 90 volts for 1 hour before imaging using Imagequant 100 (UV trans illuminator).

Table 4-2: Contents of 5X TBE (Tris/Borate/EDTA). A 1:10 dilution in dH₂O was used to make and run the gel.

Material	Amount
Tris base	54 g
Boric acid	27.5 g
0.5 M EDTA (pH: 8.0)	20 ml
Distilled water	1 L

4.2.3.4 Real-time quantitative reverse transcription PCR (Real –Time qRT-PCR)

This advanced version of PCR has the ability to detect accurately the amount of the assembled DNA after each cycle rather than the final product. Principally, it is of two types based on detectors; either TaqMan® probe, which contains flourogenic reporter restricted to quencher and primer extension results in reporter release and fluorescence detection. Opposately, the other detector is DNA- binding dye or SYBR® Green, is inert during its unbound phase and release fluorescence after adhering to DNA (Arya *et al*, 2005).

The cDNA was diluted 1:4 with nanopure water and a master mix was prepared [10 µl Sensi Mix™ SYBR H-ROX Kit (Bioline, London, UK), 2 µl of (5µM) forward primer, 2 µl of (5µM) reverse primer and 3 µl distilled autoclaved water).

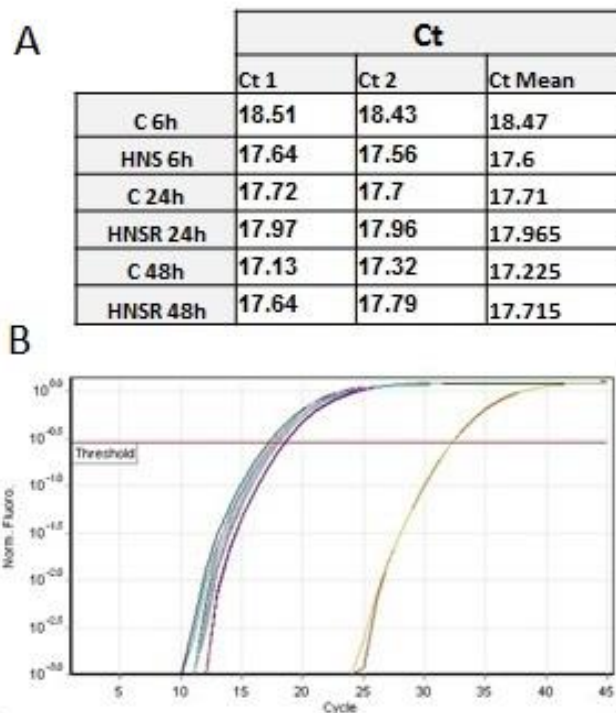
In strips of 4 tubes and caps, 17 µl of the master mix was added to 3 µl of diluted cDNA (from experiment and control samples) and the same amount of the master mix was added to 3 µl of water (negative control). All test and negative control samples were run in

duplicate using Corbett Rotor-Gene™ 6000 machine and software. The results were analysed according to the Livak method to measure the expression ratio ($2^{-\Delta\Delta CT}$) (Schmittgen and Livak, 2008) and Microsoft office Excel (2010) was used to calculate the normalisation of target genes to housekeeping genes (Table 4-3). Beta 2 microglobulin ($\beta 2M$) was used as housekeeping gene due to stability of its expression across experimental groups and their related controls (Table 4-4).

Table 4-3: A template for calculating the normalisation of target genes to housekeeping ones depending on measuring expression ratio ($2^{-\Delta\Delta CT}$). Reference Ct: housekeeping gene. Target Ct: Examined gene.

		Reference Ct				Target Ct				$\Delta Ct(\text{test}) = Ct(\text{target}) - Ct(\text{ref})$	$\Delta Ct(\text{calibrator}) = Ct(\text{target}) - Ct(\text{ref})$	$\Delta\Delta Ct = \Delta Ct(\text{test}) - \Delta Ct(\text{calibrator})$	$2^{-\Delta\Delta Ct}$
		1	2	3	Average	1	2	3	Average				
T1	Calibrator	Tube 1			#DIV/0!	Tube 1			#DIV/0!	#DIV/0!	#DIV/0!	#DIV/0!	#DIV/0!
	Test	Tube 2			#DIV/0!	Tube 2			#DIV/0!	#DIV/0!	#DIV/0!	#DIV/0!	#DIV/0!
T2	Calibrator	Tube 3			#DIV/0!	Tube 3			#DIV/0!	#DIV/0!	#DIV/0!	#DIV/0!	#DIV/0!
	Test	Tube 4			#DIV/0!	Tube 4			#DIV/0!	#DIV/0!	#DIV/0!	#DIV/0!	#DIV/0!
T3	Calibrator	Tube 5			#DIV/0!	Tube 5			#DIV/0!	#DIV/0!	#DIV/0!	#DIV/0!	#DIV/0!
	Test	Tube 6			#DIV/0!	Tube 6			#DIV/0!	#DIV/0!	#DIV/0!	#DIV/0!	#DIV/0!
T4	Calibrator	Tube 7			#DIV/0!	Tube 7			#DIV/0!	#DIV/0!	#DIV/0!	#DIV/0!	#DIV/0!
	Test	Tube 8			#DIV/0!	Tube 8			#DIV/0!	#DIV/0!	#DIV/0!	#DIV/0!	#DIV/0!

Table 4-4: Shows expression of $\beta 2M$ from experimental groups of HNSR *in vitro* model (A) and quantification report (B). Expression was presented as cycle threshold (Ct).



4.2.4 Enzyme Linked Immunosorbent Assay (ELISA)

4.2.4.1 Principles

Enzyme linked immunosorbent assay, ELISA, is a commonly used assay to quantify proteins, hormones and other antigens as well as antibodies in specific samples. It is an immunological-based technique that depends on colorimetric assessment of antigen-antibody binding interaction (Gan and Patel, 2013).

Generally, although they are sharing the same principles, ELISA has several variants. They are indirect, competitive, sandwich, multiple as well as portable ELISA. The sandwich one is based on preparing the well before adding the antigen with a preliminary antigen-specific antibody (capture Ab) enabling to isolate the target antigen from a mixture. The antigen will be packed (sandwich) between this Ab and detection Ab. The antigen-antibody complex is linked to a chromogenic-enzyme (via detection Ab) developing color after interaction with substrates and the intensity of the colour is directly related to the amount of proteins (Gan and Patel, 2013).

4.2.4.2 Technique

In order to assess the effect of HNSR model on TFF3 synthesis from HK-2 cells, ELISA was performed using supernatants, which were collected from experimental groups. The procedure was performed according to the manufacturer protocol (R&D systems™, Quantikine® ELISA; Minneapolis, USA).

Firstly, 100 µl of Assay Diluent RD-68 (buffered protein base with preservatives) was added to an already coated 96-well plate with a monoclonal antibody against human TFF3. Then, 50 µl of serially diluted standards, recombinant human TFF3, (2500-39 pg/ml) beside neat supernatants (from experimental groups) were pipetted into the well and incubated for 2h at room temperature on a horizontal orbital microplate shaker (Shaked-thermostate from ELMi Ltd, Riga, Latvia) set at 500 rpm. After that, washing 4 times using 1:25 wash buffer (buffered surfactant with preservatives), adding 200 µl of a polyclonal antibody against human TFF3 conjugated to horseradish peroxidase (TFF3 conjugate) to each well and incubation at room temperature on the shaker for 2h. Next,

washing was done again before adding 200 μl of substrate solution (hydrogen peroxide + tetramethylbenzidine). The plate was incubated in dark place at room temperature for 30 minutes before a 50 μl of stop solution (2N sulfuric acid) was pipetted onto each well. Absorbance (OD) was measured at 450nm with wavelength correction at 540nm.

4.2.5 Transmission electron microscopy (TEM)

4.2.5.1 Principle

The need for visualising tiny objects (less than 0.5 μm) that cannot be seen by light microscope encouraged scientist to develop electronic microscope (EM) which based on creation of electronic image using electronic beam. Generally, it is of two types; transmission (TEM) and scanning (SEM). In TEM, camera detect images that were generated from transmission of electronic beam through examined objects after magnifying those using magnetic lenses. The EM has the ability to magnify images up to 2 million times with high resolution showing fine details; however, it is a highly demanding, expensive tool and very complicated requiring well trained staff as well as special place (JIC, 2015).

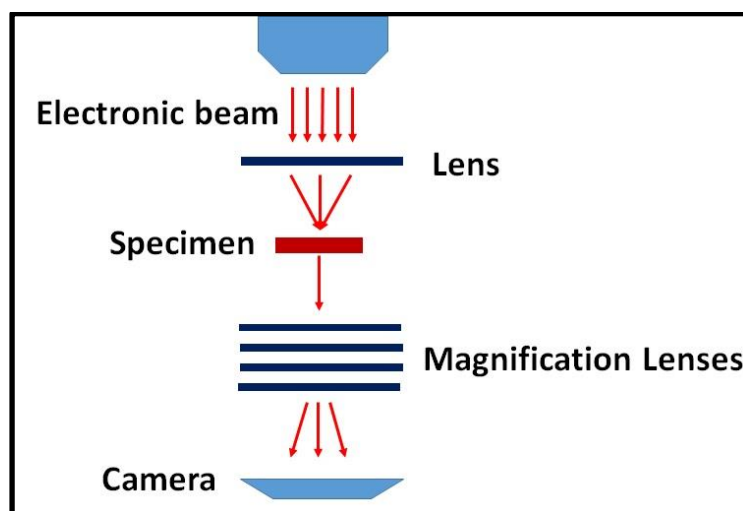


Figure 4-1 A cartoon showing the main parts of transmission electron microscope (TEM).

4.2.5.2 Technique

After setting up the HNSR model, a positive control was conducted via adding 0.2 μ M tunicamycin (Sigma-Aldrich, MO, USA) to flask with the same cell density for 16 hour (Gozuacik *et al*, 2008; Moon *et al*, 2014). When each time point finished, the cells were fixed with cacodylate buffered fixative (4% glutaraldehyde, 2% formaldehyde, 0.1 M sodium cacodylate and 2 mM calcium chloride) overnight. Then, the cells were washed with washing buffer (0.1 M sodium cacodylate+ 2 mM calcium chloride). Following a protocol of Dr Simon Byrne, after spinning down the cells at 2.3 g for 3 minutes, the supernatant was discarded and 200 μ l of 2% osmium tetroxide was added to the cells for one hour (in this step the pellet turned black) to impart electron density of the cells. Then, the cells were washed with serial dilutions of ethanol (70%, 90 % and 100%). The cells were spun down (10 X for 3 minutes) and were drained between each dilution. An intermediate solution 1, 2 epoxypropane was used. Sparr's epoxy resin was made up, and 3 dilutions were made (33%, 50% and 66%) in epoxypropane. These increasing concentrations of resin were used to infiltrate the cell (incubation for 15 minutes followed by spinning down between adding each concentration). Later, an overnight incubation of the cells with fresh resin was done.

On the next day, spinning down the cells was done followed by removal of the supernatant. The pellet was transferred to a BEEM capsule before covering it with fresh resin and a paper label was added after spinning down the capsule. The capsules were baked for 16 h at 60 $^{\circ}$ C then the polymerized resin blocks were removed from the plastic capsule. Ultramicrotome (Ultracut) was used in order to cut firstly semi- thin (40 μ m) and secondly ultra-thin sections. The first cutting was necessary in order to stain by toluidine blue and examine under light microscope for the presence of cells. After that, ultra-thin silver-pale gold sections were picked up on 300 square grid (Copper, 3.05 mm). Then, staining of the grid was performed. Firstly, incubation with 2% uranyl acetate was done for 2 minutes followed by 10 times washing in a special cabinet. Finally, these grids were stained with Reynold's lead citrate and were examined under electron microscope. This step was done with Natalie Allcock, UoL Electron Microscopy Suite.

4.2.6 Statistics

Experiments were repeated three times and readings were in triplicate (unless stated). Data interpretation, standard curve, nonlinear regression and interpolation (for ELISA) were calculated using Microsoft Excel ® 2010 and GraphPad Prism ® 6.07. Data were presented as mean \pm SD and ANOVA and Tukey's multiple comparison tests were used for analysing unpaired parametric data while Kruskal-Wallis and Dunn's multiple comparison tests were used for comparing nonparametric results. Data was described as significant when p value was < 0.05 .

4.3 Results

4.3.1 Effect of HNSR on HK-2 cell mRNA expression of cytokines and inflammatory markers

The purpose of these tests was to quantify candidate gene responses in a model of HNSR using PTEC of human kidney, HK-2. The results were normalised to both control groups and housekeeping gene beta 2 microglobulin ($\beta 2M$) and presented as expression ratio ($2^{-\Delta\Delta CT}$) (Schmittgen and Livak, 2008).

4.3.1.1 Alternative pathway

Complement 3 (C3) mRNA was abundantly expressed by HK-2 cells in response to HNS for 6h alone without replenishment. Expression was significantly lowered after HNSR for 24h ($p=0.034$) and increased six folds after HNSR for 48h ($p=0.0012$) but was not significant in relation to HNS for 6h ($p=0.076$) (Figure 4-2 A).

Properdin mRNA expression from HK-2 cells showed a different pattern although peak was from cells exposed to HNSR for 48h (1.338 ± 0.037). It was significantly higher than HNS 6h ($p<0.0001$) but insignificantly higher than HNSR 24h ($p>0.05$). However, the gene expression was significantly higher after HNSR for 24h than HNS for 6h ($p=0.007$) (Figure 4-2 B).

Similar to the expression pattern of properdin, HK-2 cells exposed to HNSR for 48h expressed factor B (fB) mRNA significantly higher than both HNSR for 24h ($p=0.005$) and HNS for 6h ($p=0.004$). Although fB mRNA expression was higher from cells exposed to HNSR for 24h than HNS for 6h alone, it was not significant ($p=0.12$) (Figure 4-2 C).

Results for factor H (fH) mRNA expression from HK-2 cells revealed insignificant drop after HNSR for 24h stimulation in comparison to HNS for 6h alone ($p=0.43$). This was followed by an incremental increase in expression after HNSR for 48h stimulation which

was significant in relation to HNS for 6h and HNSR for 24h ($p=0.042$ and 0.0012 respectively) (Figure 4-2 D).

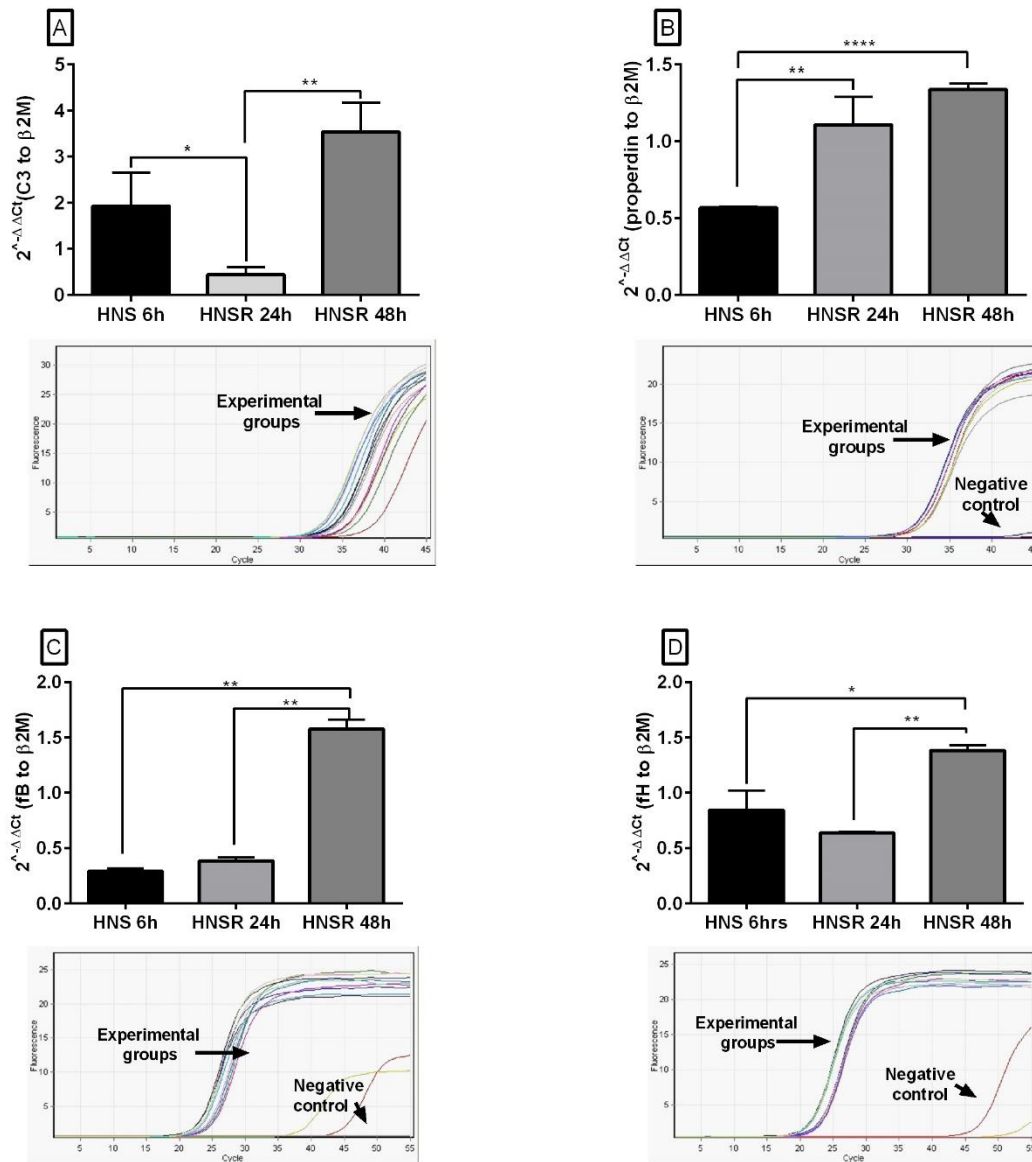


Figure 4-2: Quantitative measuring of mRNA expression of AP markers from *in vitro* renal HNSR model. C3 (A), Properdin (B), fB (C) and fH (D) mRNA expression from PTEC of human kidney (HK-2) among the three experimental groups. Results were calculated as ($2^{-\Delta\Delta Ct}$) in comparison to β_2 -M mRNA expression as endogenous control. Quantitative report of each marker showing the expression curve for experimental groups and negative controls were shown below each graph respectively; $n=3$ in duplicates, data were presented as mean \pm SD, $p(*) < 0.05$, $(**) \leq 0.01$, $(***) \leq 0.001$; HNS, hypoxia and nutrient starvation; HNSR 24h and 48h, hypoxia and nutrient starvation followed by replenishment for 24 and 48 hours respectively.

4.3.1.2 Cytokines and inflammatory markers

All three experimental groups have shown an expression of tumor necrosis factor α (TNF- α) mRNA in incremental curve. HK-2 cells stimulated with HNSR for 48h expressed TNF- α mRNA significantly higher than both HNS for 6h-treated cells ($p=0.012$) and HNSR for 24h-treated group ($p=0.015$); however the latter was insignificantly greater than HNS for 6h ($p=0.175$) (Figure 4-3 A).

Similarly, interleukin 6 (IL-6) mRNA was expressed from all stimulated groups. The greatest expression was from HNSR for 48h cells which was significantly higher than both HNSR for 24h ($p=0.0026$) and HNS for 6h ($p=0.0008$) groups. IL-6 expression from HNS for 6h was significantly less than HNSR for 24 group ($p=0.0009$) (Figure 4-3 B).

The pattern of both caspase-3 and kidney injury molecule-1 (KIM-1) mRNA expression from HK-2 cells across the *in vitro* model was the same. Caspase-3 was expressed from HNS 6h (1.735 ± 0.454) before falling (insignificantly) in HNSR 24h and ended with its maximum expression after HNSR for 48h, which was significantly higher than HNSR for 24h and HNS for 6h ($p=0.0008$ and 0.0102 respectively). Similarly, KIM-1 was abundantly expressed from HNS for 6h then fell significantly after HNSR for 24h ($p=0.013$) stimulation before elevation back (peak) after HNSR for 48h (Figure 4-3 C, D). The latter elevation was significant in comparison to HNSR for 24h ($p=0.024$) but not with HNS for 6h ($p=0.445$).

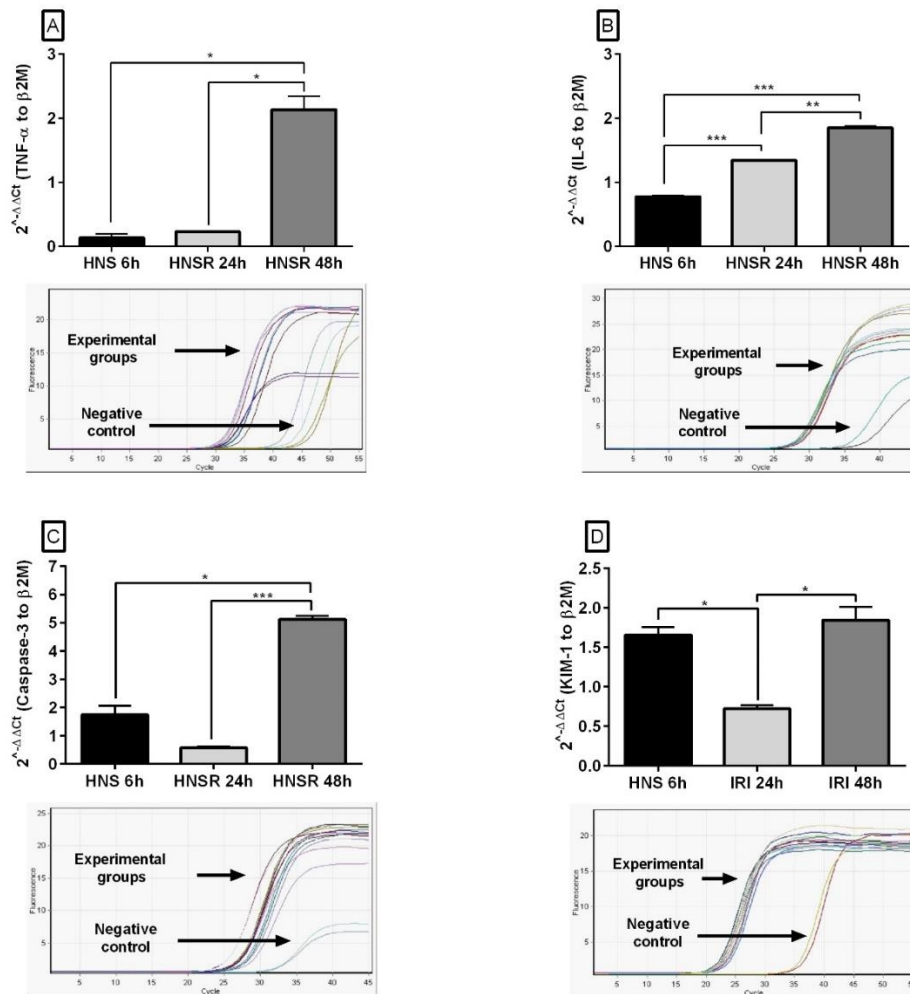


Figure 4-3: Quantitative calculation of mRNA expression of inflammatory markers from *in vitro* renal HNSR model. TNF-α (A), IL-6 (B), Caspase-3 (C) and KIM-1 (D) mRNA expression from PTEC of human kidney (HK-2). Quantitative report of each marker were shown below each graph respectively; n=3 in duplicates, data were presented as mean ± SD, $p(*) < 0.05$, $(**) \leq 0.01$, $(***) \leq 0.001$; HNS, hypoxia and nutrient starvation; HNSR 24h and 48h, hypoxia and nutrient starvation followed by replenishment for 24 and 48 hours respectively.

4.3.1.3 Hypoxia markers

Hypoxic markers were also studied in this renal HNSR *in vitro* model. Expression of tissue growth factor-β (TGF-β1) mRNA from HK-2 cells was the greatest at HNS 6h then fell significantly to the lowest at HNSR for 24h ($p=0.024$). The expression was significantly raised after HNSR for 48h in relation to HNSR for 24h ($p=0.018$) although it stayed significantly less than after HNS for 6h ($p=0.039$) (Figure 4-4A).

VCAN, also called versican, mRNA was expressed by HK-2 cells after HNS for 6h (15.14 ± 0.445) significantly higher than both after HNSR for 24h ($p=0.0005$) and HNSR for 48h ($p=0.001$) while VCAN

mRNA expression from HK-2 cells after HNSR for 24h was significantly less than HNSR for 48h ($p=0.0054$) (Figure 4-4B).

Similarly, vascular endothelial growth factor (VEGF) mRNA was expressed by HK-2 cells stimulated with HNS for 6h was higher than both HNSR for 24h and HNASR for 48h though differences were not significant ($p=0.076$ and 0.105 respectively). Meanwhile the difference between HNSR for 24h and 48h was significant ($p=0.0049$) (Figure 4-4C).

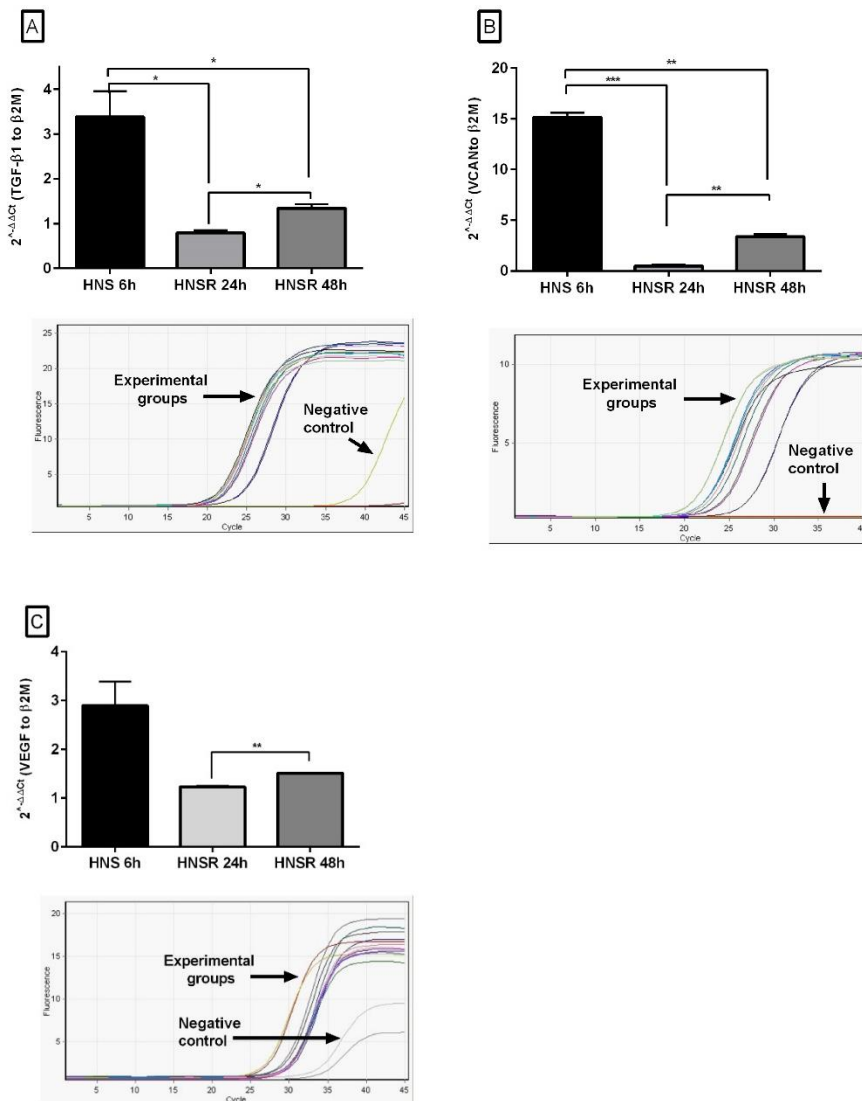


Figure 4-4: Quantitative calculation of mRNA expression of hypoxia markers from *in vitro* renal IRI model. TGF-β (A), VCAN (B), and VEGF (C) mRNA expression from PTEC of human kidney (HK-2). Results were calculated as $(2^{-\Delta\Delta Ct})$ in comparison to β2-M mRNA expression as endogenous control. Quantitative report of each marker were shown below each graph respectively; $n=3$ in duplicates, data were presented as mean \pm SD; $p(*) < 0.05$, $(**) \leq 0.01$, $(***) \leq 0.001$. HNS, hypoxia and nutrient starvation; HNSR 24h and 48h, hypoxia and nutrient starvation followed by replenishment for 24 and 48 hours respectively.

In summary, all alternative complement pathway genes investigated are most prominent at a late time point (48 h). Similarly, cytokines (IL-6) gene, inflammatory marker gene (TNF- α), tissue injury marker gene (KIM-1) as well as apoptosis marker gene (caspase-3) shows most expression after 48 h of media replacement as well. In contrast, hypoxia markers genes TGF- β , VCAN and VEGF were highest before replenishment; however, they were higher in HNSR for 48 h than for 24 h. These results pose a question about whether damage or repair processes are predominant after 48 h of media replenishment.

4.3.2 Effect of HNSR on HK-2 cell expression of cytokines and inflammatory markers proteins

After assessing the mRNA expression of different cytokines and inflammatory markers from human PTEC (HK-2) cells that were exposed to renal HNSR. Western blot assay, microarray proteome profiler (see appendix), ELISA were used to identify the type and quantity of proteins expressed from HK-2 cells stimulated with our *in vitro* renal HNSR model.

4.3.2.1 ELISA

The commercial ELISA, which was (R&D systems™, Quantikine® ELISA; Minneapolis, USA), could not detect TFF3 in the cell supernatant of any of the experimental groups of HNSR model, therefore, TFF3 was deemed to be below the detection limit of 39 pg/ml (data not shown).

Part of the results from this chapter were published in an article about causes of TFF3 release from human PTEC. The article showed that the HNSR model was a trigger to promote TFF3 protein synthesis in lysates from HK-2 cells, and this was maintained during the replenishment phase at 24 and 48 h. The article concluded that while it is known that TFF3 is regulated by HIF-1 α , HNSR can cause intracellular abundance of TFF3 in the absence of TFF3 release (Zwaini *et al*, 2016).

4.3.3 Effect of HNSR on auto-phagosome formation in HK-2 cells

In order to investigate whether HK2 cells produce auto-phagosomes in response to HNSR injury or not, electron microscope was performed. Tunicamycin, which is N-linked glycosylation inhibitor and ER stressor that causes abnormal protein assembly was used as a positive control for autophagy. The hallmark of autophagy is the formation of auto-phagosomes (Gozuacik *et al*, 2008).

In this study, the normal control did not show any auto-phagosomes (Figure 4-5 A) unlike the positive control (which was exposed to tunicamycin) in which the autophagosomes were obvious (Figure 4-5 B). Interestingly, there was no evidence of autophagy after exposing the HK-2 cells to ischemia (hypoxia and Locke's buffer) for 6 h only without reperfusion as there was not observable autophagosome (Figure 4-5 C) instead there were apoptotic cells (nuclear condensation, membrane blebbing). There were noticeable autophagosome formations after reperfusion for 24 h and 48 h (fig 9 D) which were more pronounced with signs of disintegration after 48 h (Figure 4-5 E). Images of each time point were investigated by 4 observers.

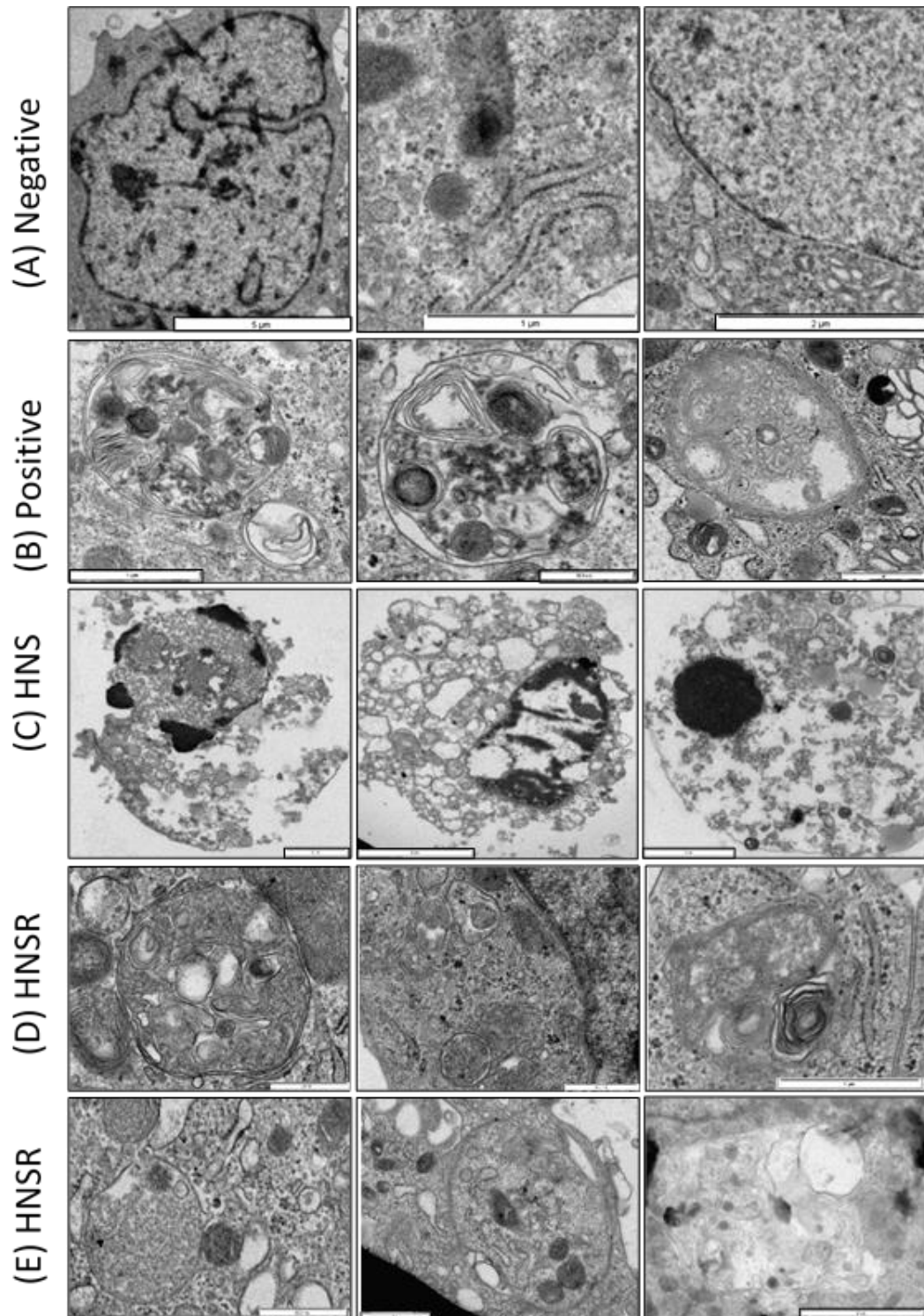


Figure 4-5: Representative transmission electron micrographs analysis (TEM) of HK-2 cells exposed to IRI model showing the autophagosome (arrow). (A) Cells at normoxia, negative control (B) Positive control (HK-2 cells treated with 0.2 μm Tunicamycin for 16 hours). (C) Ischemia for 6 h. (D) Ischemia for 6 hours followed by 24 hours replenishment. (E) Ischemia for 6 hours followed by 48 hours replenishment. Intact organelles are visible in early autophagosomes (row 4), whereas content is amorphous in late autophagosomes (row 5).

4.4 Discussion

A well-designed *in vitro* model is crucial in understanding effectively cellular responses of PTEC while studying IRI and gives a foundation to subsequent *in vivo* work or analyses therein as well (Russ, Haberstroh and Rundell, 2007; Kurian and Pemaih, 2014).

The study underlined that the conditions provoke a significant change in the mRNA expression of versican and IL-6 and that their responses are a quick, suitable control measure of the success of hypoxia (versican) and of inflammatory reaction expressed by the epithelial cells (IL-6).

The profiler documents different states of activation/stress in HK-2 cells because the expression patterns are not only distinct between conditions but certain groups of proteins show similar dynamics. The array nicely showed that while some proteins were downregulated, implying perhaps a compromised state of the cell, others were upregulated. This indicates the complexity of the reaction that was captured in the *in vitro* model, and underlined the justification to first attempt a replacement strategy of animal modelling, where a multitude of factors impact on the target cells (Schumer *et al*, 1992).

4.4.1 HK-2 response to injury

The study showed that hypoxia and nutrient starvation increased trefoil factor 3 (TFF3) abundance in lysates from HK-2 cells, which continued during the replenishment phase. At HNSR 24 hours, hypoxia-induction markers (VEGF, FABP1, CXCL16) as well as HIF-1 α were greatly increased compared to control cells; however, VEGF mRNA was higher from HNS group than replenishment ones. Other studies emphasised the pivotal role of TFF3 during both restitution where cells are migrated toward lesion site to promote healing; and regeneration through enhancing cellular differentiation and proliferation of epithelia (Hernandez *et al*, 2009; Guleng *et al*, 2012). Conversely, the opposite to other genes of TFF peptide family, TFF3 mRNA was expressed in the cortex of the kidney and TFF3 peptide is detectable in urine samples from patients with renal stone (Rinnert *et al*, 2010) and in serum of patients with chronic kidney disease stages 1-5 (Du *et al*, 2013)

In vitro studies revealed that exposing cells (gastric) to hypoxia upregulates VEGF, HIF-1, and TFF3 mRNA transcription (Hernandez *et al*, 2009; Guleng *et al*, 2012). Also,

CXCL6 gene promoter has a hypoxia-sensitive response element and is upregulated by HIF-1 in hepatocarcinoma cells (Tian *et al*, 2014) and CXCL16 was shown to be a pro-inflammatory chemokines that is produced by HK-2 cells (Poveda *et al*, 2014).

In vivo, PTEC can produce fatty Acid Binding Protein (FABP) that has been defined as a marker of hypoxic renal cell damage (Yamamoto *et al*, 2007), and CXCL 16, which is a chemokine that can mediate inflammatory cell recruitment and enhance renal injury (Poveda *et al*, 2014).

4.4.2 Autophagosome

As noticed from above results, it seems to be that apoptosis has been reported in this model where evidence of autophagy in the replenishment phase, which becomes more aggressive in 48 hours, were recorded suggesting that autophagy plays a role in protecting the PTEC from ischemia reperfusion injury. Several researches showed that autophagy could play a role in IRI (Jiang *et al*., 2010). Autophagosome could be defined as a vesicle like structure surrounded by double membrane in which sequestration of malfunctioning protein and organelles are accumulated (Suzuki *et al*., 2008). It is a way to eliminate waste material from the cell after being injured and in the same time, it could be a method of cell death. Furthermore Autophagy is a cellular sequential process involves up taking, transport to lysosome, digestion and recycling intracellular malfunctioning protein and destructive apparatus in order to achieve cellular homeostasis (Mizushima, 2007). Recently, there is a debate whether autophagy is a mechanism of cell death or a compensation step for cellular welfare. Autophagy is involved in many clinical applications such as neurodegenerative disease and ischemia reperfusion injury. In addition, there is very little known about the contribution of autophagy in pathogenesis of ischemia reperfusion injury of human kidney (Jiang *et al*., 2010).

Autophagy could play a dual effect in cellular homeostasis in response to cellular stress (specifically and in our context is HNSR injury) (Jiang *et al*., 2010). It has been found that blockade of Beclin-1 and autophagy related 5, ATG5 (the hallmark genes of autophagy) by 3-methyladenine, primes the tubular epithelial cells to hypoxia induced apoptosis. Interestingly, autophagy was not evident during ischemia itself, but it is more prominent during reperfusion. Therefore, autophagy may be regarded as a protective

mechanism in IRI of renal tubular epithelial cells. This is consistent with *in vitro* (rat) and *in vivo* (mice) studies which were done by Jiang and his colleagues in 2010 demonstrating the possibility of defensive effect of autophagy against cell injury during reperfusion phase of IRI (Jiang *et al.*, 2010).

5 Chapter five (mouse model of renal IRI and the
role of complement properdin)

5.1 Introduction

Acute kidney injury (AKI) occurs in various clinical settings, prolongs hospitalization and leads to overall mortality rate of 50% in the past 5 decades (Khajuria *et al*, 2014; Ympa *et al*, 2005). IRI is an inflammatory process that is considered as a major cause of AKI and is associated with chronic kidney disease (CKD). Renal transplantation transforms the lives of patients with end stage renal disease (ESRD). Unfortunately, different complications including IRI sometime cause the failure of renal allograft again (Hesketh *et al*, 2014). Efforts to prevent IRI compete in targeting both ischemia and reperfusion phases (Morris *et al*, 2013). Nevertheless, the exact mechanism of IRI-mediated damage is still unclear, but the activation of the complement systems has pleotropic roles in the pathogenesis of renal IRI (Leshner *et al*, 2013). More recent attention has focused on the harmful effect of complement activation, which results in more tissue damage and exacerbates renal fibrosis, during renal IRI in humans while its downregulation reduces renal injury morphologically and functionally (Danobeitia, Djamali and Fernandez, 2014).

5.1.1 Discovery and structure of properdin

Pillemer *et al.*, (1954) discovered a haemolytic activity distinct from i.e. alternative to, the classical pathway of complement activation and subsequently identified a plasma protein that was named by properdin later (Pillimer *et al*, 1954). It is glyco-oligomer of dimers, trimers, and tetramers (circulating in blood in 1: 2: 1 ratio) with each monomer being functionally active (capable of C3b binding) (Gaarkeuken *et al*, 2008; Schwaeble and Reid, 1999). The monomer has seven thrombospondin repeat type I domains (TSR0-6) and 442 amino acids subunits resulting in a molecular weight of about 53 kDa. The serum concentration is 5-25 µg/ml for humans (Cortes *et al*, 2012) but there is variability between populations (Stover *et al*, 2015). Unlike other complement components which are synthesised and secreted from liver, properdin is secreted in response to inflammatory markers from various cell types such as monocytes, T lymphocytes, granulocytes and dendritic (myeloid, Langerhans, dermal, and plasmacytoid) cells; endothelial cells release properdin secondary to trauma or shear stress (Cortes *et al*, 2012).

5.1.2 Properdin function

Complement properdin is the only positive regulator of the alternative pathway of complement activation via stabilising the C3bBb and C5 convertases (Ruseva *et al*, 2013). Interestingly, properdin showed another role after a number of researchers having reported that properdin can act as a pattern recognition molecule (Kemper and Hourcade, 2008; Xu *et al*, 2008). It is released from activated neutrophils, binds directly to apoptotic T cells *in vitro* before being engulfed by phagocytic cells (macrophage and dendritic cells) in a non-complement pathway (Kemper, Atkinson and Hourcade, 2009).

The aim from this chapter is to explore the underlying mechanism of properdin in a mouse model of *in vivo* renal IRI; its association with caspase-3, in the context of immunity, inflammation, apoptosis, autophagy, proliferation and repair, at both early and later stage of renal IRI. Lastly, the effect of modulating properdin on these injuries, in order to validate new mechanistic insights and benefit diagnosis and intervention.

5.2 Materials and methods

5.2.1 Experimental design

An *in vivo* renal IRI model was established in mice, which would allow when using congenic properdin-deficient (P^{KO}) and wild type (WT) mice to assess the role of properdin. Both age and sex matched C57BL/6 wild type (WT) and properdin knockout (P^{KO}) mice were exposed to renal ischemia by bilateral clamping of pedicles for 30 minutes followed by perfusion for 72 hrs, and the model was summarised in (Figure 5-1). 3 (1 WT and 2 P^{KO}) mice were excluded from the study due to their prompt deterioration postoperatively. The experiment was terminated after about 24 hrs for 4 (3 WT and 1 P^{KO}) mice, after 48 hrs for another 3 (1 WT and 2 P^{KO}) animals, and one (P^{KO}) after 72 h. Thereafter, mice were classified into WT sham (n=4), P^{KO} sham (n=5), WT IRI (n=9) and P^{KO} IRI (n=7). There was no significant difference in survival rate among the four experimental groups ($p > 0.05$), although that all sham mice survived and the survival rate of P^{KO} mice exposed to surgery was less than that of wild type (Figure 5-2).

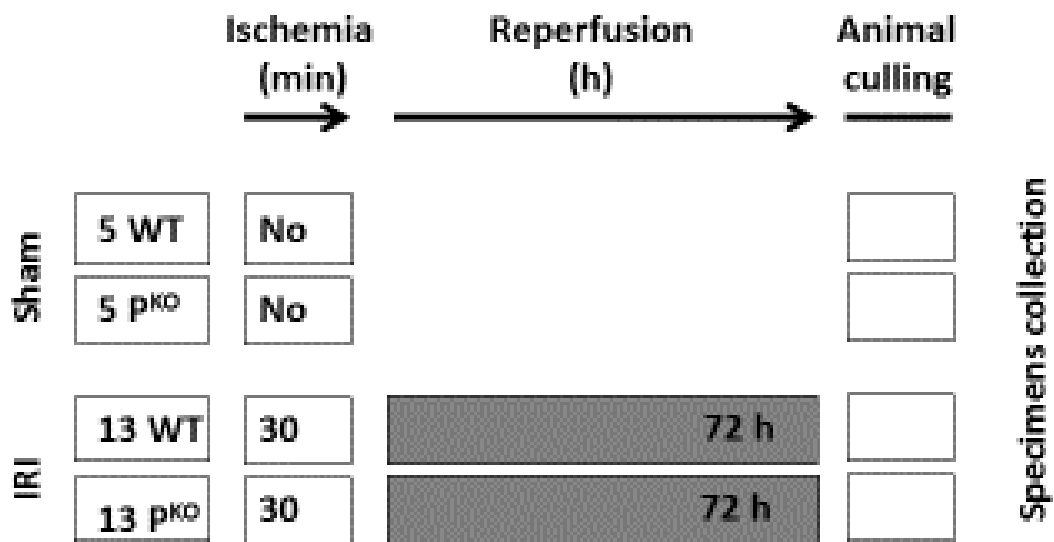


Figure 5-1: Experimental design of in-vivo murine renal IRI. Ischemia for 30 minutes was induced followed by reperfusion for 72 hrs. Wild type (WT), properdin knockout (PKO), Ischemia reperfusion injury (IRI).

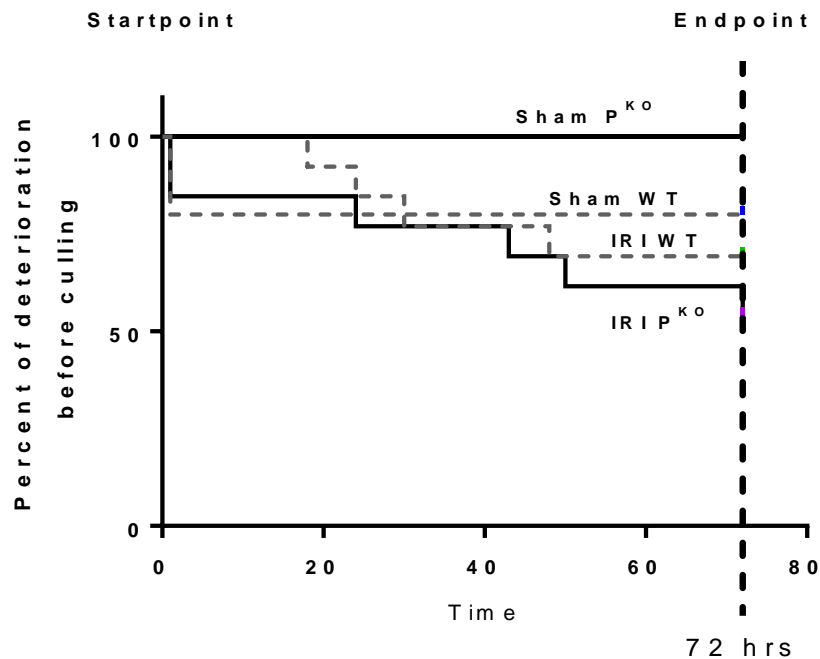


Figure 5-2 Deterioration rate of mice before culling using Kaplan–Meier. The period was measured from time of surgery until termination with animal euthanasia at 72 hrs post operation. WT: wild mice, P^{KO}: properdin knockout, IRI: ischemia-reperfusion injury

5.2.2 Induction of renal IRI

Male properdin knockout (P^{KO}) and congenic C57BL/6 wild type (WT) mice (8-12 weeks old) were taken from a colony maintained at University of Leicester (Stover et al., 2008). Mice were housed in groups in ventilated cages at 21°C, 50% humidity, with 12/12 h light/dark cycle, and had *ad libitum* access to food (TestDiet, 5LF2) and tap water. The *in vivo* ischemia reperfusion model was conducted in the surgical unit in the Central Research Facility at University of Leicester under the auspices of the Named Veterinary Surgeon. The procedure was performed in accordance with regulations of the Home Office (Scientific Procedure Act 1986, UK) and ethical approval of the institution (PPL70/8169, PIL IA536CDE7), and optimised according to a previous study and published paper (Wei and Dong, 2012).

Mice were weighed, anaesthetised (by inhalation of oxygen and 5% isoflurane), and, in supine position under inhalation of oxygen and 2% isoflurane, prepared for surgery by clipping fur and wiping with 70% alcohol swab. Analgesics (10 mg/kg Carprofen (Carprieve®, 50 mg/ml), 0.1mg/kg Buprenorphine (Vetergesic®)) were subcutaneously injected. Mice were positioned on a heated mat.

This was followed by local subcutaneous injection of 40 µl 1:10 diluted bupivacaine hydrochloride (Marcaine®, 2.5 mg/ml) at wound site (maximum dose is 2 mg/kg). Thereafter, the mouse was turned to its side, approaching kidney in the retroperitoneal space through oblique loin incision. Then the renal pedicle was isolated where both renal artery and vein were clamped using a non-traumatic microvascular clips. Occlusion was confirmed by observing patched blanching of the entire kidney surface and change of colour of the kidney from red to dark purple after several minutes (Figure 5-3). After 30 minutes, the clip was released from the pedicle permitting renal blood flow restoration (kidneys were observed for a further five minutes to ensure colour change) which represented the beginning of the reperfusion phase. The kidney was returned back to its position, the incision was sutured in two layers (Yang *et al*, 2013), then the mouse was turned on its other side and the procedure repeated contralaterally after injection of Marcaine as before. Before suturing this last incision, 1 ml saline (pre-warmed at 37°C) was administered into the abdomen to counteract dehydration.

Postoperatively, after supervised recovery from anaesthesia, mice were transferred to their holding area with some food available on cage floor. General appearance was closely monitored (starry coat, hunched, piloerection) and mouse grimace scale, a 0-2 facial expression- based scoring system to assess pain in animals which based on monitoring five criteria (orbital tightening, nose bulge, cheek bulge, ear position, and whisker change) (Sotocinal *et al*, 2011), was used as well. Second dose of both drugs carprofen and buprenorphine were given next day, and some time they need another dose the day after.

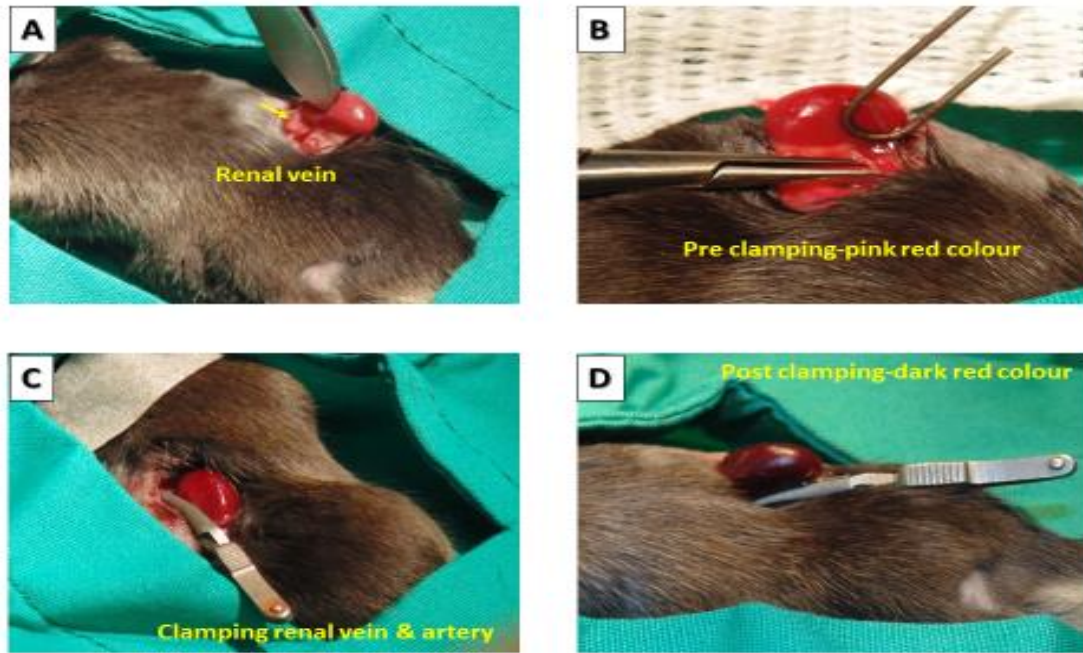


Figure 5-3 Surgical operation for renal IRI induction in mouse. A loin incision and renal pedicle recognition (A), the pink red kidney before clamping (B), clamping of both renal artery and vein for 30 minutes (C) and the dark red colour of the kidney due to ischemia (D).

5.2.3 Harvesting kidneys and tissue collection

All procedures were performed as described in project licence (PPL) where the perfusion stage stopped at 72 h. At this time point, mice were bled by cardiac puncture under terminal anaesthesia (inhalation of oxygen and 5% isoflurane) and drops of urine were collected.

In order to harvest kidneys, the abdominal wall was opened through midline laparotomy followed by dissection of internal viscera reaching the retroperitoneal space for careful harvesting of both right and left kidneys intact from their surrounding fascia after dissecting renal artery, vein and ureter. Thereafter, each kidney was divided into 4 pieces; the first one was preserved in CellStor Pot (03704206) containing 4% formaldehyde (w/v) in normal saline overnight at room temperature. It was sent to pathology laboratory in Royal infirmery hospital/Leicester (LRI) in order to prepare paraffin-embedded tissue and slides for haematoxylin (H) and eosin (E) staining.

The remaining three pieces were transferred to cryotube and stored in liquid nitrogen after few tiny pieces approximately 1-2 mm³ were cut (from second one) and kept in fixative for electron microscope assessment (2% v/v formaldehyde, 2.5% v/v glutaraldehyde, 100

μ M sodium cacodylate and 2 mM calcium chloride) for 24 h at 4 °C. These pieces were transferred to buffer containing only 0.1 mM sodium cacodylate and 2 mM calcium chloride at 4 °C until they were processed. A small portion was cut from the third quarter and was stored in an optimum cutting temperature (O.C.T ®) compound (Thermo Scientific, IL, USA), a glycol- based cryoprotective embedding medium, before freezing in liquid nitrogen. In the meantime, the collected blood was centrifuged at 10000 g for 10 minutes at room temperature to separate serum, which was transferred to a clean sterile 1.5 ml reaction tube and stored at -20 °C.

5.2.4 Tissue homogenisation

Soluble proteins were isolated from renal tissues of the four experimental groups using FastPrep-24™ 5G (MP biomedical, CA, USA) homogeniser. Firstly, a piece of the renal tissue was mixed with 50 mM/l tris/ acetate buffer (TA) in a ratio of 9 μ l/mg of renal tissue. Then, the mixture was processed by the homogeniser for 20 second and was kept on ice for 5 minutes. The process was repeated three times before centrifuging the contents at 13000 rpm at 4°C for 10 minutes (Fresco17, Thermo Scientific, IL, USA). The supernatant was transferred to another tube to be frozen at -20°C.

5.2.5 Total protein quantification

Determination the relative differences in protein levels among experimental samples in ELISA (in western blot as well) requires loading same amounts of protein in each well in which later considers as reference for normalising protein of interest (Eaton *et al*, 2013).

According to the manufacturer's standard microplate protocol, quantification of total protein was measured using Coomassie Plus™ assay kit (Thermo Scientific, IL, USA). First, albumin (BSA) standard was prepared via serial dilution to get standard samples with concentrations of 2000, 1500, 1000, 750, 500, 250, 125, 25 μ g/ml in addition to blank (0 μ g/ml). Next, a 10 μ l of each standard and unknown sample and 300 μ l of Coomassie Plus Reagent were loaded in microplate well and mixed on plate shaker for 30 seconds. The plate was incubated at room temperature for 10 minutes. Absorbance was measured at 595 nm with plate reader (Biorad, iMark).

Absorbance of standard samples were corrected by blank absorbance subtraction. Linear standard curve were created ($r= 0.943$) via plotting the corrected absorbance of standards against their concentrations. Concentrations of unknown samples were calculated via interpolating their absorbance against standard curve. Graphpad Prism version 6.04 (GraphPad Software, San Diego California USA).

5.2.6 Evaluating renal function

5.2.6.1 Blood urea nitrogen (BUN)

Protein catabolism leads to formation of toxic ammonia, which the body discards by excreting its final product (urea) through the kidneys. The measurement of blood urea nitrogen (BUN) is an indicator of kidney function. Bioassay System creatinine assay kit is designed to calculate urea directly in serum. The principle of its action is through formation of chromogenic reagent that forms a coloured complex with urea and the intensity of the colour, measured at 492nm, is linearly proportional to serum urea concentration. According to the manufacturer protocol (QuantiChrome™ Creatinine Assay Kit (DIUR-500); BioAssay Systems, Hayward, USA), 5 µl of diluted serum (1:10), standard 50mg/dl and water (blank) was transferred to the Maxisorp 96-well plate in duplicate. A premixed of 100 µl working reagent A and 100µl reagent B were added to each well before being incubated for 20 minutes at room temperature. The optical density (OD) was measured at 492 nm in a plate reader TECAN™ infinite f50 V7.0. The data were exported to excel file and the blood urea nitrogen concentration was calculated according to the formula:

$$[\text{BUN}(\text{simple})] = [\text{OD}(\text{Sample}) - \text{OD}(\text{Blank A})] / [\text{OD}(\text{STD}) - \text{OD}(\text{Blank B})] * \text{Dilution factor} * [\text{STD}]$$

5.2.6.2 Serum creatinine

Measuring serum creatinine is routinely carried out to evaluate kidney function. It gives a rough guide of renal creatinine $\text{C}_4\text{H}_7\text{N}_3\text{O}$, which results from degradation of an endogenous amino acid named creatine $\text{C}_4\text{N}_9\text{H}_3\text{O}_2$ that plays role in energy preservation. Renal glomeruli filter creatinine and excrete it intact with urine (Sana *et al*, 2008; Leelahavanichkul *et al*, 2014). Bioassay System creatinine assay kit is designed to assess

creatinine from blood serum directly without any pre-treatment. This assay depends mainly on colorimetric analysis of different intensities of the coloured creatinine complex (red) which is measured at 492 nm. According to the manufacturer protocol (QuantiChrome™Creatinine Assay Kit (DICT-500); BioAssay Systems, Hayward, USA), 30 µl of diluted serum (1:10) and standard (2 mg/dl) was transferred in duplicate into Maxisorp 96-well plate. 200 µl of equal amount of pre-mixed solution working reagent A and reagent B was added to each well. Then, the optical density was read immediately (OD₀) and after 5 minutes (OD₅). The data were exported to Excel file and the concentration was calculated as follow:

$$\text{Serum creatinine}_{(\text{Sample})} = \frac{[\text{OD}_{(\text{Sample}5)} - \text{OD}_{(\text{Sample}0)}]}{[\text{OD}_{(\text{STD}5)} - \text{OD}_{(\text{Sample} \text{ STD}0)}]} * [\text{STD}](\text{mg/dl}) * \text{Dilution factor.}$$

5.2.7 Microscopic features

Gross examination of retrieved kidneys from different study groups was performed to record shape, patterns of outer layer or cortex (pink) and inner layer or medulla (dark) as well as macroscopic differences between kidneys.

5.2.7.1 Haematoxylin and eosin (H and E) stain and Periodic Acid-Schiff (PAS) stain

After preparing H&E stained slides from all kidneys, 12 fields from cortical areas sides were examined using light microscope (Olympus, Japan) under magnification power of 40 X objectives by two independent observers to evaluate the histological changes before scoring them. Wilcoxon matched-pairs signed rank test was used to assess the interobserver error. There was no significant difference between data of the two observers ($p > 0.05$) with successful pairing. Scoring was ranged from 1-4 based on six microscopic morphologic observations: interstitial oedema (widening of the space between the proximal tubular epithelium), interstitial infiltration, dilatation of tubular lumen, detachment of cells inside the lumen, protein cast and tubular vacuolisation. Grade 1 is representing histologic changes <25%, 2= 25%-50%, 3= 50%-75% and 4= >75% respectively. The mean of the 12 fields for both right and left kidney of each mouse were

calculated (Yang *et al*, 2006). Additionally, the slides were stained with PAS to detect the brush border of proximal renal tubules (Yabuki *et al*, 2001).

Mitotic figure counting during the metaphase of cellular meiosis is an indicator for cell proliferation or division (Cireşan *et al*, 2013). During metaphase, the chromosomes are aligned in the middle of nucleus forming metaphase plate by the help of spindle fibres (Bill Grimes, Rick Hallick, Ken Williams, 2004).

5.2.7.2 Transmission electron microscopy (TEM)

Transmission electronic microscope (TEM) was used to assess the cellular changes of the renal proximal tubules of murine kidneys which were harvested from 4 mice (2 WT and 2 P^{KO}) exposed for our *in vivo* IRI model. Ten fields at the same magnification power were chosen to be examined for each kidney before calculating the summation of the average. The criteria for scoring were depending on the appearant health of the mitochondria, brush border, state of nucleus, presence of autophagosome and cytoplasmic vacuole. For each criterion, findings were scored from 0-3 based on observed degrees of damages. Regarding mitochondrial status; 0=healthy one; 1 and 2= abnormal swollen mitochondria observed in less than 50% and 50%-75% respectively; 3= totally damaged mitochondria. Observing normal brush border was scored 0; 1 (and 2) = damage of less than 50% (and 50%- 75%) of brush border; 3= total absence of brush border. Scoring of nucleus condition was 0= normal nucleus; 1= swollen nucleus; 2= more damage to the nucleus in terms of irregular indentations of the nuclear membrane and condensation of chromatin materials; 3= damaged nucleus. Meanwhile, presence of no or scanty autophagosome (the same for vacuoles) equalled to 0; 1 (and 2) when autophagosome (vacuoles) observed over less than 50% (and 50%- 75%) of the field; 3= autophagosome (vacuoles as well) distributed all over the field and/ or presence of lysosomal autophagosome.

5.2.8 Investigating the underlying mechanism of injury during renal IRI

In order to detect the possible molecular mechanism that resulted in the deterioration in renal structure and function of both wild and properdin knockout mice after renal IRI, production of various proteins were measured in both serum and tissue homogenates of murine kidneys using several techniques.

5.2.8.1 Western immunoblotting

In this chapter, it was used to detect protein synthesis in renal tissue homogenate of P^{KO} mice and their WT mates that were exposed to surgical IRI as well as their correspondent sham.

5.2.8.1.1 Principle

It is a commonly used analytic technique, which enables researchers to identify the nature or the amount semi- quantitatively of proteins that were separated and then were transferred to a membrane. An electrical current is used to mobilise protein from the gel and adhere to the membrane where it is stained with antibody (Mahmood and Yang, 2012).

5.2.8.1.2 Sample preparation and gel electrophoresis

The percentage of the resolving gel was varied depending on the molecular weight of the protein of interest. Both resolving and stacking gels (Table 5-1 and Table 5-2Table 5-2) were prepared according to the laboratory protocol. 20 µg of measured protein was added after mixing it with 2X Laemmli sample buffer (Biorad, Hertfordshire, UK) containing 5% mercaptoethanol (Sigma-Aldrich, MO, USA) in a ratio of 1:1 leaving a lane (well) for 10 µl of precision plus protein dual colour standard ladder (Biorad) to assess the relative molecular weight of each protein. Later, the gel was run first at 90 V for half hour then at 120 volts for 1.5 hrs using 1 X SDS running buffer (Table 5-3). Finally, the gel was ready to be blotted.

Table 5-1 Reagents and quantities were used to prepare different percentages of resolving gel (10 ml). SDS: Sodium dodecyl sulphate, APS: Ammonium per sulphate, TEMED: Tetramethylethylenediamine.

Material	8%	10%	12%	15%
Water	4.6 ml	4 ml	3.3 ml	2.3 ml
30% Acrylamide: bisacrylamide (37.5:1)	2.7 ml	3.3 ml	4 ml	5 ml
10% SDS	0.1 ml	0.1 ml	0.1 ml	0.1 ml
1.5 M tris (pH: 8.8)	2.5 ml	2.5	2.5	2.5 ml
10% APS	0.1 ml	0.1 ml	0.1 ml	0.1 ml
TEMED	0.006 ml	0.006 ml	0.004 ml	0.004 ml

Table 5-2 A Regents and quantities used to prepare 5m of 5% stacking gel. SDS: Sodium dodecyl sulphate, APS: Ammonium per sulphate, TEMED:Tetramethylethylenediamine.

Material	Amount
Water	3.4 ml
30% acrylamide	0.83 ml
1 M tris pH 6.8	0.63 ml
10% SDS	0.05 ml
10% APS	0.05 ml
TEMED	5 µl

Table 5-3 Reagents and quantities were used to prepare 10 X of SDS running buffer. SDS: Sodium dodecyl sulphate.

Material	Amount
Tris base (Thermo Fisher scientific, USA)	30 g
Glycine (Thermo Fisher scientific, EC 200-272-2)	144 g
Sodium Dodecyl Sulphate (Fisher scientific)	10 g
Distilled water	Up to 1 L

5.2.8.1.3 Electro blotting

It is used to transfer the protein from the gel and adsorb it into the membrane. In the first place, the transfer stack or sandwich is prepared. It is composed from gel and polyvinylidene fluoride membrane (PVDF) and surrounded by filter (Whatman) papers and sponge. More importantly, to arrange them in a correct way (the gel is toward cathode while the membrane toward anode) as the electrical current is move in a perpendicular line from cathode (black) to anode (red) to permit protein to move from gel to membrane. Then, in the presence of 1 X blotting buffer (Table 5-4), blotting was done either at 100V at room temperature using ice pack or overnight at 15V at 4 °C depending on the optimum condition for the individual protein (Figure 5-4).

Table 5-4 Reagents and quantities were used to prepare 10 X of transfer (blotting) buffer.

Material	Amount
Tris base (Fisher scientific)	30 g
Glycine (Fisher scientific)	144 g
Distilled water	Up to 1 L

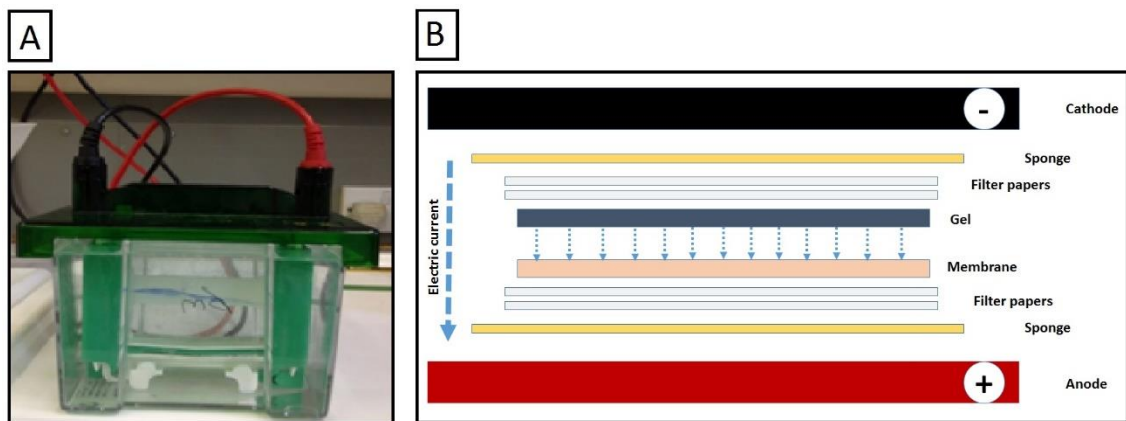


Figure 5-4 Western blot from (Bio-Rad). The running of the gel inside the tank (A) and the arrangements of the cassette between the two poles during electro-blotting (B).

5.2.8.1.4 Probing with primary and secondary antibodies

The membrane is immersed in a blocking buffer (5% non-fat milk in TBS-T) for 1 h to block the empty surface of the membrane, which is characterised by high affinity to protein binding. This will reduce the interference through preventing the unwanted binding of the detecting antibodies. Afterward, incubation with various antibodies (Table 5-5 Table 4-1) diluted in 1X TBS Tween 20 was performed. Normalisation of target protein were performed against endogenous loading control (β -actin).

Table 5-5 Primary and secondary antibodies were used in western blot.

Name of protein	primary antibodies	Origin	Dilution	Secondary antibody	Origin	Dilution	Band size
NFkB	Rabbit NFkB polyclonal antibody	Santa Cruz	1: 500	Swine Antirabbit	Dako Denmark	1 3000	65 kDa
HMGB-1	Rabbit HMGB1 polyclonal antibody	Proteintech/ Uourpe	1: 500	ChemoMate En Vision detection kit HRB – rabbit / mouse labelled polymer	Dako Denmark	1 40	29 kDa
PCNA	Monoclonal Mouse Anti-Proliferation cell nuclear antigen	Dako Denmark	1: 1000			1 40	36 kDa
TGF- β	Rabbit anti - TGF- β	Santa Cruz	1: 500			1 40	12.5,25 kDa
Caspase 3	Rabbit polyclonal antibody	Santa Cruz	1: 400			1 40	32 the procaspase 3,17 and 11 the cleavage product
β -actin	Monoclonal Mouse Anti-ACTB Antibody	Abcam	1: 5000			1 40	42 kDa

The probing with primary antibody was performed either at room temperature for 2 h or overnight at 4 °C depending on the optimization of each antibody used. Then, washing with 0.05% (v/v) Tween 20 (Sigma-Aldrich, MO, USA) in TBS. Thereafter, probing with horseradish peroxidase (HRP)-conjugated secondary antibody for 1 h was performed at room temperature and finally was washed.

5.2.8.1.5 Detection

The end step, detection and staining, was done by using Pierce® ECL Western Blotting Substrate (Thermo Scientific, USA). A mixture of enhanced-chemiluminescence (ECL) reagent (1 ml reagent A or luminol and 1ml reagent B) was applied to the membrane; wrapped in plastic sheet protector; and exposed to film (Bio-Max Light, Sigma-Aldrich, MO, USA) in a light-tight cassette until antibody-reactive bands were detected (exposure: 1-30 minutes). Next, the film was immersed in developer solution for 1 minute, washed by water, immersed in fixer solution (1 minute), washed with water again and left to dry. An alternative, easier and faster, method for detection has been used later where after ECL applying to the membrane, detection was performed using ChemiDoc™ Imaging quantitatively using rolling disk method to subtract background and lane profile to assess a three-dimension quantity. Both lanes and bands were firstly detected before measuring volume (density) for both protein of interest and endogenous protein for each sample (Figure 5-5). Data of both target proteins and endogenous controls (β - actin) were exported to Microsoft excel for further analysis where, at the beginning, the correction factor for each sample was calculated by dividing the average density of endogenous control by individual sample. Then, the normalised density of each time point where measured by multiplying the density (volume) of protein of interest by its correction factor (see equation below). Finally, ratio of experiment to its control was considered in our figures.

Normalised density of Protein of interest= Protein of interest (Volume) X [Mean density of endogenous control (Volume)/ Density of specific endogenous control (Volume)]

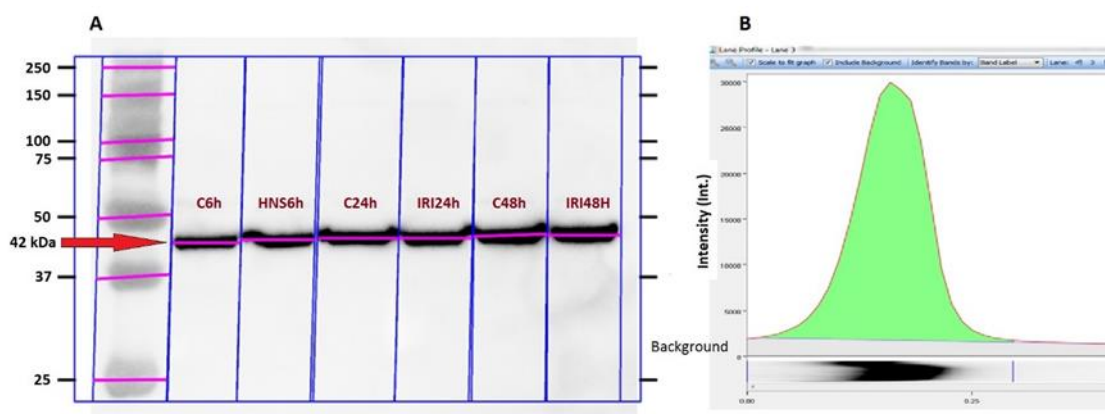


Figure 5-5 Method illustration of semi quantitative calculation of protein expression from different HNSR model groups by detecting lanes and bands (A) and measuring density (volume) (B) using V.5 Image Lab software from Bio-Rad.

5.2.8.2 Enzyme Linked Immunosorbent Assay (ELISA)

Both sera and tissue homogenates of WT and P^{KO} mice were taken (5.2.3) to measure quantitatively multiple inflammatory and complement proteins production in the four mice groups. While the principles of sandwich ELISA were elaborated before (chapter 3), the technique followed the manufacturers' guidance as detailed below.

A. Serum complement factor C5a

Initially, the protocol used in Dimitrova et al., 2010 (arthritis model in properdin-deficient mouse) was followed to measure C5a in serum (Dimitrova *et al.*, 2010). Because of technical difficulties to quantify the amount of complement, a commercial ELISA assay kit was used to measure natural and recombinant mouse complement component C5a; following the manufacturer's protocol (Duo Set® ELISA, DY2150, R and D Systems, Minneapolis, USA). Firstly, 100 µl of 4µg/ml capture antibody rat anti-mouse C5a (842652) was coated on the maxisorp 96-well plate and incubated overnight at room temperature. Then, washing was done using 0.05% (v/v) Tween ® 20 in PBS twice for three washes. The plate was blocked using 300 µl of 1% (w/v) BSA for 1 hour. After washing three times again, a 100 µl serially diluted standards (recombinant mouse C5a,

842654) (1000 pg/ml) were added to the samples and incubated for 2 hours. Optimisation was performed with different dilution factors (1:200, 1:400 and 1:1000) in order to get the sample on the standard curve. Washing was repeated and 100 µl of the detection antibody (biotinylated goat anti-mouse C5a, 842653) (200 ng/ml) was added for 2 hours. Another wash was done and 100 µl of the streptavidin –HRP (890803) (1:200) was added for 20 minutes in dark. Last washing was done before adding the 100 µl of substrate solution TMB [made from dissolving a TMB tablet (Sigma-Aldrich, MO, USA) in phosphate buffer] and it was incubated for 20 minutes. Sulphuric acid (2 N) as a stopping solution (50 µl) was added before the two reading at 450 nm and 570 nm was done in the Varioscan. The OD of the standard was calculated and subtracted from the 0 reading and concentrations were calculated via interpolating absorbance against a four parameter logistic (4-PL) curve fit standard curve using Graph Pad PRISM 6.07 analysis software (GraphPad Software, La Jolla, California, USA).

B. Serum chemokine CXCL16

Sandwich ELISA also was used to measure natural and recombinant mouse CXCL16 in accordance with manufacturer's protocol (abcam®, USA). Firstly, multiple standards (recombinant mouse CXCL16) were prepared via serial dilution (80 pg/ml – 1.25 pg/ml) and zero and samples were diluted 1:100. A 100 µl from standards and the samples were added to antibody- coated plate containing capture antibody specific for mouse CXCL16 and were incubated at room temperature for 2.5 hours. Plate was washed four times with 1 X wash solution, 100 µl the detection antibody (biotinylated CXCL16) was added and incubated for 1 hour and washing was repeated. A 100 µl streptavidin –HRP was added for 45 minutes in dark with gentle shaking. Lastly, washing was done before adding the 100 µl substrate solution TMB and the plate was incubated for 30 minutes with gentle shaking. A stopping solution (50 µl) was added before reading at 450 nm.

C. Serum monocyte chemoattractant protein-1 (MCP-1/ CCL2)

According to the manufacturer's protocol (Mouse CCL2 ELISA Ready-SET-GO, eBioscience, 88-7391, USA), 100 µl capture antibody (Pre-titrated, purified antibody) in 1 X coating buffer was added to a 96-well plate of Coat Corning Costar and incubated

overnight at 4 °C. Next day, the wells were aspirated and washed (3 times for about 1 minute each) with washing buffer (0.05% tween-20 in 1 X PBS) before commencing blocking by adding 200 µl of 1 X ELISA/ELISPOT diluent for 1.5 hour at room temperature and followed by single washing with wash buffer. The maximum standard was prepared (2000 pg/ml) first performed and followed by adding 100 µl of serial diluted standards (maximum 2000 pg/ml) and the diluted serum(1:50) and incubated overnight at 4 C⁰ to maximize the sensitivity. Washing 3 times, then 100 µl of detection antibody for 1 hour at room temperature. After that, another 3 time washes, then 100 µl of Avidin-HRP was added and incubated for 30 minutes, another 5 times wash done with soaking time 2 minutes ,then 100 µl of 1 x TMB was added and incubated or 15 minutes at room teprature then 50 µl stop solution added. Then the plate was read at 450 nm with correction wavelength at 570 nm at the Varioskan machine.

D. Serum C5b-9

Sandwich ELISA kit (TCC C5b-9, CUSABIO, Hubei, China) was used for quantitative determination of mouse terminal complement complex (C5b-9) in serum. According to the manufacturer's guidance, all reagents were prepared, samples were diluted 1: 200, and standards were prepared via serial dilution (50, 25, 12.5, 6.25, 3.12, 1.56, 0.78 ng/ml) and 0 standard. 100µl of standard and sample well were added for their correspondent well and covered with the adhesive strip. After 2 hours incubation at 37°C, the liquid of each well was aspirated without washing. Next, 100µl of Biotin-antibody (1x) was added to each well and was covered with a new adhesive strip. Then, well was incubated for 1 hour at 37°C before aspirating each well and washing, which was performed by filling the well with 200µl of wash buffer for 2 minutes, three times. 100µl of HRP-avidin (1x) was added to each before covering the microtiter plate with a new adhesive strip and incubating it for 1 hour at 37°C. The aspiration/wash process was repeated 5 time as before and 90µl of TMB substrate was added to each well. Another incubation for 15-30 minutes at 37°C was conducted and 50µl of stop solution was added to each well. The optical density of each well was measured within 5 minutes, using a microplate reader set to 450 nm and wavelength correction at 570 nm.

E. MCP-1/ CCL2 in tissue homogenate

Monocyte chemoattractant protein 1 (MCP-1) which also known as CCL2 was measured in tissue homogenate of mice using mouse MCP-1/CCL2 ELISA Kit (Sigma-Aldrich, MO, USA). Other studies revealed a wide range of MCP-1 level from more than 1000 pg/ μ g of total protein in a mouse model of haemolytic uremic syndrome (Keepers, Gross and Obrig, 2007) to less than 5 pg/mg in murine IRI (Stroo *et al*, 2015). Therefore, the total protein loading was firstly optimised with different amount (500,250,100 and 50 μ g). The result showed a loading protein of 20 μ g was best amount that fit in the middle of the standard curve. According to the manufacturer's protocol guidance, all reagents were brought to room temperature (18-25 $^{\circ}$ C) and before preparing appropriate dilutions of the materials. The standard stock was prepared in a concentration of 2000 pg/ml and from this; a serial dilutions were pipetted to have 666.7, 222.2, 74.07, 24.69, 8.23, 2.74, and 0 pg/ml. 100 μ l of both sample and standard were added to a ready MCP-1 antibody-coated plate in duplicate for 2.5 h at room temperature. Solutions were discarded and plate was washed four times with 300 μ l of 1X buffer. 100 μ l of 1X biotinylated detection antibody was added to each well and incubated for 1 h at room temperature with slight shaking. Thereafter, the solution was aspirated and the plate was washed 4 times as above before adding 100 μ l HRP streptavidin reagent for 45 minutes at room temperature as well. Again, the solution was removed and washing was performed as before. Finally, a 100 μ l of ELISA colorimetric TMB solution was added, incubated at room temperature in dark place for 30 minutes, 50 μ l stop solution was added and read by plate reader (Biorad, iMark) instantly at 450 nm.

A best fit (second polynomial) standard curve ($r= 0.9991$) was created using Graph Pad PRISM, 6.07 (GraphPad Software, La Jolla, California, USA). Absorbance of samples were subtracted from background then were interpolated against standard curve to calculate MCP-1 concentrations.

F. Lectin pathway activity

Functional ELISA for LP was done following Kotimaa *et al*, 2015, using polyclonal antiserum (pAb) against recombinant mouse C9 (MyBioSource; San Diego, USA) with serum dilution of 1:4 in BVB⁺⁺ buffer (Veronal buffered Saline/0.5 mM MgCl₂/2 mM

CaCl₂/0.05% Tween 20/1% BSA, pH 7.5) on plates coated with mannan (*Saccharomyces cerevisiae*, Sigma-Aldrich, MO, USA).

According to the manufacturer's guidance and our laboratory optimisation (H. Al-Aridhee, PhD project), each well was coated with 100 µl 10µg/ml anti mannan antibody after dilution 1:1000 in CB buffer (100mM Na₂CO₃/NaHCO₃, pH 9.6) and plate was incubated for 16 h at 4⁰C. Then, each well was washed 3X5 minutes with 200 µl PT buffer (PBS/0.05% Tween 20) before blocking each well with 150 µl PB buffer (PBS/1% BSA) for 90 minutes at 37⁰C. The wells were washed again with 200 µl/ well of PT buffer 3X5 minutes before adding 100 µl of diluted serum (1:4) for each well and the plate was incubated for 1 h at 37⁰C. The plate was washed for the third time with 200 µl/ well of PT buffer 3X5 minutes; 100 µl of 0.2 mg/ml of 1:200 polyclonal rabbit complement component 9 (C9) antibody was added to each well and was incubated for 1 h at 37⁰C. Thereafter, fourth run of wash with 200 µl/ well of PT 3X5 minutes was performed and 100 µl of 1mg/ml polyclonal swine anti-rabbit HRP antibody (with 1:200 dilution) was added for each well before 1 h incubation at 37⁰C. Last wash with 200 µl/ well of PT 3X5 minutes was done before adding 100 µl of coloured substrate (TMB) for each well and left at room temperature for 5-10 minutes. 50 µl of stop solution was added to each well and optical densities were read using ELISA reader at 450 nm wavelength.

G. Serum interleukin 6 (IL-6)

A sandwich ELISA was used to detect IL-6 (Mini ELISA Development Kit 900-M50, PeproTech, London, UK). The capture antibody of antigen-affinity purified rabbit anti-IL6 was diluted with PBS to a concentration of 1µg/ml. 100µl of this solution were added to each well of ELISA microplates (NuncMaxiSorp) which was sealed and left overnight. After preparation of all the solutions and reconstitution of the component of the experiment at room temperature, the well was aspirated and washed four times using 300 µl of washing buffer per well. Then, 300 µl block buffer [1% (w/v) BSA-PBS] was added for 1 hour followed by washing four times again. After that, the standard was diluted from 4 ng/ml to zero in diluent. The mouse serum was diluted in ratio of 1:10 and was mixed by vortexing. Immediately, the standard/samples (100µl) were added and were incubated

for 2 hours. Next, aspiration and washing was done again to be followed by adding 100µl detection biotinylated antibody (antigen-affinity purified rabbit anti-m16) in a concentration of 0.5 µg/ml for 2 hours. ABTS Chromogen / substrate (Invetrogen from Thermo Fischer Scientific, USA) (100 µl) was added after aspiration of the excess detection antibody and washing. The colour development was monitored each 10 minutes for a maximum of 1 hour until the zero reading of standard was 0.1. The reading was done with Elisa reader (Biorad, iMark) at 405nm with wavelength correction at 655nm.

5.2.8.3 In Situ End Labelling for the detection of Apoptotic Cells

The principle of this assay is terminal deoxynucleotidyl transferase dUTP nick end labeling (TUNEL) assay where DNA fragmentation is detected by enzymatically labelling the free 3' OH terminal with modified nucleotides to examine the presence of apoptosis. These DNA ends are characteristically localised in morphologically distinguishable nuclei and apoptotic bodies.

A. Method

The tissues were fixed in 10% neutral buffered formalin before embedding them in paraffin and cut to 4 µm thickness. ApopTag Peroxidase *In Situ* Apoptosis Detection Kit (Millipore, S7100) was used to label fragmented nuclear DNA *in situ* with digoxigenin-deoxyuridine (dUTP) by terminal deoxynucleotidyl transferase (TdT). According to the manufacturer's protocol, the slides were deparaffinised by washing with Xylene 2 x 5 minutes each, then another two washes with 100% IMS (5 minutes each), followed by another washing in 70% (v/v) IMS. Lastly wash with water twice, 2 minutes each and then the slides were put in PBS until they were ready. After that, the tissue was pre-treated by applying freshly diluted Proteinase K (20µg/ml) to the specimen for 10 minutes at room temperature and the specimen was washed with distilled water twice for 2 minutes each. Quenching of endogenous peroxidase was done with 3% (v/v) hydrogen peroxide for 5 minutes at room temperature. Washing with PBS twice (5 minutes) was done. Then excess of liquid was tapped and was blotted carefully. After that, Equilibration buffer was applied directly on the slides for 10 seconds. Again excess of liquid was blotted and the working strength TdT enzyme was applied for 1 hour at room temperature. Then the reaction was stopped by adding working strength stop/wash buffer for 10 minutes.

Then Anti-digoxigenin conjugate was added and was incubated for 30 minutes at room temperature. After washing, Peroxidase substrate 3-amino-9-ethylcarbazole was added for 10-15 minutes at room temperature. Thereafter, rinsing with distilled water and PBS were performed and the slides were counter-stained with haematoxylin solution for 2-4 min followed by washing with water and mounting with glycerol. Finally, 20 fields were examined under 400 magnification power of Olympus light microscope.

5.2.9 Statistics

Data interpretation, standard curve, nonlinear regression and interpolation (for ELISA) were calculated using Microsoft Excel ® 2010 and GraphPad Prism ® 6.07. Data were presented as mean \pm SEM. ANOVA and Tukey's multiple comparison tests were used for analysing unpaired parametric data while Kruskal-Wallis and Dunn's multiple comparison tests were used for comparing nonparametric results. Student unpaired t-test was used for single comparison of parametric data while Mann-Whitney test was used for non-parametric ones. Data was described as significant when p value was < 0.05 .

5.3 Results

The typical change observed after 72 h post operatively (pale colour cortex of kidneys in contrast to the red colour cortex of sham kidneys) were considered as an evidence to confirm the existence of IRI in this animal model (Figure 5-6).

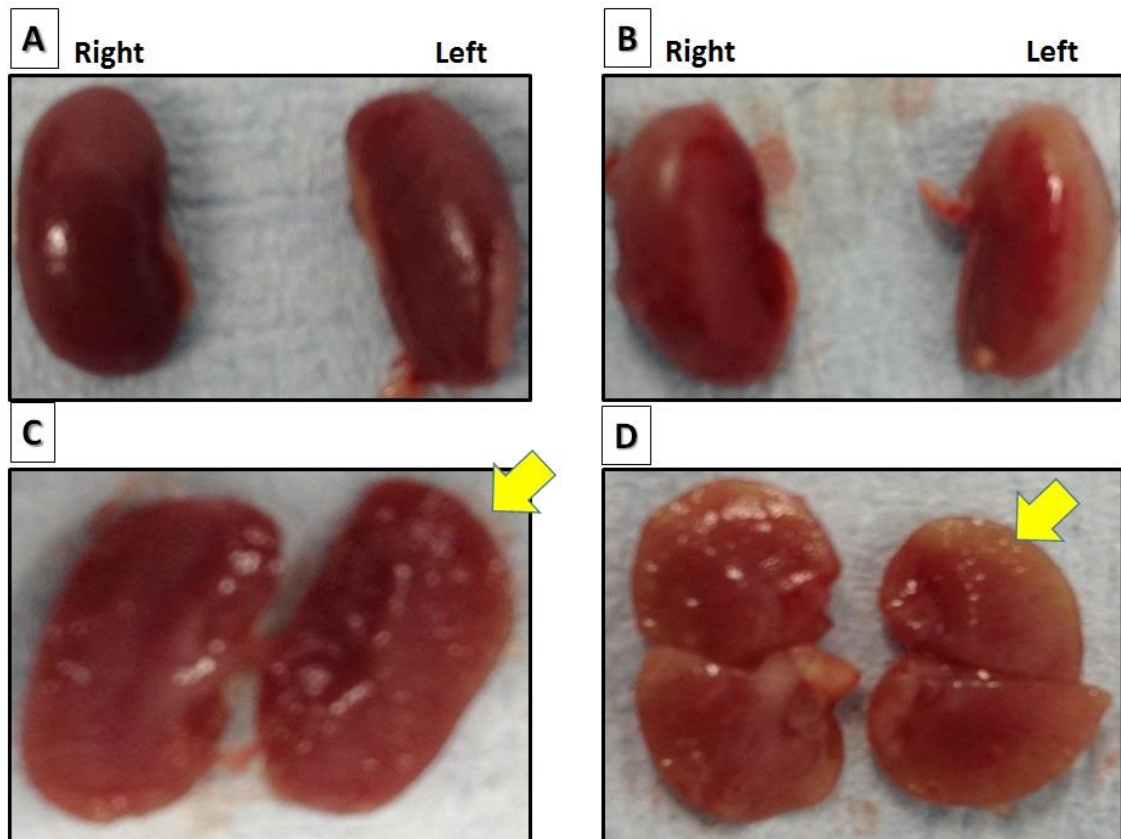


Figure 5-6: Macroscopic pictures of normal and damaged kidney. Intact right and left kidneys with red external surface from sham control (A) comparing with pale colour from IRI group (B). Sagittal section through kidney shows red cortex in sham mouse (C) and pale cortex in IRI mouse (D).

5.3.1 Renal function

The first set of questions aimed to evaluate the influence of IRI *per se* on function of murine kidney as well as the effect of complement properdin. It can be seen from the data in (Figure 5-7 A) that both IRI groups (WT and P^{KO}) reported higher BUN than their corresponding shams. What was interesting in this data was that properdin-deficient mice that exposed to IRI showed significant rising of BUN in relation with WT one ($p= 0.03$).

Similarly, serum creatinine levels (Figure 5-7 B) were more in IRI groups (WT and P^{KO}) with IRI than sham mice and P^{KO} mice with IRI had significant higher serum creatinine than WT mice with IRI ($p= 0.046$).

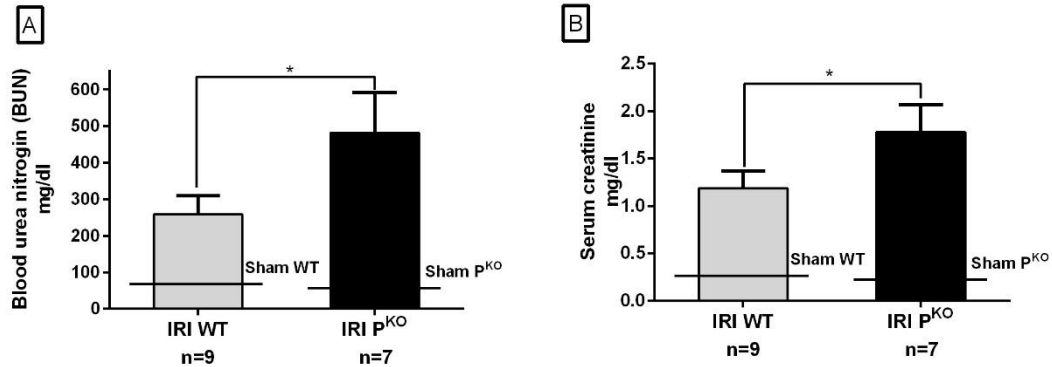


Figure 5-7 Renal function of the four experimental groups. Blood urea nitrogen (BUN) (A) and serum creatinine (B). Data was in triplicates and presented as mean \pm SEM p (*) < 0.05, IRI: ischemia reperfusion injury; P^{KO}: properdin knockout mice; WT: wild type

5.3.2 Microscopic feature

The results obtained from the preliminary analysis of histopathological scoring for H and E stain slides of murine kidneys revealed that both IRI (WT and P^{KO}) groups had more histological changes in comparison with shams. The results, as seen in Figure 5-8 E, indicated significantly higher histopathological score in P^{KO} mice with IRI than WT mice ($p= 0.023$).

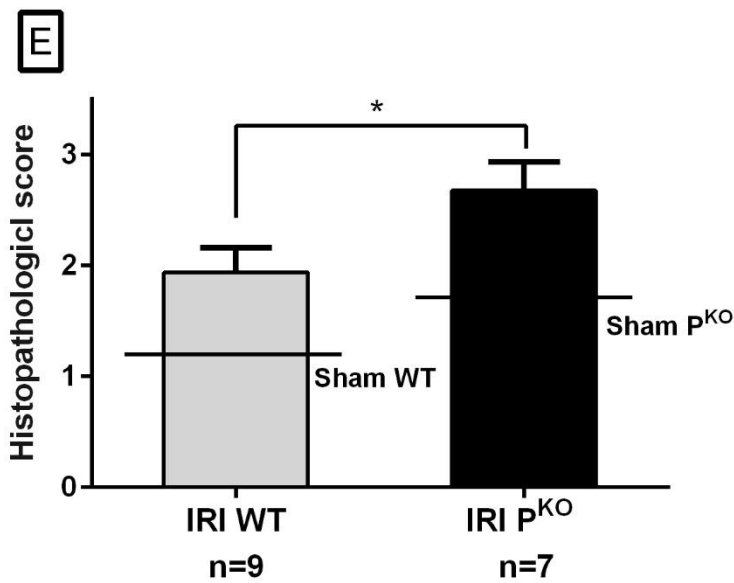
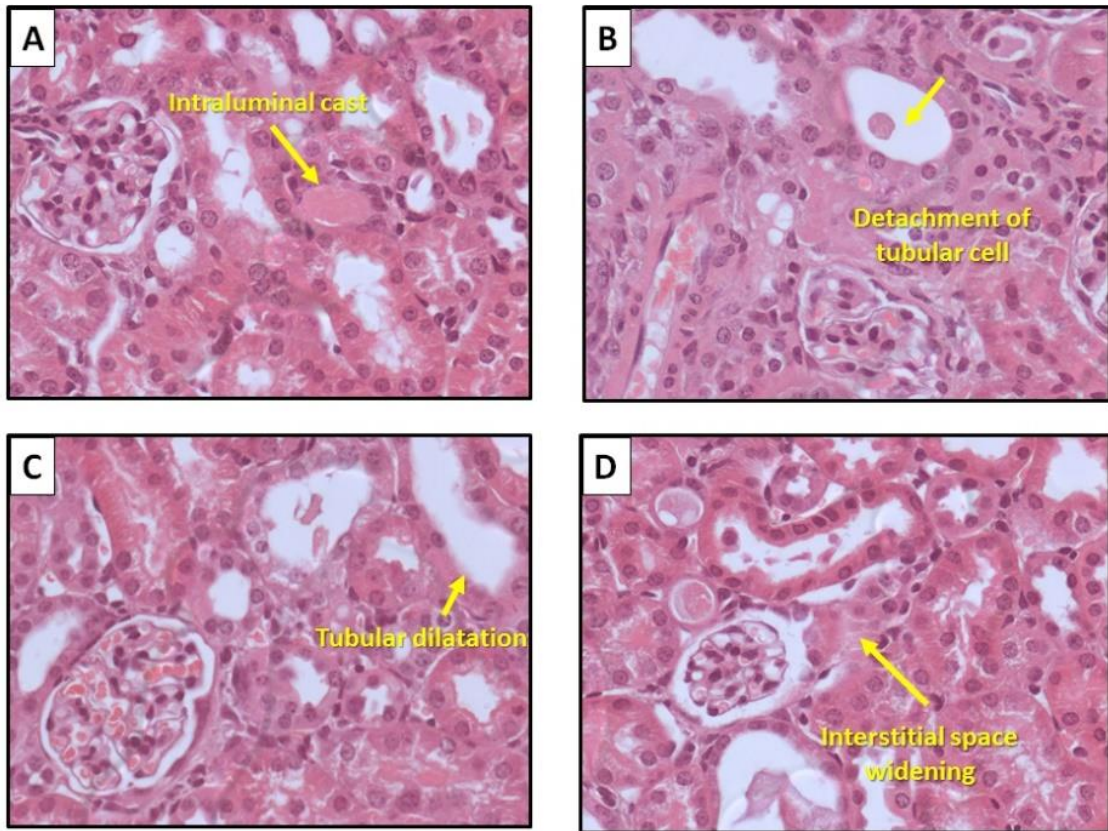


Figure 5-8: H and E stain of renal tissue of mice. Multiple sections for kidney show tissue injury due to IRI. There is intraluminal cast accumulation (A), detachment of tubular cell (B), tubular dilatation (C) and interstitial space widening (D). 40 X (Image-Pro plus 7, Micropublisher 5.0 RTV). There was significant elevation in histopathological injury in IRI groups. Slides were examined by two independent observers and data was presented as mean \pm SEM. p (*) < 0.05. IRI: ischemia reperfusion injury; P^{KO}: properdin knockout mice; WT: wild type.

These results were supported by PAS stain findings where brush border, a characteristic of proximal tubular epithelium, was less pronounced in IRI groups but not in sham control (Figure 5-9) but there was no obvious difference between the genotype.

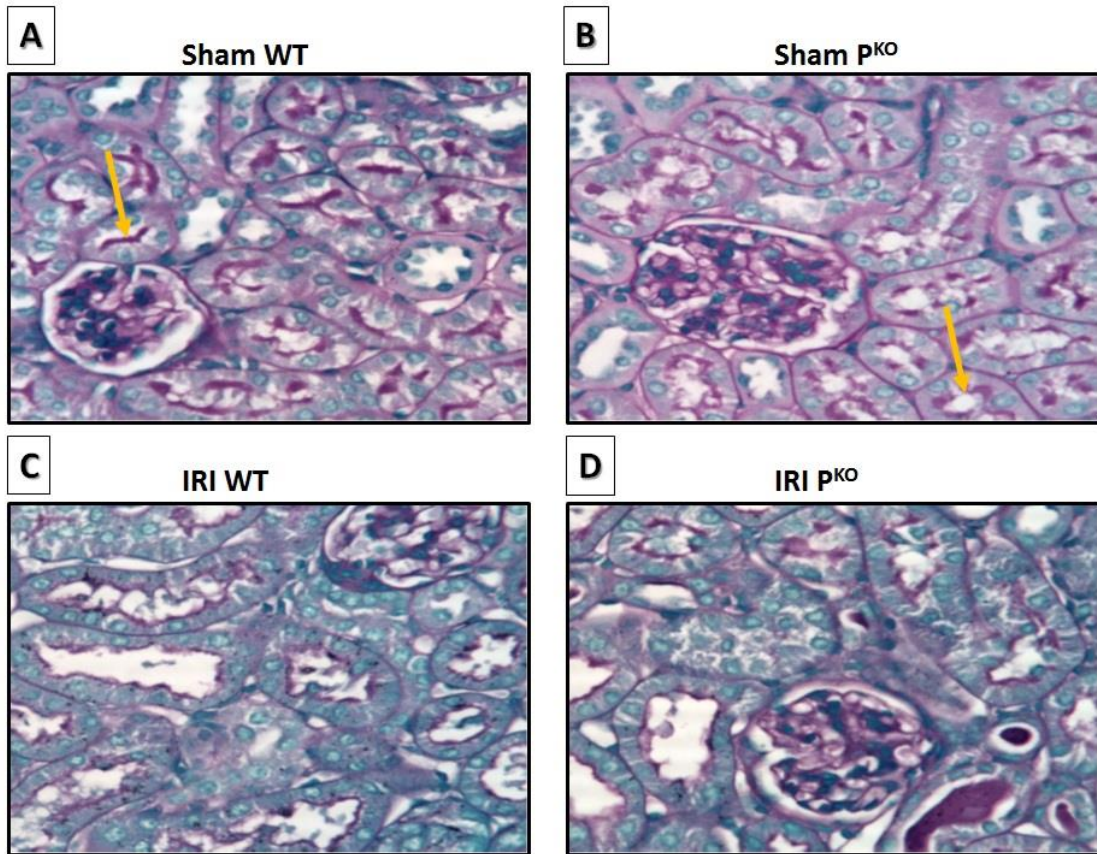


Figure 5-9: PAS stain of kidney. Under light microscope X 100, a violet stain indicates PAS positivity of brush border of renal proximal tubules particularly basement membrane (arrows) in kidneys from sham mice (A, B) in comparison with absence in IRI groups (C, D).

Similarly, mitotic figure counting, revealed more mitotic figures in IRI than sham in both WT ($p > 0.05$) and P^{KO} mice ($p = 0.04$). The mean mitotic figures in sham groups (wild and P^{KO}) was the same (0.1) while IRI P^{KO} group was double that of the IRI WT (3.4 vs 1.7; $p > 0.05$) (Figure 5-10).

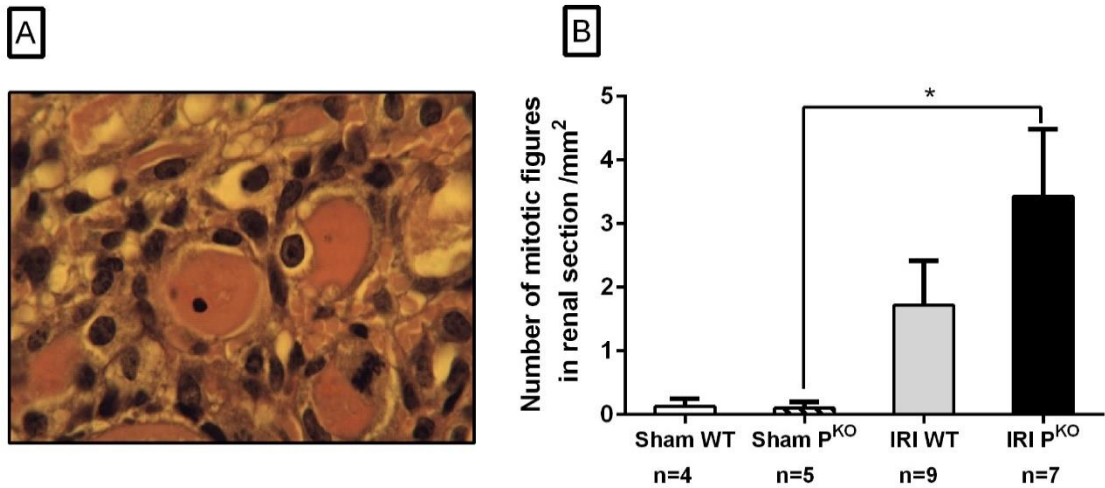


Figure 5-10: Mitotic figure. Mitotic figures were counted using light microscope X40 oil objective in slides from kidney. Arrow indicates chromosome aligned in metaphase (A). The mean of right and left kidneys were calculated and the mean of kidneys from each groups were presented in graph (B). p (*) < 0.05. IRI: ischemia reperfusion injury; P^{KO}: properdin knockout mice; WT: wild type.

Furthermore, ultrastructure analysis of kidneys using TEM supported the injurious effect of IRI in both WT and P^{KO} mice (Figure 5-11).

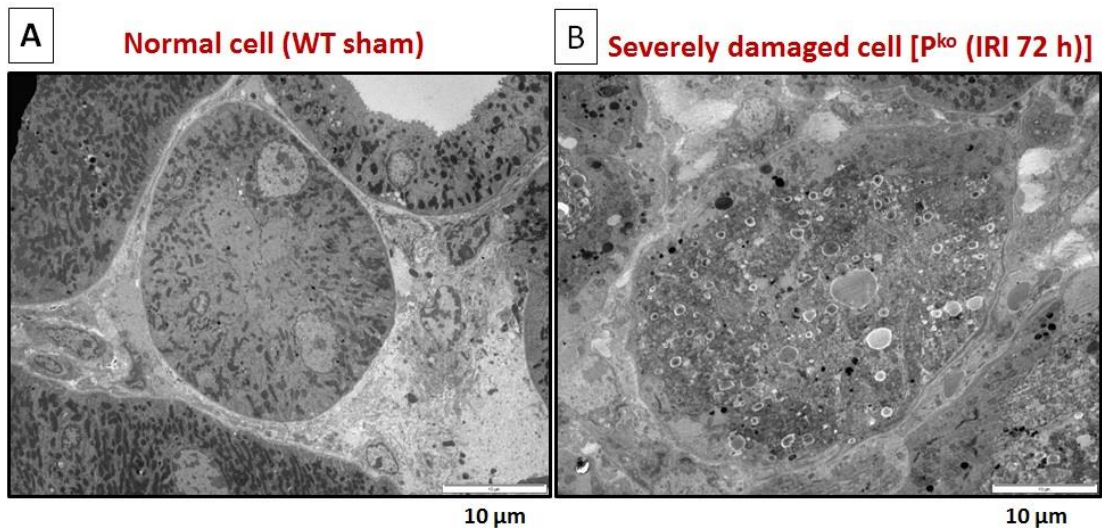


Figure 5-11 Transmission electron microscope (TEM). Normal cell (A) and severely damaged one after exposure to IRI: dissolved architecture, unclear nuclei, and presence of vacuoles (B). The criteria for TEM scoring based on the wellbeing of the mitochondria, brush border, state of nucleus, presence of auto phagosome and cytoplasmic vacuole. For each criterion, findings were scored from 0-3 based on observed degrees of damages.

5.3.3 The underlying mechanism

The next set of analyses examined molecular signalling due to renal IRI and the impact of properdin deficiency in an attempt to understand the underlying mechanisms behind functional and structural injurious changes that have been observed.

5.3.3.1 Western Blot

Protein production of multiple inflammatory (NF- κ B, HMGB-1 and caspase-3) and proliferative marker (PCNA) were measured from renal tissue homogenate of the four experimental groups, using western blot analysis.

To start with, nuclear factor NF- κ B protein (around 65 kDa) was investigated. It is a transcriptional protein with a pro-inflammatory role and is expressed in renal tissue (podocytes, tubular endothelial cells and vascular endothelial cells) due to upregulation of various inflammatory markers (such as IL-1 β , IL-6 and TNF- α) during renal IRI (Yan *et al*, 2015; Sanz *et al*, 2010). Although results were statistically not significant ($p > 0.05$), both wild and properdin- deficient mice with renal IRI produced more NF- κ B protein in comparison to sham mice (Figure 5-12).

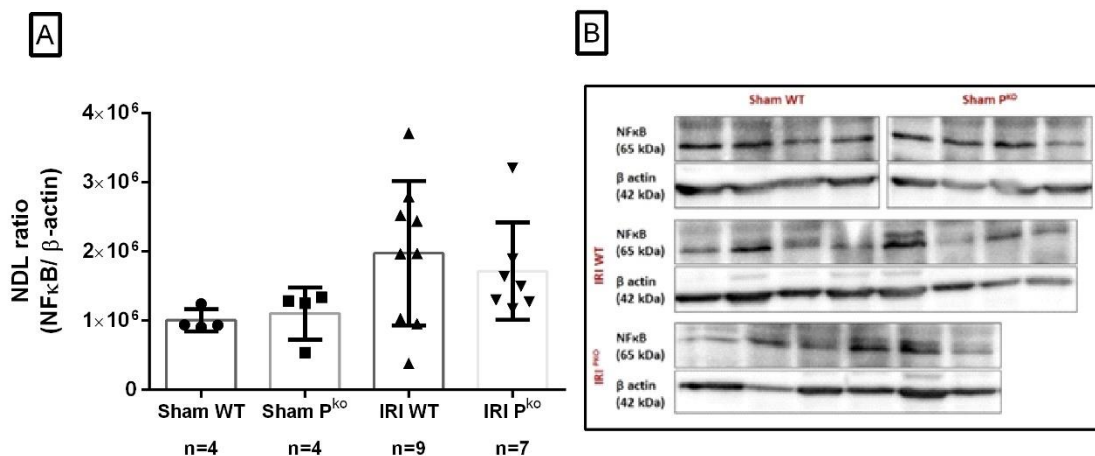


Figure 5-12 Densitometry (A) and western blot (B) of NF- κ B against β -actin. NF- κ B protein were measured from renal tissue homogenate of wild and properdin- deficient mice exposed to renal IRI. Data was presented as mean \pm SEM and p (*) < 0.05 . IRI: ischemia reperfusion injury; P^{KO}: properdin knockout mice; WT: wild type; NDL: normalised densitometry of loading control.

From the data in Figure 5-13, it is apparent that wild-type mice with renal IRI as well as properdin deficient littermate produced more high mobility group box 1 (HMGB-1) protein (29 kDa) compared to sham mice ($p > 0.05$, 0.018 respectively). Additionally, the P^{KO} mice that had exposed to renal IRI showed greater HMGB-1 protein than WT mice ($p = 0.049$). HMGB-1, which is a non-histone nuclear protein that belongs to the damage-associated molecular patterns (DAMPs) family, is translocated to outside cells secondary to cell injury resulting in an inflammatory activity via stimulating innate immune cells (such as PMN) via binding to Toll-like receptor (TLR) (Wu *et al*, 2010).

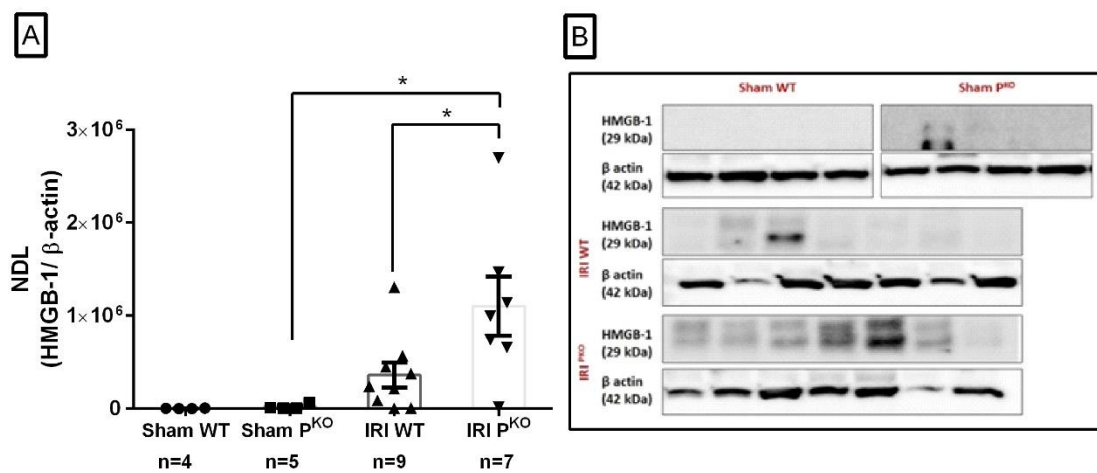


Figure 5-13 Densitometry (A) and western blot (B) of HMGB-1 against β -actin. HMGB-1 protein were measured from renal tissue homogenate of wild and properdin-deficient mice exposed to renal IRI. Data was presented as mean \pm SEM and p (*) < 0.05 . IRI: ischemia reperfusion injury; P^{KO} : properdin knockout mice; WT: wild type; NDL: normalised densitometry of loading control.

The results, as shown in Figure 5-14, indicated that both wild and P^{KO} mice, which suffered from renal IRI, produced more cleaved products (17 kDa) of pro-caspase-3 protein (32 kDa) than sham mice; moreover, caspase-3 synthesis was significantly higher in P^{KO} mice with IRI than wild-type group ($p = 0.017$).

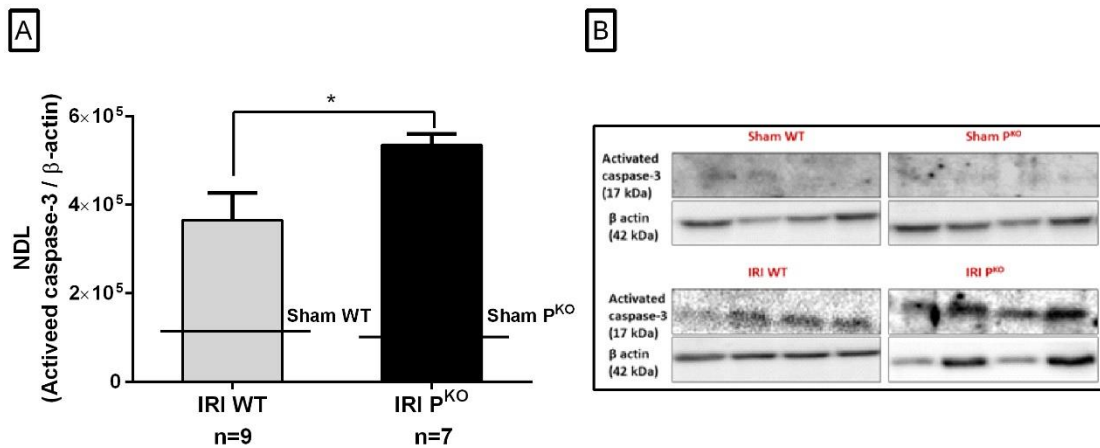


Figure 5-14 Densitometry (A) and western blot (B) of caspase-3 against β -actin. Caspase-3 protein fragment (17 kDa) was measured from renal tissue homogenate of wild and properdin-deficient mice exposed to renal IRI. Data was presented as mean \pm SEM and p (*) < 0.05 . IRI: ischemia reperfusion injury; P^{KO}: properdin knockout mice; WT: wild type; NDNL: normalised densitometry of loading control.

Finally, it can be seen from the data in Figure 5-15, proliferating cell nuclear antigen (PCNA) protein (36 kDa) was expressed abundantly from both IRI, wild-type and P^{KO}, groups in comparison with sham mice ($p = 0.003$ and < 0.0001 respectively). Moreover, PCNA was greater, although not significant, in P^{KO} mice with renal IRI than WT group ($p > 0.05$).

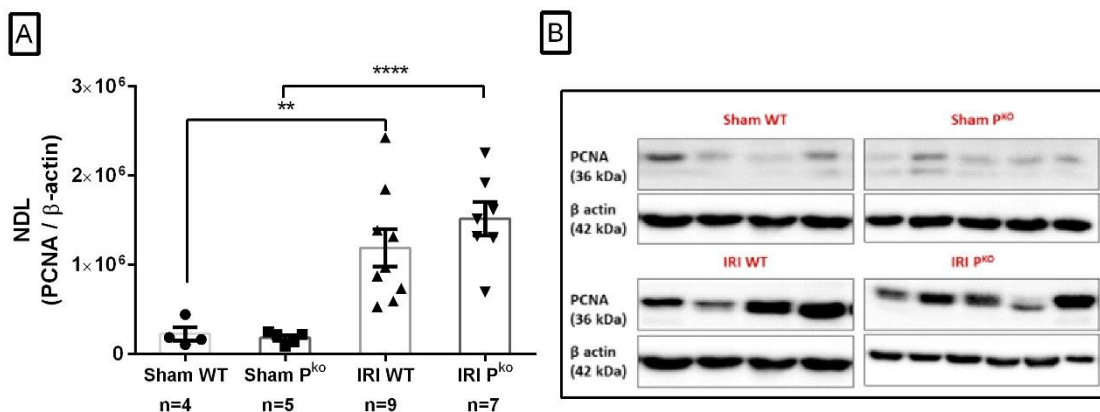


Figure 5-15 Densitometry and western blot of PCNA against β -actin. PCNA protein was measured from renal tissue homogenate of wild and properdin-deficient mice exposed to renal IRI. Data was presented as mean \pm SEM and p (**) < 0.01 , (****) < 0.0001 . IRI: ischemia reperfusion injury; P^{KO}: properdin knockout mice; WT: wild type; NDNL: normalised densitometry of loading control.

5.3.3.2 ELISA

ELISA was used to assess serum level of IL-6, a cytokine marker of epithelial cell damage (Stadnyk, 1994) and CXCL16, a chemokine, was characterised as a sensitive marker of PTEC stress *in vitro* (Zwaini *et al*, 2016). Furthermore, complement C5a (a byproduct of complement activation) and C5b-9 (the end-product of complement activation) also named membrane attack complex, MAC) were investigated in serum as they were described as promoters for renal IRI (Zhou *et al*, 2000; Peng *et al*, 2012).

From the graph in Figure 5-16, data revealed more interleukin 6 (IL-6) release, although not significant, in serum of wild-type mice with renal IRI than sham ($p > 0.05$). A similar relationship, but significant, was found between operative and sham P^{KO} mice ($p = 0.017$) while there was no significant difference between wild-type and P^{KO} mice, which were exposed to renal IRI ($p > 0.05$).

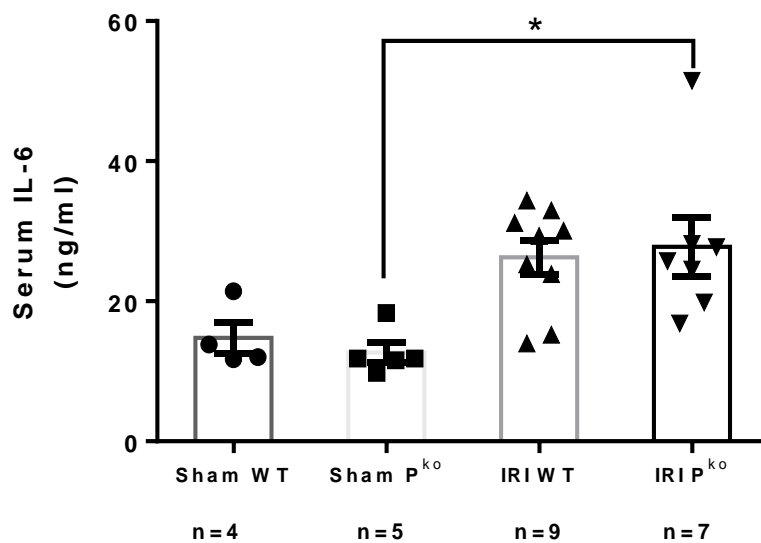


Figure 5-16 IL-6 in serum of mice. IL-6 was measured in murine serum of both wild and PKO mice that have been exposed to renal IRI and compared with sham groups using ELISA. Data were shown as mean \pm SEM; p was considered to be significant (*) < 0.05 . IRI: ischemia reperfusion injury; P^{KO}: properdin knockout mice; WT: wild type.

Despite there being no significant difference in serum CXCL-16 between wild-type and properdin-deficient mice with renal IRI ($p > 0.05$), results found more serum CXCL-16 in surgical (WT and P^{KO}) groups than sham ($p > 0.05$ and 0.047 respectively) (Figure 5-17).

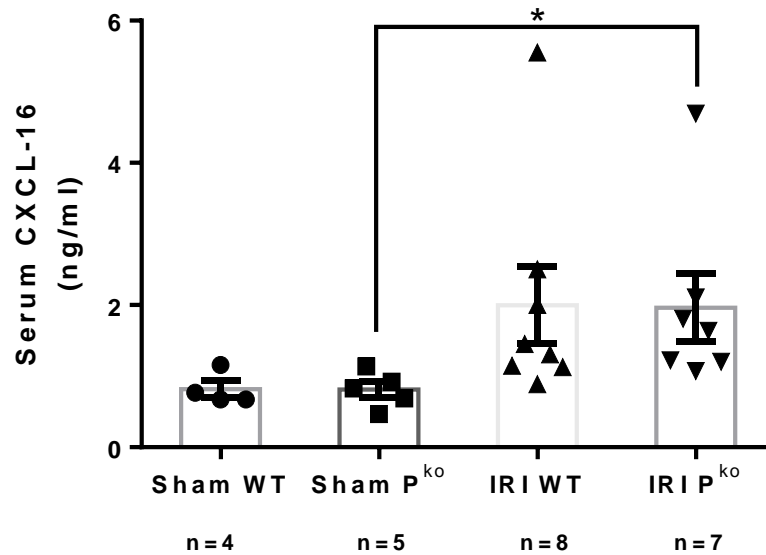


Figure 5-17 CXCL-16 in serum of mice. CXCL-16 was measured in murine serum of both wild and PKO mice that have been exposed to renal IRI and compared with sham groups using ELISA. Data were shown as mean \pm SEM; p was considered to be significant (*) < 0.05 . IRI: ischemia reperfusion injury; P^{KO} : properdin knockout mice; WT: wild type.

Similarly, it can be seen from the data in Figure 5-15 A, that complement by-product, C5a, was present abundantly in murine serum of both IRI, wild and P^{KO} , groups in comparison with sham mice. However, 5 results (3 Wild IRI and 2 PKO IRI) were excluded because they were higher than the maximum limit of the kit despite 1:1000 dilution. Moreover, C5a was less, although not significantly, in P^{KO} mice with renal IRI that WT group ($p > 0.05$). Although results were statistically not significant ($p > 0.05$), both wild-type and properdin-deficient mice with renal IRI produced less C5ab-9 in comparison to sham mice; nonetheless, it was higher in wild than P^{KO} in both sham and surgical groups (Figure 5-18 B). However, there was a significant reverse relation between C5a and C5b-9 release in sera of the four experiment groups ($r = -0.98$; $p = 0.015$) (Figure 5-18 C).

Functional ELISA results for of C9 in serum of experimental mice revealed elevation but not significant among wild type mice exposed to IRI in comparison to sham mates ($p > 0.05$), while it was significant in relation with properdin deficient ones ($p= 0.008$). This indicated that MBL pathway was stimulated due to IRI in wild-type mice but not in properdin deficient ones (Figure 5-18 D).

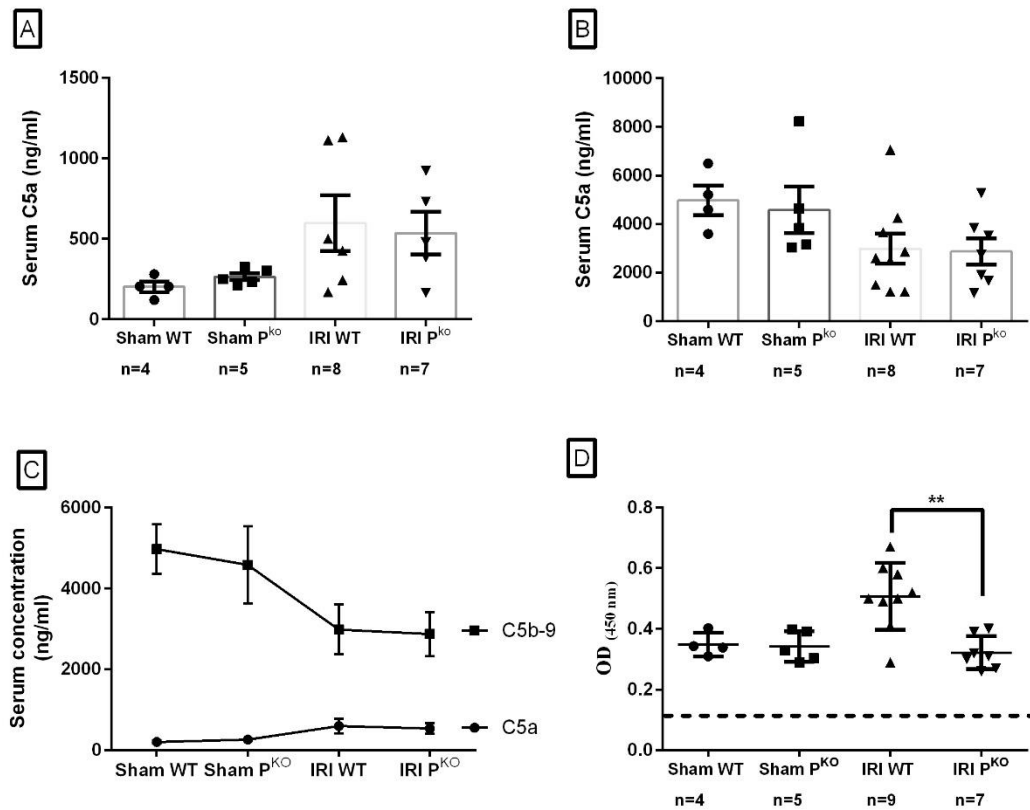


Figure 5-18 Complement proteins in serum of mice. C5a (A, C), C5b-9 (B, C) were measured in murine serum of both wild and PKO mice that have been exposed to renal IRI and compared with sham groups using ELISA. Lectin pathway activity was determined by activation of mouse serum (sham/IRI) on mannan coated plates. The dot line indicates the background absorbance of serum with 10mM EDTA and heat inactivated serum analysed for lectin pathway activity in parallel (D); Data were shown as mean \pm SEM; p was considered to be significant (*) < 0.05 , (**) < 0.01 . IRI: ischemia reperfusion injury; P^{ko}: properdin knockout mice; WT: wild type.

From the data in Figure 5-19 A, it is apparent that serum of wild mice with renal IRI as well as properdin deficient litter-mate contained slightly more MCP-1 in relation with sham mice; nevertheless, they were not significant ($p > 0.05$). Additionally, P^{KO} mice showed greater serum MCP-1 than WT mice in both surgical and sham groups ($p > 0.05$). On the other hand, MCP-1 assessment from renal tissue homogenates of the four mice experimental groups, which illustrated in Figure 5-19 B, revealed nearly equal amount of expression in wild-type mice that were exposed to renal IRI and sham; while P^{KO} mice data revealed significant increase in tissue MCP-1 in comparison with sham group ($p = 0.038$).

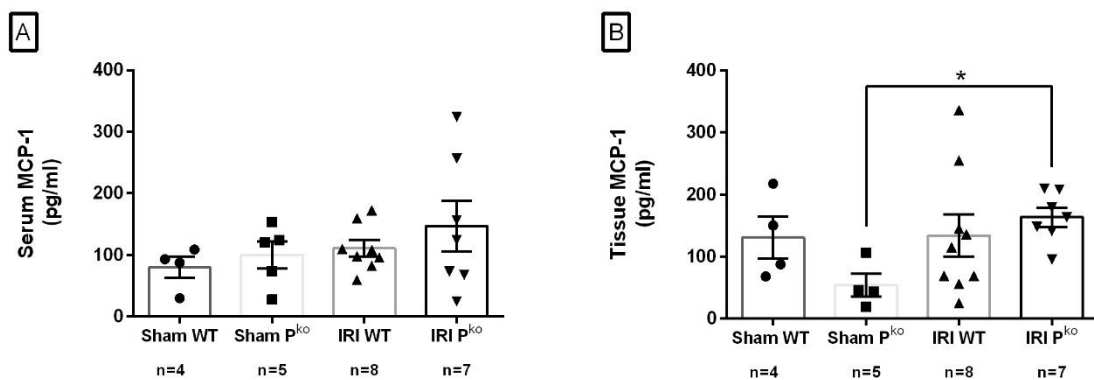


Figure 5-19 MCP-1 in serum and renal tissue homogenate of mice. MCP-1 was measured in murine serum (A) and renal tissue homogenate (B) of both wild and P^{KO} mice that have been exposed to renal IRI and compared with sham groups using ELISA. Data were shown as mean \pm SEM; p was considered to be significant (*) < 0.05 , (**) ≤ 0.01 . IRI: ischemia reperfusion injury; P^{KO} : properdin knockout mice; WT: wild type.

5.3.3.3 Indirect TUNEL assay

Detecting of apoptotic bodies in different kidney parts: tubular area, tubular lumen and interstitium, to assess degree of apoptosis was conducted as seen in (Yang *et al*, 2003).

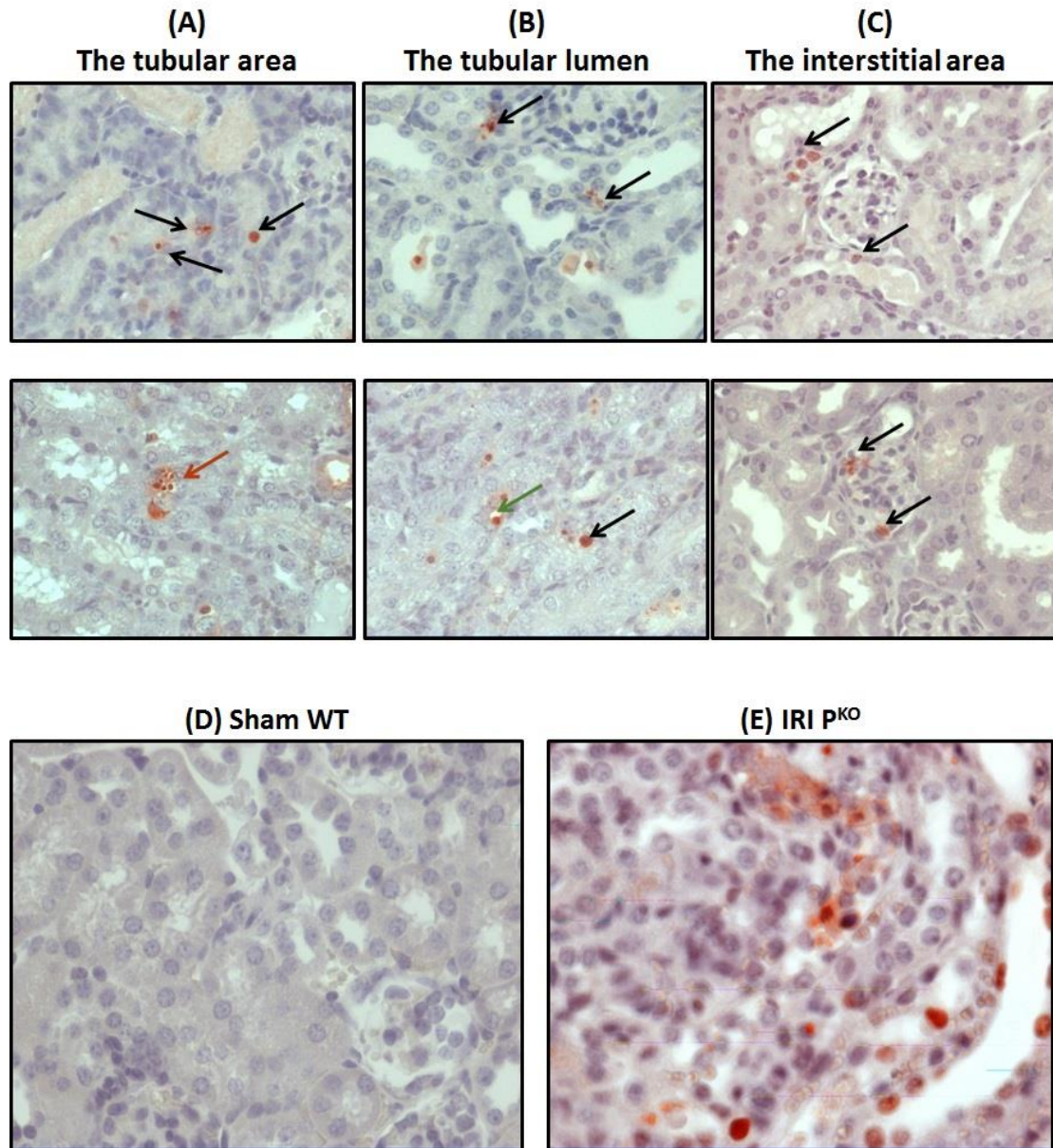


Figure 5-20 Apoptotic bodies in different parts of murine kidney. Single (black arrow) and cluster (red arrow) of apoptotic bodies as well as apoptotic body with halo (green arrow) were observed and calculated in tubular area (A), tubular lumen (B), and interstitial area (C) of murine kidney. A slide from sham wild (D) shows no apoptotic bodies in comparison with multiple apoptotic bodies in slide from kidney with IRI P^{KO} mice (E). Slides were assessed under light microscope (Olympus CX41) 40X,

Further analysis, as shown in Figure 5-21, revealed that both wild and P^{KO} mice, which suffered from renal IRI, had more apoptotic bodies than sham mice as well as a significant increase among PKO mice suffered from IRI in relation with WT mice exposed to renal IRI ($p = 0.024$) (Figure 5-21).

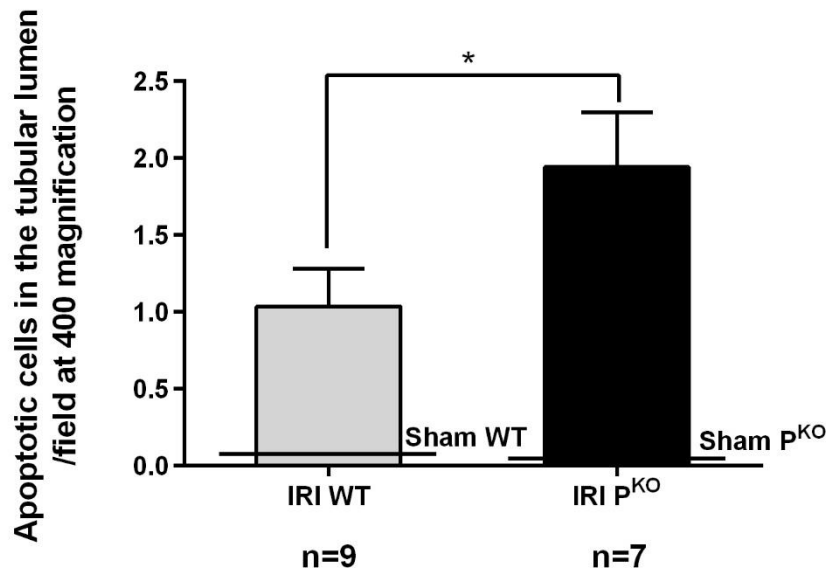


Figure 5-21 Apoptotic cells in murine renal tissue. Average of apoptotic bodies in 20 slides were counted under light microscope (Olympus CX41) 40X. Data were shown as mean \pm SEM; p was considered to be significant (*) < 0.05 . IRI: ischemia reperfusion injury; P^{KO}: properdin knockout mice; WT: wild type.

5.4 Discussion

Prior studies, where clamping renal vessels were performed to induce renal IRI in mice, have concluded that complement activation shows a pivotal role in renal IRI through its participation in immune complex cleansing, tissue homeostasis and other self-defence mechanisms (Bonventre, 2010; Bonventre and Yang, 2011). It has been found that inhibition of the alternative pathway (AP) via targeting properdin, which is the sole positive regulator, using a blocking monoclonal anti properdin antibody will ameliorate renal IRI in murine model (Miwa et al., 2013 and Miao et al., 2014). Miwa et al., 2013 established renal IRI in mice, which were generated with compound knockouts for complement down-regulators CD59 (halts MAC assembly) and decay accelerating factor (DAF) or CD55 (inhibits C3 and C5 convertases) via clamping both renal pedicles for 22 minutes and reperfusion for 24 hours. Results revealed a significant improvement of renal impairment at 24 hours when given anti properdin (intra-peritoneal injection of 2mg/mouse of mouse anti-mouse properdin mAb 14E1) treatment 24 hours before clamping renal pedicles. Similar results were observed in triple -deleted mice (CD59, DAF and properdin) in comparison with double (CD59 and DAF) deleted mice. Likewise, Miao et al., 2014 performed renal IRI in mice via bilateral clamping of renal pedicles for 25 minutes followed by reperfusion for 24 hours. Mice with a proximal tubular epithelial cell specific deletion of the complement down-regulator Crry, were treated with anti properdin antibody 2 hours prior clamping of renal pedicles and showed significant reduction in renal damage and significant inhibition in tubular C3 staining and presence of F4/80⁺ macrophages at 24 hours. The above studies created a platform for the hypothesis that properdin-deficient mice in the presence of all down-regulators would express an improved phenotype in comparison to their congenic wildtype controls in a model of renal IRI.

5.4.1 Specifications of our renal IRI model

With respect to the renal IRI models descriptions, substantial differences in their design were noticed which affect markedly development and outcomes of the murine phenotypes in renal IRI. The present study was designed to determine the role of properdin on wildtype C57BL/6 mice exposed to bilateral clamping of renal pedicles and reperfusion

for 72 hours thereafter in relation with congenic properdin deficient mice. Mice were anaesthetised generally using isoflurane inhalation which has a renoprotective effect (Wei and Dong, 2012). Additionally, analgesic drugs (carprofen, a prostaglandin synthesis inhibitor, and buprenorphine, a partial opioid agonist) were subcutaneously injected repeatedly. Both NSAID and buprenorphine have shown a direct anti-inflammatory effect (Volker et al., 2000) and neutrophil migration inhibition (Hish et al., 2014).

5.4.2 Properdin deficiency impaired renal function

It was an unanticipated finding that impairment in renal function (serum creatinine and blood urea nitrogen) as well as tissue damage (more tubular dilatation, cast formation, cell detachment and less prominent brush border) following renal IRI are significantly worse in properdin deficient mice than the wildtype group. This is pointing to a significant value of a properdin sufficient state in IRI induced acute renal failure and are in agreement with data obtained by Ruseva et al, 2012 when a nephrotoxic nephritis (NTN) was induced by a nephrotoxic serum, sheep anti-mouse glomerular basement membrane (GBM) antibody, injection intraperitoneally in complement factor H (CFH) knockout and/ or P^{KO} mouse. They found that properdin depletion aggravates C3 deposition and subsequent renal glomerulopathy in CFH knockout mice (Ruseva *et al*, 2013).

5.4.3 Inflammatory mediators circulating in P^{KO} mouse after 72 h from IRI

In an attempt to understand the underlying molecular mechanism behind the harmful effect of properdin deficiency on renal tissue following IRI, our study found that caspase-3 protein fragments (17 kDa) production and apoptotic cell assembly were significantly higher in properdin deficient mice compared to congenic wild type. These are in line with study undertaken by others where both human proximal tubular epithelial cells (subjected to hypoxia/re-oxygenation in vitro) and renal tissue of mice (exposed to ischemia for 30 minutes followed by reperfusion for 24 hours) express higher cleaved caspase-3 protein as well as more apoptotic bodies comparing with control/ sham groups respectively (Chen *et al*, 2013b).

Caspase-3 is one of the executioner intracellular proteases that is found in inactive phase in normal renal tissues and can be stimulated through extrinsic pathway through death receptor- mediated pathway (such as tumour necrosis factor receptor) or intrinsic pathway via mitochondrial stimulation; whereas both pathways resulting in caspases activation cycle (McIlwain, Berger and Mak, 2013). Active caspase-3, i.e. cleavage, has the ability to regulate programmed cell death, apoptosis, during renal IRI (Lien, Lai and Silva, 2003) where it dismantles affected cells via its proteolytic activity, developing apoptotic bodies and upregulating ligands attracting phagocytic cells (Elmore, 2007).

Phagocytosis is a vital process in clearing apoptotic cells. It is conducted by either professional phagocytes, when it is their primary function (such as macrophage and dendritic cells), or nonprofessional, when it commences by adjacent cells (such as epithelial cells and endothelial cells); nonetheless, both types will follow the same steps of phagocytosis which are detection, decision, engulfing and degradation (Elliott and Ravichandran, 2010). Phagocytosis is usually initiated by up regulating membranous receptors on phagocytic cells that could be complement related via activation complement 3 receptor or non-complement through Fc gamma receptors (Fc γ R) (Caron and Hall, 1998).

Properdin deficiency may cause accumulation of apoptotic cells in kidneys exposed to IRI due to disruption in phagocytic mechanism. This is due to the fact that properdin, in addition to its positive regulator for CP, has a non-complement recognition role for diseased cells, helping in eliminating them via phagocytic action of macrophages and dendritic cells (Kemper, Atkinson and Hourcade, 2009). The recognition occurs through properdin binding to early apoptotic T-cells (not live or necrotic ones), which promotes C3b deposition on T-cell surface directly and bypassing CP and LP. This is an alternative route to the usual complement-mediated phagocytosis pathway. A similar binding capability of properdin has also been shown (in *in vitro* studies) on late apoptotic and necrotic cells rather than early apoptosis (Kemper, Atkinson and Hourcade, 2009; Xu *et al*, 2008; Xu *et al*, 2008). It could be suggested that phagocytic pathway via Fc γ R stimulation, which will be intact in both sham and surgical P^{KO} groups, can compensate properdin-mediated phagocytosis during ordinary apoptosis in sham groups but will be overwhelmed in IRI mice. Accordingly, it is highly possible that more apoptotic cells

were found in renal tissue of properdin deficient mice in relation to congenic wildtype after renal IRI due to over production and less clearance.

Moreover, results indicated that high-mobility group box 1 (HMGB1) protein was significantly elevated in renal tissue homogenate in P^{KO} mice comparing to wildtype group. Additionally wildtype mice exposed to IRI showed less pronounced interleukin 6 (IL6) and monocyte chemoattractant protein (MCP1) release compared to properdin deficient mice.

HMGB1 is a 30 kDa endogenous ligand that may be found either inside nucleus helping in DNA transcription or extracellularly as a pro-inflammatory cytokine during cellular injury (Yang *et al*, 2005). During renal IRI, it is released from either macrophages and/or necrotic cells (Yang *et al*, 2005) or probably from apoptotic cells prior to death after translocation into vacuoles called apoptotic cell derived membranous vesicles (ACMV) (Schiller *et al*, 2013). HMGB1 binds to TLR4, which is also upregulated as well after IRI, on tubular epithelial cells surfaces, causing activation of several mitogen activated protein kinase (MAPKinase) pathway proteins (i.e. phosphorylation of extracellular signal-regulated kinase (ERK), c-Jun N-terminal kinase (JNK) and p38). HMGB1-TLR4-MAPK pathway aggravates renal IRI by triggering innate immunity through activating various inflammatory cytokines such as IL-6 and chemokines (MCP-1) (Wu *et al*, 2010; Chen *et al*, 2013b). It seems that an inflammatory loop will be accomplished secondary to the effect of inflammation on renal cells particularly tubular epithelial cells (Figure 5-22). Furthermore, HMGB1 blocking via anti HMGB1 Ab injection prior to surgical clamping of renal vessels ameliorates renal IRI in wild-type mice (Wu *et al*, 2010).

Another aspect of our study showed significant rise in CXCL16 protein production following IRI in comparison with sham control with no difference between P^{KO} and wild-type mice while changes in NFκB protein among groups were insignificant although slight elevation among IRI mice were recorded. Although no *in vivo* study about the function of CXCL16 during renal IRI could be found, study by Zhao *et al*, 2013 proved that CXCL16 steps up after cardiac IRI in mice and its blockage protects murine heart muscle (Zhao *et al*, 2013).

CXCL16 is a chemokine, which is expressed in both tubular cells and fibroblasts in normal kidney at low level and upregulates after acute kidney injury. It elicits leukocyte

recruitment (Izquierdo *et al*, 2012) as well promoting chemotaxis of cells expressing CXCR6 (such as bone marrow-derived fibroblasts) to enhance inflammation and fibrosis (Chen *et al*, 2011; Schramme *et al*, 2008). Nevertheless, *in vitro*, CXCL16 shows no role in cell apoptosis or proliferation (Izquierdo *et al*, 2012). Further analysis of the CXCL16 pathway is recommended to evaluate its role during *in vivo* renal ischemia reperfusion injury.

5.4.4 Activation of complement system

Shedding of glycocalyx in IRI, release of DAMPs and loss of cell bound regulators generate an altered cell surface which promotes complement activation and activation of the coagulation cascade (Duehrkop and Rieben, 2014). All three complement pathways are activated during renal IRI where they results in generation of pro inflammatory molecules (C3a, C5a, and C5b-9) which have fundamental role in tissue injury and inflammation (Danobeitia, Djamali and Fernandez, 2014). We found serum levels of C5a and serum C5b-9 to be inversely correlated i.e. greater levels of C5a in IRI compared to sham, lower levels of C5b-9 in IRI compared to sham (supplementary **Error! Reference source not found.**). It has been found that C5a plays a vital role in renal IRI and blocking C5a receptor or knocking it out in mice ameliorate renal injury at 24 h and 48 h after renal IRI (de Vries *et al*, 2003; Peng *et al*, 2012). On the other hand, C5a could be generated after renal IRI under the influence of coagulative system activation where thrombin can exert an effect analogous to C5a convertase in generating the C5a (Huber-Lang, Sarma *et al*. 2006). The coagulation process on sample preparation may generate relatively less terminal complex in samples from IRI animals because of *in vivo* consumption of activity (Krisinger *et al.*, 2012). It seems that the source of C5b-9 to be via the alternative pathway is unlikely because of the lack of a difference in levels in the absence of properdin, nor is it likely to be via the classical pathway because of a lack of a properdin dependent difference inconsistent with a contribution from the amplification loop. For this reason, lectin pathway activity was assessed in sera from experimental animals as ischemic cell surfaces can be sufficient triggers of lectin pathway activation (Schwaeble *et al.*, 2011). Measurement of lectin pathway activity in serum revealed a significant increase in activity in the IRI WT group, contrasting with previous findings of a consumption of complement activity at the earlier time point of 24 hours (Kotimaa *et al.*, 2015). Our

results are in line with *in vivo* work on mice (bilateral ischemia for 55 minutes and reperfusion for 6 hours) where MBL is activated via Mannan-binding lectin-associated serine protease 2 (MASP-2) during renal IRI (Asgari *et al.*, 2014). Nevertheless, lectin pathway activity in serum from properdin deficient mice did not differentiate between IRI and sham groups.

5.4.5 Aftermath repair

In addition to the injurious role, complement system activation during IRI may participate in tissue repair (Danobeitia, Djamali and Fernandez, 2014). In a mouse model of laser induced choroidal neovascularisation, the local generation of C5b-9 was linked to the release of CCL2 in the repair stage of tissue injury (Liu *et al.*, 2011). There was a positive correlation of CCL2 levels and histological score only in wildtype mice. Because of the experimental design, only endpoint analyses were made and no definite conclusions can be drawn regarding disease kinetics which might differ in the genotypes. Absent reactivity of lectin pathway activity at 72 hours after IRI and production of CCL2 which does not bear relation to the extent of histopathological injury, unlike WT, may suggest a beneficial effect of the absence of properdin for longterm fibrotic reactions (Sahin and Wasmuth, 2013).

Other evidence for the presence of repairing mechanisms in our model were presence of mitotic figures (Humbert and Gödde, 2015) as well as the elevation of proliferating cell nuclear antigen (PCNA) protein in renal tissues harvested from both IRI groups comparing with sham counterpart. PCNA plays a pivotal role in DNA replication as well as recruiting its components in response to DNA damage (Mailand, Gibbs-Seymour and Bekker-Jensen, 2013) and it was used as a marker for renal epithelial cell proliferation where the less PCNA the less cellular proliferation (White *et al.*, 2014).

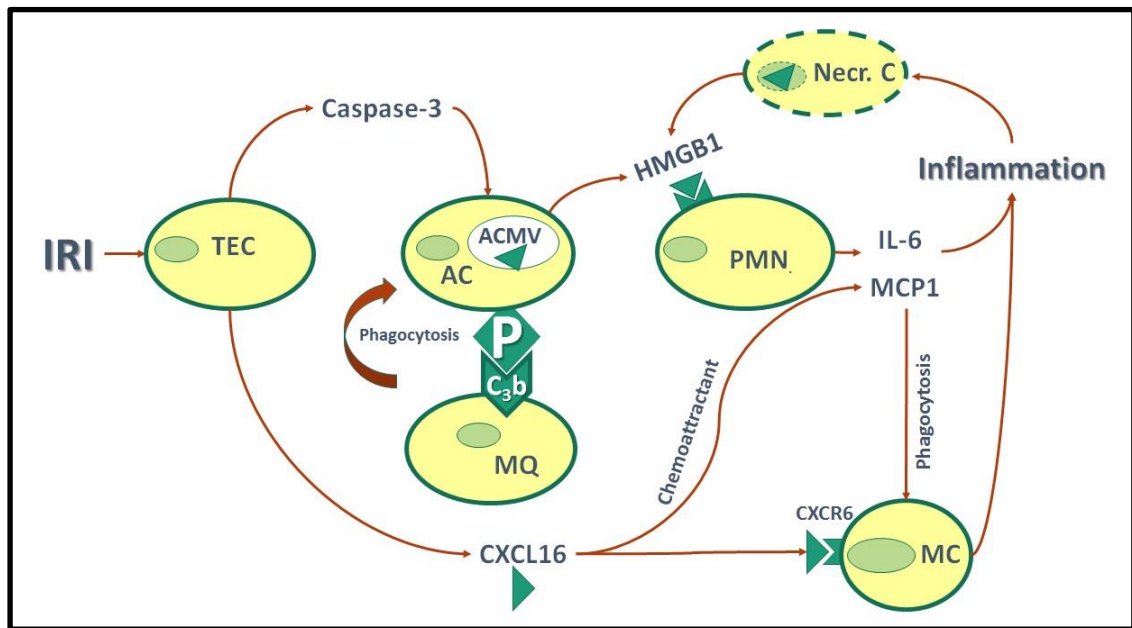


Figure 5-22 Role of properdin as a pattern recognition molecules in renal IRI. AC= Apoptotic cell; ACMV= Apoptotic cell- derived membrane vesicles MC= Monocytes; MQ= Macrophage; Necr. C= Necrotic cell; PMN= Polymorph neutrophil; TEC= Tubular endothelial cell.

In summary, it is possible that renal IRI in properdin- deficient mice results in more HMGB1 secondary to accumulation of apoptotic cell causing activation of HMGB1-TLR4 pathway that ends with more inflammation and renal tissue damage due to activation of various pro-inflammatory cytokines and chemokines. However, proving this mechanism requires further analysis.

The reperfusion was around 24 hours in the majority of animal renal IRI models while our model extended to 72 hours that may influence the molecular signalling of complement pathway and gave time for tissue repair establishment.

6 Chapter six (conclusions)

6.1 Conclusions

Our HNSR model is a new *in vitro*, dependable and easily applicable model that can simulate and may replace *in vivo* renal IRI in certain circumstances. The model was designed to simulate both phases of IRI (6 hours and 24 hours) and was extended to cover the healing phase as well (48 hours). Ischemia was simulated via combined treatment of human PTEC (HK-2) with serum-free, glucose-free Locke's buffer and incubation in hypoxic chamber while incubation with normal media inside oxygenated chamber represented conditions similar to the reperfusion phase with oxygen and nutrient resupply.

The study results revealed that the conditions provoke a significant change in the mRNA expression of versican and IL-6 and that their individual responses are a quick, acting a suitable control measure of the success of hypoxia (versican) (Leonardo *et al*, 2008) and of inflammatory reaction expressed by the epithelial cells (IL-6) (Zhang *et al*, 2015).

It is thought that establishing a well-designed *in vitro* model is essential to understand effectively cellular responses of PTEC while studying IRI and gives a foundation to subsequent *in vivo* work or analyses therein as well (Russ, Haberstroh and Rundell, 2007; Kurian and Pemaiah, 2014).

In vivo, properdin deficient mice were significantly impaired in their renal function compared to wildtype mice (significant rising in blood urea nitrogen and serum creatinine). Properdin deficient mice showed worse histopathology, greater numbers of apoptotic cells in renal tissue (mainly intraluminal), significantly elevated danger associated molecule HMGB1, and corresponding caspase-3 activation. *Ex vivo* reactivity of the lectin pathway of complement activation was significantly impaired in properdin deficient mice after IRI. Wildtype mice responded with local and systemic CCL2 production commensurate with the extent of damage while properdin deficient mice did not.

The model was able to examine the repair period after IRI due to the longer reperfusion phase (72 h). The data indicated an increase in number of mitotic figures, which is an indicator of cell division and thus repair (Cireşan *et al*, 2013). Furthermore, the model expressed more proliferation markers (PCNA) protein in IRI groups compared to sham (Mailand, Gibbs-Seymour and Bekker-Jensen, 2013). Overall, the use of congenic

properdin deficient mice has shown that properdin has a significant role to play in the normal postischemic recovery of renal injury

6.2 Strengths and limitation

The *in vitro* NHR model seems to be reproducible, easy to monitor, affordable and standardisable. Also, can offer a model for the use in the field of renal cell pathology. In addition, its applications are in line with the 3 Rs concepts, particularly the replacement, where cell line could replace animal model in underlining the initial phase of future researches. However, as isolated cells can only be used in this context, the isolation is limited, and cannot account for the host's reactivities and influence on the allograft.

Regarding *in vivo* animal model IRI, simulating the concurrence of factors relevant to human intervention (renoprotective anaesthesia, peri- and postoperative analgesia, volume substitution) in mice deficient of properdin and congenic controls were performed. The model allowed longer-term observation of renal outcome, including renal repair phase after IRI (72h).

On the other hand, the animal model excluded neutrophil infiltration mice. This is because mice had to receive painkiller before and during surgery as well as postoperatively (during reperfusion phase) as part of animal welfare (refinement) to reduce animal suffering. These drugs were carprofen, a prostaglandin synthesis inhibitor, and buprenorphine, a partial opioid agonist and both have shown a direct anti-inflammatory effect (Volker et al., 2000) and neutrophil migration inhibition (Hish et al., 2014).

6.3 Future work

This model can reliably deliver insight in IRI mechanisms via evaluating both injury phases (ischemia and hypoxia) as well as exploring reactive and repair pathways. Our model can be used for preclinical analysis as described, and can be adapted to answer research questions involving anoxic or hyperbaric conditions for eukaryotic cells, or customised conditions for microbes.

With reference to the animal model, it would be better if a new time point (24 hours reperfusion) was added in order to investigate the acute phase of renal IRI. Moreover, reversing the effect of properdin deficiency via giving properdin to the P^{KO} group could be vital to confirm its role during renal IRI.

7 Chapter seven (appendix)

7.1 Human proximal tubular epithelial cells (HK-2)

7.1.1 Simulation of ischemia by mineral oil immersion

7.1.1.1 Assessing cell viability by trypan blue (TB)

Under laminar flow cabinet, after HK-2 cells reached confluency in their flask, they were plated out into a 48-well plate then were transferred to a humidified incubator at 37 °C, 5% CO₂. The next day, the HNSR model was set up with two control groups (media contained 10% and 0.25% FCS, respectively) without oil, experimental groups where overlaid with mineral oil for 1, 3, and 6h and followed by media replenishment for 24 and 48 hours respectively. At the end point for each group, the well was washed twice with PBS before being stained with pre-diluted TB 0.4% (100 µl Trypan Blue: 100 µl PBS) to detect the compromised cells as they stain blue under the microscope. Counting these cells was done by taking the average number of blue cells for four fields in each well (for 3 wells for each time point) using magnification power of 40 X (data not shown).

7.1.1.2 Assessing LDH release

HK-2 cells were seeded in 36 wells of 48-well plate and were distributed as experimental wells and their control (4 well per time points) followed by induction of HNSR model for 1, 2 and 3h using mineral oil immersion as mentioned above and analysed after 24 and 48h of substrate replacement. LDH release from supernatant, which was aspirated through the oil, was measured at OD 490 nm and showed a general reduction in LDH release from HNSR groups in comparison to their controls. There was significant reduction in HNSR 24h with HNS 1h ($p=0.0002$) as well in HNSR 48h with HNS 1h ($p=0.05$). Furthermore, LDH release from HNSR 48h for the three time points (1, 2, and 3 h) and their controls was higher than relative groups of HNSR 24h (Figure 7-1).

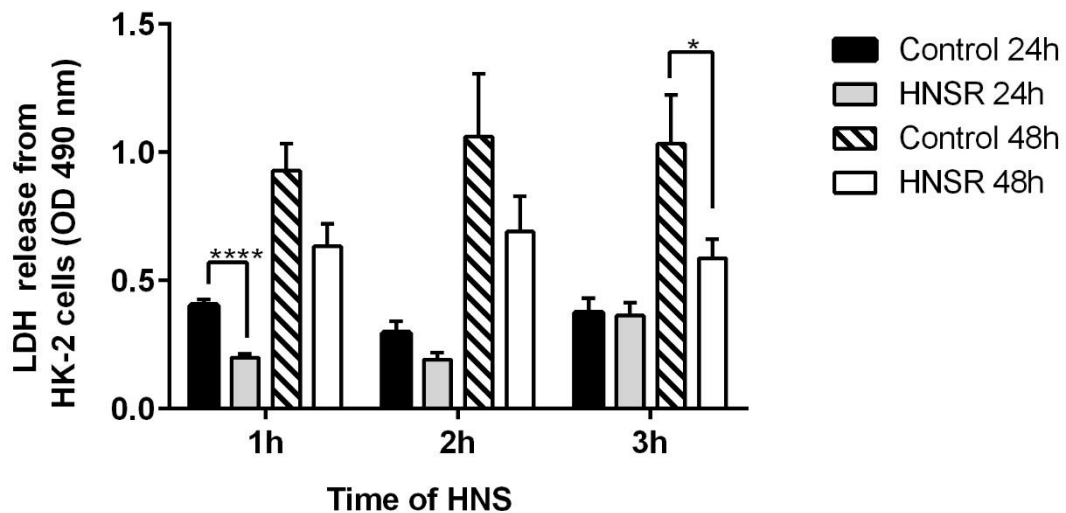


Figure 7-1 Stimulation of renal IRI by oil immersion and subsequent measurement of cell cytotoxicity using LDH release. The induction of hypoxia and nutrient starvation was done by immersion the HK-2 cells with mineral oil for 1, 2 and 3 hours followed by substrate replacement for 24 and 48 hours. The injury was examined by reading out the LDH release from the compromised cell in ELISA reader at optical density (OD) 490; n=4, data were presented as mean \pm SD, p (*) < 0.05, (***) \leq 0.001, HNSR: hypoxia/nutrient starvation-replenishment.

7.1.2 Simulation of ischemia by Locke's buffer and / or hypoxia

HK-2 cells were grown in culture media DMEM:F12 containing EGF in 25 cm² flask to become almost confluent. To start with, 3 injurious stimuli mimicking ischemia were used (Locke's alone, hypoxia alone, and both). Firstly, to induce starvation by nutrient deprivation, media was replaced with serum- free glucose- free Locke's buffer (154 mM NaCl, 5.6 mM KCl, 2.3 mM CaCl₂, 1 mM MgCl₂, 3.6 mM NaHCO₃ and 5 mM HEPES , pH 7.2) for 3 and 6 h. The cells were replenished with normal media and were kept in the incubator for 48 hours. Secondly, the flasks were transferred to an oxygen-low environment in hypoxic chamber that circulates a hypoxic gas mixture of 94.5% N₂, 0.5% O₂ and 5% CO₂ (Galaxy R, New Brunswick Scientific Ltd) for 3 and 6 hours. Later, the flasks were returned back to oxygen- containing incubator (21% oxygen and 5% CO₂) for 48 hours. The last group was exposed to both Locke's buffer and hypoxic environment where media was replaced with Locke's buffer before incubating flasks at hypoxic

chamber for 3 and 6 hours. Later, the cells were replenished with normal media and return back to oxygen- containing incubator (21% oxygen and 5% CO₂) for 48h. Reading was done via measuring LDH release from the supernatant of the cells using LDH kit (Promega, WI, USA).

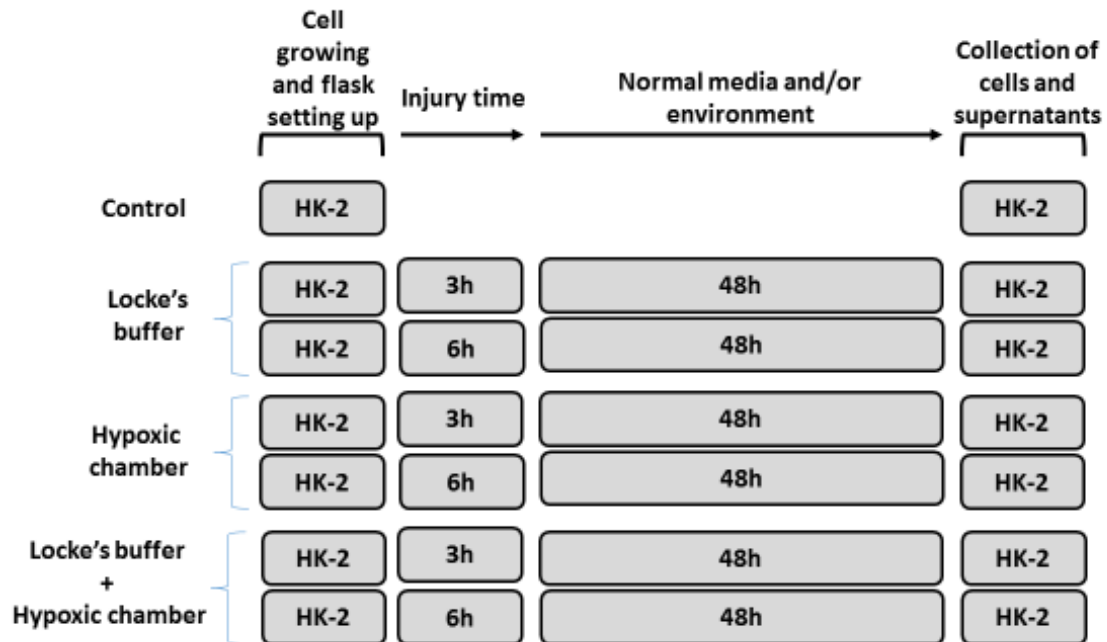


Figure 7-2 the initial experimental design of in-vitro renal HNSR model. Three pairs of experiment and one control flasks of human renal proximal tubular epithelial (HK-2) cells were grown in 25 cm² flasks. Experimental groups were exposed to and nutrient starvation (Locke's buffer), hypoxia (hypoxic chamber) and both for 3 and 6 h with replenishment for 48 h. Supernatant was collected for analysis.

The results revealed more LDH release with combinatorial stimulation (Locke's buffer and hypoxia) than from stimulation by each separately with slight incremental after stimulation for 6h than 3h (Figure 7-3 A). Hence, the experiments was repeated using only the combined stimuli for 3 and 6h followed by replenishment for 24 and 48h in order to assess the impact of replenishment time (Figure 7-3 B). Results showed higher LDH release after 48h than 24h of replenishment as well as more after 6h treatment than 3h (Figure 7-12 B).

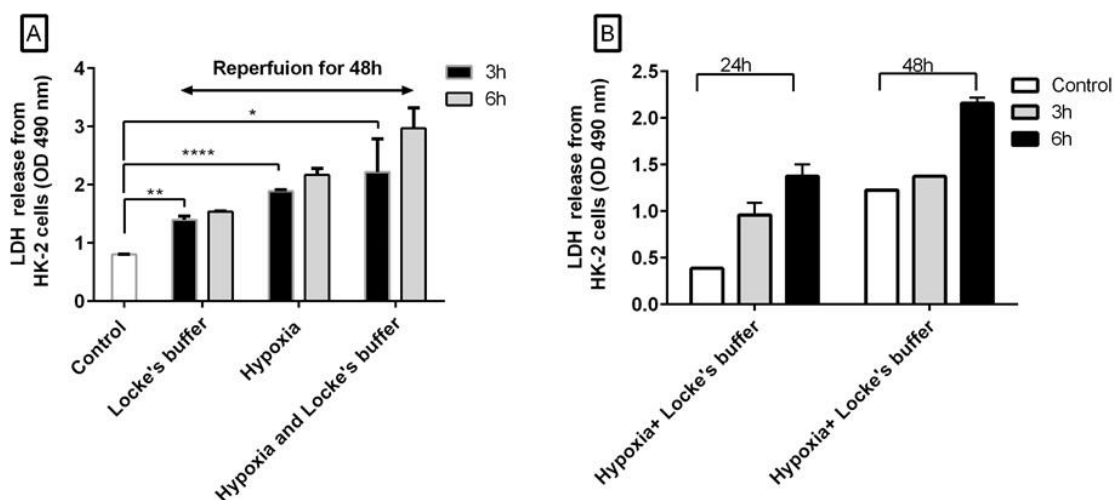


Figure 7-3 Quantitative assessment of lactate dehydrogenase (LDH) cell cytotoxicity from in vitro initial renal HNSR models. The graph shows effect of nutrient starvation (Locke's buffer) and / or hypoxia for 3 and 6 hours with media replenishment for 48 hours on LDH release from supernatant of human proximal tubular epithelial (HK-2) cells (A) and the differences in LDH release after HK-2 cells stimulation with both nutrient starvation (Locke's buffer) and hypoxia for 3 and 6 hours with media replenishment for 24 and 48 hours (B); data were presented as mean \pm SD, p (*) < 0.05, (**) \leq 0.01, (****) \leq 0.0001.

7.1.3 Effect of HNSR model on TNF- α production by renal PTEC (HK2)

Expression of tumor necrosis factor- α (TNF- α) protein from all experimental groups was measured and compared to their respective controls in order to assess the pro-inflammatory influence of HNSR on renal HK-2 cells.

7.1.3.1 Technique

Immediately, after serial dilution of the standard sample from 2000pg/ml to zero, 100 μ l of each standard and sample were added to each well in triplicate and subsequently were incubated for 2 h at room temperature. Again, aspiration and washing of the plate for 4 times were done. After that, a 100 μ l of 0.5 μ g/ml detection antibody was added to each well and was incubated for 2 h at room temperature. After aspiration and washing as previous, a 100 μ l of diluted (1:2000) Avidin- HRP Conjugate was added to each well and incubated at room temperature for 45 minutes. This is followed by another 4

aspiration/washing cycles a 100 μ l of substrate solution (TMB; Sigma-Aldrich, MO, USA) was added to each well and incubated at room temperature for 30 minutes to develop color then 100 μ l of stop solution (1 N HCl) was added. Finally, ELISA plate reader (Bio-Rad, iMark) was used at 405 nm with wave correction set at 650 nm for measuring absorbance.

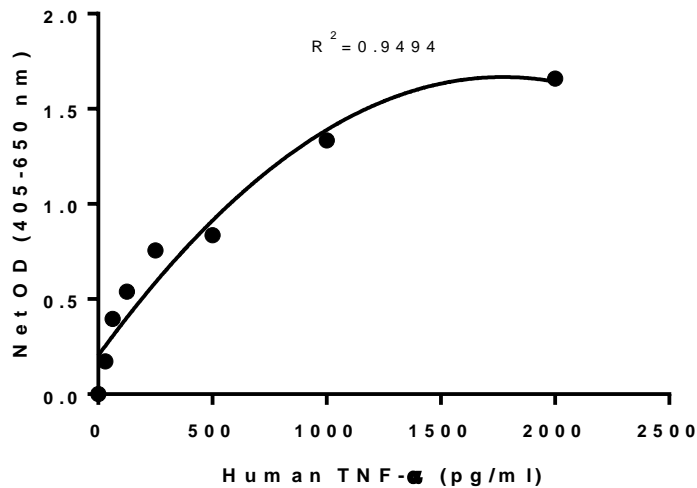


Figure 7-4 Standard curve of TNF- α . The cut off value is 31.25 pg/ml and the range of detection is 16-2000 pg/ml

On day one, the capture antibody was diluted with PBS to reach 1 μ g/ml which followed immediately by adding a 100 μ l to each ELISA plate well before sealing plate and incubating it overnight at room temperature. Next day, the liquid was aspirated from the wells before washing the plate for 4 times using 300 μ l of wash buffer for each well each time. To drain residual buffer, the plate was inverted and was blotted on paper towel after the last wash. Finally, 300 μ l block buffer was added to each well and was incubated for 1h at room temperature before aspiration and washing plate for 4 times as above.

From the ELISA kit, both capture antibody (21 μ g of antigen- affinity purified rabbit anti ETNF- α + 0.5mg D-mannitol); and detection antibody (11 μ g of biotinylated antigen- affinity purified rabbit anti-h TNF- α + 0.5mg D-mannitol) were diluted to have a concentration of 100 μ g/ml. Simultaneously, the human TNF- α standard (1 μ g of recombinant hTNF- α + 2.2mg BSA+ 11 mg D-mannitol) was reconstituted in sterile water for a concentration of 1 μ g/ml. Meanwhile, the Avidin-HRP Conjugate was aliquoted into two vials and stored at -20 $^{\circ}$ C.

7.1.3.2 Results

The pattern of TNF- α protein expression among experimental groups stimulated for 3h did not show any significant changes either to each other ($p > 0.05$) or to control although the greatest expression was from HK-2 cells stimulated with both hypoxia and Locke's buffer (646 ± 78.8). In the meantime, 6h treated groups showed more reproducible results. There was a significant rise in TNF- α protein expression from HK-2 cells with Locke's buffer and combined stimulations in comparison to control. Cells stimulated with hypoxia alone expressed TNF- α more than control and less than those with combined stimulation although results were not significant (Figure 7-5).

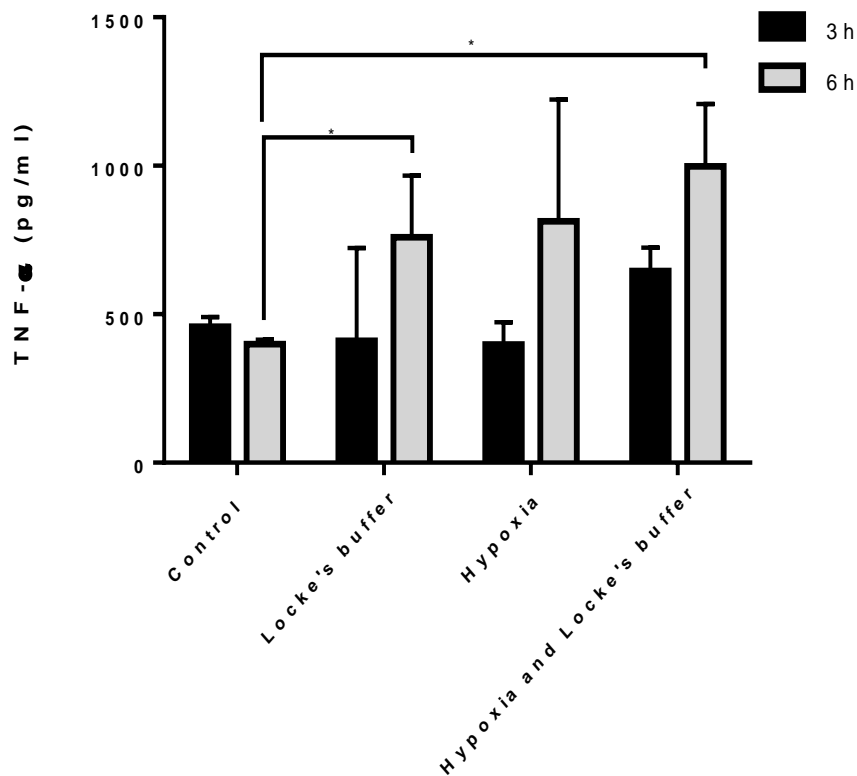


Figure 7-5 ELISA for TNF- α protein. Effect of HNSR stimulants on renal PTEC (HK-2). Quantitative measuring of TNF- α protein expression from different type of stimulation for 3 and 6h; $n=3$, data were presented as mean \pm SD, p (*) < 0.05 .

7.1.4 Western blotting

7.1.4.1 Collecting cells and protein measurement

From each time point of the experiment, cells were frozen at -20°C after washing them with PBS. Then, a lysis buffer were prepared according to our laboratory protocol. 500 μl of lysis buffer (Table 7-1) was added to each flask and the cells were re-suspended by pipetting up and down. Then, the flasks were rocked gently for 30 minutes at $2-8^{\circ}\text{C}$. After that, the lysate was collected into a reaction tube and centrifugation (Heraeus Fresco 17™, Thermo Scientific, Langenselbold, Germany) was done at 14000 Xg for 5 minutes. The clean supernatant was transferred and total protein was measured. To do this, a fresh standard stock of 2000 $\mu\text{g}/\text{ml}$ of bovine serum albumin (PAA, Passion, Austria) was prepared in distilled water and serially diluted. Next, 10 μl from either standards or samples were loaded into 96-well plate followed by adding 150 μl of Pierce Reagent (Thermo Scientific, Langenselbold, Germany) to each well. After 5 minutes incubation at room temperature, the optical density were measured at wavelength of 650 nm by plate reader (Bio-Rad, iMark).

The proteins that were examined are shown in Table 7-2. Finally, Pierce® ECL Western Blotting Substrate (Thermo Scientific, USA), ChemiDoc™ Imaging Systems and software (Bio-Rad, USA) were used to detect and analyse protein band (detail in chapter 4). Normalisation of target protein were performed against endogenous loading control (β -actin).

Table 7-1 Ingredients required to prepare 10 ml of lysis buffer. Lysis buffer usually prepared in ice; EDTA: Ethylene diamine tetra acetic acid, EGTA: Ethylene glycol tetra acetic acid, PMSF: phenyl methyl sulfonyl fluoride.

Stock solution	Amount
1 M β glycerophosphate (pH: 7.4)	100 μ l
0.5 M EDTA (pH: 8.0)	20 μ l
40 mM EGTA	250 μ l
1 M Tris-HCL (pH: 7.5)	500 μ l
100 mM Sodium orthovanadate	100 μ l
1 M Benzimidazole	10 μ l
100 mM PMSF	20 μ l
β -Mercaptoethanol	10 μ l
10% (v/v) Triton X-100	1 mL
500 Mm Sodium Floride	1 mL
Proteinase inhibitor cocktail (Sigma-Aldrich, MO, USA)	10 μ g/ml
Nanopure water	6.971 mL

Table 7-2 Primary and secondary antibodies were used during western blot.

	Primary antibody	Origin	Dilution	Secondary antibody	Origin	Dilution	Molecular weight
HIF-1 α	Rabbit polyclonal anti-HIF-1 α	Biorbyt Cambridge, UK	1:500	Swine anti-rabbit, polyclonal/HRP	Dako, Denmark	1:3000	90 kDa
Factor H	Rabbit polyclonal anti-factor H	Santacruz, Europe	1:500	Swine anti-rabbit, polyclonal/HRP	Dako, Denmark	1:3000	150 kDa
Factor B	Mouse monoclonal anti-factor B	Santacruz, Europe	1:500	Donkey anti-goat IgG-HRP	Santacruz, Europe	1:2000	100 kDa
C3	Polyclonal goat C3 anti human	Biorbyt Cambridge, UK	1:5000	Donkey anti-goat IgG-HRP	Santacruz, Europe	1:2000	110 kDa
PCNA	Monoclonal Mouse Anti-PCNA	Dako, Denmark	1:1000	Polyclonal goat anti-mouse	Dako, Denmark	1:1000	36 kDa
Properdin	Goat polyclonal anti properdin	Santacruz, Europe	1:500	Donkey anti-goat IgG-HRP	Santacruz, Europe	1:2000	53 kDa
TFF3	Monoclonal mouse antihuman TFF3	Biorbyt, Cambridge, UK	1:500	Polyclonal goat anti-mouse	Dako, Denmark	1:1000	7 KDa
HMGB 1	Rabbit polyclonal anti-HMGB1	Proteintech, IL, USA	1:500	Swine anti-rabbit, polyclonal/HRP	Dako, Denmark	1:3000	25 KDa
NF κ B	Rabbit polyclonal anti-NF κ B p 65	Santacruz, Europe	1:500	Swine antirabbit polyclonal/HRP	Dako, Denmark	1:3000	65 KDa
β -actin	Monoclonal Mouse anti- β -actin	Sigma-Aldrich, MO, USA	1:5000	Polyclonal goat anti-mouse	Dako, Denmark	1:1000	42 kDa

7.1.4.2 Western immunoblotting

7.1.4.2.1 Alternative pathway

The pattern of **protein synthesis** in HNSR model varied from mRNA expression. Both C3 and fH proteins revealed higher production after HNSR comparing to HNS, with peak after 24 hours. Moreover, properdin showed upregulation after 48 hours with no difference between HNS for 6h and HNSR for 24h while fB western blot data indicated a higher protein production after HNS that decreased with increasing replenishment time (less properdin from HK-2 cells after HNSR for 48 h than for 24 h).

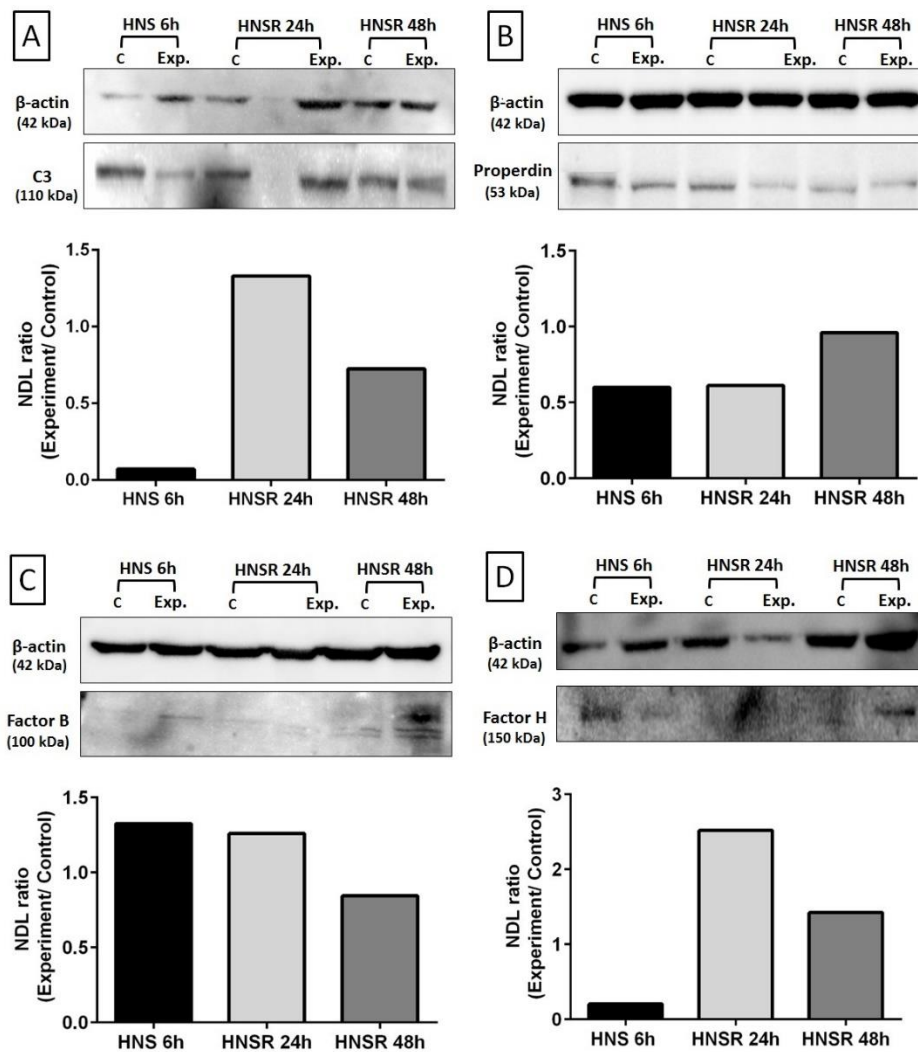


Figure 7-6: Semi-quantitative calculation of protein expression of AP markers from in vitro renal IRI model. C3 fragment (A), properdin (B), fB (C) and fH (D) Protein from PTEC of human kidney (HK-2) among the three experimental groups. Results were calculated as NDL ratio of experiment to its control in comparison to β -actin protein expression as endogenous control.

7.1.4.2.2 Cytokines and inflammatory markers

Western blot data for NfκB showed higher protein production after replenishment, which is more after 48 hours than 24 hours, in comparison to HNS for 6h alone. The highest protein synthesis of HMGB-1 was at HNSR for 24 h while PCNA protein was more after HNS for 6 h than after replenishment (Figure 7-7). Both HIF-1 α and trefoil factor 3 (TFF3) data revealed that HK-2 cells produce these two proteins in response to HNSR model with peak synthesis after 24h of replenishment. The results were published in article (Zwaini *et al*, 2016).

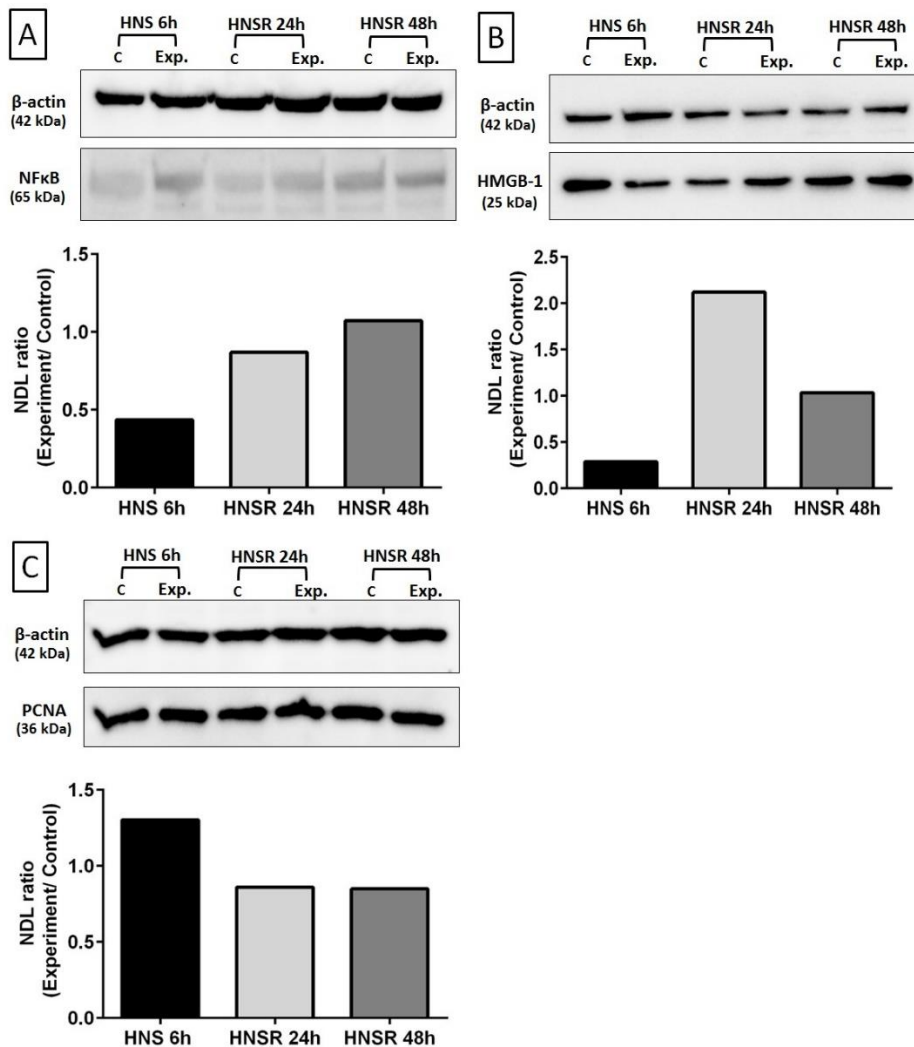


Figure 7-7: Semi-quantitative calculation of protein expression of inflammatory markers from in vitro renal IRI model. NfκB (A), HMGB-1 (B), PCNA (C). Protein from PTEC of human kidney (HK-2) among the three experimental groups. Results were calculated as ND L ratio of experiment to its control in comparison to β- actin protein expression as endogenous control.

7.1.5 Microarray proteome profiler

7.1.5.1 Principle

It is a modified version of enzyme linked immunoassay (same principle of ELISA) to detect qualitatively and semi-quantitatively presence of specific proteins in biological samples. It is a paper-based assay where primary antibodies of interest (35-40) are blotted as separate spots on nitrocellulose membrane (two adjacent spots for each antibody) and after recognition with secondary antibodies, they are detected using chemiluminescent tools. It is a relatively easy and rapid method to detect wide range of biomarkers in single test, which could be useful in preliminary investigations (in our experiment, the effect of HNSR on expression of 38 human kidney biomarkers).

7.1.5.2 Preparation of lysis buffer

The lysis buffer for the HK-2 cells was prepared as recommended in the manufacturer's protocol with some modification: 1% Igepal CA-630, 20 mM Tris-HCL (pH: 8.0), 137 mM NaCl, 10% Glycerol, 2 mM EDTA, and 10 µg/ml of proteinase inhibitor cocktail (Sigma-Aldrich, MO, USA).

7.1.5.3 Setting up the experiment

As the kit contains 4 membranes, the HNSR model was set up with seeding density of 0.7×10^5 as always with only one control for the 48 h time point. After each time point, supernatant was discarded; cells were washed with PBS and frozen. On the day of the experiment, 500 µl of the lysis buffer was added to each flask. Resuspension of the cells was done by pipetting up and down. Then, gentle rocking of the cells was performed at 4 °C for 30 minutes. After that, centrifugation at 14000 xg for 5 minutes was done. Then, the supernatant was collected into a new clean reaction tube. Protein measurement was done using Pierce assay (Pierce™ 660 nm Protein Assay, Thermo Scientific, IL, USA) and samples were adjusted to 300 µg protein. After preparing all the reagents as directed in the protocol, 2 ml of blocking buffer (Array Buffer 6) was added to each well of the 4-Well Multi-dish and the blocking buffer was incubated with each membrane to be used

in the experiment for one hour on a rocking platform shaker. Upon contact of the blocking buffer with the membrane, the blue dye of the spot disappeared; however, the already captured antibody was reserved in their specific location. Meanwhile, samples were suspended in 1.5 ml Array Buffer 5 (Buffered protein base). Furthermore, 500 µl of Array Buffer 6 and 15 µl of Detection Antibody Cocktail were added to the sample and were incubated for 1 h at room temperature. After aspiration of the Buffer 6 from the 4-multidish, the mixture of the above was added and incubated overnight at 4 °C on a rocking platform shaker. A 3 X 10 minutes wash was done with 1 X washing buffer for each membrane to be followed by adding the diluted streptavidin –HRP for 30 minutes at room temperature on a rocking platform shaker. Another 3 x 10 minutes wash was done. After that, the membranes were removed from the washing buffer and 1 ml of already prepared Chemi Reagent Mix was added to each membrane for 1 minute. Then, after wrapping the membranes and ensure there is no air bubbles, the membranes were exposed to an autoradiography film in a cassette with the identification number directed up toward the film. Lastly, multiple exposure times (1-10 minutes) were done.

7.1.5.4 Analysis

Image J 1.49 software was used to measure the integrated pixel density for each spot after background subtraction. Readings for each biomarker were calculated in duplicate and analysed separately by two different persons.

7.1.5.5 Results

In order to understand the molecular mechanism behind HNSR injury affecting HK-2 cells, proteins for renal injury biomarkers were scanned using proteome profiler array. It showed that human PTEC in HK-2 cells HNSR model expressed variable types of proteins, which are different in their mechanism of action, relation to hypoxia as well as glucose deprivation. Therefore, data of biomarker molecules that did not present any noticeable differences among experimental groups were not shown and only 18 proteins, which showed remarkable changes, were described respectively.

7.1.5.5.1 Peak protein production at HNSR for 24 h

Synthesis of trefoil factor 3 (TFF3), which plays a pivotal role in restitution (cell migration to heal superficial lesions) and regeneration of epithelial cells, as well as effectors of hypoxia induction (VEGF, CXCL-16, and FABP-1) by HK-2 cells showed significant elevation after HNS for 6 hours compared with control. This increment in production reached its peak after HNSR for 24 hours and dropped back (though still significantly higher than control) after HNSR for 48 hours; however, data were illustrated in published article (Zwaini *et al.*, 2016).

7.1.5.5.2 Down regulation in protein synthesis

Protein profiler results showed 6 kidney biomarkers with significant downregulation in protein synthesis after exposing PTEC (HK-2 cells) to HNSR injury where the peak was from control and the lowest was from HNSR 48h.

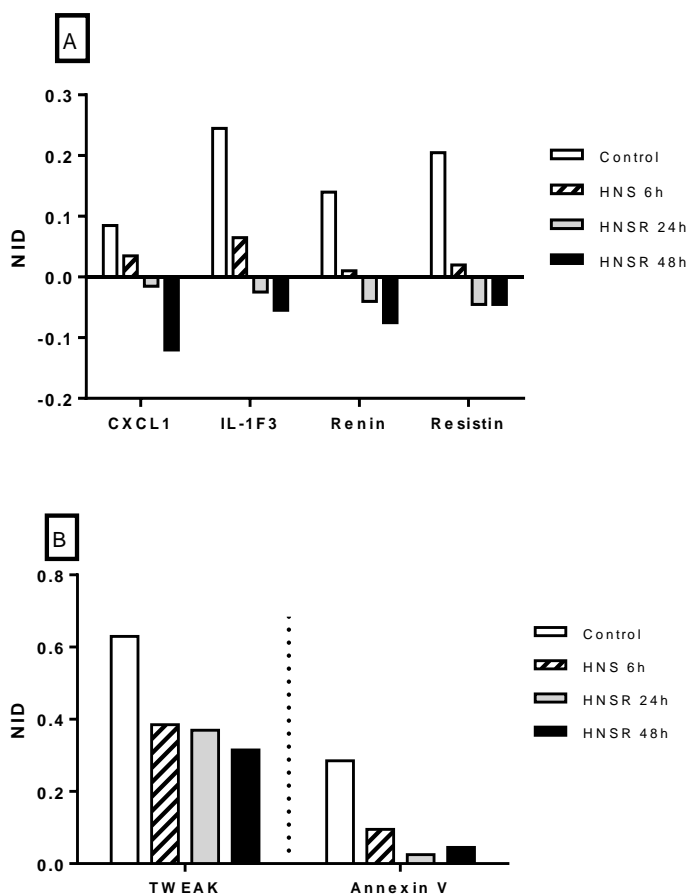


Figure 7-8: Proteome profiler of HK-2 cells showed downregulation in protein synthesis. . HNS/R: hypoxia-nutrient starvation/ replenishment, NID: normalised integrated density.

7.1.5.5.3 Lowest protein production at HNSR 48h

Results of other sets of renal injury biomarkers revealed a different pattern of protein expression from HK-2 cells after HNSR injury exposure with lowest level after replenishment for 48 h.

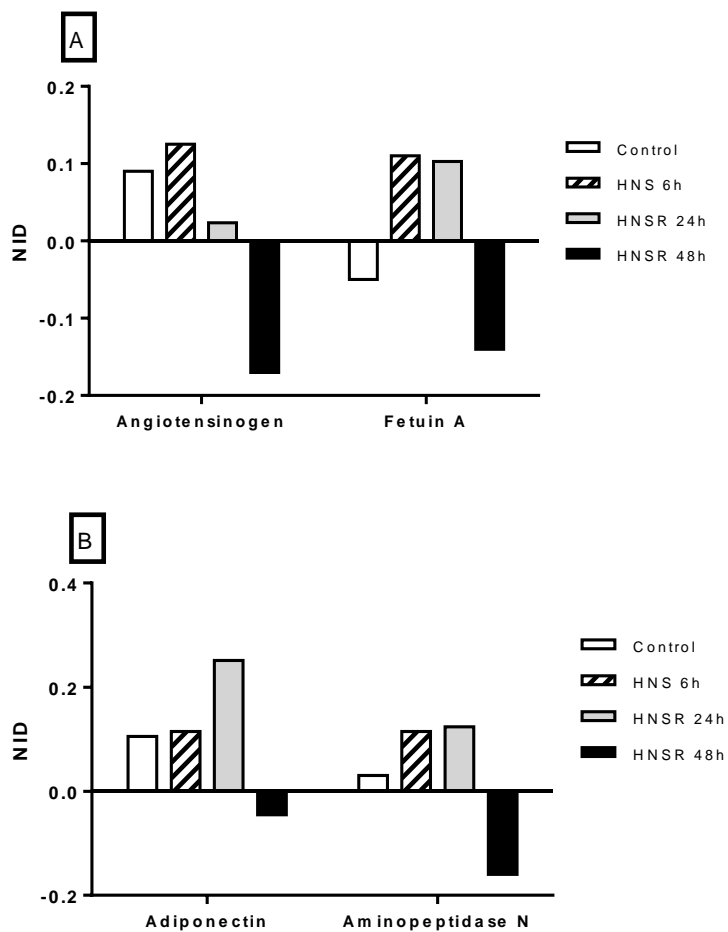


Figure 7-9: Proteome profiler of HK-2 cells showed lowest protein synthesis at HNSR 48h.). HNS/R: hypoxia-nutrient starvation/ replenishment, NID: normalised integrated density.

7.1.5.5.4 Protein production from HNSR 6 h is less than control and peaks after 48 hours

On the other hand, HK-2 cells exposed HNSR model produced 4 renal injury proteins in a different manner from the above. Results indicated lower protein synthesis in HNS 6h than control group followed by stepping up in production in both HNSR 24 and 48 hours.

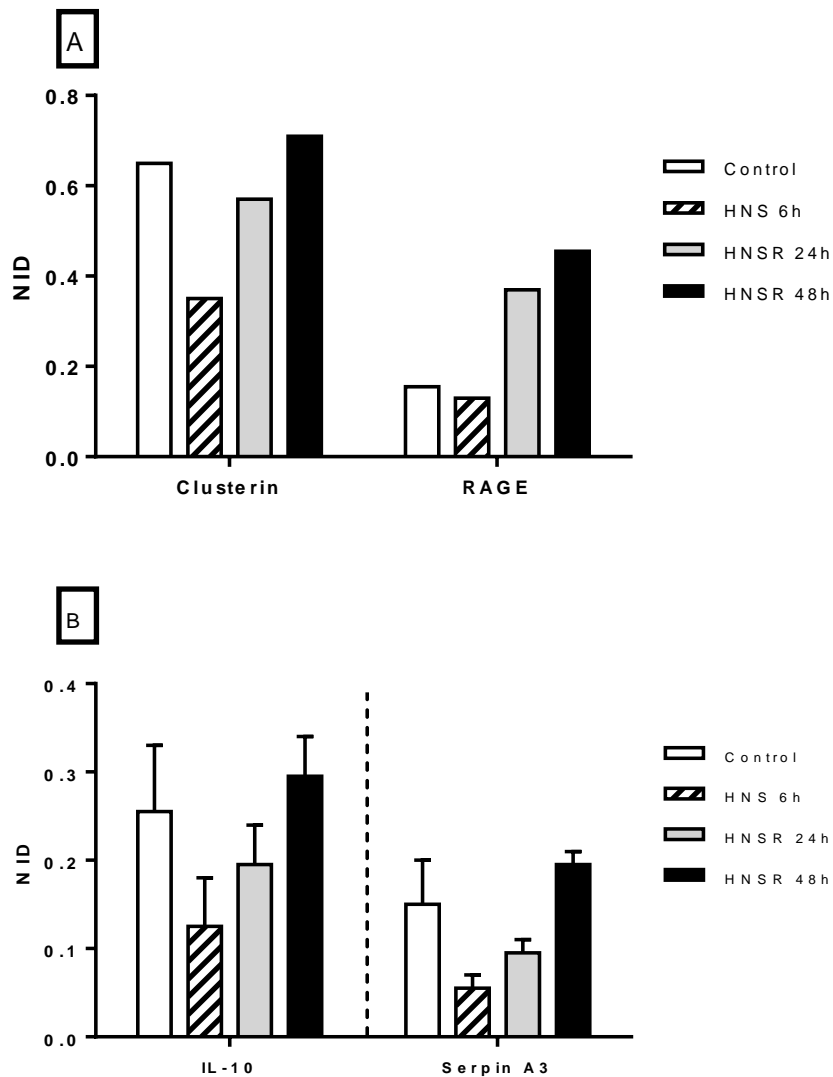


Figure 7-10: Proteome profiler of HK-2 cells showed lower protein synthesis from HNS 6h than control group.. HNS/R: hypoxia-nutrient starvation/ replenishment, NID: normalised integrated density.

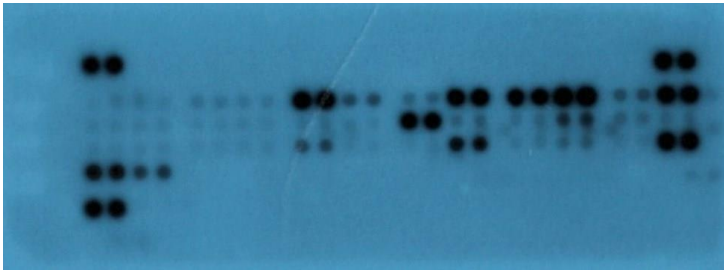
Intriguingly, proteins of renin, angiotensinogen and IL-1 revealed a different pattern. The proteins were found more in control group than HNS for 6h to be reduced in 24 hours and 48 hours replenishment groups. These three proteins are known as VEGF stimulator, which means that VEGF expression in our model did not follow RAS pathway nor IL-1. Additionally, angiotensin II has been suggested to accelerate inflammation and enhance chronic kidney diseases through promoting cell proliferation and mediating pro-inflammatory molecules (Ni *et al*, 2013).

Adiponectin (ADPN) is a 30 kDa protein (Raucci *et al*, 2013) and it is one of the adipokine family. In addition to its metabolic role in controlling glucose metabolism and fat breaking down, adiponectin is an anti-inflammatory cytokine that is secreted from various cells mainly adipocytes (Oh and Rabb, 2013; Perri *et al*, 2013). Both ADPN mRNA and protein were shown to be expressed in human PTEC, which is escalated with inflammation (Perri *et al*, 2013) with a protective role against renal IRI (Oh and Rabb, 2013). Our results revealed that ADPN protein is expressed from human PTEC *in vitro* after exposing to hypoxia and nutrient starvation. Furthermore, the protein increases in abundance during replenishment for 24 hours and diminishes after replenishment for 48 hours. The molecular mechanism is still uncertain (Oh and Rabb, 2013).

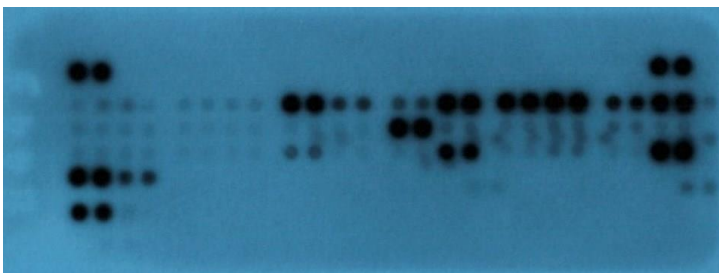
Resistin is another member of adipokine family in addition to other proteins such as IL-6 and TNF- α (Raucci *et al*, 2013). Its protein was found at higher levels in the control group but started diminishing in hypoxia and starvation group as well as replenishment groups. Park *et al*, 2011 suggested an inflammatory function for resistin. They emphasised that different cytokines like IL-6 and TNF- α can stimulate resistin expression from adipocyte and monocytes (Park *et al*, 2011; Raucci *et al*, 2013) which thereafter can reverse the action of adiponectin (McTernan *et al*, 2003). In contrast, low glucose level may stimulate resistin expression from adipocytes (McTernan *et al*, 2003).

7.1.5.5.5 Proteome profiler

HNS 6 hours



HNSR 24 hours



HNSR 48 hours

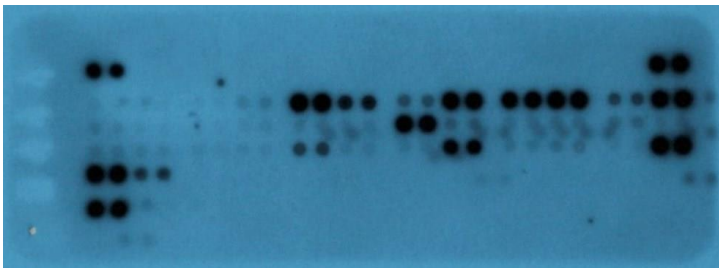


Figure 7-11 Microarray protein proteome profiler of HK-2 cells were exposed to HNSR injury.

7.1.6 Induction of HK-2 cells injury by LPS stimulation

In acute renal impairment, injury might be aggravated by lipopolysaccharide (LPS) endotoxin through potentiating the effect of hypoxia on the cells in the proximal tubular epithelium of the kidneys (Zager *et al*, 2007). Accordingly a trial to assess the effect of LPS on hypoxic cells were performed.

Firstly, in order to find the best concentration for LPS, HK-2 cells were grown as usual and seeded at a density of 8×10^4 cells in a six well plate. Two of them were stimulated with 100 ng/ml LPS (*E Coli 0111:B4*) for 6 and 20 h respectively and the other two were stimulated with 10 μ g/ml LPS for the same time points. The last two plates remained untreated as controls. The supernatants were measured in triplicate by LDH release assay and whole experiment repeated twice. Results showed that LDH release was increased with increasing LPS concentration and/ or duration of stimulation (Figure 7-12 A).

Next, an attempt to design a HNSR model, cells were grown as above before being stimulated by LPS (10 μ g/ml) for 6h and 20h and/ or transferred to an oxygen-free environment in hypoxic chamber for the same periods. The experiment was repeated twice and injury was assessed by LDH release assay. There was more LDH release after stimulation for 6h than 3h (Figure 7-12 B). However, we did not pursue any further analysis due to time constraint.

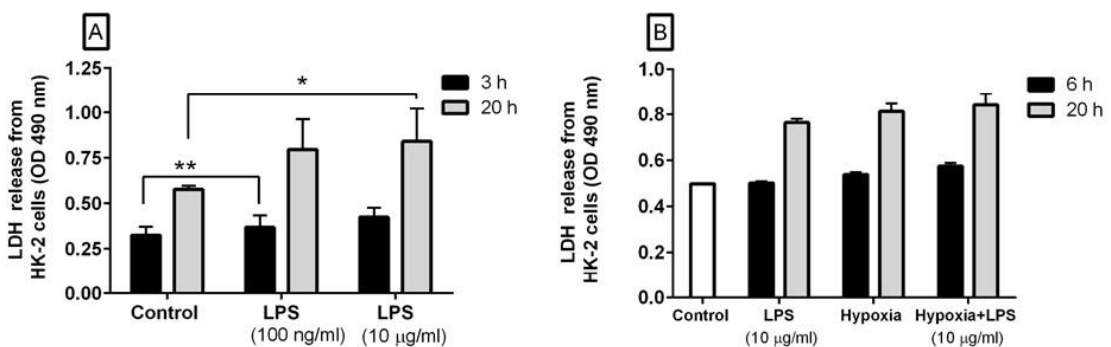


Figure 7-12 Effect of LPS on renal PTEC. A quantitative assessment of LDH release from supernatant of human proximal tubular epithelial (HK-2) cells treated with 100 ng/ml and 10 μ g/ml LPS (*E Coli*, 0111:B4) for 3 and 6 hours (A) and the differences in LDH release after HK-2 cells stimulation with LPS (10 μ g/ml) and / or hypoxia for 6 and 20 hours (B); n=2, data were presented as mean \pm SD, p (*) < 0.05, (**) \leq 0.01.

7.1.6.1 Response of renal PTEC to LPS and hypoxia

TNF- α protein expression from HK-2 cells was measured using sandwich ELISA as an indication for inflammation. There were no significant differences in protein expression among the experimental groups in comparison to control at 6h treatment time ($p > 0.05$). Meanwhile, stimulation of HK-2 cells for 20h revealed significant elevation in TNF- α protein expression from hypoxia-treated cells in relation to LPS alone ($p = 0.026$) but not significant (although still higher) than control ($p = 0.097$). Combined stimulation resulted in maximum TNF- α expression which was significantly higher than LPS-treated and control cells ($p = 0.0005$ vs 0.007) but not significant in relation to hypoxic cells ($p = 0.37$).

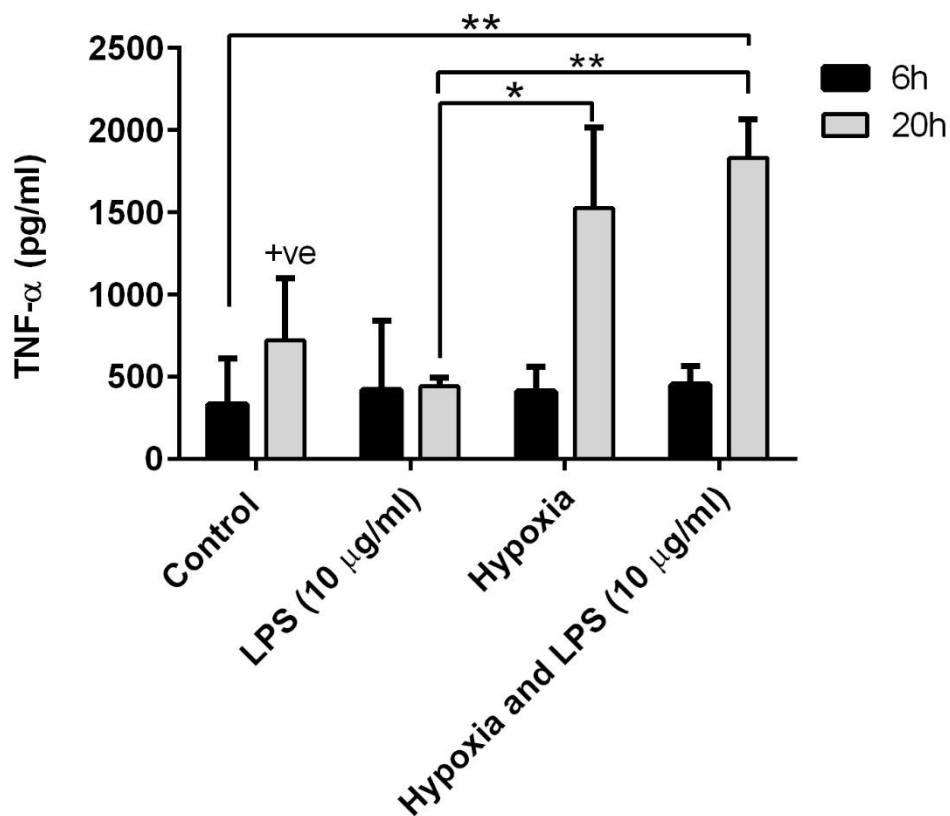


Figure 7-13 Expression of TNF- α protein from PTEC of human kidney after stimulation with LPS (10 μ l/mg) and/ or hypoxia for 6 and 20h in comparison to control and positive control; n=3, data were presented as mean \pm SD, p (*) < 0.05, (**) \leq 0.01, (***) \leq 0.001. LPS: lipopolysaccharide.

7.1.7 Treatment with human erythropoietin recombinant protein

Erythropoietin (EPO) is a glycoprotein originating predominantly from kidneys of adult humans (peri-tubular cells) although brain and neonatal liver are other possible sources for it (Kristensen *et al*, 2013; Yang *et al*, 2011). Its production is under the control of HIF-1 α and it is involved in erythrocyte formation. Pharmaceutically, during the last 2 decades a recombinant human EPO (r-hu-EPO) has been prepared and frequently used to treat anaemia of chronic illnesses such as in end stage renal diseases, malignancy and post operation (Bernhardt *et al*, 2010).

A cytoprotective effect of erythropoietin especially after ischemia reperfusion injury has been recorded through pleotropic mechanism; Hochhauser *et al.*, (2008) found that erythropoietin could decrease the hepatic injury in transplanted liver. Later, Fu *et al.*, (2013) confirmed this conclusion using a rat model. Although the exact mechanism of hepatocyte protection is not clear, it could be due to stimulation of intracellular signals like c-Jun N-terminal Kinase (JNK) and phosphatidylinositol 3-kinase which inhibit cell apoptosis (Hochhauser *et al*, 2008; Fu *et al*, 2013). Similarly, erythropoietin showed a protective effect on cardiac myocytes against IRI after myocardial infarction (Calvillo *et al*, 2003) and other heart diseases such as cardiomyopathy, arrhythmia and heart failure which generate ischemic conditions in heart muscle (Kim, Oudit and Backx, 2008; Burger *et al*, 2009; Ammar *et al*, 2011). Furthermore, studies showed similar protective impact of EPO against IRI in retina, reproductive system and neurons (Sasaki, 2003). Hence, the ischemia reperfusion injury in different tissues could be abrogated by treatment with EPO.

Interestingly, EPO has a remarkable prophylactic influence in renal IRI though the exact mode of protection is unclear (Spandou *et al*. 2006). According to Westenfelder *et al.* , (1999), renal cells such as mesangial, proximal tubular and medullary collecting duct cells have its own erythropoietin receptor (EPO-R). Direct binding to EPO-R activates JNK, mitogen-activated protein kinase (MAPK), and the phosphatidylinositol 3-kinase (PI3/Akt). Consequently, this activation leads to up-regulation of both anti-apoptotic (Pallet *et al.*, 2009) and anti-oxidative (Katavetin *et al.*, 2007) genes. In addition, EPO has an anti-inflammatory role by ameliorating apoptosis via a decrease of PML in the interstitial tissue (Hu *et al*, 2012).

7.1.7.1 EPO treatment after ischemia

The HNSR model was set as above using HK-2 cell line but 50 U/ml of human erythropoietin recombinant protein (eBioscience) was added to the media during reperfusion period. Then, reading was done via measuring LDH release from the supernatant of the cells using LDH kit (Promega).

7.1.7.2 EPO treatment before and after ischemia

The experiment was performed similar to the above model but 50 U/ml of human erythropoietin recombinant protein (eBioscience, 14-8992) was added 1 hour before induction of ischemia and another 50 U/ml during reperfusion.

Erythropoietin may have a protective effect against renal IRI (Sharples *et al*, 2004; Yang *et al*, 2011). To investigate the above renoprotective effect IRI model was performed. In this experiment the conditions were similar to the set up model where IRI for HK-2 cells were induced by hypoxia and or Locke's buffer but a 50 U/ml Erythropoietin was added for the reperfusion media for 48 hours after exposing the HK-2 cells to the ischemia. The most protective effect for EPO was obtained with combination of hypoxia and Locke's rather than with hypoxia and Locke's buffer alone.

A comparison was done between two modalities of EPO treatment in order to find the method of EPO treatment that gives best protective effect. In the first, the EPO (50 U/ml) was added to the reperfusion media after exposure to ischemia. While in the second, the EPO (50 U/ml) was added also one hour before exposure to ischemia and after exposure to ischemia). According to Sharples *et al* (2004) EPO treatment for 1 hrs before ischemia has protective effect against IRI (data not shown). In summary, these were a preliminary experiments that should be confirmed by further analysis.

7.1.8 Immunohistochemistry (IHC) for examining C5-9 in HNSR model

7.1.8.1 Technique

HK-2 cells were grown on coverslip in 6-well plate and were incubated until 80% confluent. Cells were exposed to HNSR as mentioned in chapter 3 before quick rinsing with PBS. Secondly, cells were fixed using methanol at room temperature for 5 minutes followed by PBS washing three times for 5 minutes each. Thereafter, the adherent cells were incubated with PBS containing 0.1–0.25% Triton X-100 for 10 minutes (to improve the penetration of the antibody) followed by three 5 minute washes with PBS.

Next, cells incubated with 1% BSA (bovine serum albumin), 22.52 mg/mL glycine in PBST (PBS+ 0.1% Tween 20) for 30 minutes for blocking unspecific binding of the antibodies. Then cells were incubated in anti-C5b-9 antibody [aE11] (ab66768) (Abcam, Cambridge, USA) in 1% BSA in PBST in a humidified chamber for 1 h. Later, the solution was discarded and cells were washed three times in PBS, 5 min each wash. 100 µl DAKO chemoMate En Vision detection kit HRP – rabbit / mouse labelled polymer (K5007 ENV) was added for 30 min at room temperature followed by another run of washing with PBS (3X5 min). and diluted DAB peroxidase chromogen was added for 3 minutes sharp. Finally, PBS washing 3X5 min was performed, and then the slides were counterstained with 0.5 % (w/v) Toluidine Blue and / or Haematoxylin- eosin stain in 1% acetic acid (5 min) and followed by cover slipping with DPX to be examined under light microscope 40X (oil).

7.1.9 Fluorescence-activated cell sorting (FACS)

7.1.9.1 Principle

Fluorescence activated cell sorting (FACS) is a flow cytometric technique measuring and analysing the scattered light and fluorescence emitting from target cells after stimulating them with light beam (laser).

Cells are suspended in fluid media and are channelled singly through a laser beam. Then light scattering from cells or their components are produced as a result of light beam reflection and refraction from each cell. There are two types of scattering; Forward (FSC),

which is used to measure cell sizes, and side (SSC) to assess the granularity of cells. Fluorescent dyes (fluorochromes) that are excited at various wave lengths conjugated to specific antibodies to detect those cells expressing the antigen of interest. The most commonly used couple of fluorochrome are fluorescein isothiocyanate (FITC) and phycoerythrin (PE) because their peak emission spectra are well separated. Light signals (FSC and SSC) and fluorescence (FITC and PE) are detected and are converted to electrical charges for analysis via specific software).

To prepare a plot that can be used for the coming experimental samples, a gate is performed when the collected values from the FSC and SSC are recognised and boundaries set up to confine the test to the target sample. This is followed by fluorescence compensation by which data from both fluorochromes (FITC and PE) are calculated to measure the percentage of interference between them.

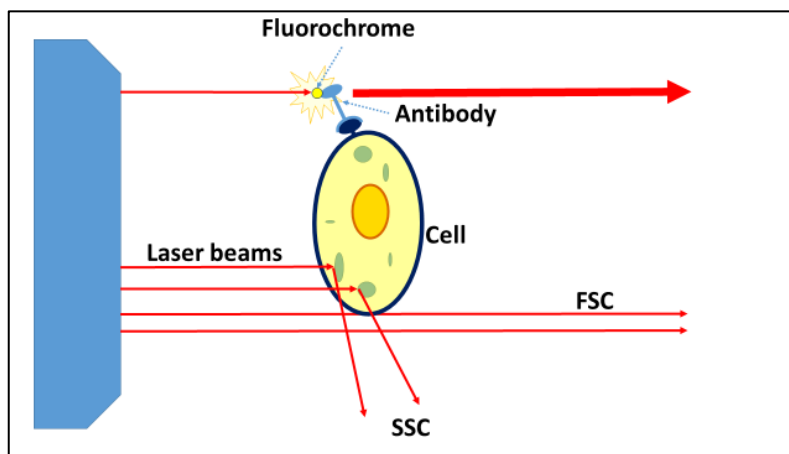


Figure 7-14 Light scattering and fluorescence emission from single cell. The Laser beams reflect and refract from cell (or its components) resulting forward scattering (FSC) and side scattering (SSC). A fluorescent emission excite from the fluorochrome-labelled antibody after its binding to cellular antigen.

7.1.9.2 Technique

Proximal tubular epithelial cell of human kidney (HK-2) were resuscitated from frozen stocks and grown in their usual media before seeding them in 6 medium size (25 cm²) flasks. 0.7×10^6 cells were seeded in each flask and were incubated overnight to adhere. The HNSR model was performed as usual (chapter 3) with control and experimental groups for each time points. Suspended cells were isolated from supernatant by centrifugation at 1500 rpm for 5 minutes at room temperature while the adherent cells

were collected from flasks by trypsin treatment followed by two cycles of washing with normal media and centrifugation at 1500 rpm for 5 minutes at room temperature. The pellet was washed twice with bovine serum albumin (BSA)-containing buffer solution after discarding media. According to the manufacturer's protocol (FITC Annexin V Apoptosis Detection Kit with PI, San Diego, USA), cells were re-suspended in Annexin V binding buffer at a concentration of 0.25×10^7 cells per ml. Thereafter, a 100 μ l of cell suspension was transferred in a 5 ml test tube and both 5 μ l of FITC Annexin V and 10 μ l of propidium iodide solution were added. After mixing with mild vortex cells were incubated at room temperature (25 °C) in dark place for 15 minutes. Thereafter, 400 μ l of Annexin V binding buffer was added and analysed using FACS DIVA machine and software.

7.1.9.3 Results

FACS was used to assess the presence of both apoptotic and necrotic cells after exposing HK-2 cells to HNSR injury. Results showed no differences among experimental groups and their controls.

Table 7-3 FACS for HK-2 cells exposed to HNSR injury

	Q1				Q2				Q4			
	Necrotic cells				Late apoptosis/ necrotic cells				Early apoptotic cells			
	Annexin V ^{-ve} / PI ^{+ve}				Annexin V ^{+ve} / PI ^{+ve}				Annexin V ^{+ve} / PI ^{-ve}			
	n=1	n=2	n=3	Mean	n=1	n=2	n=3	Mean	n=1	n=2	n=3	Mean
Control 6 h	0.5	1.5	0	0.67	4.4	3.4	0	2.6	0.6	1.1	3	1.57
HNS 6 h	0.2	0.6	0.8	0.53	3.2	4	11.6	6.27	0.8	0.7	1.8	1.1
Control 24 h	0.3	0.3	1.9	0.83	2.8	1.1	11.1	5	0.7	0.4	2.7	1.27
HNSR 24 h	0.3	0.4	0.9	0.53	2.5	1.8	6.5	3.6	0.8	0.2	1.2	0.73
Control 48 h	0.4	0.5	2.1	1	5.2	1.6	9.8	5.53	1.4	0.6	3.5	1.83
HNSR 48 h	0.3	0.3	1	0.53	3.3	1.3	6.2	3.6	1.5	0.6	1.2	1.1

7.2 Human podocyte

Podocyte cells were a gift from Professor Saleem Moin from Bristol University. The podocyte cells were grown in 25 cm² flask using RPMI (PAA, 1640) containing L-glutamine (20 mM), 10% Fetal Calf serum (FCS), 200 µg /ml recombinant human epidermal growth factor HEGF (Sigma-Aldrich, MO, USA), penicillin (100 IU/ml) and streptomycin(100 µg/ml) . These cells express a temperature sensitive SV40 promoter that allows proliferative, undifferentiated growth at 33 °C where the cells take on a cobblestone appearance while differentiated growth at 37⁰ C leads to cessation of the bodies of the cells are unevenly distended and spindle- shaped projections are formed (Figure 7-15 A). That is why the cells were kept in 33⁰ C incubator for 7 days until they become confluent then transferred to a 37⁰ C incubator to allow them to be differentiated. These cells were then split and were maintained in the same way as for HK-2 cells (Oshima *et al*, 2011).

Podocytes were stimulated with the 3 injurious stimuli (Locke's alone, hypoxia alone, and both) following the same protocol of HK-2 cells (**Error! Reference source not found.**). Results were similar to those of HK-2 cells where LDH release was increased with increased duration of treatment as and was more in combined treatment than exposure to each stimulus separately (Figure 7-15 B).

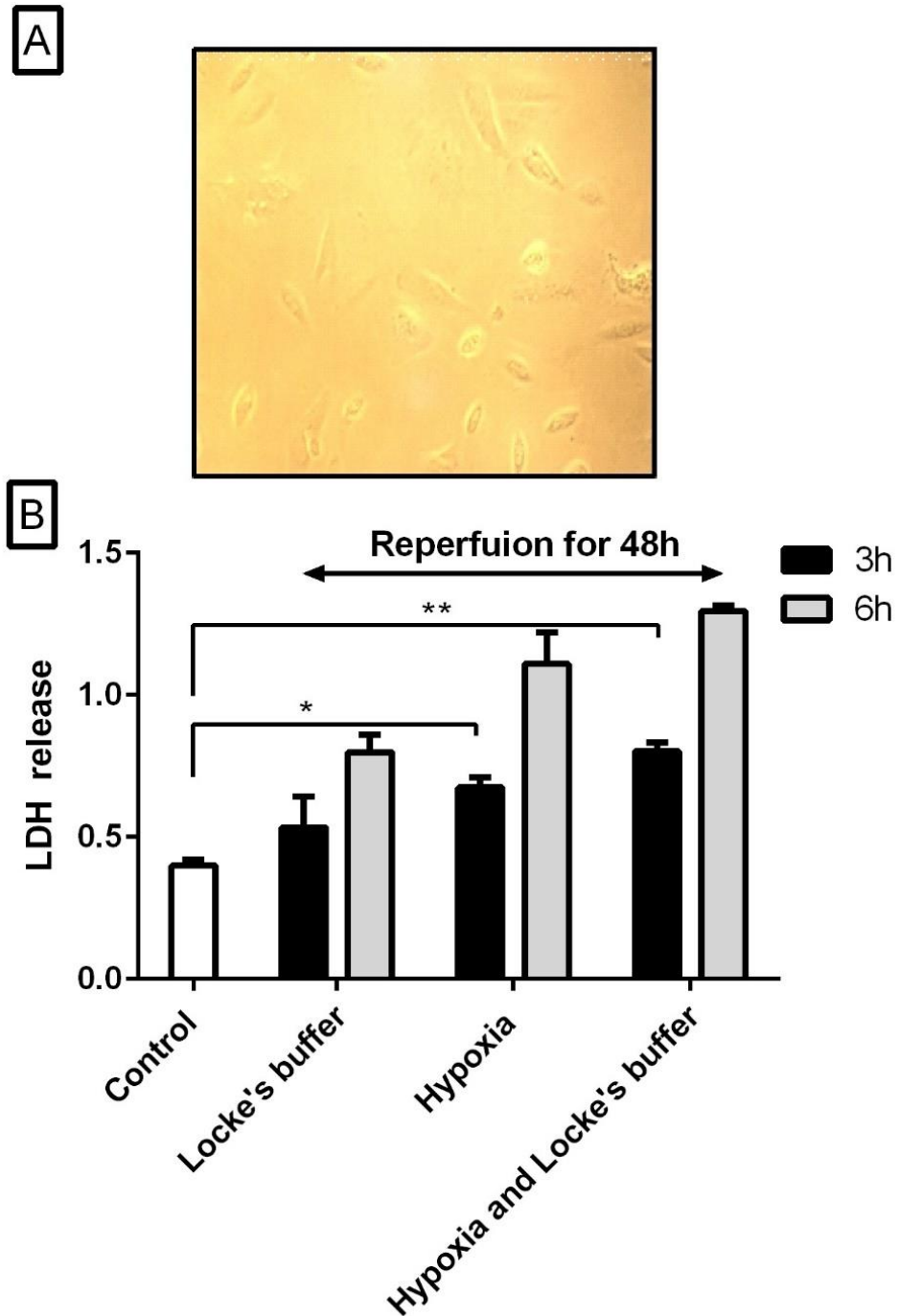


Figure 7-15 Confluent human podocytes under light microscope (X 40) (A) and a graph shows effect of nutrient starvation (Locke's buffer) and / or hypoxia for 3 and 6 hours with media replenishment for 48 hours on LDH release from supernatant of human podocytes (B); Data were presented as mean \pm SD, p (*) < 0.05 , (**) ≤ 0.01 .

7.3 Primary mouse renal tubular cells (RTC)

7.3.1 Mouse renal tubular cell (RTC) culture

Many attempts to culture mouse RTC were made using protocols obtained from other studies; the method of Chana, Sidaway and Brunskill, 2008 gave a good yield of RTC with predictable monolayers at 30 days. To prepare RTCs from mice, explanted kidneys from schedule 1 culled mice were collected in to HBSS (20 ml). Under strictly sterile conditions, the kidneys were transferred to a Petri dish of Hank's balanced salt solution (HBSS). The capsule of the kidneys was removed with scalpel blade and forceps, and the outmost layer of the cortex was carefully pared off.

The collected cells were centrifuged for 5 min. at 1000 rpm. Thereafter, the formed pellets were washed twice with HBSS and were re-suspended with 9.5 ml HBSS and 100 μ l of collagenase type II enzyme (Sigma-Aldrich, MO, USA). After incubation for 2 min at 37^oC incubator, digestion was stopped by adding 20 ml DMEM: F12 containing 10% FCS. Another two washes with 20 ml DMEM:F12 media was done, then the pellet was re-suspended with 5 ml of DMEM:F12 media which contained specific substances suitable for mouse RTC as mentioned below. Lastly, 2.5 ml of media was plated out and these flasks were kept in the incubator without any movement for 7 days until the cells could be seen under microscope. Finally, the developed cells were maintained as usual for the human PTEC culture but with the DMEM:F12 media that contains insulin (5 μ g/ml) (Sigma-Aldrich, MO, USA), triiodothyronine (4 pg/ml) (Sigma- Aldrich, MO, USA) and hydrocortisone (36 ng/ml) (Sigma- Aldrich, MO, USA).

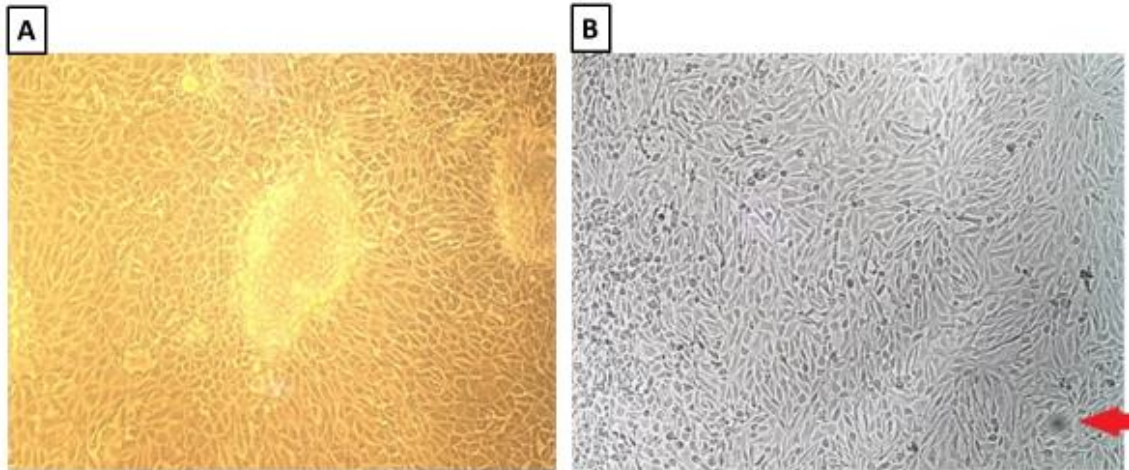


Figure 7-16 PTEC cells of WT (A) and P^{KO} mouse (B). Numerous dome formations due to the existence of tight junctions and an intact transcellular transport process are characteristic manifestations of confluent cultures

7.3.2 Testing the sensitivity of mouse RTC to HNSR model

The HNSR model with hypoxic environment and Locke's buffer that was used in the HK-2 cells was implemented to the RTC, which are prepared from both properdin knockout and wild type mice for the same time points. The media used for reperfusion is the same media used for culturing these primary cells.

7.3.3 Properdin knockout mouse

To assess if HNSR can be established for mouse RTC and if the sensitivity of mouse RTC depends on properdin, the established model of *in vitro* IRI was used to establish two sets of experiments for the RTC of properdin knockout and wild-type mice. Regarding the properdin deficient, the result showed that there were no significant differences in the LDH release in comparison to the control group although there was less cell membrane damage when the time of ischemia was 3 hours compared to 6 hours and control. These results would recommend for further studies on both knockout and wild-type mice to compare two genotype.

7.4 Cadaveric kidneys

7.4.1 Introduction

7.4.1.1 Kidney preservation

A key predictive factor of success in kidney transplantation is the method of preservation of the retrieved organ (Jamieson and Friend, 2008). To reduce ischemic insults, the harvested organ is immersed in cold isotonic buffers that minimise metabolic activity and decrease cell damage (Vogel *et al*, 2012; Jamieson and Friend, 2008). Various types of preservation solutions are used in daily practice; nonetheless, cold static solution (Table 7-4) is the most commonly used buffer (Hosgood, Hunter and Nicholson, 2012). Reducing temperature by 10 °C results in a 2-3 fold decrease in metabolic activity and subsequently, less consumption of adenosine triphosphate (ATP) and decreased phospholipid hydrolysis. This method influences favourably the damage from consequent reperfusion through reducing the deposited waste products metabolised during reperfusion (Jamieson and Friend, 2006; Hosgood, Hunter and Nicholson, 2012). This preservation method is both time-controlled and much less effective with increasing storage time as the generation and accumulation of metabolite and toxic substances slows to 10% but does not cease (Jamieson and Friend, 2006; Jamieson and Friend, 2008).

Table 7-4 components of cold static solutions that are widely used in kidney preservation before renal transplantation surgery. * Essential components that are common in all formulas (Adapted from: (Hosgood, Hunter and Nicholson, 2012).

	Components	Examples	Effects
1	Impermeants*	Glucose, lactobionate, mannitol, raffinose, sucrose	Decrease swelling and provide stability to the ultra-structure of the cell
2	Colloid	Hydroxyethyl starch (HES), polyethylene glycol (PEG)	Maintain osmotic pressure
3	Buffers*	Citrate, histidine, phosphate	Decrease intracellular acidosis and minimize cellular swelling
4	Electrolyte*	Calcium, chloride, magnesium, magnesium sulphate, potassium, sodium	Decrease intracellular acidosis and minimize cellular swelling
5	Anti-oxidants	Allopurinol, glutathione, tryptophan	Preserve cell viability
6	Additives	Adenosine, glutamic acid, ketoglutarate	Nucleotide metabolism?

7.4.1.2 Normothermic perfusion (NP)

Normothermic perfusion (NP) could be defined as perfusing an organ that is prepared for transplant surgery at a physiologically normal temperature. Usually, NP is performed after organ dissection from the donor body and prior to implantation and restoring circulation into the organ within the recipient body. Unlike cold preservation, NP seeks to maintain oxygen and nutrient supply without an ischemic period (in an ideal situation) as well as preserving organ function in a normothermic environment. Accordingly, NP minimises cellular injury resulting from cooling during classical preservation, decreases IRI and enables evaluation of function and viability of the organ (Jamieson and Friend, 2006; Morris and Knechtle, 2013; Vogel *et al*, 2012).

7.4.1.3 Sources of donor kidneys

There are two sources for kidneys used in transplantation for patients with end-stage renal diseases; they are donated from either a living human or cadaver (Terasaki *et al*, 1995). The latter are also of two variants; kidneys recovered from deceased patients with brain death (BD) or circulatory (cardiac) death (CD) (Damman *et al*, 2011a). There is some reservation to use kidneys from victims of CD over BD, but the demand for using kidneys from BD and CD donors is substantial (Watson *et al*, 2010), when there is a shortage of kidneys harvested from living donors, which are by far superior (Pratschke *et al*, 2001).

Donors after brain death (DBD) refer to patients whose hearts are beating but fulfil the brainstem death criteria (Sade, 2011). If left without management, donors with BD suffer from multiple hormonal, physiological and inflammatory consequences resulting in cardiac arrest and deterioration in the outcomes after kidney transplantation (Barklin, 2009; Bugge, 2009). Conversely, donors after circulatory (cardiac) death (DCD) could be defined as individuals with irreversible cardiopulmonary arrest, irreversible brain injury, their death has been certified and inevitable but they do not satisfy the brain death criteria; however, those are grouped as Maastricht category 3 (British Transplantation Society, 2004; Steinbrook, 2007).

Brain death has both local and systemic effects. The systemic consequences are due to a combination of (i) hemodynamic disturbances through catecholamine storming because of the injured brain stem, (ii) hormonal and metabolic changes, (iii) endocrine and neuropeptide turbulences and (iv) release of mediators secondary to brain ischemia

(Kosieradzki and Rowiński, 2008; Barklin, 2009). These changes lead to organ ischemia and endothelium activation which, as a whole, cause a systemic inflammatory reaction; however, these conflicts affect many organs inside the body such as lung, liver, heart and kidneys resulting in poor outcomes after donating them for transplantation (Auråen *et al*, 2013). Nevertheless, studies about BD effects on kidneys were controversial, varying from presence and to absence of differences in the expression of various types of cytokines and adhesion molecules between kidneys harvested from living donor and brain death (Kim *et al*, 2000; Barklin, 2009).

On the other side, DCD kidneys suffer from various period of warm ischemia before usual cold storage period. This may affect negatively the outcome after implanting such kidneys though the exact post-transplant prognosis is still unclear resulting in excluding DCD kidneys from the evidence-based national organ-sharing scheme, where DBD kidneys are allocated, and are kept within individual transplant centres (Summers *et al*, 2010).

7.4.1.4 Role of complement fragment (C4d) during renal IRI

The serum of an adult contains around 200- 600 µg/ml of a glycoprotein of about 200 kDa named C4. It is composed of 3 subunits (α , β , and γ) which bind together via disulphide bonds (Odink *et al*, 1981; van den Elsen, Jean MH *et al*, 2002). C4 plays a crucial role in the activation of the complement system through leading to formation of C3 and C5 convertase. While activation of C4 occurs by both the classical and MBL pathways (Murata and Baldwin III, 2009; Nickleit *et al*, 2002), through either of them, C4 is split to a small fluid phase C4a part which diffuses away and a large C4b fragment. C4b remains active for microseconds only because of the vulnerability of its exposed thioester bond of the α chain to react with any neighbouring protein or carbohydrate. Consequently, around 95% of C4b is hydrolysed with water and is dispersed in blood or interstitial fluid. In the meantime, the active C4b binds to C2a forming C3 convertase, which cleaves C3 to C3a and C3b. This in conjugation with factor B, leads to initiation of the alternative pathway (Murata and Baldwin III, 2009). C4b is inactivated by factor I (FI) forming iC4b which is split by FI to a large fragment, C4c, that is degraded and a small functionless molecule that covalently adheres via thioester bond to the cell membrane, called C4d (Feucht and Opelz, 1996; Murata and Baldwin III, 2009) (Figure 7-17). Currently, C4d is a recognised biomarker for immune mediated graft rejection

due to its ability to permanently deposit in the tubular epithelium of transplanted organs (Feucht and Opelz, 1996; Watschinger and Pascual, 2002).

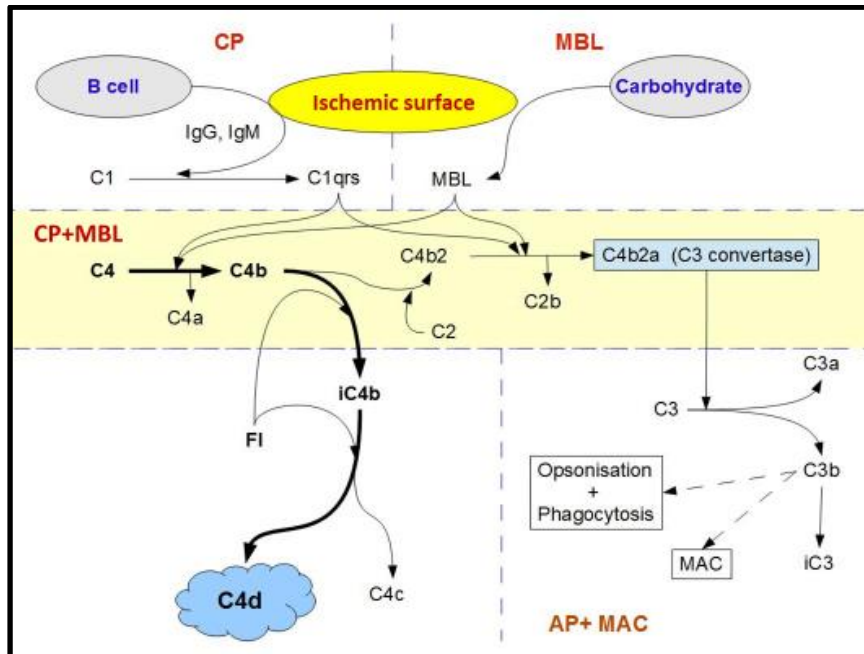


Figure 7-17 C4d formation and its relation to complements pathways. CP (complement pathway), MBL (mannose binding lectin), AP (alternative pathway), MAC (membrane attack complex).

7.4.1.5 Role of von Willebrand factor (vWF) in renal damage during IRI

vWF is important in haemostasis via changing platelets morphology, facilitating their accumulation and sticking them to each other, potentiating their adhesion to the vessel wall in addition to protecting factor VIII from destruction (Brouland *et al*, 1999; Lau *et al*, 2003). The multimeric adhesive glycoprotein, vWF, is composed of polypeptide chains, which are linked by disulfide bonds forming 500 kD dimers inside the endoplasmic reticulum then in Golgi apparatus, these dimers oligomerise to multimers that may be more than 10000 kD by creating disulfide bonds between the dimers (Brouland *et al*, 1999; Mendolicchio and Ruggeri, 2005). Eventually, the multimerised or mature vWF is stored in Weibel-Palade (WP) bodies, specialised organelles in the endothelial cell (EC) (Haberichter *et al*, 2005; Brouland *et al*, 1999). Megakaryocytes and platelets are considered another source for vWF production with presence of α - granules as storage organelles for vWF (Ruggeri, 2007).

vWF is liberated from EC to the plasma either immediately after synthesis (so called constitutive pathway) or secreted from the storage Weibel-Palade granules after

stimulation (so-called regulated pathway) (Brouland *et al*, 1999; Ruggeri, 2007; Mendolicchio and Ruggeri, 2005). *In vivo*, the circulating (i.e. plasma) vWF originates merely from EC as platelets do not secrete their vWF contents unless activated (Ruggeri, 2007). While *in vitro*, various stimulants lead to the secretion of vWF such as histamine, thrombin, oxidative stress and complement (Brouland *et al*, 1999). The mature vWF is unfolded after its secretion from the WP bodies under the influence of the shear stress at the site of the endothelial damage to participate in initiating platelet accumulation at the site of injury (Reininger, 2008). Later it is cleaved in plasma by a metalloproteinase (ADAMTS13) in order to prevent unwanted thrombi (Mendolicchio and Ruggeri, 2005; Ruggeri and Ruggeri, 2004; Levy *et al*, 2001) (Figure 7-18). Other studies illustrated the usage of vWF as an indicator for EC injury (Jahroudi and Lynch, 1994) in spite of the lack of information about its expression *in vivo* particularly after organ transplantation (Brouland *et al*, 1999). The expression of vWF increases commensurate with EC damage (Lip and Blann, 1995). Hence, expression of vWF reactivity could be a reliable marker for assessing endothelial damage during IRI.

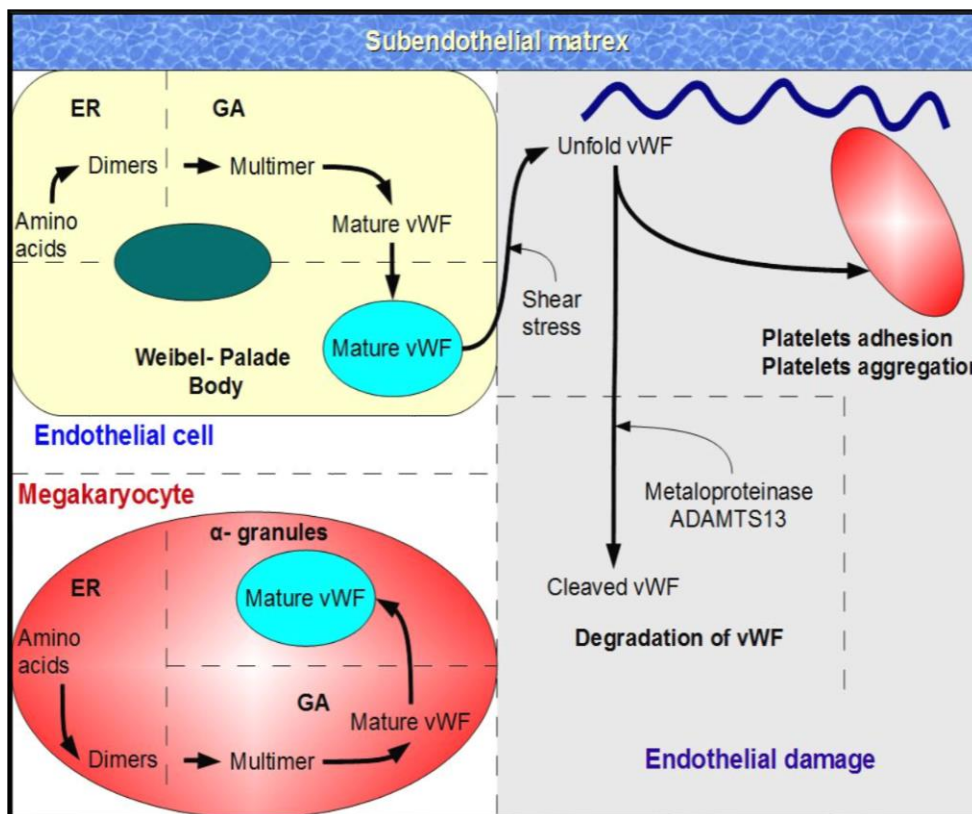


Figure 7-18 vWF synthesis and regulation during endothelial injury. ER (Endoplasmic reticulum), GA (Golgi apparatus)

The purpose of this chapter is to assess kidneys procured from DBD and DCD that were not transferred to the patient after subjective assessment by the surgical team as well as the impact of normothermic perfusion (NP) prior to surgery on these kidneys.

7.4.2 Materials and methods

This was a retrospective analysis for 60 kidneys (24 were from DBD and 36 from DCD) deemed to be unsuitable for transplantation which were perfused for 1 hour at room temperature (NP) after a variable time of storage. Clinical biopsies were collected from deceased kidneys before and after perfusion and embedded in paraffin wax (Leicester General Hospital) for further analysis.

7.4.2.1 Ethics

From October 2012 to October 2013, 60 kidneys, which were considered unsuitable for transplantation were recruited in this laboratory research project by the renal transplant group team at Leicester General Hospital (headed by Professor Michael L. Nicholson). The transplant coordinators before organ retrieval obtained consent from the donor family for the use of the organs for research. Ethical approval was granted for the study by the national research ethics commission in the UK (Ref UHL 77018; Ex-vivo normothermic perfusion of disused human kidneys; REC: 12/EM/0143; principle investigator: Professor Michael L Nicholson).

7.4.2.2 Immunohistochemistry (IHC)

7.4.2.2.1 Principle

Immunohistochemistry (IHC) is a method to detect presence of antigens (including protein expression) and their distribution within examined tissue cell. It involves multiple steps of tissue preparation and treatment that deploys biochemical, histological and immunological principles and enables a labelled antibody to interact with and localise the antigen of interest (Dabbs, 2013; Ramos-Vara, 2011).

7.4.2.2.2 Technique

In this chapter, IHC was used to assess semi-quantitatively the deposition of vWF in endothelial cells of renal glomeruli and C4d in renal tubules of the discarded kidneys.

Five-micrometer microtome sections from these blocks were floated on water at 52⁰ C and were attached to glass slides. The sections were de-waxed in two changes of xylene (5 min) and brought to water via methanol (99% IMS). Thereafter, slides were immersed in PBS for 7 min. Initially, for antigen retrieval, digestion of protein in tissue section was tried using proteinase K (40 µg/ml) after warming at 37⁰C. This step was cancelled as the results were better without it. Next, a 100 µl DAKO chemoMate Peroxidase blocking solution (DAKO) was added for 5 min at room temperature then was drained. As blocking agent, 3% (w/v) bovine serum albumin (BSA) 0.5% Tween-20 in PBS was used (20 min, room temperature). Later, slides were washed in PBS, 3X5 min.

Mouse monoclonal antihuman C4d antibody (Quidel) (1:250) or polyclonal vWF were added as primary antibody and the slides were incubated overnight at 4⁰ C. Optimisation of vWF concentration was necessary as all the starting dilution (1/100) and subsequent ones (1/1000, 1/2000, 1/5000) showed too much reactivity. After washing (3 x 5 min), a 100 µl DAKO chemoMate En Vision detection kit HRP – rabbit / mouse labelled polymer (K5007 ENV) was added for 30 min at room temperature. Then, another run of washing with PBS (3X5 min) and diluted DAB peroxidase chromogen (diaminbenzidine tetrahydrochloride) was added for 3 min sharp. Finally, PBS washing 3X5 min was performed, and then the slides were counterstained with 0.5 % (w/v) Toluidine Blue and / or Haematoxylin- eosin stain in 1% acetic acid (5 min) and followed by cover slipping with DPX to be examined under light microscope 40X (oil).

7.4.2.3 Western immunoblotting

While its principle was explained in chapter 5, this well-known protein assay was launched in this chapter to examine semi-quantitatively C3, β-actin and vWF protein expression from renal tissues of collected kidneys.

7.4.2.3.1 Preparation of tissue homogenate:

At the beginning, tissue biopsies were selected randomly. Then, each tissue is weighed before adding 9 volumes Tris acetate (TA) buffer solution (50 mM) pH to 7.5.

The tissue was mashed using pestle and mortar. Next, centrifugation of the homogenate was performed at 13000 rpm for 10 minutes 4⁰C. Later, the supernatant was collected in 1.5 ml reaction tubes after proper labelling. Finally, it is fundamentally important to carry out the procedure under liquid nitrogen.

7.4.2.3.2 Protein assay

Total protein in tissue homogenate of each specimen was measured accurately and loading volumes were adjusted accordingly to get equal amounts of protein in each well (methods were explained at appendix page).

DC protein assay (Bio-rad, Hertfordshire, UK) kit was used to assess protein concentration of the homogenate. Serial dilutions of Bovine serum albumin (Sigma-Aldrich, MO, USA) from 2000 µg/ml until 750 µg/ml) with PBS were performed. The sample had to be diluted with dH₂O to yield a total volume of 50µl. Then, using 96- well plate, 25 µl of already provided reagent A and 200 µl of reagent B were added to the well. Both the standard and the sample had to be vortexed before withdrawing from them a 5 µl aliquot. A duplicate of each were added to the plate. Then, the plate was shaken for 5 second before absorbance was read using the plate reader (Labsystem, multiskan EX) (program 630, ABORT once mixed). Absorbance results were plotted against standard (BSA) serial concentrations getting standard curve where absorbance were interpolated to calculate total protein concentrations of specimens (Figure 7-19).

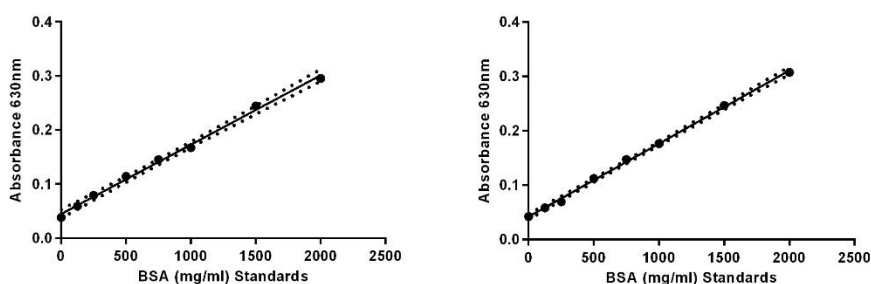


Figure 7-19: Standard curve of total protein assay of tissue homogenate from deceased kidneys (DBD and DCD donors) in preparation for western immunoblotting.

7.4.2.3.3 Running the gel

Precast Bio-Rad miniprotein TGX 4-20% 10 well (456-1093) were used as a readymade SDS gel. 20 µg of protein were loaded with sample loading buffer 1: 1 (4% β-mercaptoethanol) in each well together with the ladder (BIO RAD#161-0374) which followed by running the gel run at 150 Volts for 90 min. The recipe of 10 X running buffer for 1 L 25 mM Tris (30.3g), 192 mM (Glycine (144g), SDS (10g), pH 8.3.

7.4.2.4 Histopathological assessment

Evaluating histopathological changes were based on Remuzzi scoring system that examines four different parameters: Glomerular global sclerosis, tubular atrophy, interstitial fibrosis and vascular lesions (Remuzzi *et al*, 2006). Sections were scored by a consultant pathologist who was blinded to the donor types. The score ranged from a minimum of zero (indicating the absence of renal lesions) to three (severe). The sum of the four parameters was calculated where a score of 0-3 indicated mild changes, 4-6 moderate and 7-12 severe.

7.4.2.5 Statistics

Data were presented as mean ± SD and were compared using Students' two way ANOVA and multiple t-test. Categorical variables were analysed by Pearson's test. $P < 0.05$ was considered statistically significant. GraphPad Prism 6.07 was used for statistical analysis (GraphPad Software, La Jolla, California, USA).

7.4.3 Results

The results of the *ex vivo* work were collected, analysed and presented in this part in sections. Firstly, data about C4d deposition comparing between two sources of donated kidneys were illustrated, followed by identifying the relations with histopathological changes, renal functions and storage time. Data on vWF reactivity, C3 and β-actin were presented in the same fashion. Lastly, the effect of NP on C4d deposition and vWF production from deceased kidneys was shown; some supportive results were explained in the appendix.

7.4.3.1 Renal tubular epithelial deposition of C4d before NP

Epithelial C4d reactivity has been described in allograft rejection and IgA nephropathy (Xu et al., 2009; Maeng et al., 2013). Renal proximal epithelial cells are especially sensitive to ischemia-induced injury (Yu et al., 2013). Therefore, reactivity for thioester bonded C4 activation product C4d was examined in tubular epithelium. Immunohistochemical analysis was performed using a monoclonal antihuman C4d antibody as primary antibody. The slides were examined under light microscope at 40X. Two to three independent observers blinded to the sample groups evaluated the slides. Initially, the number of C4d deposits per 10mm² was established, but was found to be too variable between observers. Next, we refined our evaluation by qualitatively scoring the extent of tubular involvement for C4d deposition which proved reproducibility between observers (Figure 7-21 A-E). Kidneys were categorised into four subgroups according to degree and pattern of C4d deposition in the renal tubular area. This was in line with Banff scoring system for detecting post-transplant renal rejection where 0% of tubules had shown C4d staining equal to nil, while up to 10% and 19-50% immunostaining were considered minimal and focal, respectively. When more than 50% of renal tubules were stained, it was marked as diffuse (Cohen *et al*, 2012).

Results revealed no significant differences in C4d deposition between DBD and DCD groups ($p > 0.05$) although presence of more C4d deposition in kidneys of DCD than DBD (Figure 7-21 F). Moreover, within DBD group, there was no significant variation among degrees of C4d deposition ($p=0.28$). Within DCD group, there was also no variation ($p=0.074$).

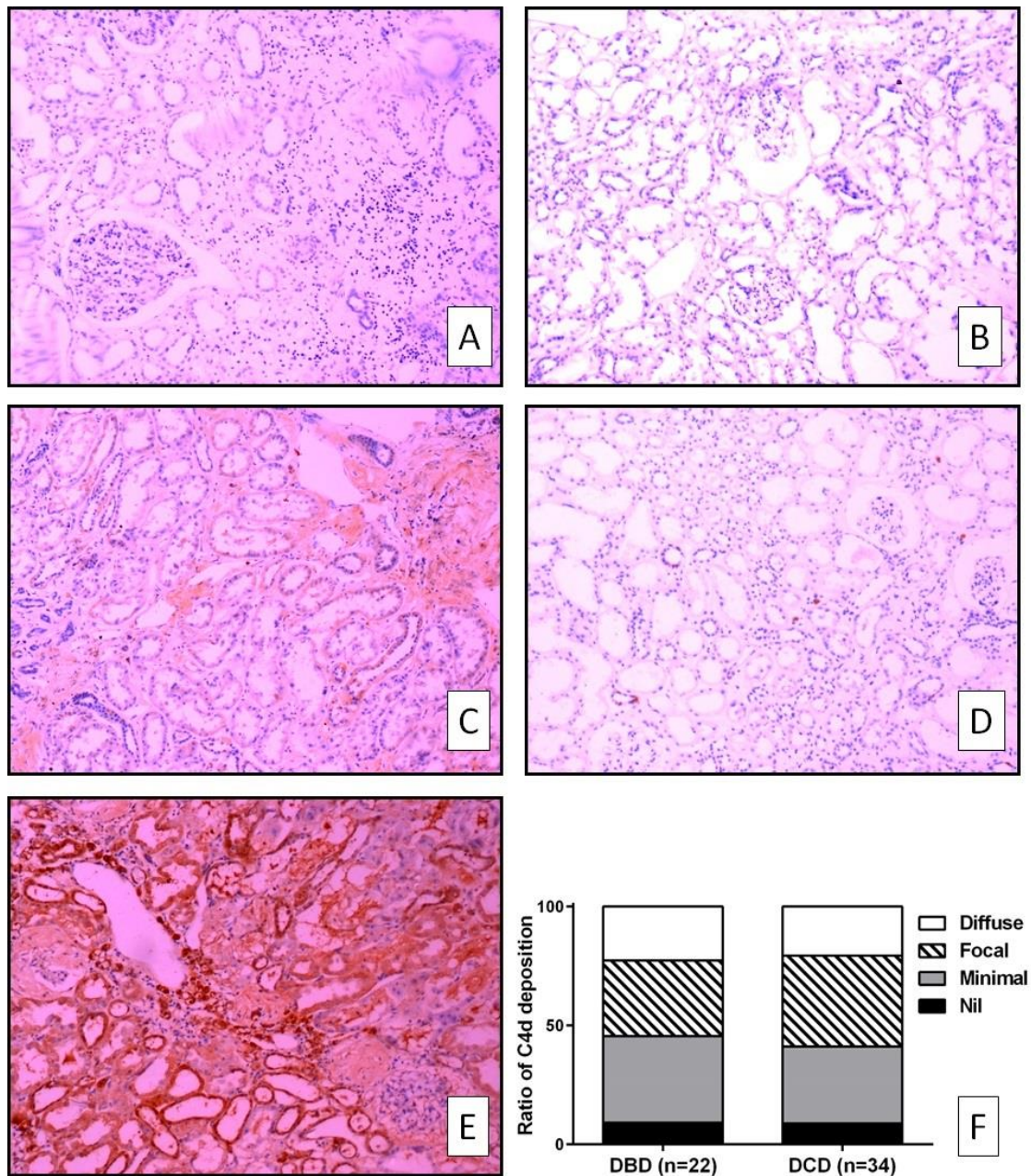


Figure 7-20 Immunohistochemical analysis of C4d deposition in tubular epithelium under light microscope (Olympus CX41) 10X using image Pro plus and Q imaging microPublisher 5.0 RTV; A: -ve control, B: no deposition, C: minimum deposition, D: focal deposition and E: diffuse deposition. F, comparison of scoring for C4d reactivities in DBD and DCD kidneys (n=22 and 34, respectively)

7.4.3.1.1 Relation of C4d deposition with histopathological scoring

Histopathological scoring is designed to assess the viability of donated kidneys for the purpose of transplantation via examining numbers of intact nephrons in these kidneys. A score of up to 3 assumes functioning kidney could be used for single transplants while a score between 4-6 means kidney is feasible for dual transplant while a score above six are not amenable to be transplanted (Remuzzi *et al*, 2006).

The degree of structural damage (histopathological score) among DBD and DCD kidneys as well as its relation with storage time are illustrated in appendix (7.4.3.3.4).

DBD kidneys showed increased diffuse C4d deposition in renal tubular epithelium with increased histopathological score ($r=0.97$; $p=0.15$). Oppositely, focal and minimal C4d deposition decreased with higher score ($r= -0.866$; $p= 0.33$ and $r= -0.427$; $p= 0.72$) respectively. In the meantime, nil C4d deposition in renal tubular epithelium was shown only in kidneys with the lowest histopathological score (Figure 7-21 A).

Similarly, in DCD kidneys, diffuse C4d deposition showed insignificant direct relation to histopathological score ($r= 0.879$; $p= 0.317$) while, focal and minimal C4d deposition decreased with higher score ($r= -0.991$; $p= 0.086$ and $r= -0.762$; $p= 0.448$) respectively. None of the kidneys with severe histopathological score had nil C4d deposition (Figure 7-21 B).

9.1% of DBD and 3% of DCD Kidneys showed mild histopathological score and no C4d deposition; 13.6% of DBD and 12% of DCD specimens revealed mild histopathological score and minimal C4d deposition.

These results suggested that C4d could be a marker of renal damage as its deposition, in renal tubular epithelium, was increased in the more damaged kidney although statistically this was not significant. In conclusion, C4d is not a discriminator between DBD and DCD pre-NP.

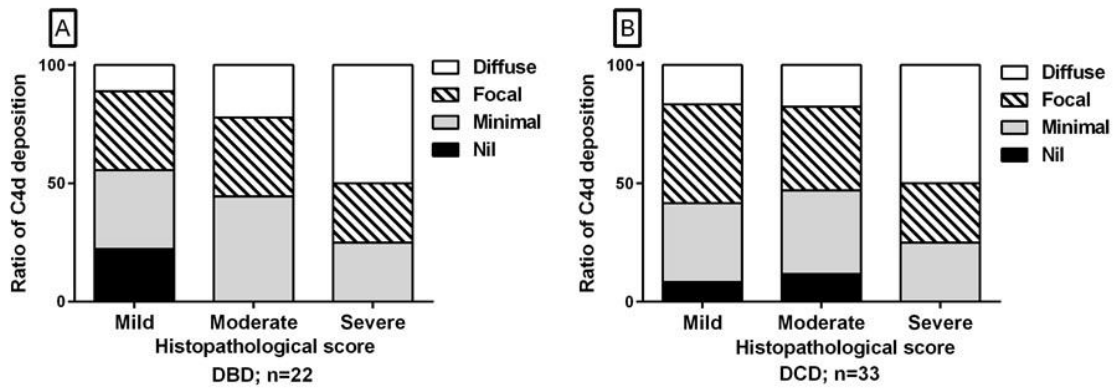


Figure 7-21 Semiquantitative analysis of C4d deposition in renal tubular epithelium plotted against histopathological damage in DBD (A) and DCD (B)

7.4.3.1.2 The relation of sum score with C4d deposition in renal tubular epithelium of DBD vs DCD kidneys

The distribution of the severity of C4d deposition over the grades of sum score in both DBD and DCD groups showed some patterns of increment in C4d accumulation with measuring of score grades. The sum score is a composite of functional measures and visual appearance. It is graded from better function (1) to worst (5) by finding the total summation of three factors (renal blood flow, urine output and visual score).

In DBD group, diffuse C4d deposition was raised over grades 1, 3 and 4. Nevertheless, the relations among sum score grades and C4d deposition were weak (r sum score vs nil = -0.74; sum score vs minimal = 0.27; sum score vs focal = -0.27; and sum score vs diffuse = 0.15) with p value equal to 0.15, 0.65 and 0.65 and 0.8 respectively (Figure 7-22 A).

Concurrently, the pattern of the diffuse C4d deposition in DCD specimens was significantly increased with higher sum score grades ($r = 0.88$; $p = 0.05$). By contrast, the focal deposition exhibited a significantly paradoxical pattern ($r = -0.9$; $p = 0.036$). There was no obvious correlation between sum score and either nil ($r = 0.46$; $p = 0.43$) or minimal ($r = -0.41$; $p = 0.49$) C4d deposition in tubular epithelium of kidneys harvested from DCD (Figure 7-22 B).

From these sum score results, data shown proposed greater C4d deposition with deterioration of renal function in both donor kidneys and the relation was significant in DCD but not in DBD

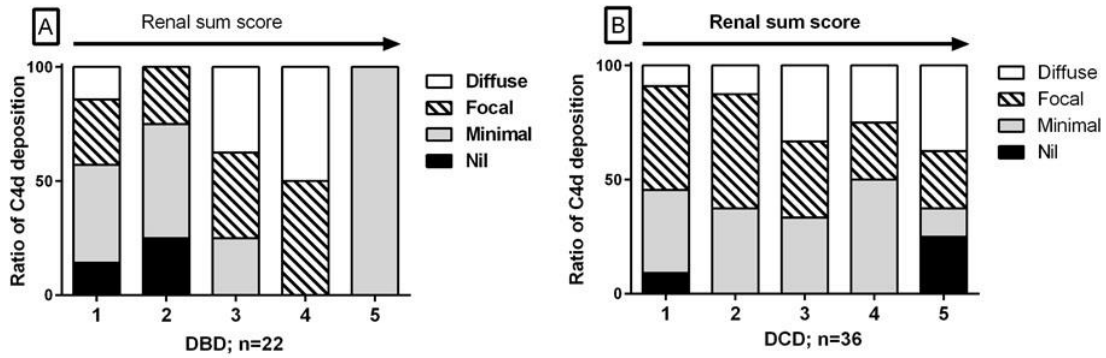


Figure 7-22 Semi-quantitative analysis of C4d deposition in renal tubular epithelium plotted against sum score in DBD (A), DCD (B). The sum score is a cumulative score of renal blood flow; urinary output and visual score calculated from 1-5.

7.4.3.1.3 Effect of cold ischemic time (CIT) and warm ischemic time (WIT) on C4d expression in DBD vs DCD kidneys

The cold ischemia represents the period from kidney retrieval until transplantation (Hosgood, Hunter and Nicholson, 2012) and in our model; it was calculated until starting NP. Each of the DBD and DCD kidneys groups were subdivided according to the duration of cold ischemia into two subgroups [at or below 24 h (≤ 24 h) and more than 24 h (>24 h) respectively]. These time points were chosen because during current practice, the CIT is less than 24 h in most of centres and does not exceed 48 h (Hosgood, Hunter and Nicholson, 2012) and a cohort study on the relation of CIT with graft survival in kidneys donated from DCD identified the prolong CIT as more than 24 h (Summers *et al*, 2013).

The severity of C4d deposition in renal proximal tubular epithelium was unexpectedly more in (≤ 24 h) than (> 24 h) groups in both DBD and DCD kidneys.

While half of cases in DBD and DCD kidneys with CIT > 24 h showed focal and diffuse C4d deposition, there were fewer cases in DBD group with CIT ≤ 24 h (n= 2/22) than in the corresponding DCD group (n=9/34) (Figure 7-23).

Kidneys from DBD did not experience a period of warm ischemia, the period from circulatory arrest till harvesting of kidney, unlike the DCD group. The latter was subdivided according to the period of warm ischemia into ≤ 16 minutes and more than 16 minutes.

The relation of C4d deposition DCD groups with time of warm ischemia revealed a pattern similar to CIT where the focal and diffuse C4d deposition were increased in ≤ 16 min and equally distributed with mild/minimal C4d deposition at > 16 min (Figure 7-23 B).

Hence, these results might signify that with increase CIT (DBD and DCD) and WIT (DCD), there were less activation of complement in donor kidneys.

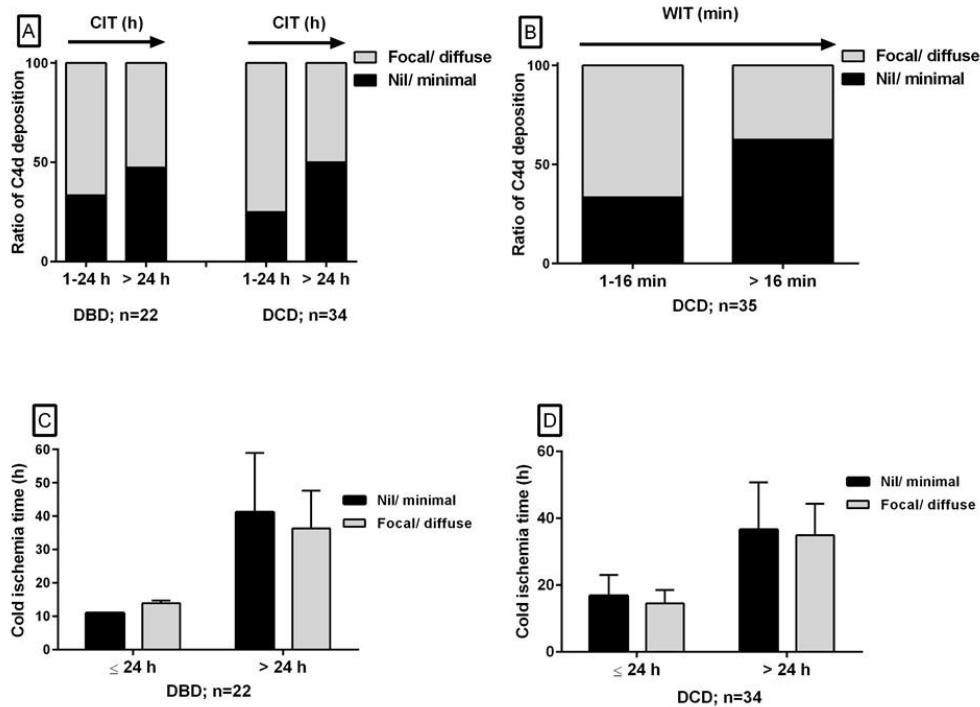


Figure 7-23 Semi-quantitative analysis of C4d deposition in renal tubular epithelium plotted against cold ischemic time in DBD and DCD (A, C, D) and against warm ischemic time in DCD (B); data were presented as mean \pm SD and $p < 0.05$ is significant.

7.4.3.2 Assessing vWF accumulation in renal glomeruli before NP

In normal kidneys, glomeruli do not stain with vWF (Pusztaszeri *et al*, 2006). Accordingly, vWF reactivity in the glomeruli of the declined kidneys was assessed under light microscope at 40 X and classified according to its intensity (Nil= -ve; mild= +ve; moderate= ++ve and strong= +++ve). Two independent observers blinded to the sample groups assessed the sections using predefined criteria (Figure 7-24 A-E). Results showed a highly significant abundance in vWF deposition in glomeruli of kidneys donated from DBD ($p=0.0003$) while abundance among DCD kidneys was not significant ($p=0.0523$). Data showed no significant differences in vWF deposition between DBD and DCD

groups ($p > 0.05$) although presence of stronger vWF deposition was more in kidneys of DCD than DBD (Figure 7-24 F). It seems that the renal glomeruli in both groups were positively reactive to vWF and this was a constant observation in DBD in comparison to DCD.

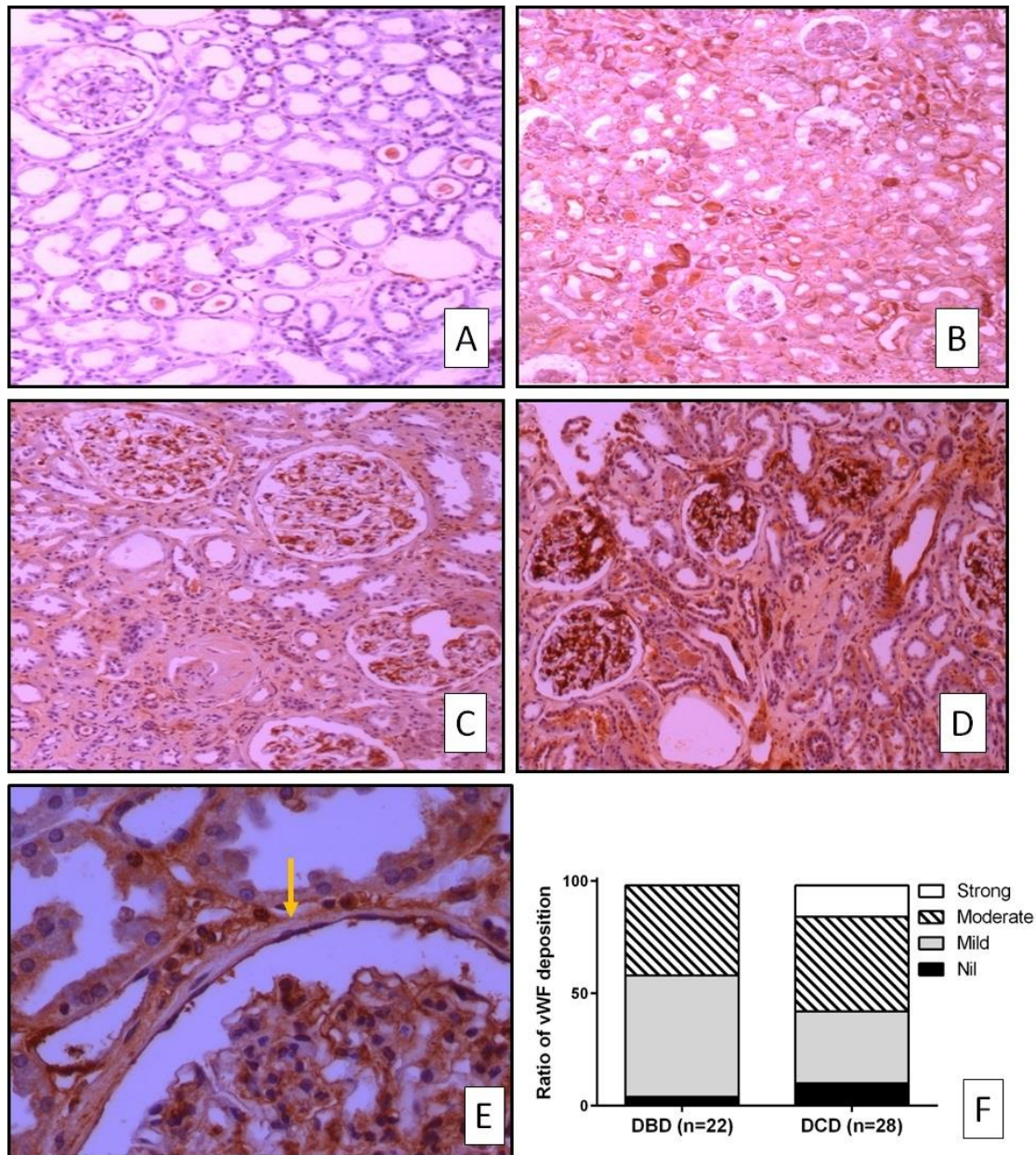


Figure 7-24: Immunohistochemical analysis of vWF reactivity in glomeruli. (A-D): examples of subjective staging of reaction intensity; A: Nil (-ve), B: Mild (+ve), C: Moderate (++)ve, D: Strong (+++ve) (10X). The vWF reactivity appears within the capillary convolute, (E) (40X). Olympus CX41 light microscope and image Pro plus /Q imaging microPublisher 5.0 RTV was used to capture images. (F), comparison of scoring for vWF reactivities in DBD and DCD kidneys (n=22 and 28, respectively).

7.4.3.2.1 Relation of vWF reactivity with histopathological scoring

There was no strong vWF reactivity in any of the DBD kidneys and only those with mild histopathological score showed no vWF reactivity. The moderate vWF reactivity was decreased with increase histopathological score ($r = -0.967$; $p = 0.163$). Oppositely, mild vWF reactivity was increased with increase histopathological scoring ($r = 0.945$; $p = 0.212$). (Figure 7-25 A). In addition, results of DBD kidneys revealed significant relation between mild and moderate vWF reactivity ($r = -0.997$; $p = 0.049$) as well as moderate and severe histopathological scoring ($r = 0.985$; $p = 0.015$). Hence, when the extent of vWF reactivity declined, kidneys were more damaged.

In DCD kidneys, vWF deposition did not show any significant relation with the histopathological score ($p > 0.05$) (Figure 7-25B). However, 4.5% of DBD and 3.4% of DCD kidneys showed mild histopathological score with no vWF reactivity and 13.6% of DBD and 3.4% of DCD groups showed mild histopathological score and moderate vWF reactivity.

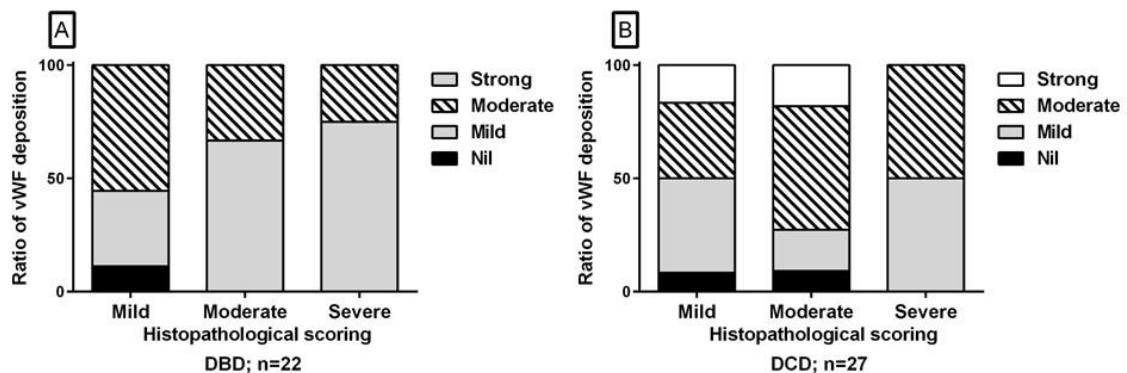


Figure 7-25 Semi-quantitative analysis of vWF reactivity blotted against histopathological damage in DBD (A) and DCD (B).

7.4.3.2.2 The relation of sum score with vWF deposition in DBD vs DCD kidneys

There were no significant relations of sum score with either donor groups. In DBD group, r of sum score vs nil = 0.35; sum score vs mild = 0.46; sum score vs moderate = -0.64 with p value equal to 0.56, 0.43 and 0.24 respectively (Figure 7-26 A). In comparison to the DCD group, a possible relation (but not significant) was noticed between sum score and strong vWF expression ($r = -0.87$; $p = 0.058$). This was not applicable to nil and mild vWF reactivity from glomeruli of DCD (r sum score vs nil = 0.81; sum score vs mild = 0.22;

sum score vs moderate= -0.38) with p equal to 0.096, 0.72 and 0.52 respectively (Figure 7-26 B).

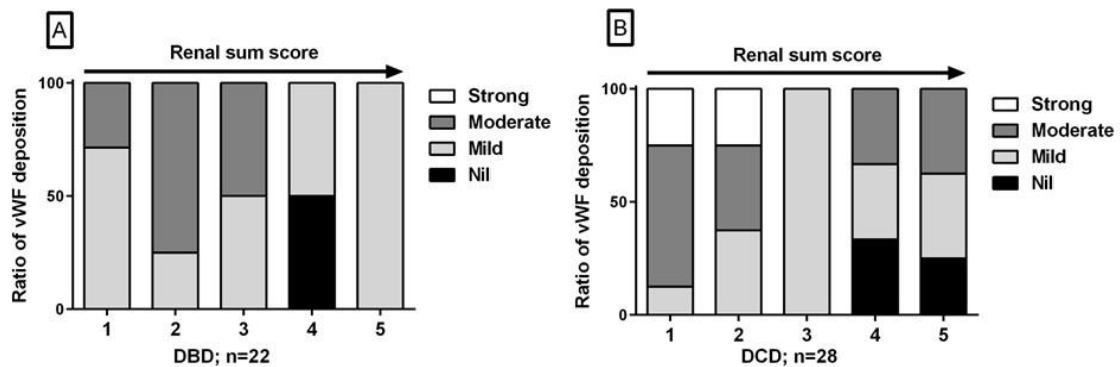


Figure 7-26 Semiquantitative analysis of vWF reactivity plotted against sum score in DBD (A), DCD (B). The sum score is a cumulative score of renal blood flow; urinary output and visual score calculated from 1-5.

7.4.3.2.3 Effect of cold ischemic time (CIT) and warm ischemic time (WIT) on vWF reactivity in DBD vs DCD kidneys

There was a direct relation between time of cold ischemia and vWF reactivity from renal glomeruli among donated kidneys in which ratios of moderate and strong vWF reactivity were doubled in >24 h group over \leq 24 h in DBD and DCD samples (Figure 7-27 A). Moreover, in DBD group exposed to cold ischemia for more than 24 h, moderate to strong vWF reactivity group had significantly longer CIT than nil to moderate group ($p=0.002$) (Figure 7-27 C).

In DCD kidneys, both groups (nil to mild and moderate to strong) were significantly higher in > 24 h than \leq 24 h ($p= 0.003$ and 0.004 respectively). However, after 24 h of cold ischemia, the moderate to strong vWF reactivity showed longer CIT than nil to mild group but not significant ($p > 0.05$) (Figure 7-27 D).

With regard to WIT for DCD, vWF reactivity was more with longer ischemia. Strong vWF reactivity was nearly equal in both groups (≤ 16 min = 15%; > 16 min = 16.667%); however the moderate vWF reactivity was more in >16 min (50%) than ≤ 16 min (35%). The ratios of combined moderate and strong vWF reactivity were increased with increased WIT (Figure 7-27 B).

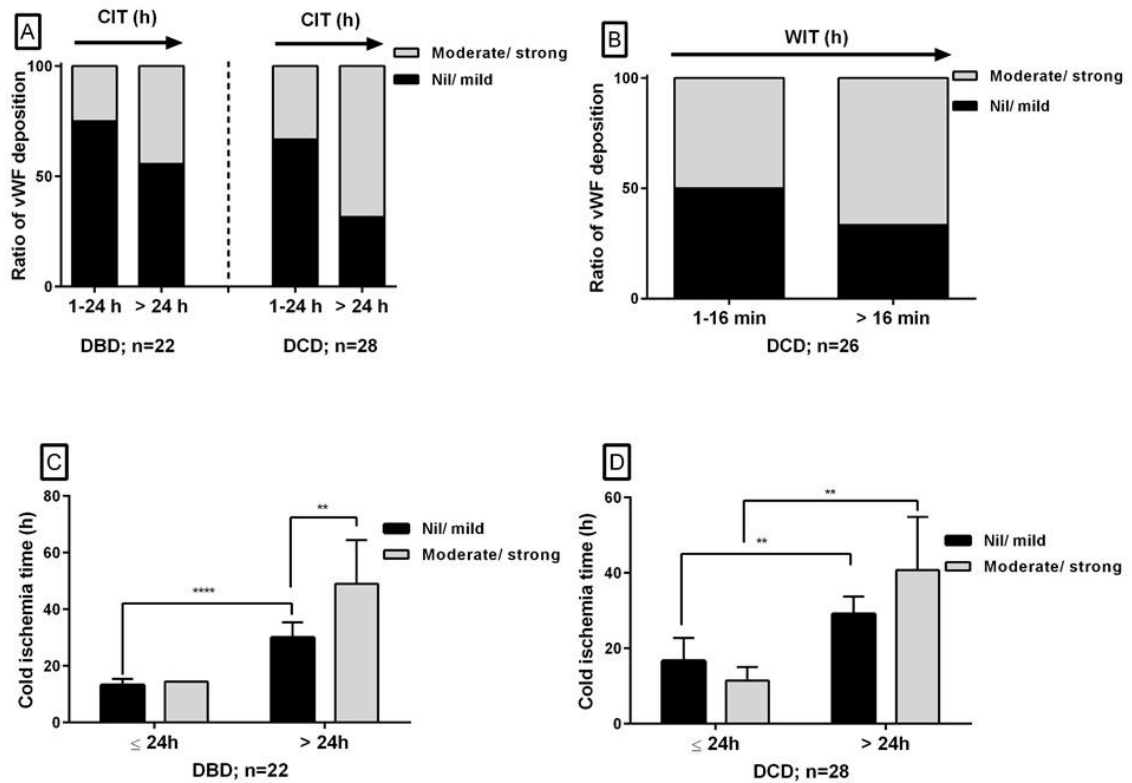


Figure 7-27 Semiquantitative analysis of vWF reactivity plotted against cold ischemic time in DBD and DCD (A, C, D) and against warm ischemic time in DCD (B). p (*) < 0.05, (**) \leq 0.01, (***) \leq 0.001, (****) \leq 0.0001; data presented as mean \pm SD.

7.4.3.2.4 Small extra fragment of vWF by western blot ADAMTS13 in kidneys from DBD and DCD

A vWF reactive band at 115 kDa was found most predominantly in samples scored +++, while a 60 kDa species were found at relatively lowest abundance in these samples. This compares to a figure found in Xiang *et al*, 2011, where vWF band decreases over time when ADAMTS13 is added, and a cleavage product appears (Xiang *et al*, 2011). This is contrary to our expectation that there would be more ADAMTS13 mediated cleavage of vWF when endothelial cells are damaged, i.e. we predicted it to be in the +++ samples.

But because the abundance of bands appears to follow a pattern (Xiang *et al*, 2011), we thought we should repeat this one blot with the same samples one last time. We did long and short exposures aiming for 115 kDa (weak at 1 min) and 60 kDa (very strong at 1 min) bands separately.

The western blot repeated for those samples and unfortunately, there was no difference in the presence of extra fragment in those 4 classes apart from band between 37 and 50) found in those sample 21(-ve score in IHC) and sample 3(+++ve score by IHC).

7.4.3.3 Analysis of pre-NP complement C3 fragment and β -actin in kidney lysates using immunoblotting

All the three complement cascades act on C3 and C5 resulting in their cleavage. By IHC, complement C3 is present in both basement membrane of Bowman's capsule and renal tubules of normal kidney (Brar and Quigg, 2014). Because IHC using a polyclonal antibody identifies and localises C3 and perhaps its activation fragments, if present, western blot was used to identify unequivocally those samples in which C3 had been activated (Bokisch, Dierich and Muller-Eberhard, 1975). There was C3 expression from all samples of DBD kidneys and approximately all that of DCD (88.57%) as four samples were negative for C3 only. The C3 expressions were more abundant in DBD group than in DCD (Figure 7-28 A). Although β -actin is a well-known housekeeping marker, it was variable in this study. It was expressed more in DCD kidneys than DBD as well as the negative expression in DCD was half than of DBD group (20% vs 39.13%). However, one sample of the DCD group was negative for both, β -actin and C3, even though proteins were visualised on the gel (Figure 7-28 B).

Samples exhibiting reactivity with the polyclonal anti C3 antibody of bands smaller than 68 kDa (the β -chain of C3) were recorded positive for C3 activation. While 70.8% of DBD samples were positive of C3 activation products (iC3b, 43kDa; C3dg, 41 kDa; C3c, 27 kDa), only 44.1% of DCD samples were affected in this way.

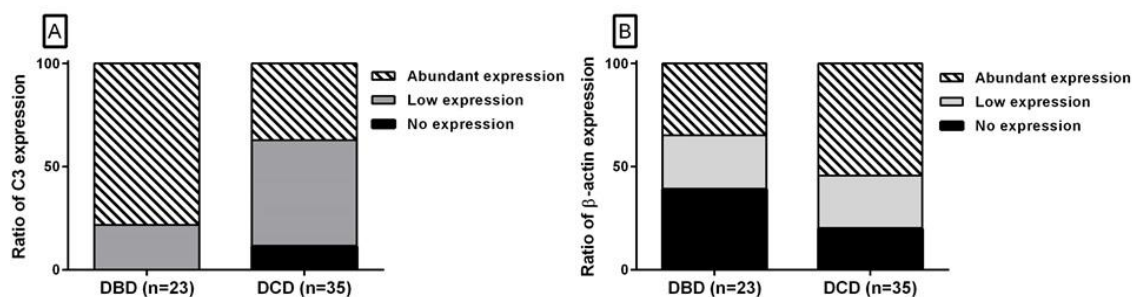


Figure 7-28 Semi-quantitative analysis of C3 fragment (A) and β -actin (B) expression using western blot in DBD and DCD.

7.4.3.3.1 The relation of histopathological scoring to C3 fragment and β -actin expressions

The patterns of C3 fragment expressions in relation to histopathologic changes in DBD samples showed more C3 fragment expression with increase in severity of tissue injury. Abundant expression of C3 fragment was directly related ($r= 0.969$; $p= 0.16$) while low expression was inversely related to histopathological scoring ($r= - 0.969$; $p= 0.156$) (Figure 7-29 A).

Unfortunately, the pattern of C3 fragment expression in renal tissue lysate was not clear among DCD kidneys. There was no changes in ratio of low C3 fragment expression among the three histopathological grades. There was insignificant relation between both no and abundant C3 expression and histopathological damage ($r= - 0.689$; $p= 0.516$ and $r= 0.565$; $p= 0.618$ respectively) (Figure 7-29 B).

Relatively, β -actin did not show a clear pattern in its expression from kidney in relation to the severity of histopathological changes in both DBD and DCD kidneys. In DBD kidneys, both abundant and low β -actin expression were directly related to histopathological score but not significant ($r= 0.514$; $p= 0.508$ and $r= 0.933$; $p= 0.234$ respectively) (Figure 7-29 C). Comparatively, there was a fair increase in the severity of β -actin expression in relation to histopathological scoring among kidneys from DCD samples. Both no and low β -actin expression groups were directly related (not significant) to histopathological scoring ($r= 0.937$; $p= 0.228$ and $r= 0.644$; $p= 0.555$ respectively) while the relation between abundant β -actin expression with histopathological damage was inverse and not significant ($r= - 0.782$; $p= 0.429$) (Figure 7-29 D).

It seems that all kidneys that scored severe in the histopathological assessment were positive for activated C3 and β -actin for DCD and DBD kidneys. Activated C3 discriminates severe histopathology in DBD.

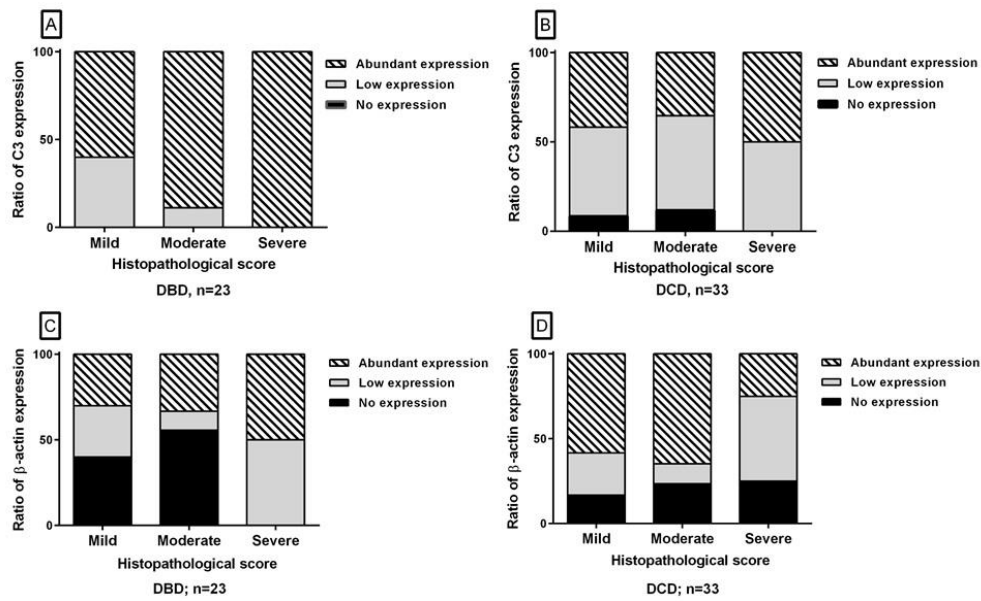


Figure 7-29 Semiquantitative analysis of C3 and β -actin expression using western blot. C3 fragment expressions were plotted against. C3 expressions were blotted against histopathological score in DBD (A) and DCD (B). β -actin expressions were blotted against histopathological score in DBD (C) and DCD (D).

7.4.3.3.2 Effect of sum score on complement C3 fragment and β -actin

Activated C3 was expressed in all samples of DBD over the 5 grades of sum score. The expression was more abundant with higher grades of sum score because low expression of C3 fragment was significantly inversely related to sum score ($r = -0.884$; $p = 0.047$) while abundant expression was directly related ($r = 0.884$; $p = 0.047$) (Figure 7-30 A, E). Interestingly, all three degrees of β -actin among DBD kidneys were inversely related to sum score (r for no expression, -0.189 ; low expression, -0.97 ; abundant expression; -0.609) although the relation was significant only in kidneys with low expression ($p = 0.006$) (Figure 7-30 B, F).

In DCD groups, both no and low expression of C3 from renal tubules were inversely related while abundant expression was directly related to sum score although the relations were not significant with $p > 0.05$ (r for no expression, -0.169 ; low expression, -0.22 ; abundant expression; 0.291) (Figure 7-30 C, E).

By contrast, DCD specimens with no expression of β -actin were significantly related to sum score ($r = 0.938$; $p = 0.018$) while both low and abundant expression showed inverse relation though not significant ($r = -0.771$; $p = 0.127$ and $r = -0.816$; $p = 0.092$) (Figure 7-30 D, F).

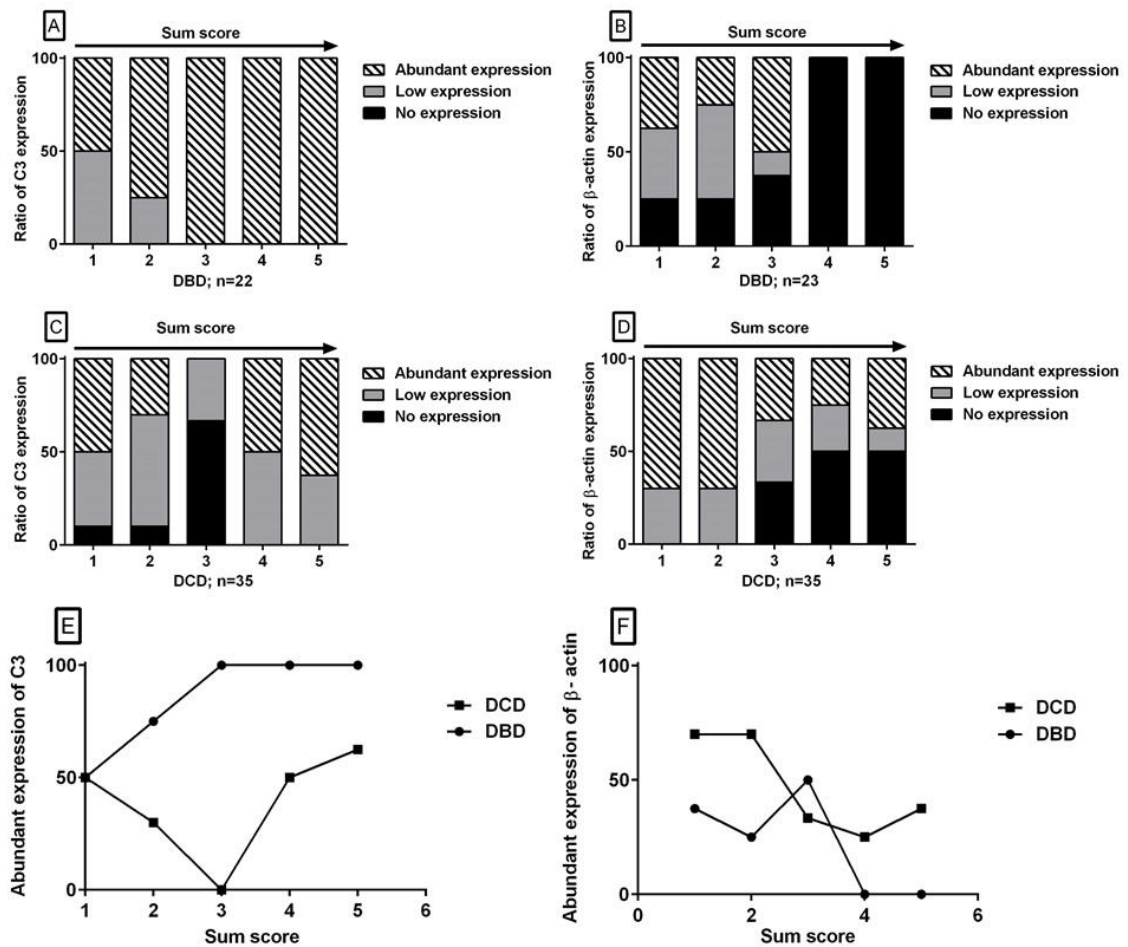


Figure 7-30 Semiquantitative analysis of C3 and β -actin expression using western blot. Comparison of C3 (A) and β -actin (B) reactivity in DBD and DCD kidneys. C3 expressions were plotted against sum score in DBD (C) and DCD (E). β -actin expressions were blotted against sum score in DBD (D) and DCD (F). Strong (abundant expression) C3 (G) and β -actin (H) were plotted against DBD and DCD. The sum score is a cumulative score of renal blood flow; urinary output and visual score (1-5)

7.4.3.3.3 Effect of CIT and WIT on expression of C3 fragment and β -actin

C3 expressions from renal tissue were stronger with less period of cold ischemia in both DBD and DCD groups. In DBD kidneys, abundant C3 expression was found in all specimens with cold ischemic time (≤ 24 h) and in 70% of (>24 h) group. Likewise, in kidneys from DCD, although abundant C3 expression saw a minor decline with increased CIT but ratio of low C3 expression doubled in (≤ 24 h) group in comparison with (> 24 h) group. Results also showed that ratio of no C3 expression was depressed 5 fold in kidneys with CIT (≤ 24 h) in comparison with (> 24 h) group (Figure 7-31 A).

The expression of β -actin showed two opposite patterns in relation with CIT between the two kinds of donor kidneys. In the DBD group, the more time the less expression where no β - actin expression group nearly doubled in (≤ 24 h) in relation to (> 24 h) and abundant β - actin expression was decreased respectively. In the DCD group, the opposite was found where ratio of no expression of β - actin was observed 3 times more in the short of CIT ≤ 24 h than in > 24 h groups while low expression was increased 4 times, respectively. The abundant β - actin was nearly equal between the two CIT groups (Figure 7-31 B).

In DCD kidneys, there was more C3 fragment expression in group experiencing >16 min WIW than in ≤ 16 min WIT group where both abundant and low expression were increased while activated C3 expression was detectable in all samples from > 16 min WIT group (Figure 7-31 C).

In the same manner, β -actin expression from kidneys of DCD was expressed abundantly with increased WIT. Kidneys with ≤ 16 min WIT showed various degree of β - actin expression while all kidneys with WIT > 16 min had abundant expression only (Figure 7-31 D).

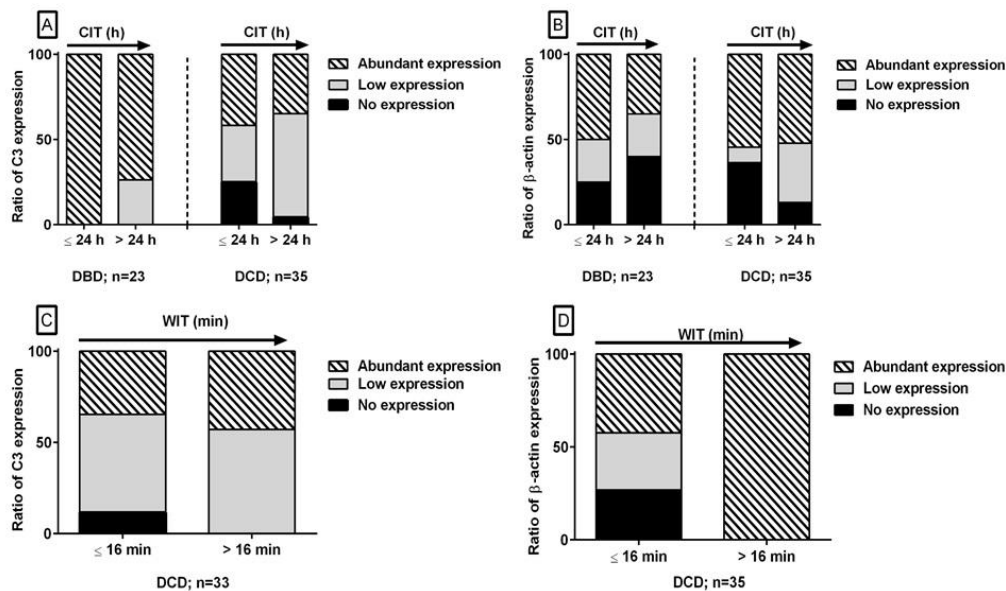


Figure 7-31 Semiquantitative analysis of C3 fragment and β -actin expression using western blot. C3 expressions were plotted against cold ischemic time in DBD and DCD (A) as well as against warm ischemic time in DCD (C). β -actin expressions were blotted against cold ischemic time in DBD and DCD (B) as well as against warm ischemic time in DCD (D).

7.4.3.3.4 Histopathology

Results showed no difference in grades of histological score between DBD and DCD kidneys (Figure 7-32 A). The relationship between cold storage time with histopathological score was not strong either in DBD ($r = -0.4$; Figure 7-32 B) or DCD ($r = 0.24$; Figure 7-32 C); nevertheless, data revealed more histopathological damage in kidneys with CIT more than 24 h than those with or less than 24 h in both DBD and DCD (Figure 7-32 E). Furthermore, results of WIT in DCD kidneys showed a strong relation with histopathological score i.e. the more ischemia time, the more kidney damage ($r = 0.9$; Figure 7-32 D).

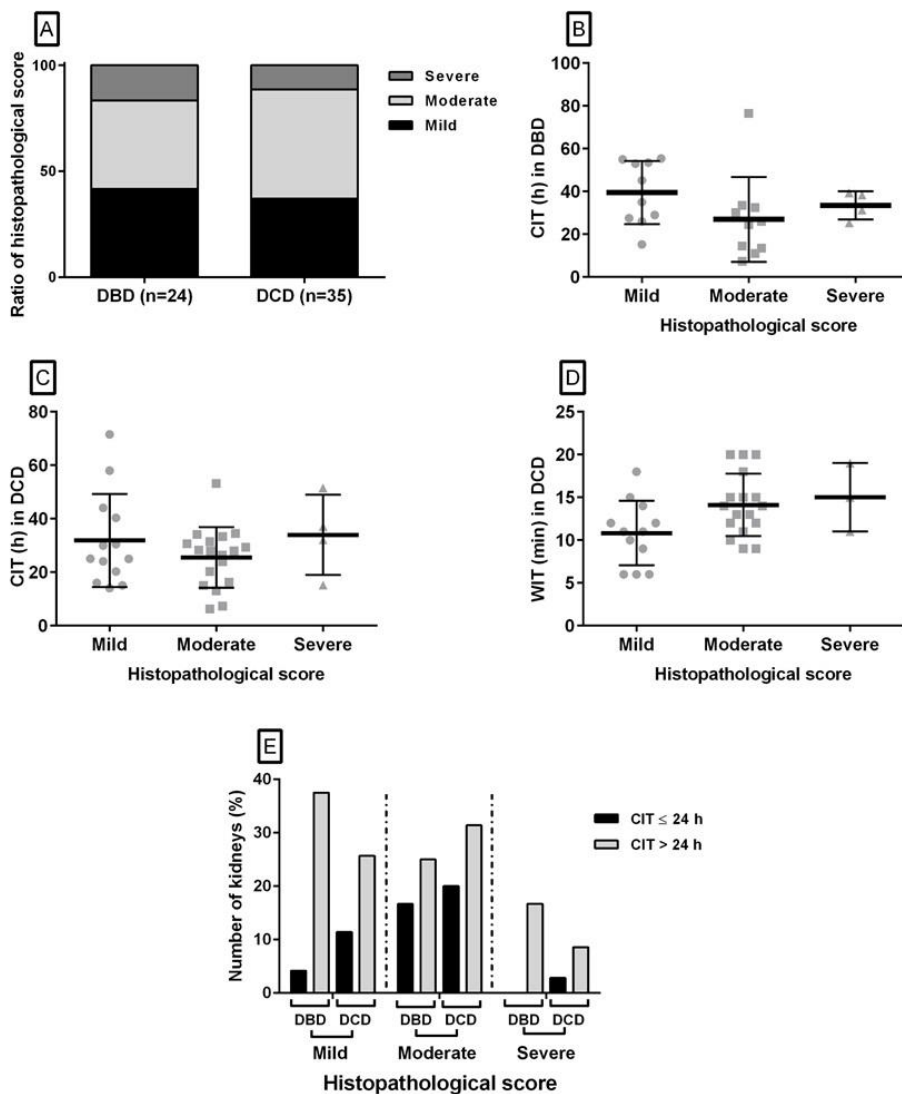


Figure 7-32: Histopathological scoring grades in DBD and DCD kidney before exposing to NP (A) and its relation with CIT in DBD (B, E), DCD (C, E), and with WIT in DCD group (D).

7.4.3.4 Effect of NP on expression of vWF, C4d

Recent trials showed that NP on marginal kidneys may improve surgical outcomes and open the door to invest kidneys in transplantation which are declined previously (Nicholson and Hosgood, 2013). After exposure to *ex vivo* NP, human kidneys that were donated from both brain death and cardiac death donors were classified into pre and post NP groups to assess both C4d and vWF expressions.

There was a decrease in vWF reactivity after exposing both DBD and DCD kidneys to NP although the majority of kidneys showed no differences. Among DBD kidneys, nearly two third of kidneys revealed same grade of vWF reactivity pre and post NP while kidneys that showed a decrease in vWF reactivity were more than those that showed an increment after NP. Similarly, half of DCD kidneys did not reveal any differences in vWF reactivity between pre and post NP; however, kidneys that showed decrease in vWF reactivity were double those that showed an increase in reactivity after treatment them with NP (Figure 7-33 A, C). Exposing both DBD and DCD kidneys to NP resulted in an increase in C4d deposition despite the majority of kidneys not revealing any changes in abundance of C4d expression. In DBD specimens, severity of expression of C4d was equal between pre and post NP in about two third of kidneys; nevertheless, kidneys that showed escalation in C4d expression were three times more than those that showed diminution after NP. In the same way, half of DCD kidneys did not reveal any changes in C4d expression after NP; however, kidneys that showed an increase in C4d expression were double those that revealed a reduction in expression post NP (Figure 7-33 B, D).

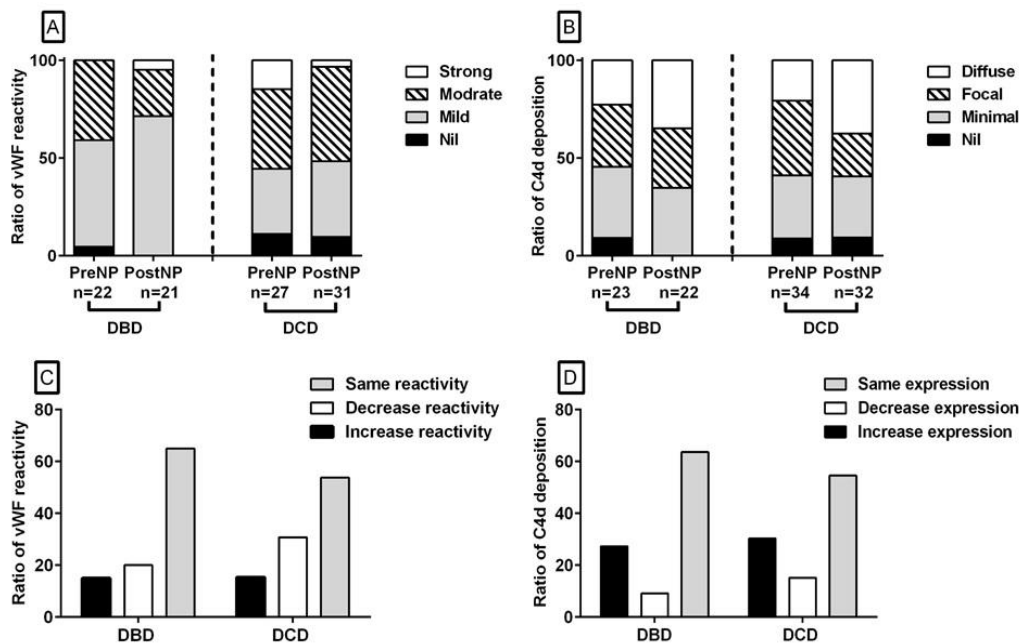


Figure 7-33 Effect of normothermic perfusion on vWF reactivity and C4d expression. Immunoblotting to assess semi-quantitatively ratios of vWF reactivity (A,C) and C4d expressions (B,D) in declined kidneys that have been donated from both DBD and DCD donors.

7.4.4 Discussion

7.4.4.1 Cadaveric kidneys, the best source.

One of the greatest challenges that surgeons are faced with is the high demand for allograft donor kidneys. This escalating demand has arisen from the widening in the gap between numbers of patients with ESRD and both numbers of donated kidneys and transplant operations (Binnani, Gandhi and Bahadur, 2012). The United Network for Organ Sharing (UNOS) reported that each year the number of ESRD patients waiting for renal transplant is increasing by 10% in comparison with an increase of only 4% rising in renal transplant surgeries (Gopalakrishnan and Gourabathini, 2007). This is supported by a report that was released by Scientific Registry of Transplant Recipients/ Organ Procurement and Transplantation Network (SRTR/ OPTN) declaring that around 40,000 patients were waiting for transplant surgery in 1998 while in 2011 the numbers were increased nearly threefold (Binnani, Gandhi and Bahadur, 2012).

As a result and despite the superiority of live-donor kidneys, a strategy was established to procure kidneys from cadaveric donor post brain (DBD) and/ or cardiac (DCD) death.

Additionally, the criteria of kidney selection were extended to include kidneys that previously were held to be inappropriate for transplantation such as those from elderly donors, obese patients and patients with chronic diseases (e.g. hypertension and diabetes) (Ojo *et al*, 2001; Gopalakrishnan and Gourabathini, 2007). However, about 41% of extended criteria donors (ECD) kidneys were rejected by the surgical teams ascribing to measures related to the size of the kidney, appearance, age of the patients, kidney perfusion as well as biopsy results (Binnani, Gandhi and Bahadur, 2012; Aubert *et al*, 2015). Furthermore, there was large incongruity in ratios of ECD to standard criteria donors (SCD) among countries. While only 16.6% of renal transplant patient in USA get ECD kidneys, in France, it was 47% while only 30% in the rest of Europe (Aubert *et al*, 2015).

In our study, it was very difficult to address exactly whether DBD and DCD kidneys, which were originally declined, could be implanted successfully or not depending on their complement expression; however, this pilot study gave insight into the possibility of complement activation, which may result in early post-transplant renal dysfunction. Furthermore, this chapter presents for the first time that **vWF, the vascular endothelial marker, could be used as a predictor for the severity of renal damage particularly in donor kidneys prior to transplant surgery.**

This study was limited by the absence of control group of living donor kidneys as well as no specimens from successfully transplanted organ. In addition, a major limitation to the study is, since kidneys were not transplanted, that no association with graft function after transplantation could be performed.

These results were in agreement with Qureshi *et al* 2012, where they assessed prospectively and retrospectively a 60 patient cohort with combined pancreas and kidney transplantation (organs were procured from 20 DCD and 40 DBD donors). They revealed no significant difference in short term survival between DCD and DBD kidneys as Kaplan–Meier 1-year survival estimates of 84% and 95% respectively (Qureshi *et al*, 2012). Another cohort study on 71 renal transplant surgeries performed in China using DCD kidneys for the period from 2007-2012 found that despite the high delayed graft function rate (28.2%), the 1 and 3 years survival rate were 95.7% and 92.4% respectively (Chen *et al*, 2013a). Furthermore, our results seem to be consistent with a study from

University of Wisconsin/ Department of Organ Transplantation. They compared the outcomes of 1038 kidneys donated from DCD with 3740 from DBD over three decades (1980- 2008) and they showed similarity in patient survival rate after 1 year, 3 years and 10 years between DBD and DCD kidneys (95.2%, 88.4%, 60.7%, and 92.3%, 84.6%, 59.7%) (Bellingham *et al*, 2011).

However, the findings of the current study do not support the retrospective research by Singh *et al* 2011 on 70 DCD and 508 DBD transplanted kidneys at University of Minnesota School of Medicine/ Department of General Surgery/ Division of Transplantation, USA over a period from 2001 until 2008. They revealed that long term prognosis of transplanted kidneys from DCD donor is better than DBD with significantly higher mortality rates due to graft failure (12.5% DCD vs. 31% DBD), primary non-function (0 DCD vs. 10% DBD) and greater mean serum creatinine levels after 2 years (1.4 DCD vs. 2.7 mg/dL DBD) (Singh *et al*, 2011).

A review by Floerchinger et al 2011 proposed that organs (including kidneys) from DBD are inferior to DCD because brain death will activate various molecular and inflammatory cytokines such as activation of both complement system (increased circulating C3a) and extrinsic pathway of clotting system (increased von Willebrand factor) (Floerchinger, Oberhuber and Tullius, 2012).

7.4.4.2 Complement fragment (C4d) and C3

The study found no difference in extent of complement C4d protein expression from renal tubules of kidneys donated from DBD and DCD (Figure 7-20). C4d deposition showed positive relation in comparison with structural damage (histopathological score) where the more tissue damage, the greater the abundance of C4d deposition in both DBD and DCD kidneys. Another finding was that C4d deposition related positively with renal dysfunction (sum score) as kidneys with higher sum score revealed abundant C4 deposition. Hence, C4d could be used as a biomarker of renal damage in deceased kidneys prior to transplantation.

This study showed more abundance of C3 protein in kidneys obtained from DBD than DCD. Among DBD, C3 protein synthesis was directly related with structural changes where the more damage (higher histopathological score), the more abundant the

production. Similarly, there was an increase in C3 production in DBD kidneys with deterioration in renal damage (direct relation with sum score). Conversely, C3 production did not show any significant correlation with either histopathological scoring or sum score among DCD specimens.

When relating the presence of C3 activation products and of C4d reactivity as a measure of complement activation within the kidney tissue, a greater proportion of DBD samples showed evidence of complement activation compared to DCD samples. Interestingly, 8.8% of DCD samples did not show neither C3 activation products by Western blot or deposition of C4d by immunohistochemistry.

Clinically, C4d staining was widely extended from being merely a biomarker for detecting antibody-mediated graft failure to cover all antibody-related conditions, including autoimmunity and pregnancy (Cohen *et al*, 2012). In the early nineties, a study of 596 patients with renal transplantation from cadaveric donors in Munich, Germany concluded the potential for using C4d as a prognostic as well as pathologic marker post renal transplant surgeries to detect graft rejection (Feucht *et al*, 1993). Later, a prospective study by Collens *et al* 1999 examined C4d deposition in peritubular capillaries by immunofluorescence to distinguish between humoral and cell-mediated rejection in kidneys that suffered from acute graft failure at the Massachusetts General Hospital (Collins *et al*, 1999). These studies resulted in considering C4d staining as a cardinal sign of acute antibody-mediated renal rejection (Racusen *et al*, 2003). Later, these criteria were integrated into the Banff classification, a group of clinical, immunological, serological and morphological criteria to diagnose antibody-mediated kidney rejection in 2007 (Corrêa *et al*, 2013). Damman *et al* 2011 showed that C4d is elevated significantly in serum of deceased donors compared to live donors and is associated with acute graft rejection (Damman *et al*, 2011b).

There is some disagreement about the sensitivity of C4d staining due to its appearance in renal biopsy with ABO-mismatching despite lack of graft dysfunction (Cohen 2012). Another debate was raised about its specificity as well. This is mainly due the presence of antibody-mediated rejection with negative C4d staining (Corrêa *et al*, 2013).

The complement cascade has an essentially injurious role during kidney transplantation (Serinsöz *et al*, 2005). Upregulation of C3 could come from the tubular epithelium of the

donor kidney itself or be circulating in the recipient (Damman *et al*, 2011a). While the latter yields no effect on transplantation outcomes, Pratt *et al*, emphasised that absence of C3 in the donor kidneys improves survival in mice (Damman *et al*, 2011a; Pratt, Basheer and Sacks, 2002). Interestingly, Damman *et al*, proved that kidneys donated from brain death patients produce C3, i.e activation of complement system, before and immediately after transplantation as sequelae to brain death and IRI, respectively.

7.4.4.3 Role of vWF

This study set out with the aim of assessing the significance of vWF in evaluating the viability of deceased kidneys for transplantation. The results revealed that vWF was variously abundant in almost all glomeruli of deceased kidneys (DBD: 96% and DCD: 90%) with stronger reactivity in DCD than DBD. Nevertheless, vWF reactivity in renal glomeruli showed no clear relation in deceased specimens either with structural (histopathological score) or functional (sum score) changes apart from its inverse relation to histopathological score and vWF reactivity in glomeruli of DBD kidneys (i.e. more damage, less reactivity).

Prior studies have noted the importance of plasma vWF protein as an indicator for endothelial activation and injury secondary to inflammation (Zezos *et al*, 2005; Aversa *et al*, 2001). vWF has been proposed as a marker for disease activity in patients with ulcerative colitis due to the direct relation of its plasma level with disease severity and also acute-phase proteins (ESR and CRP) as well (Zezos *et al*, 2005). Likewise, it has been used as a biomarker for diagnosing sepsis in a prospective study on patients at University Hospital of Geneva (Switzerland) and Lille (France) although it was not useful to distinguish disease level (Scherpereel *et al*, 2006).

In relation to vWF production during renal diseases, a clinical study on uraemia patients, complication of chronic kidney diseases (CKD), noticed high plasma and low platelet vWF protein levels (Casonato *et al*, 2001). Similar clinical study by Shen *et al*, 2012 confirmed the elevation in plasma vWF protein secondary to renal endothelial injury in CKD patients (Shen *et al*, 2012). Interestingly, an experimental renal transplantation on monkeys reported that vWF protein deposition in renal glomeruli is exacerbated during chronic, rather than acute, rejection (Lagoo *et al*, 2000).

vWF reactivity from renal vessels of donor kidneys could be an indicator of arterial injury which may result in development of atherosclerosis that results in with decreased graft survival due to chronic rejection (Ota *et al*, 2005; Blann, 2000). This was supported by an *in vivo* study on rats exposed to brain death (BD) where it showed an elevation in plasma vWF after 2 h after brain death. In addition, the same study revealed platelets trapped in the vascular lumen of donor kidney after ½ h of BD (Morariu *et al*, 2008); however, our results of increased staining for vWF in DCD could come from platelets that are stuck in glomeruli when no blood is flowing. This explanation could be supported by the higher β -actin production in DCD than DBD kidneys.

7.4.4.4 Role of CIT and WIT in deceased kidney on complement (C4d and C3) and vWF

Studies showed that CIT and WIT duration play a vital role in post-transplant kidney function as well as survival. Both DBD and DCD kidneys suffer from cold ischemia (CI) injury following removal. CI injury usually results from ATP depletion secondary to hypoxia (absence of oxygen). Several molecular and metabolic processes will be initiated ending with lysosomal enzyme stimulation, lactic acid production and acidosis, cellular swelling and both free radicles and mineral (calcium and iron) accumulation. After restoring blood flow, the CI injury progresses to IRI causing damage to both renal glomeruli and tubules (Halazun *et al*, 2007; Hosgood, Hunter and Nicholson, 2012). Summers *et al*, 2013 found in a cohort study on 6490 deceased kidneys that prolonged CIT (> 24 h) of kidneys procured from DCD resulted in worse graft survival than those from DBD while CIT did not affect graft survival of DBD kidneys (Summers *et al*, 2013).

In addition to CI injury, kidneys harvested from DCD suffer a period of warm ischemia (WI), where blood is not reaching a normothermic kidney, from the time of heart stops beating until kidney is transferred to cold preservation. Renal insults due to WI injury exacerbates the CI injury making DCD kidneys less favourable for transplantation (Hosgood, Hunter and Nicholson, 2012; Halazun *et al*, 2007).

In our study, DBD kidneys showed lower C4d deposition as well as C3 protein production with increase CIT. DCD kidneys showed similar pattern of C4d deposition to that of DBD

with increase CIT and WIT while the C3 production was opposite. C3 production in DCD kidneys was increased with prolonged CIT and WIT.

In kidney transplantation, a study examined around 2500 kidneys procured from cadaveric donors over 8 years since 2000, revealed that CIT has a great impact on graft survival where prolonged CIT associated with higher rate of delayed graft function (DGF), where patients need haemodialysis during the first week after surgery, and graft rejection (Valdivia *et al*, 2011). Meanwhile, a similar study covering nearly the same period on 9082 deceased donor kidney was conducted by Kayler *et al*, suggested that despite the unfavourable effect of prolonged CIT on DGF, CIT has **no** effect on graft survival (Kayler, Srinivas and Schold, 2011).

It seems likely that higher C4d and C3 production are indicators of more renal damage after transplantation and prolonged CIT and WIT have harmful effect on implanted kidneys. Results also showed evidence of complement activation (might be indicated from expression of C3 fragments in DBD specimens); however, C4d deposition did not express these relations with CIT and WIT. The fact that these kidneys are already damaged, not suitable for transplantation and renal cells die with prolonged CIT and WIT is a possible explanation of lowering complement synthesis with increase ischemic time.

The study revealed a positive relationship between CIT and vWF reactivity in renal glomeruli of both DBD and DCD kidneys as well as with WIT in DCD specimens. This may be an indication of more renal damage with prolonged ischemic time.

Another issue that could not be addressed in this study was that no effluents were available to study complement activation in fluid phase in addition to the unknown stability of epitopes when monoclonal antibodies were used (C4d). Another factor which was not been assessed, was the WIT in DBD kidneys during the period from clamping renal vessels until starting cold preservation.

7.4.4.5 Role of NP

Ex-vivo normothermic perfusion (NP) could be considered as a cleansing technique to reduce the side effects of storage time in donated kidneys prior to transplantation (Nicholson and Hosgood, 2013). However, there were no significant variations in C4d

deposition in renal tubular epithelium or vWF accumulation among pre NP and post NP groups. These findings drawn from kidney samples from both DBD and DCD groups; however, the findings of the current study do not support the previous research. A clinical study on 18 kidneys harvested from extended criteria donor (ECD) exposed to NP for about 60 minutes prior to transplantation revealed reduction in delay graft reduction in comparison to kidney with traditional cold storage (5.6% vs 36.2%) respectively (Nicholson and Hosgood, 2013). A greater number of samples is required to make conclusions.

In summary, the study has indicated a great deal of variability in kidneys declined for transplantation. The warm ischaemic insult in DCD kidneys did not appear to have any added effect on cellular injury, complement activation or renal function. This highlights the need to employ assessment techniques to determine the suitability of marginal kidneys for transplantation.

In addition, C4d staining of renal tubules did not differentiate between DBD and DCD kidneys but vWF, the vascular endothelial marker, could be used as a predictor for the severity of renal damage in donor kidneys prior to transplant surgery. Furthermore, both DBD and DCD may be good sources of transplantable material.

7.4.5 Conclusion

In terms of kidneys that were harvested from cadaveric donors, the present study was designed to assess deceased kidneys harvested from DBD and DCD that were declined from transplantation as well as the effect of *ex vivo* NP as preservative technique. The study has shown that C4d staining of renal tubules did not differentiate between DBD and DCD kidneys while activated C3 protein in renal tissue homogenate produced more in DBD than DCD specimens. However, among healthier kidneys, those with mild histopathological score, DBD kidneys with no C4d deposition were three fold more than that of DCD kidneys. The second finding identified more vWF staining in renal glomeruli and β -actin protein synthesis in tissue homogenate of DCD than DBD kidneys that could be from platelets that were stacked in kidneys after circulatory halt. Kidneys from DBD may be healthier so they can express proteins while DCD have too much damage to their cells so are not able to react. In that event, it could be assumed that kidneys with mild

histopathological score and no C4d deposition (9.1% of DBD and 3% of DCD) might be healthy enough for transplantation.

The study on diseased kidneys has included human kidneys that are the target in all IRI researches, and from cadaveric donors where current studies are focussed to expand the numbers of donors. The data indicated a possibility that no significant differences between kidneys from DCD and DBD origin and both could be used for transplantation. The study also, proposes von Willebrand factor as a possible marker to assess the kidney's susceptibility prior to transplant surgery.

It is unfortunate that the study was not able to include data from live control as well as post-transplant data although these were not possible because the kidneys were not suitable for implantation. Additionally, an increase sample size may be recommended to get statistically more meaningful results as well as to evaluate the influence of NP more accurately. Lastly, we could not normalise our data against β -actin due its inconstant expression although it would be interesting to investigate mechanisms of cell death via assessing the role of β -actin, ROS generation and mitochondrial activity (Li *et al*, 2004).

Increasing numbers of human kidneys that included are in future studies as well as more focusing on the role of vWF will probably give more clear results in *ex vivo* work.

7.5 Participations, presentations and publications

1. British Transplantation Society (BTS) congress 2014; 26 – 28 February, SECC Glasgow (poster and abstract)

<http://www.btscongress.com/posters-p105-113.html>



The Inflammatory and Complement Mediated Response to *Ex-vivo* Normothermic Perfusion in Human Kidneys

SA Hosgood, Z Zwaini, M Patel, C Stover and ML Nicholson
University of Leicester, Department of Infection, Immunity and Inflammation and Transplant Group



Introduction

Ex-vivo normothermic perfusion (EVNP) is a novel technique of kidney preservation. Renal function is restored *ex-vivo* by circulating a red blood cell based solution through the kidney at normal body temperature. Little is known about the response of donation after brain death (DBD) and donation after circulatory death (DCD) kidneys to a short period of EVNP. The aim of this study was to quantify and compare the inflammatory effects of EVNP in human DCD and DBD kidneys.

Methods

Sixty human kidneys that were declined for transplantation underwent 60 minutes of EVNP at 37°C with an oxygenated packed red blood cell based solution after a period of static cold storage (figure 1, 2). Thirty five kidneys were from DCD and 25 from DBD donors. The reasons for decline are listed in table 1.

October 2012 – July 2013
60 kidneys declined for transplantation

Reasons for Decline	
PMH	15
Poor Flush	13
Donor Age	9
HMP Parameters	8
Technical/Anatomical	6
Histology	5
Prolonged CIT	4

Table 1. Reasons for decline for transplantation

Results

Donor demographics are listed in table 2. There were significantly more male donors in the DCD group (P = 0.036).

There was no significant difference in the perfusion parameters between the two groups (Figure 3). However, the DCD kidneys had a higher level of proteinuria compared the DBD kidneys (0.73 ± 0.52 vs 0.46 ± 0.22pg/ml; P = 0.032).

Levels of TNF α , IL1 β or IL-8 were not detectable in the plasma pre or post perfusion in either group.

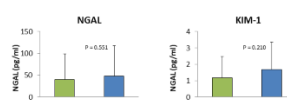


Figure 4. Urinary biomarkers, neutrophil gelatinase-associated lipocalin (NGAL) and kidney injury molecule (KIM-1) in the urine after 60 minutes of EVNP.

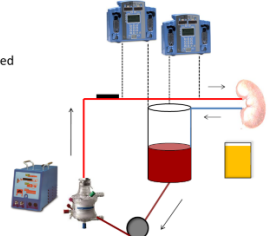


Figure 2. Schematic diagram of the ex-vivo normothermic perfusion (EVNP) system



Figure 1. A picture of a kidney during EVNP

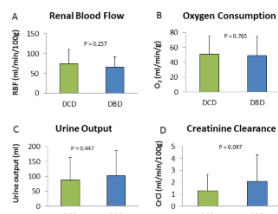


Figure 3. Perfusion parameters during EVNP. (A) The mean renal blood flow (RBF), (B) oxygen consumption, (c) total urine output and (D) creatinine clearance (CrCL) after 60 minutes of perfusion.

	DCD n = 35	DBD n = 25	P value
Donor Age (y)	60.5 ± 12.1	61.0 ± 14.4	0.878
M : F	24 : 11	10 : 15	0.036
L : R kidney	16 : 19	14 : 11	0.601
WIT (min)	12.9 ± 4.0	0	-
CIT (h)	27.7 ± 13.4	34.3 ± 17.1	0.099

Table 2. Donor demographics and ischaemic times. Donor age, male or female, left or right kidney, warm ischaemic time (WIT) and cold ischaemic time (CIT).

C4d staining	Nil	<10%	<50%	>50%
Pre perfusion				
DCD	9.7%	25.8%	41.9%	22.6%
DBD	9.1%	36.4%	31.8%	22.7%
Post perfusion				
DCD	11.1%	33.3%	18.5%	37.1%
DBD	0%	31.8%	31.8%	36.4%

Table 3. The level of C4d staining the per and post perfusion biopsies in the DCD and DBD kidneys.

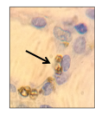


Figure 5. C4d positive staining in the renal biopsy.

Conclusion

Kidneys from DCD and DBD donors had similar perfusion characteristics during 60 minutes of EVNP. However, DCD kidneys were associated with a higher level of proteinuria. Inflammatory cytokines were not up-regulated during perfusion in DCD or DBD kidneys. Almost a quarter of DCD and DBD kidneys had diffuse C4d positive staining after static cold storage. The pattern of staining changed somewhat after EVNP with some kidneys expressing more and some less positive staining. EVNP does not appear to up-regulate inflammatory or complement pathways in human DCD or DBD kidneys.

194

Investigations of human kidneys pre-transplantation

Z Zwaini (zdrz2@le.ac.uk)^{1,2}, SA Hosgood³, M Patel¹, C Stover¹ and ML Nicholson³

¹ Department of Infection, Immunity and Inflammation, University of Leicester, UK. ² College of Medicine, University of Kufa, Iraq. ³ Department of Surgery, University of Cambridge, UK

Introduction:

Ex-vivo normothermic perfusion (EVNP) is a novel technique of kidney preservation. It is performed outside human body by circulating a red blood cell based solution through the kidney at normal body temperature. Normothermic perfusion of kidneys may improve surgical outcomes and open the door to use kidneys in transplantation, which were previously declined.

The aim of this study is to compare kidneys obtained from donors with brain death (DBD) and donors with circulatory death (DCD) using novel markers of inflammation and renal damage.

Method:

Sixty human kidneys underwent 60 minutes of *Ex-vivo* normothermic perfusion (EVNP) at 37°C (Figure 1 and 2). Thirty five kidneys were from DCD donors and 25 from DBD donors. Von Willebrand Factor (vWF) and complement fragment C4d were measured in tissue during perfusion.

October 2012 – July 2013

60 kidneys declined for transplantation

Reasons for Decline

PMH (Past medical history)	15
Poor Flush	13
Donor Age	9
HMP (Hypothermic machine perfusion) Parameters	8
Technical/Anatomical	6
Histology	5
Prolonged CIT (Cold ischemic time)	4

Table 1. Reasons for decline for transplantation

Results:

9.1% of DBD and 3% of DCD Kidneys showed mild histopathological score and no C4d deposition (Figure 3).

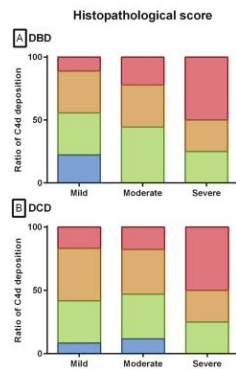


Figure 3. Semiquantitative analysis of C4d deposition in renal tubular epithelium plotted against histopathological damages in DBD (A) and DCD (B)

Conclusion: C4d staining of renal tubules did not differentiate between DBD and DCD kidneys. But vWF, the vascular endothelial marker, could be used as a predictor for the severity of renal damage in donor kidneys prior to transplant surgery. Furthermore, both DBD and DCD may be good sources of transplantable material.

Acknowledgement:

This work was partially funded by Iraqi Higher Committee for Educational Development (HCED) (Dr Z Zwaini)

References: Jamieson, R.W. and Friend, P.J. (2008) 'Normothermic organ preservation', *Transplantation reviews*, 20(4), pp. 172-178. Cohen, D., Colvin, R.B., Daha, M.R., Drachenberg, C.B., Haas, M., Nickleleit, V., Salmon, J.E., Sis, B., Zhao, M. and Bruijn, J.A. (2012) 'Pros and cons for C4d as a biomarker', *Kidney international*, 81(7), pp. 628-639. Ruggeri, Z.M. (2007) 'The role of von Willebrand factor in thrombus formation', *Thrombosis research*, 120, pp. S5-S9.



Figure 1. A picture of a kidney during EVNP

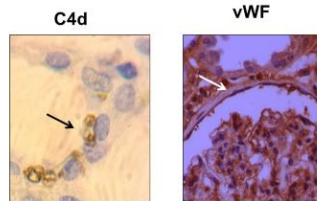


Figure 4. C4d (left) and vWF (right) positive staining in the renal biopsy

The pattern of the diffuse C4d deposition in DCD specimens (Figure 5) was significantly increased with higher renal impairment grades ($r = 0.88$; $p = 0.05$).

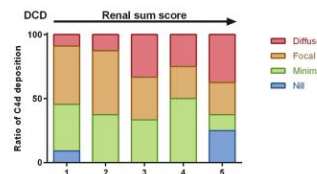


Figure 5. Semiquantitative analysis of C4d deposition in renal tubular epithelium blotted against sum score in DCD. The sum score is a cumulative score of renal blood flow; urinary output and visual score calculated from 1-5.

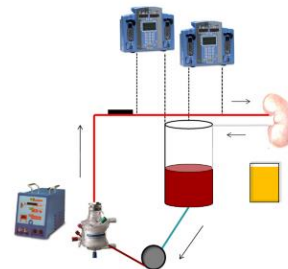


Figure 2. Schematic diagram of the ex-vivo normothermic perfusion (EVNP) system

In terms of vWF, 4.5% of DBD and 3.4% of DCD kidneys showed mild histopathological score with no vWF reactivity. There were significantly more DBD kidneys (13.6%) that showed mild histopathological score and moderate vWF reactivity (Figure 6).

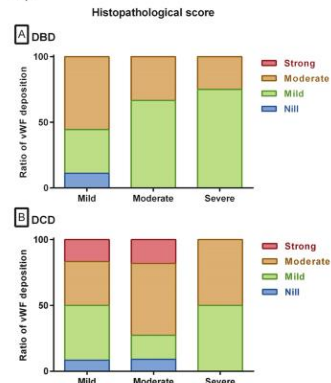


Figure 6. Semiquantitative analysis of vWF deposition in renal tubular epithelium plotted against histopathological damages in DBD (A) and DCD (B)

3. UK kidney week (UKKW), Birmingham 7th-10th June, 2016 (poster)

Properdin deficiency aggravates renal injury of ischemia reperfusion

Zinah Dheyaa Zwaini^{1,3}, Nigel J. Brunskill^{1,2}, Wilhelm Schwaeble¹, Cordula M Stover¹ and Bin Yang^{1,2,4}.

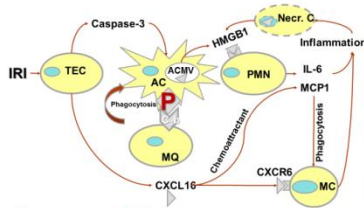
¹Infection, Immunity and Inflammation, University of Leicester; ²Renal Group, University Hospitals of Leicester, UK; ³College of Medicine, University of Kufa, Iraq; ⁴Basic Medical Research Centre of Medical School, Nephrology, Affiliated Hospital of Nantong University, China



Introduction and aims

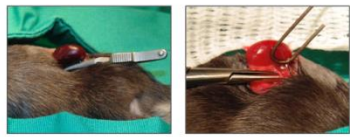
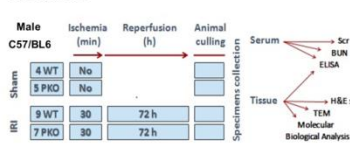
Ischemia reperfusion injury (IRI) is one of major causes of acute renal injury. Properdin stabilizes C3bBb convertase and positively regulates the alternative complement pathway (AP), which may play key roles in renal IRI.

The aim of this study is to investigate the effect of properdin knockout (P^{KO}) on renal IRI.



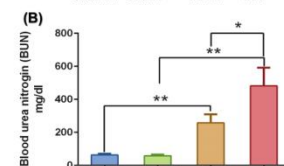
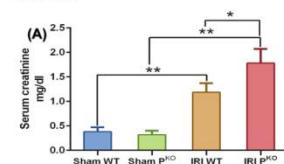
AC= Apoptotic Cell; ACMV= Apoptotic Cell-derived Membrane Vesicles; MC= Monocytes; MΦ= Macrophage; Necr. C= Necrotic Cell; PMN= Polymorph Neutrophil; TEC= Tubular Endothelial Cell;

Methods

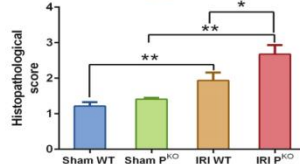


A pink red kidney before clamping (left) and the dark red colour due to ischemia (right).

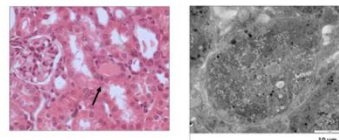
Results



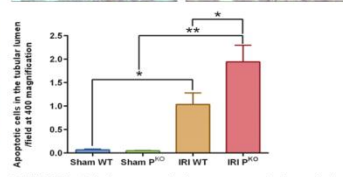
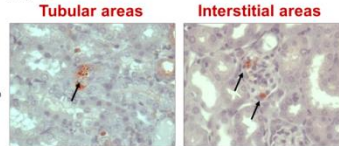
Renal function; serum creatinine (A) and blood urea nitrogen (B); p (*) ≤ 0.05, (**) ≤ 0.01.



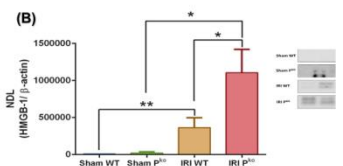
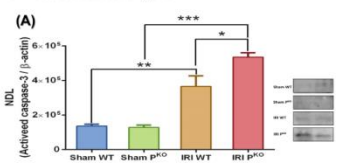
Microscopically, P^{KO} results in more tissue damage in kidney comparing to congenic wild type.



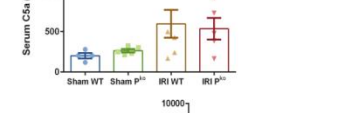
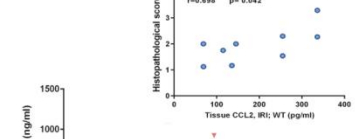
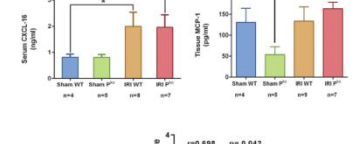
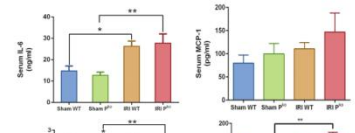
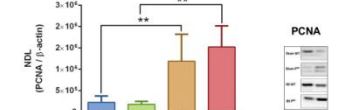
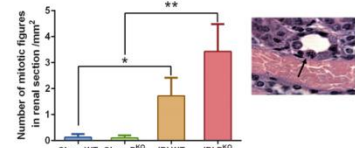
H&E staining of kidney sections showing accumulation of protein cast (left). Ultrastructural cellular damages were observed under TEM (right).



TUNNEL staining revealed more apoptotic cells in P^{KO} mice than wild type.



The expression of inflammatory marker HMGB1 and activated caspase-3 were significantly higher in P^{KO} mice.



There was no statistically significant change in complement C5a and C5b-9.

Conclusions

- Renal IRI was significantly enhanced in P^{KO} mice, which may be associated with increased inflammation and compromised clearance of apoptotic cells.
- Detected complement pathways did not show significant difference between P^{KO} and wild type mice, but the difference in *in situ* binding of complement elements cannot be ruled out.

References: (1) Hesketh EE, Czopek A, Clay M, et al. *J Vis Exp*. 2014; 88, e51816. (2) Kolimaa JP, van Werkhoven MB, O'Flynn J, et al. *J Immunol Methods*. 2015 Apr;419:25. (3) Leshner AM, Zhou L, Kimura Y, et al. *J Am Soc Nephrol*. 2013;24:53

Dr Zinah Dheyaa Zwaini: zddrz2@le.ac.uk; Dr Bin Yang: by5@le.ac.uk

4. American Society of Nephrology (ASN) Kidney week 2015. San Diego, CA, USA, 3RD-8TH Nov. 2015. (Abstract p.888).

[file:///C:/Users/x121e/Downloads/KW15Abstracts%20\(1\).pdf](file:///C:/Users/x121e/Downloads/KW15Abstracts%20(1).pdf)

5. 53rd ERA-EDTA Congress, Vienna, Austria, 21st-24th May 2016 (free communication)





EACCME
European Accreditation Council for Continuing Medical Education

CERTIFICATE

53rd ERA-EDTA Congress
Vienna, Austria (21-24.05.2016)

has been accredited by the European Accreditation Council for Continuing Medical Education (EACCME) to provide the following CME activity for medical specialists:

53rd ERA-EDTA Congress
is designated for a maximum of, or up to 24 European CME credits (CMEC).

Dr. Zinah Zwaini

Number of credits

9

Prof. Gert Mayer
53rd Congress President

Prof. Danilo Fliser
*Chair of the Scientific Committee
of 53rd ERA-EDTA Congress*

Prof. Jorge Cannata Andia
*President of UEMS
Section of Nephrology*



Each medical specialist should claim only those credits that he/she actually spent in the educational activity. The EACCME is an institution of the European Union of Medical Specialists (UEMS), whose services, through an agreement between the Association of Medical Specialists and the American Medical Association, physicians may convert EACCME credits to an equivalent number of AMA-PPA Category 1 CreditSM. Information on the process to convert EACCME credit to AMA credit can be found at www.ama-assn.org/pressroom/education. The educational activities occurring outside of Europe, organized by the U.E.A.C.C.M.E. for C.M.E. credits are controlled by Accredited Group Learning Activities Section. This section is defined by the bylaws of the Council Program of The Royal College of Physicians and Surgeons of Canada.

6. Mode of Proximal Tubule Damage: Differential Cause for the Release of TFF3?
(article at *Frontiers in Immunology*. 2016;7:122. doi:10.3389/fimmu.2016.00122)



Mode of Proximal Tubule Damage: Differential Cause for the Release of TFF3?

Zinah Zwaini^{1,2†}, Dalia Alammari^{1†}, Simon Byrne¹ and Cordula Stover^{1*}

¹Department of Infection, Immunity and Inflammation, College of Medicine, Biological Sciences and Psychology, University of Leicester, Leicester, UK, ²Kufa College of Medicine, Najaf, Iraq

Proximal tubular epithelial cells are particularly sensitive to damage. In search of a biomarker, this study evaluated the potential of different cell activation models (hypoxia/replenishment and protein overload) to lead to a release of trefoil factor 3 (TFF3). Surprisingly, we found disparity in the ability of the different stimuli to enhance the intracellular abundance of TFF3 and its release: while conditions of nutrient starvation and damage associated with replenishment lead to intracellular abundance of TFF3 in the absence of TFF3 release, stimulation with an excess amount of albumin did not yield accumulation of TFF3. By contrast, incubation of cells with a purified λ light chain preparation from a patient with multiple myeloma provoked the presence of TFF3 in the cell supernatant. We, therefore, propose that elevations of TFF3 in renal disease might be more revelatory for the cause of restitution than previously thought.

Keywords: trefoil factor 3, nutrient starvation, hypoxia, renal, protein-induced damage

OPEN ACCESS

Edited by:

Uday Kishore,
Brunel University London, UK

Reviewed by:

Taruna Madan,
National Institute for Research in
Reproductive Health, India
Miki Nakao,
Kyushu University, Japan

***Correspondence:**

Cordula Stover
cms13@le.ac.uk

[†]Zinah Zwaini and Dalia Alammari
contributed equally

Specialty section:

This article was submitted to
Molecular Innate Immunity,
a section of the journal
Frontiers in Immunology

Received: 14 January 2016

Accepted: 18 March 2016

Published: 30 March 2016

Citation:

Zwaini Z, Alammari D, Byrne S and
Stover C (2016) Mode of Proximal
Tubule Damage: Differential Cause for
the Release of TFF3?
Front. Immunol. 7:122.
doi: 10.3389/fimmu.2016.00122

INTRODUCTION

Trefoil factor 3 (TFF3) has a role in restitution (cell migration to heal superficial lesions) and regeneration (differentiation and proliferation as repair) of epithelia. Contrasting with genes that encode other members of the TFF peptide family, TFF3 mRNA is expressed in the cortex of the kidney (1). TFF3 peptide was readily detectable in urine from patients with nephrolithiasis compared to normal urine (1). Elevated levels were also found in urine from patients with incident chronic kidney disease as part of a nested study with a median follow up time of nearly 9 years (2) as well as in serum of patients with chronic kidney disease stages 1–5 (3). Possible triggers for the release of TFF3 may include damage or inflammation (2).

We have developed *in vitro* models that target cells of the proximal tubular epithelial cell line HK-2 in different ways: a phase of hypoxia/nutrient starvation (HNS) and subsequent replenishment with medium models the injury observed in ischemia reperfusion; stimulation of HK-2 cells with immunoglobulin light chains (LCs) or albumin devoid of fatty acids models effects of monoclonal gammopathy and elevated protein, respectively.

The aim of this study was to compare and contrast TFF3 release in response to these experimental conditions.

MATERIALS AND METHODS

For the HNS–replenishment (HNSR) model, phenolphthalein containing growth medium [DMEM:F-12 (Thermo Fisher Scientific Ltd.) with L-glutamine (200 mM), 10% (v/v) fetal calf serum (FCS), 200 μ g/ml recombinant human epidermal growth factor (Sigma-Aldrich Company

Bibliography

Biobibliography

Aktas, S., Boyvat, F., Sevmis, S., Moray, G., Karakayali, H. & Haberal, M. (2011) 'Analysis of vascular complications after renal transplantation', *Transplantation proceedings* Elsevier, pp. 557.

Alangaden, G.J., Thyagarajan, R., Gruber, S.A., Morawski, K., Garnick, J., El-Amm, J.M., West, M.S., Sillix, D.H., Chandrasekar, P.H. and Haririan, A. (2006) 'Infectious complications after kidney transplantation: current epidemiology and associated risk factors', *Clinical transplantation*, 20(4), pp. 401-409.

Ammar, H.I., Saba, S., Ammar, R.I., Elsayed, L.A., Ghaly, W.B. and Dhingra, S. (2011) 'Erythropoietin protects against doxorubicin-induced heart failure', *American journal of physiology. Heart and circulatory physiology*, 301(6), pp. H2413-21.

Arumugam, T.V., Tang, S.C., Lathia, J.D., Cheng, A., Mughal, M.R., Chigurupati, S., Magnus, T., Chan, S.L., Jo, D.G., Ouyang, X., Fairlie, D.P., Granger, D.N., Vortmeyer, A., Basta, M. and Mattson, M.P. (2007) 'Intravenous immunoglobulin (IVIG) protects the brain against experimental stroke by preventing complement-mediated neuronal cell death', *Proceedings of the National Academy of Sciences of the United States of America*, 104(35), pp. 14104-14109.

Arya, M., Shergill, I.S., Williamson, M., Gommersall, L., Arya, N. and Patel, H.R. (2014) 'Basic principles of real-time quantitative PCR', *Expert review of molecular diagnostics*,

Asgari, E., Farrar, C.A., Lynch, N., Ali, Y.M., Roscher, S., Stover, C., Zhou, W., Schwaeble, W.J. and Sacks, S.H. (2014) 'Mannan-binding lectin-associated serine protease 2 is critical for the development of renal ischemia reperfusion injury and mediates tissue injury in the absence of complement C4', *FASEB journal : official publication of the Federation of American Societies for Experimental Biology*, 28(9), pp. 3996-4003.

Aubert, O., Kamar, N., Vernerey, D., Viglietti, D., Martinez, F., Duong-Van-Huyen, J.P., Eladari, D., Empana, J.P., Rabant, M., Verine, J., Rostaing, L., Congy, N., Guilbeau-Frugier, C., Mourad, G., Garrigue, V., Morelon, E., Giral, M., Kessler, M., Ladriere, M., Delahousse, M., Glotz, D., Legendre, C., Jouven, X., Lefaucheur, C. and Loupy, A.

(2015) 'Long term outcomes of transplantation using kidneys from expanded criteria donors: prospective, population based cohort study', *BMJ (Clinical research ed.)*, 351, pp. h3557.

Auråen, H., Mollnes, T.E., Bjørtuft, Ø., Bakkan, P.A., Geiran, O., Kongerud, J., Fiane, A. and Holm, A.M. (2013) 'Multiorgan procurement increases systemic inflammation in brain dead donors', *Clinical transplantation*, 27(4), pp. 613-618.

Averna, M., Barbagallo, C.M., Ganci, A., Giammarresi, C., Cefalù, A.B., Sparacino, V., Caputo, F., Basili, S., Notarbartolo, A. and Davì, G. (2001) 'Determinants of enhanced thromboxane biosynthesis in renal transplantation', *Kidney international*, 59(4), pp. 1574-1579.

Banda, N.K., Mehta, G., Ferreira, V.P., Cortes, C., Pickering, M.C., Pangburn, M.K., Arend, W.P. and Holers, V.M. (2013) 'Essential role of surface-bound complement factor H in controlling immune complex-induced arthritis', *Journal of immunology (Baltimore, Md.: 1950)*, 190(7), pp. 3560-3569.

Banda, N.K., Takahashi, M., Takahashi, K., Stahl, G.L., Hyatt, S., Glogowska, M., Wiles, T.A., Endo, Y., Fujita, T. and Holers, V.M. (2011) 'Mechanisms of mannose-binding lectin-associated serine proteases-1/3 activation of the alternative pathway of complement', *Molecular immunology*, 49(1), pp. 281-289.

Bakris, G.L., Fonseca, V.A., Sharma, K. and Wright, E.M. (2009) 'Renal sodium–glucose transport: role in diabetes mellitus and potential clinical implications', *Kidney international*, 75(12), pp. 1272-1277.

Barklin, A. (2009) 'Systemic inflammation in the brain-dead organ donor', *Acta Anaesthesiologica Scandinavica*, 53(4), pp. 425-435.

Basile, D.P., Donohoe, D.L., Roethe, K. and Mattson, D.L. (2003) 'Chronic renal hypoxia after acute ischemic injury: effects of L-arginine on hypoxia and secondary damage', *American journal of physiology.Renal physiology*, 284(2), pp. F338-48.

Basile, D.P., Fredrich, K., Chelladurai, B., Leonard, E.C. and Parrish, A.R. (2008) 'Renal ischemia reperfusion inhibits VEGF expression and induces ADAMTS-1, a novel VEGF inhibitor', *American journal of physiology.Renal physiology*, 294(4), pp. F928-36.

Basu, R.K., Hubchak, S., Hayashida, T., Runyan, C.E., Schumacker, P.T. and Schnaper, H.W. (2011) 'Interdependence of HIF-1 α and TGF- β /Smad3 signaling in normoxic and hypoxic renal epithelial cell collagen expression', *American journal of physiology.Renal physiology*, 300(4), pp. F898-905.

Bellingham, J.M., Santhanakrishnan, C., Neidlinger, N., Wai, P., Kim, J., Niederhaus, S., Levenson, G.E., Fernandez, L.A., Foley, D.P. and Mezrich, J.D. (2011) 'Donation after cardiac death: a 29-year experience', *Surgery*, 150(4), pp. 692-702.

Benítez, C., Londoño, M., Miquel, R., Manzia, T., Abraldes, J.G., Lozano, J., Martínez-Llordella, M., López, M., Angelico, R. and Bohne, F. (2013) 'Prospective multicenter clinical trial of immunosuppressive drug withdrawal in stable adult liver transplant recipients', *Hepatology*, 58(5), pp. 1824-1835.

Bernhardt, W.M., Wiesener, M.S., Scigalla, P., Chou, J., Schmieder, R.E., Gunzler, V. and Eckardt, K.U. (2010) 'Inhibition of prolyl hydroxylases increases erythropoietin production in ESRD', *Journal of the American Society of Nephrology : JASN*, 21(12), pp. 2151-2156.

Bill Grimes, Rick Hallick, Ken Williams (2004) *The Biology project. Cell Biology*. Available at: http://www.biology.arizona.edu/cell_bio/tutorials/cell_cycle/cells3.html

Binnani, P., Gandhi, B. and Bahadur, M.M. (2012) *Renal transplantation from expanded criteria donors*. INTECH Open Access Publisher.

Blann, A. (2000) 'Endothelial cell activation, injury, damage and dysfunction: separate entities or mutual terms?', *Blood Coagulation & Fibrinolysis*, 11(7), pp. 623-630.

Boackle, S.A., Morris, M.A., Holers, V.M. and Karp, D.R. (1998) 'Complement opsonization is required for presentation of immune complexes by resting peripheral blood B cells', *Journal of immunology (Baltimore, Md.: 1950)*, 161(12), pp. 6537-6543.

Bokisch, V.A., Dierich, M.P. and Muller-Eberhard, H.J. (1975) 'Third component of complement (C3): structural properties in relation to functions', *Proceedings of the National Academy of Sciences of the United States of America*, 72(6), pp. 1989-1993.

Bonventre, J.V. (2010) 'Pathophysiology of AKI: injury and normal and abnormal repair', *Contributions to nephrology*, 165, pp. 9-17.

- Bonventre, J.V. (2003) 'Dedifferentiation and proliferation of surviving epithelial cells in acute renal failure', *Journal of the American Society of Nephrology : JASN*, 14 Suppl 1, pp. S55-61.
- Bonventre, J.V. and Weinberg, J.M. (2003) 'Recent advances in the pathophysiology of ischemic acute renal failure', *Journal of the American Society of Nephrology : JASN*, 14(8), pp. 2199-2210.
- Bonventre, J.V. and Yang, L. (2011) 'Cellular pathophysiology of ischemic acute kidney injury', *The Journal of clinical investigation*, 121(11), pp. 4210-4221.
- Brar, J.E. and Quigg, R.J. (2014) 'Complement activation in the tubulointerstitium: AKI, CKD, and in between', *Kidney international*, 86(4), pp. 663-666.
- Breggia, A.C. and Himmelfarb, J. (2008) 'Primary mouse renal tubular epithelial cells have variable injury tolerance to ischemic and chemical mediators of oxidative stress', *Oxidative medicine and cellular longevity*, 1(1), pp. 33-38.
- Briggs, J.D. (2001) 'Causes of death after renal transplantation', *Nephrology, dialysis, transplantation : official publication of the European Dialysis and Transplant Association - European Renal Association*, 16(8), pp. 1545-1549.
- Brouland, J.P., Egan, T., Roussi, J., Bonneau, M., Pignaud, G., Bal, C., Vaiman, M., Andre, P., Herve, P., Mazmanian, G.M. and Drouet, L. (1999) 'In vivo regulation of von willebrand factor synthesis: von Willebrand factor production in endothelial cells after lung transplantation between normal pigs and von Willebrand factor-deficient pigs', *Arteriosclerosis, Thrombosis, and Vascular Biology*, 19(12), pp. 3055-3062.
- Bugge, J. (2009) 'Brain death and its implications for management of the potential organ donor', *Acta Anaesthesiologica Scandinavica*, 53(10), pp. 1239-1250.
- Burger, D.E., Xiang, F.L., Hammoud, L., Jones, D.L. and Feng, Q. (2009) 'Erythropoietin protects the heart from ventricular arrhythmia during ischemia and reperfusion via neuronal nitric-oxide synthase', *The Journal of pharmacology and experimental therapeutics*, 329(3), pp. 900-907.

- Burns, A.T., Davies, D.R., McLaren, A.J., Cerundolo, L., Morris, P.J. and Fuggle, S.V. (1998) 'Apoptosis in ischemia / reperfusion injury of human renal allografts', *Transplantation*, 66(7), pp. 872-876.
- Calvillo, L., Latini, R., Kajstura, J., Leri, A., Anversa, P., Ghezzi, P., Salio, M., Cerami, A. and Brines, M. (2003) 'Recombinant human erythropoietin protects the myocardium from ischemia-reperfusion injury and promotes beneficial remodeling', *Proceedings of the National Academy of Sciences of the United States of America*, 100(8), pp. 4802-4806.
- Caron, E. and Hall, A. (1998) 'Identification of two distinct mechanisms of phagocytosis controlled by different Rho GTPases', *Science (New York, N.Y.)*, 282(5394), pp. 1717-1721.
- Carroll, M.C. (2004) 'The complement system in regulation of adaptive immunity', *Nature immunology*, 5(10), pp. 981-986.
- Carroll, S. and Georgiou, G. (2013) 'Antibody-mediated inhibition of human C1s and the classical complement pathway', *Immunobiology*, 218(8), pp. 1041-1048.
- Casonato, A., Pontara, E., Vertolli, U.P., Steffan, A., Durante, C., De Marco, L., Sartorello, F. and Girolami, A. (2001) 'Plasma and platelet von Willebrand factor abnormalities in patients with uremia: lack of correlation with uremic bleeding', *Clinical and applied thrombosis/hemostasis : official journal of the International Academy of Clinical and Applied Thrombosis/Hemostasis*, 7(2), pp. 81-86.
- Chana, R.S., Sidaway, J.E. and Brunskill, N.J. (2008) 'Statins but not thiazolidinediones attenuate albumin-mediated chemokine production by proximal tubular cells independently of endocytosis', *American Journal of Nephrology*, 28(5), pp. 823-830.
- Chen, G., Shiu-Chung Ko, D., Wang, C., Qiu, J., Han, M., He, X. and Chen, L. (2013) 'Kidney transplantation from donors after cardiac death: an initial report of 71 cases from China', *American Journal of Transplantation*, 13(5), pp. 1323-1326.
- Chen, J., Wang, W., Zhang, Q., Li, F., Lei, T., Luo, D., Zhou, H. and Yang, B. (2013) 'Low molecular weight fucoidan against renal ischemia–reperfusion injury via inhibition of the MAPK signaling pathway', *PloS one*, 8(2), pp. e56224.

Chen, G., Lin, S.C., Chen, J., He, L., Dong, F., Xu, J., Han, S., Du, J., Entman, M.L. and Wang, Y. (2011) 'CXCL16 recruits bone marrow-derived fibroblast precursors in renal fibrosis', *Journal of the American Society of Nephrology : JASN*, 22(10), pp. 1876-1886.

Chen, M., Harris, M.P., Rose, D., Smart, A., He, X.R., Kretzler, M., Briggs, J.P. and Schnermann, J. (1994) 'Renin and renin mRNA in proximal tubules of the rat kidney', *The Journal of clinical investigation*, 94(1), pp. 237-243.

Chmurzyńska, A. (2006) 'The multigene family of fatty acid-binding proteins (FABPs): function, structure and polymorphism', *Journal of Applied Genetics*, 47(1), pp. 39-48.

Cireşan, D.C., Giusti, A., Gambardella, L.M. and Schmidhuber, J. (2013) 'Mitosis detection in breast cancer histology images with deep neural networks', in Anonymous *Medical Image Computing and Computer-Assisted Intervention–MICCAI 2013*. Springer, pp. 411-418.

Cockman, M.E., Masson, N., Mole, D.R., Jaakkola, P., Chang, G.W., Clifford, S.C., Maher, E.R., Pugh, C.W., Ratcliffe, P.J. and Maxwell, P.H. (2000) 'Hypoxia inducible factor- α binding and ubiquitylation by the von Hippel-Lindau tumor suppressor protein', *The Journal of biological chemistry*, 275(33), pp. 25733-25741.

Cohen, D., Colvin, R.B., Daha, M.R., Drachenberg, C.B., Haas, M., Nickeleit, V., Salmon, J.E., Sis, B., Zhao, M. and Bruijn, J.A. (2012) 'Pros and cons for C4d as a biomarker', *Kidney international*, 81(7), pp. 628-639.

Cohen, B., Smits, J.M., Haase, B., Persijn, G., Vanrenterghem, Y. and Frei, U. (2005) 'Expanding the donor pool to increase renal transplantation', *Nephrology, dialysis, transplantation : official publication of the European Dialysis and Transplant Association - European Renal Association*, 20(1), pp. 34-41.

Collins, A.B., Schneeberger, E.E., Pascual, M.A., Saidman, S.L., Williams, W.W., Tolkoff-Rubin, N., Cosimi, A.B. and Colvin, R.B. (1999) 'Complement activation in acute humoral renal allograft rejection: diagnostic significance of C4d deposits in peritubular capillaries', *Journal of the American Society of Nephrology : JASN*, 10(10), pp. 2208-2214.

Conde, E., Alegre, L., Blanco-Sanchez, I., Saenz-Morales, D., Aguado-Fraile, E., Ponte, B., Ramos, E., Saiz, A., Jimenez, C., Ordonez, A., Lopez-Cabrera, M., del Peso, L., de

- Landazuri, M.O., Liano, F., Selgas, R., Sanchez-Tomero, J.A. and Garcia-Bermejo, M.L. (2012) 'Hypoxia inducible factor 1-alpha (HIF-1 alpha) is induced during reperfusion after renal ischemia and is critical for proximal tubule cell survival', *PLoS one*, 7(3), pp. e33258.
- Corrêa, R.R.M., Machado, J.R., da Silva, M.V., Helmo, F.R., Guimarães, C.S.O., Rocha, L.P., Faleiros, A.C.G. and dos Reis, M.A. (2013) 'The importance of C4d in biopsies of kidney transplant recipients', *Clinical and Developmental Immunology*, 2013.
- Cortes, C., Ohtola, J.A., Saggi, G. and Ferreira, V.P. (2012) 'Local release of properdin in the cellular microenvironment: role in pattern recognition and amplification of the alternative pathway of complement', *Front Immunol*, 3(412.10), pp. 3389.
- Cravedi, P. and Heeger, P.S. (2014) 'Complement as a multifaceted modulator of kidney transplant injury', *The Journal of clinical investigation*, 124(6), pp. 2348-2354.
- Dabbs, D.J. (2013) *Diagnostic immunohistochemistry*. Elsevier Health Sciences.
- Daemen, M.A., de Vries, B. and Buurman, W.A. (2002) 'Apoptosis and inflammation in renal reperfusion injury', *Transplantation*, 73(11), pp. 1693-1700.
- Daha, M.R. (2013) 'Unexpected role for properdin in complement C3 glomerulopathies', *Journal of the American Society of Nephrology : JASN*, 24(1), pp. 5-7.
- Damman, J., Nijboer, W.N., Schuurs, T.A., Leuvenink, H.G., Morariu, A.M., Tullius, S.G., van Goor, H., Ploeg, R.J. and Seelen, M.A. (2011) 'Local renal complement C3 induction by donor brain death is associated with reduced renal allograft function after transplantation', *Nephrology, dialysis, transplantation : official publication of the European Dialysis and Transplant Association - European Renal Association*, 26(7), pp. 2345-2354.
- Damman, J., Seelen, M.A., Moers, C., Daha, M.R., Rahmel, A., Leuvenink, H.G., Paul, A., Pirenne, J. and Ploeg, R.J. (2011) 'Systemic complement activation in deceased donors is associated with acute rejection after renal transplantation in the recipient', *Transplantation*, 92(2), pp. 163-169.

- Danobeitia, J.S., Djamali, A. and Fernandez, L.A. (2014) 'The role of complement in the pathogenesis of renal ischemia-reperfusion injury and fibrosis', *Fibrogenesis & tissue repair*, 7(1), pp. 1-11.
- Day, C., Patel, R., Guillen, C. and Wardlaw, A.J. (2009) 'The chemokine CXCL16 is highly and constitutively expressed by human bronchial epithelial cells', *Experimental lung research*, 35(4), pp. 272-283.
- De Rosa, P., Muscogiuri, G. and Sarno, G. (2013) 'Expanded criteria donors in kidney transplantation: the role of older donors in a setting of older recipients', *ISRN Transplantation*, 2013.
- de Vries, B., Matthijsen, R.A., van Bijnen, A.A., Wolfs, T.G. and Buurman, W.A. (2003) 'Lysophosphatidic acid prevents renal ischemia-reperfusion injury by inhibition of apoptosis and complement activation', *The American journal of pathology*, 163(1), pp. 47-56.
- de Vries, B., Matthijsen, R.A., Wolfs, T.G., van Bijnen, A.A., Heeringa, P. and Buurman, W.A. (2003) 'Inhibition of complement factor C5 protects against renal ischemia-reperfusion injury: inhibition of late apoptosis and inflammation¹', *Transplantation*, 75(3), pp. 375-382.
- de Vries, B., Kohl, J., Leclercq, W.K., Wolfs, T.G., van Bijnen, A.A., Heeringa, P. and Buurman, W.A. (2003) 'Complement factor C5a mediates renal ischemia-reperfusion injury independent from neutrophils', *Journal of immunology (Baltimore, Md.: 1950)*, 170(7), pp. 3883-3889.
- Delves, P.J., Martin, S.J., Burton, D.R. and Roitt, I.M. (2011) *Roitt's essential immunology*. John Wiley & Sons.
- Dimitrova, P., Ivanovska, N., Schwaeble, W., Gyurkovska, V. and Stover, C. (2010) 'The role of properdin in murine zymosan-induced arthritis', *Molecular immunology*, 47(7), pp. 1458-1466.
- Du, T., Luo, H., Qin, H., Wang, F., Wang, Q., Xiang, Y. and Zhang, Y. (2013) 'Circulating serum trefoil factor 3 (TFF3) is dramatically increased in chronic kidney disease', .

- Duehrkop, C. and Rieben, R. (2014) 'Ischemia/reperfusion injury: effect of simultaneous inhibition of plasma cascade systems versus specific complement inhibition', *Biochemical pharmacology*, 88(1), pp. 12-22.
- Duffy, A.M., Bouchier-Hayes, D.J. and Harmey, J.H. (2004) 'Vascular Endothelial Growth Factor (VEGF) and Its Role in Non-Endothelial Cells: Autocrine Signalling by VEGF', *VEGF and Cancer*, , pp. 133-144.
- Dunkelberger, J.R. and Song, W. (2010) 'Complement and its role in innate and adaptive immune responses', *Cell research*, 20(1), pp. 34-50.
- Eaton, S.L., Roche, S.L., Hurtado, M.L., Oldknow, K.J., Farquharson, C., Gillingwater, T.H. and Wishart, T.M. (2013) 'Total protein analysis as a reliable loading control for quantitative fluorescent Western blotting', *PLoS one*, 8(8), pp. e72457.
- Egger, B., Procaccino, F., Lakshmanan, J., Reinshagen, M., Hoffmann, P., Patel, A., Reuben, W., Gnanakkan, S., Liu, L. and Barajas, L. (1997) 'Mice lacking transforming growth factor alpha have an increased susceptibility to dextran sulfate-induced colitis', *Gastroenterology*, 113(3), pp. 825-832.
- Ehrnthaller, C., Ignatius, A., Gebhard, F. and Huber-Lang, M. (2011) 'New insights of an old defense system: structure, function, and clinical relevance of the complement system', *Molecular medicine (Cambridge, Mass.)*, 17(3-4), pp. 317-329.
- Eickelberg, O., Seebach, F., Riordan, M., Thulin, G., Mann, A., Reidy, K.H., Van Why, S.K., Kashgarian, M. and Siegel, N. (2002) 'Functional activation of heat shock factor and hypoxia-inducible factor in the kidney', *Journal of the American Society of Nephrology : JASN*, 13(8), pp. 2094-2101.
- Ekdahl, K.N., Nilsson, B., Pekna, M. and Nilsson, U. (1992) 'Generation of iC3 at the interface between blood and gas', *Scandinavian Journal of Immunology*, 35(1), pp. 85-91.
- Elliott, M.R. and Ravichandran, K.S. (2010) 'Clearance of apoptotic cells: implications in health and disease', *The Journal of cell biology*, 189(7), pp. 1059-1070.
- Elmore, S. (2007) 'Apoptosis: a review of programmed cell death', *Toxicologic pathology*, 35(4), pp. 495-516.

- Eltzschig, H.K. and Eckle, T. (2011) 'Ischemia and reperfusion [mdash] from mechanism to translation', *Nature medicine*, 17(11), pp. 1391-1401.
- Feliers, D. and Kasinath, B.S. (2010) 'Mechanism of VEGF expression by high glucose in proximal tubule epithelial cells', *Molecular and cellular endocrinology*, 314(1), pp. 136-142.
- Ferreira, V.P., Pangburn, M.K. and Cortés, C. (2010) 'Complement control protein factor H: the good, the bad, and the inadequate', *Molecular immunology*, 47(13), pp. 2187-2197.
- Feucht, H.E. and Opelz, G. (1996) 'The humoral immune response towards HLA class II determinants in renal transplantation', *Kidney international*, 50, pp. 1464-1475.
- Feucht, H.E., Schneeberger, H., Hillebrand, G., Burkhardt, K., Weiss, M., Riethmüller, G., Land, W. and Albert, E. (1993) 'Capillary deposition of C4d complement fragment and early renal graft loss', *Kidney international*, 43(6), pp. 1333-1338.
- Flannagan, R.S., Jaumouillé, V. and Grinstein, S. (2012) 'The cell biology of phagocytosis', *Annual Review of Pathology: Mechanisms of Disease*, 7, pp. 61-98.
- Flecknell, P. (2002) 'Replacement, reduction and refinement', *Altex*, 19(2), pp. 73-78.
- Floerchinger, B., Oberhuber, R. and Tullius, S.G. (2012) 'Effects of brain death on organ quality and transplant outcome', *Transplantation reviews*, 26(2), pp. 54-59.
- Fogo, A.B., Cohen, A.H., Colvin, R.B., Jennette, J.C. and Alpers, C.E. (2014) 'Renal anatomy and basic concepts and methods in renal pathology', in Anonymous *Fundamentals of Renal Pathology*. Springer, pp. 3-17.
- Fu, W., Liao, X., Ruan, J., Li, X., Chen, L., Wang, B., Wang, K. and Zhou, J. (2013) 'Recombinant human erythropoietin preconditioning attenuates liver ischemia reperfusion injury through the phosphatidylinositol-3 kinase/AKT/endothelial nitric oxide synthase pathway', *Journal of Surgical Research*, 183(2), pp. 876-884.
- Furuhashi, M. and Hotamisligil, G.S. (2008) 'Fatty acid-binding proteins: role in metabolic diseases and potential as drug targets', *Nature reviews Drug discovery*, 7(6), pp. 489-503.

Furuta, G.T., Turner, J.R., Taylor, C.T., Hershberg, R.M., Comerford, K., Narravula, S., Podolsky, D.K. and Colgan, S.P. (2001) 'Hypoxia-inducible factor 1-dependent induction of intestinal trefoil factor protects barrier function during hypoxia', *The Journal of experimental medicine*, 193(9), pp. 1027-1034.

Gaarkeuken, H., Siezenga, M.A., Zuidwijk, K., van Kooten, C., Rabelink, T.J., Daha, M.R. and Berger, S.P. (2008) 'Complement activation by tubular cells is mediated by properdin binding', *American journal of physiology. Renal physiology*, 295(5), pp. F1397-403.

Gan, S.D. and Patel, K.R. (2013) 'Enzyme immunoassay and enzyme-linked immunosorbent assay', *Journal of Investigative Dermatology*, 133(9), pp. e12.

Gilbert, R.E., Wu, L.L., Kelly, D.J., Cox, A., Wilkinson-Berka, J.L., Johnston, C.I. and Cooper, M.E. (1999) 'Pathological expression of renin and angiotensin II in the renal tubule after subtotal nephrectomy: implications for the pathogenesis of tubulointerstitial fibrosis', *The American journal of pathology*, 155(2), pp. 429-440.

Gilg, J., Webb, L., Feest, T. and Fogarty, D. (2011) 'UK Renal Registry 13th Annual Report (December 2010): Chapter 9: haemoglobin, ferritin and erythropoietin amongst UK adult dialysis patients in 2009: national and centre-specific analyses', *Nephron. Clinical practice*, 119 Suppl 2, pp. c149-77.

Gopalakrishnan, G. and Gourabathini, S.P. (2007) 'Marginal kidney donor', *Indian journal of urology : IJU : journal of the Urological Society of India*, 23(3), pp. 286-293.

Gorsuch, W.B., Chrysanthou, E., Schwaeble, W.J. and Stahl, G.L. (2012) 'The complement system in ischemia-reperfusion injuries', *Immunobiology*, 217(11), pp. 1026-1033.

Gottlieb, R.A., Burleson, K.O., Kloner, R.A., Babior, B.M. and Engler, R.L. (1994) 'Reperfusion injury induces apoptosis in rabbit cardiomyocytes', *The Journal of clinical investigation*, 94(4), pp. 1621-1628.

Gozuacik, D., Bialik, S., Raveh, T., Mitou, G., Shohat, G., Sabanay, H., Mizushima, N., Yoshimori, T. and Kimchi, A. (2008) 'DAP-kinase is a mediator of endoplasmic reticulum stress-induced caspase activation and autophagic cell death', *Cell Death & Differentiation*, 15(12), pp. 1875-1886.

- Guleng, B., Han, J., Yang, J., Huang, Q., Huang, J., Yang, X., Liu, J. and Ren, J. (2012) 'TFF3 mediated induction of VEGF via hypoxia in human gastric cancer SGC-7901 cells', *Molecular biology reports*, 39(4), pp. 4127-4134.
- Gutwein, P., Abdel-Bakky, M.S., Doberstein, K., Schramme, A., Beckmann, J., Schaefer, L., Amann, K., Doller, A., Kämpfer-Kolb, N. and Abdel-Aziz, A.H. (2009) 'CXCL16 and oxLDL are induced in the onset of diabetic nephropathy', *Journal of Cellular and Molecular Medicine*, 13(9b), pp. 3809-3825.
- Haberichter, S.L., Merricks, E.P., Fahs, S.A., Christopherson, P.A., Nichols, T.C. and Montgomery, R.R. (2005) 'Re-establishment of VWF-dependent Weibel-Palade bodies in VWD endothelial cells', *Blood*, 105(1), pp. 145-152.
- Hag Lee, Seung Hoon Lee, Byung Hoon Oh, Heung Man Lee, Jong Ouck Choi, Kwang Yoon Jung, Sang (2001) 'Expression of mRNA of trefoil factor peptides in human nasal mucosa', *Acta Oto-Laryngologica*, 121(7), pp. 849-853.
- Hahm, K.B., Im, Y.H., Parks, T.W., Park, S.H., Markowitz, S., Jung, H.Y., Green, J. and Kim, S.J. (2001) 'Loss of transforming growth factor beta signalling in the intestine contributes to tissue injury in inflammatory bowel disease', *Gut*, 49(2), pp. 190-198.
- Halazun, K., Al-Mukhtar, A., Aldouri, A., Willis, S. & Ahmad, N. (2007) 'Warm ischemia in transplantation: search for a consensus definition', *Transplantation proceedings* Elsevier, pp. 1329.
- Han, X., Gelein, R., Corson, N., Wade-Mercer, P., Jiang, J., Biswas, P., Finkelstein, J.N., Elder, A. and Oberdörster, G. (2011) 'Validation of an LDH assay for assessing nanoparticle toxicity', *Toxicology*, 287(1), pp. 99-104.
- Harboe, M. and Mollnes, T.E. (2008) 'The alternative complement pathway revisited', *Journal of Cellular and Molecular Medicine*, 12(4), pp. 1074-1084.
- Hernandez, C., Santamatilde, E., McCreath, K., Cervera, A., Díez, I., Ortiz-Masiá, D., Martínez, N., Calatayud, S., Esplugues, J. and Barrachina, M. (2009) 'Induction of trefoil factor (TFF) 1, TFF2 and TFF3 by hypoxia is mediated by hypoxia inducible factor-1: implications for gastric mucosal healing', *British journal of pharmacology*, 156(2), pp. 262-272.

- Hesketh, E.E., Czopek, A., Clay, M., Borthwick, G., Ferenbach, D., Kluth, D. and Hughes, J. (2014) 'Renal ischaemia reperfusion injury: a mouse model of injury and regeneration', *JoVE (Journal of Visualized Experiments)*, (88), pp. e51816-e51816.
- Hillen, T. and Painter, K.J. (2009) 'A user's guide to PDE models for chemotaxis', *Journal of mathematical biology*, 58(1-2), pp. 183-217.
- Hish, G.A., Jr, Diaz, J.A., Hawley, A.E., Myers, D.D., Jr and Lester, P.A. (2014) 'Effects of analgesic use on inflammation and hematology in a murine model of venous thrombosis', *Journal of the American Association for Laboratory Animal Science : JAALAS*, 53(5), pp. 485-493.
- Hochhauser, E., Pappo, O., Ribakovsky, E., Ravid, A., Kurtzwald, E., Cheporko, Y., Lelchuk, S. and Ben-Ari, Z. (2008) 'Recombinant human erythropoietin attenuates hepatic injury induced by ischemia/reperfusion in an isolated mouse liver model', *Apoptosis*, 13(1), pp. 77-86.
- Hoffman, M.C., Rumer, K.K., Kramer, A., Lynch, A.M. and Winn, V.D. (2014) 'Maternal and fetal alternative complement pathway activation in early severe preeclampsia', *American Journal of Reproductive Immunology*, 71(1), pp. 55-60.
- Hoffmann, W. (2005) 'Trefol factors', *Cellular and Molecular Life Sciences CMLS*, 62(24), pp. 2932-2938.
- Hoffmann, W. (2008) 'Regeneration of the gastric mucosa and its glands from stem cells', *Current medicinal chemistry*, 15(29), pp. 3133-3144.
- Hosgood, S.A. (2012) *Normothermic Perfusion in Renal Transplantation*, .
- Hosgood, S., Hunter, J. and Nicholson, M. (2012) 'Cold Ischaemic Injury in Kidney Transplantation', in Kapur, S., Afaneh, C. and Aull, M.J. (eds.) *Urology and Nephrology » "Current Concepts in Kidney Transplantation"*. Online: InTech, pp. 218.
- Hosseini-Moghaddam, S., Soleimanirahbar, A., Mazzulli, T., Rotstein, C. and Husain, S. (2012) 'Post renal transplantation Kaposi's sarcoma: a review of its epidemiology, pathogenesis, diagnosis, clinical aspects, and therapy', *Transplant Infectious Disease*, 14(4), pp. 338-345.

- Hotta, K., Sho, M., Yamato, I., Shimada, K., Harada, H., Akahori, T., Nakamura, S., Konishi, N., Yagita, H. and Nonomura, K. (2011) 'Direct targeting of fibroblast growth factor-inducible 14 protein protects against renal ischemia reperfusion injury', *Kidney international*, 79(2), pp. 179-188.
- Hotter, G., Palacios, L. and Sola, A. (2004) 'Low O₂ and high CO₂ in LLC-PK1 cells culture mimics renal ischemia-induced apoptosis', *Laboratory investigation*, 84(2), pp. 213-220.
- Hourcade, D.E. (2006) 'The role of properdin in the assembly of the alternative pathway C3 convertases of complement', *The Journal of biological chemistry*, 281(4), pp. 2128-2132.
- Hu, L., Yang, C., Zhao, T., Xu, M., Tang, Q., Yang, B., Rong, R. and Zhu, T. (2012) 'Erythropoietin ameliorates renal ischemia and reperfusion injury via inhibiting tubulointerstitial inflammation', *Journal of Surgical Research*, 176(1), pp. 260-266.
- Huber-Lang, M., Sarma, J.V., Zetoune, F.S., Rittirsch, D., Neff, T.A., McGuire, S.R., Lambris, J.D., Warner, R.L., Flierl, M.A. and Hoesel, L.M. (2006) 'Generation of C5a in the absence of C3: a new complement activation pathway', *Nature medicine*, 12(6), pp. 682-687.
- Hue-Roye, K. and Vege, S. (2008) 'Principles of PCR-based assays', *Immunohematology*, 24, pp. 170-175.
- Humbert, P.O. and Gödde, N.J. (2015) 'Mitotic Spindle Orientation: Semaphorin-Plexin Signaling Flags the Way', *Developmental cell*, 33(3), pp. 243-244.
- Humes, H.D., Nguyen, V.D., Cieslinski, D.A. and Messana, J.M. (1989) 'The role of free fatty acids in hypoxia-induced injury to renal proximal tubule cells', *The American Journal of Physiology*, 256(4 Pt 2), pp. F688-96.
- Hutchens, M.P., Fujiyoshi, T., Komers, R., Herson, P.S. and Anderson, S. (2012) 'Estrogen protects renal endothelial barrier function from ischemia-reperfusion in vitro and in vivo', *American journal of physiology. Renal physiology*, 303(3), pp. F377-85.

- Hyams, C., Camberlein, E., Cohen, J.M., Bax, K. and Brown, J.S. (2010) 'The *Streptococcus pneumoniae* capsule inhibits complement activity and neutrophil phagocytosis by multiple mechanisms', *Infection and immunity*, 78(2), pp. 704-715.
- Ichimura, T., Asseldonk, E.J., Humphreys, B.D., Gunaratnam, L., Duffield, J.S. and Bonventre, J.V. (2008) 'Kidney injury molecule-1 is a phosphatidylserine receptor that confers a phagocytic phenotype on epithelial cells', *The Journal of clinical investigation*, 118(5), pp. 1657-1668.
- Isfort, K., Ebert, F., Bornhorst, J., Sargin, S., Kardakaris, R., Pasparakis, M., Bahler, M., Schwerdtle, T., Schwab, A. and Hanley, P.J. (2011) 'Real-time imaging reveals that P2Y2 and P2Y12 receptor agonists are not chemoattractants and macrophage chemotaxis to complement C5a is phosphatidylinositol 3-kinase (PI3K)- and p38 mitogen-activated protein kinase (MAPK)-independent', *The Journal of biological chemistry*, 286(52), pp. 44776-44787.
- Ivanovska, N.D., Dimitrova, P.A., Luckett, J.C., El-Rachkidy Lonnen, R., Schwaeble, W.J. and Stover, C.M. (2008) 'Properdin deficiency in murine models of nonseptic shock', *Journal of immunology (Baltimore, Md.: 1950)*, 180(10), pp. 6962-6969.
- Izquierdo, M.C., Sanz, A.B., Sánchez-Niño, M.D., Pérez-Gómez, M.V., Ruiz-Ortega, M., Poveda, J., Ruiz-Andrés, O., Ramos, A.M., Moreno, J.A. and Egido, J. (2012) 'Acute kidney injury transcriptomics unveils a relationship between inflammation and ageing', *Nefrologia*, 32(6), pp. 715-723.
- Jahroudi, N. and Lynch, D.C. (1994) 'Endothelial-cell-specific regulation of von Willebrand factor gene expression', *Molecular and cellular biology*, 14(2), pp. 999-1008.
- Jamieson, R.W. and Friend, P.J. (2006) 'Normothermic organ preservation', *Transplantation reviews*, 20(4), pp. 172-178.
- Jamieson, R.W. and Friend, P.J. (2008) 'Organ reperfusion and preservation', *Frontiers in bioscience : a journal and virtual library*, 13, pp. 221-235.
- Janeway, C.J., Travers, P., Walport, M. and Shlomchik, M. (2001) *Immunobiology: The Immune System in Health and Disease*. 5th edition edn. New York, USA: Garland Science.

Janeway, C.A., Travers, P., Walport, M. and Shlomchik, M.J. (1997) *Immunobiology: the immune system in health and disease*. Current Biology.

Jennings, R.B., Ganote, C.E. and Reimer, K.A. (1975) 'Ischemic tissue injury', *The American journal of pathology*, 81(1), pp. 179-198.

Jiang, G., Zhong, X., Cui, Y., Liu, W., Tai, S., Wang, Z., Shi, Y., Zhao, S. and Li, C. (2010) 'IL-6/STAT3/TFF3 signaling regulates human biliary epithelial cell migration and wound healing in vitro', *Molecular biology reports*, 37(8), pp. 3813-3818.

Jiang, M., Liu, K., Luo, J. and Dong, Z. (2010) 'Autophagy is a renoprotective mechanism during in vitro hypoxia and in vivo ischemia-reperfusion injury', *The American journal of pathology*, 176(3), pp. 1181-1192.

Jiang, M., Wei, Q., Dong, G., Komatsu, M., Su, Y. and Dong, Z. (2012) 'Autophagy in proximal tubules protects against acute kidney injury', *Kidney international*, 82(12), pp. 1271-1283.

Jiang, M., Liu, K., Luo, J. and Dong, Z. (2010) 'Autophagy Is a Renoprotective Mechanism During in Vitro Hypoxia and in Vivo Ischemia-Reperfusion Injury', *The American Journal of Pathology*, 176(3), pp. 1181-1192.

JIC (2015) *What is Electron Microscopy?* Available at: https://www.jic.ac.uk/microscopy/intro_EM.html

Jing, C., Beesley, C., Foster, C.S., Chen, H., Rudland, P.S., West, D.C., Fujii, H., Smith, P.H. and Ke, Y. (2001) 'Human cutaneous fatty acid-binding protein induces metastasis by up-regulating the expression of vascular endothelial growth factor gene in rat Rama 37 model cells', *Cancer research*, 61(11), pp. 4357-4364.

Jones, S.E. and Jomary, C. (2002) 'Clusterin', *The international journal of biochemistry & cell biology*, 34(5), pp. 427-431.

Joshi, D., Patel, H., Baker, D.M., Shiwen, X., Abraham, D.J. and Tsui, J.C. (2011) 'Development of an in vitro model of myotube ischemia', *Laboratory Investigation*, 91(8), pp. 1241-1252.

Kamijo, A., Kimura, K., Sugaya, T., Yamanouchi, M., Hikawa, A., Hirano, N., Hirata, Y., Goto, A. and Omata, M. (2004) 'Urinary fatty acid-binding protein as a new clinical

marker of the progression of chronic renal disease', *Journal of Laboratory and Clinical Medicine*, 143(1), pp. 23-30.

Karasawa K, Asano K, Moriyama S, Ushiki M, Monya M, Iida M, Kuboki E, Yagita H, Uchida K, Nitta K and Tanaka M (2015) 'Vascular-resident CD169-positive monocytes and macrophages control neutrophil accumulation in the kidney with ischemia-reperfusion injury.', *Journal of the American Society of Nephrology*, 26(4), pp. 896-906.

Kassianos, A.J., Sampangi, S., Wang, X., Roper, K.E., Beagley, K., Healy, H. and Wilkinson, R. (2013) 'Human proximal tubule epithelial cells modulate autologous dendritic cell function', *Nephrology, dialysis, transplantation : official publication of the European Dialysis and Transplant Association - European Renal Association*, 28(2), pp. 303-312.

Katritch, V., Cherezov, V. and Stevens, R.C. (2013) 'Structure-function of the G protein-coupled receptor superfamily', *Annual Review of Pharmacology and Toxicology*, 53, pp. 531-556.

Kaushal, G.P., Singh, A.B. and Shah, S.V. (1998) 'Identification of gene family of caspases in rat kidney and altered expression in ischemia-reperfusion injury', *The American Journal of Physiology*, 274(3 Pt 2), pp. F587-95.

Kayler, L., Srinivas, T. and Schold, J. (2011) 'Influence of CIT-Induced DGF on Kidney Transplant Outcomes', *American Journal of Transplantation*, 11(12), pp. 2657-2664.

Ke, Q. and Costa, M. (2006) 'Hypoxia-inducible factor-1 (HIF-1)', *Molecular pharmacology*, 70(5), pp. 1469-1480.

Keepers, T.R., Gross, L.K. and Obrig, T.G. (2007) 'Monocyte chemoattractant protein 1, macrophage inflammatory protein 1 alpha, and RANTES recruit macrophages to the kidney in a mouse model of hemolytic-uremic syndrome', *Infection and immunity*, 75(3), pp. 1229-1236.

Kemper, C., Atkinson, J.P. and Hourcade, D.E. (2009) 'Properdin: emerging roles of a pattern-recognition molecule', *Annual Review of Immunology*, 28, pp. 131-155.

Kemper, C. and Hourcade, D.E. (2008) 'Properdin: new roles in pattern recognition and target clearance', *Molecular immunology*, 45(16), pp. 4048-4056.

Kemper, C., Mitchell, L.M., Zhang, L. and Hourcade, D.E. (2008) 'The complement protein properdin binds apoptotic T cells and promotes complement activation and phagocytosis', *Proceedings of the National Academy of Sciences of the United States of America*, 105(26), pp. 9023-9028.

Kerr, M., Bray, B., Medcalf, J., O'Donoghue, D.J. and Matthews, B. (2012) 'Estimating the financial cost of chronic kidney disease to the NHS in England', *Nephrology, dialysis, transplantation : official publication of the European Dialysis and Transplant Association - European Renal Association*, 27 Suppl 3, pp. iii73-80.

Khajuria, A., Tay, C., Shi, J., Zhao, H. and Ma, D. (2014) 'Anesthetics attenuate ischemia–reperfusion induced renal injury: Effects and mechanisms', *Acta Anaesthesiologica Taiwanica*, 52(4), pp. 176-184.

Khor, Y.M., Lam, W.W.C., Wong, W.Y. and Goh, A.S.W. (2015) 'Role of nuclear medicine imaging in evaluation of complications following renal transplant', *Proceedings of Singapore Healthcare*, , pp. 2010105815611813.

Kim, S., Kang, Y., Kim, W., Woo, D., Lee, Y., Kim, D., Park, Y.B., Kwon, B.S., Park, J. and Lee, W. (2004) 'TWEAK can induce pro-inflammatory cytokines and matrix metalloproteinase-9 in macrophages', *Circulation Journal*, 68(4), pp. 396-399.

Kim, Y.S., Lim, C.S., Kim, S., Lee, J.S., Lee, S., Kim, S.T., Kim, H.J. and Chae, D. (2000) 'Cadaveric renal allograft at the time of implantation has the similar immunological features wit rejecting allograft ', *Transplantation*, 70(7), pp. 1080-1085.

Kim, K.H., Oudit, G.Y. and Backx, P.H. (2008) 'Erythropoietin protects against doxorubicin-induced cardiomyopathy via a phosphatidylinositol 3-kinase-dependent pathway', *The Journal of pharmacology and experimental therapeutics*, 324(1), pp. 160-169.

Kinsey, G.R., Li, L. and Okusa, M.D. (2008) 'Inflammation in acute kidney injury', *Nephron.Experimental nephrology*, 109(4), pp. e102-7.

Kishi, S., Campanholle, G., Gohil, V.M., Perocchi, F., Brooks, C.R., Morizane, R., Sabbiseti, V., Ichimura, T., Mootha, V.K. and Bonventre, J.V. (2015) 'Meclizine preconditioning protects the kidney against ischemia–reperfusion injury', *EBioMedicine*, 2(9), pp. 1090-1101.

- Kondos, S., Hatfaludi, T., Voskoboinik, I., Trapani, J., Law, R., Whisstock, J. and Dunstone, M. (2010) 'The structure and function of mammalian membrane-attack complex/perforin-like proteins', *Tissue antigens*, 76(5), pp. 341-351.
- Kosieradzki, M. & Rowiński, W. (2008) 'Ischemia/reperfusion injury in kidney transplantation: mechanisms and prevention', *Transplantation proceedings* Elsevier, pp. 3279.
- Kotimaa, J.P., van Werkhoven, M.B., O'Flynn, J., Klar-Mohamad, N., van Groningen, J., Schilders, G., Rutjes, H., Daha, M.R., Seelen, M.A. and van Kooten, C. (2015) 'Functional assessment of mouse complement pathway activities and quantification of C3b/C3c/iC3b in an experimental model of mouse renal ischaemia/reperfusion injury', *Journal of immunological methods*, 419, pp. 25-34.
- Krisinger, M.J., Goebeler, V., Lu, Z., Meixner, S.C., Myles, T., Pryzdial, E.L. and Conway, E.M. (2012) 'Thrombin generates previously unidentified C5 products that support the terminal complement activation pathway', *Blood*, 120(8), pp. 1717-1725.
- Kristensen, P.L., Pedersen-Bjergaard, U., Kjær, T.W., Olsen, N.V., Dela, F., Holst, J.J., Faber, J., Tarnow, L. and Thorsteinsson, B. (2013) 'Influence of erythropoietin on cognitive performance during experimental hypoglycemia in patients with type 1 diabetes mellitus: a randomized cross-over trial', *PloS one*, 8(4), pp. e59672.
- Kumar, H. and Choi, D. (2015) 'Hypoxia Inducible Factor Pathway and Physiological Adaptation: A Cell Survival Pathway?', *Mediators of inflammation*, .
- Kumar, R. and Boim, M.A. (2009) 'Diversity of pathways for intracellular angiotensin II synthesis', *Current opinion in nephrology and hypertension*, 18(1), pp. 33-39.
- Kumar, S., Allen, D.A., Kieswich, J.E., Patel, N.S., Harwood, S., Mazzon, E., Cuzzocrea, S., Raftery, M.J., Thiemermann, C. and Yaqoob, M.M. (2009) 'Dexamethasone ameliorates renal ischemia-reperfusion injury', *Journal of the American Society of Nephrology : JASN*, 20(11), pp. 2412-2425.
- Kunduzova, O.R., Bianchi, P., Parini, A. and Cambon, C. (2002) 'Hydrogen peroxide production by monoamine oxidase during ischemia/reperfusion', *European journal of pharmacology*, 448(2), pp. 225-230.

- Kuo, J.H., Wong, M.S., Perez, R.V., Li, C., Lin, T. and Troppmann, C. (2012) 'Renal transplant wound complications in the modern era of obesity', *Journal of Surgical Research*, 173(2), pp. 216-223.
- Kurian, G.A. and Pemaih, B. (2014) 'Standardization of in vitro cell-based model for renal ischemia and reperfusion injury', *Indian journal of pharmaceutical sciences*, 76(4), pp. 348.
- Laarman, A., Milder, F., van Strijp, J. and Rooijackers, S. (2010) 'Complement inhibition by gram-positive pathogens: molecular mechanisms and therapeutic implications', *Journal of molecular medicine*, 88(2), pp. 115-120.
- Lagoo, A.S., Buckley, P.J., Burchell, L.J., Peters, D., Fechner, J.H., Tsuchida, M., Dong, Y., Hong, X., Brunner, K.G. and Oberley, T.D. (2000) 'Increased glomerular deposits of von Willebrand factor in chronic but not acute rejection of primate renal allografts ', *Transplantation*, 70(6), pp. 877-886.
- Lau, C.L., Cantu, E., Gonzalez-Stawinski, G.V., Holzknecht, Z.E., Nichols, T.C., Posther, K.E., Rayborn, C.A., Platt, J.L., Parker, W. and Davis, R.D. (2003) 'The role of antibodies and von Willebrand factor in discordant pulmonary xenotransplantation', *American Journal of Transplantation*, 3(9), pp. 1065-1075.
- Lau, A., Wang, S., Liu, W., Haig, A., Zhang, Z.X. and Jevnikar, A.M. (2014) 'Glycyrrhizic acid ameliorates HMGB1-mediated cell death and inflammation after renal ischemia reperfusion injury', *American Journal of Nephrology*, 40(1), pp. 84-95.
- Lee, D., Shenoy, S., Nigatu, Y. and Plotkin, M. (2014) 'Id proteins regulate capillary repair and perivascular cell proliferation following ischemia-reperfusion injury', *PLoS one*, 9(2), pp. e88417.
- Lee, J., Kim, S.C., Ko, Y.S., Lee, H.Y., Cho, E., Kim, M., Jo, S., Cho, W.Y. and Kim, H.K. (2014) 'Renoprotective effect of paricalcitol via a modulation of the TLR4-NF- κ B pathway in ischemia/reperfusion-induced acute kidney injury', *Biochemical and biophysical research communications*, 444(2), pp. 121-127.
- Lee, K.E., Kim, E.Y., Kim, C.S., Choi, J.S., Bae, E.H., Ma, S.K., Park, J.S., Do Jung, Y., Kim, S.H. and Lee, J.U. (2013) 'Macrophage-stimulating protein attenuates hydrogen

peroxide-induced apoptosis in human renal HK-2 cells', *European journal of pharmacology*, 715(1), pp. 304-311.

Lee, S., Evans, M.A., Chu, H.X., Kim, H.A., Widdop, R.E., Drummond, G.R. and Sobey, C.G. (2015) 'Effect of a Selective Mas Receptor Agonist in Cerebral Ischemia In Vitro and In Vivo', *PloS one*, 10(11), pp. e0142087.

Lee, H.T. and Emala, C.W. (2002) 'Preconditioning and adenosine protect human proximal tubule cells in an in vitro model of ischemic injury', *Journal of the American Society of Nephrology : JASN*, 13(11), pp. 2753-2761.

Leelahavanichkul, A., Souza, A.C., Street, J.M., Hsu, V., Tsuji, T., Doi, K., Li, L., Hu, X., Zhou, H., Kumar, P., Schnermann, J., Star, R.A. and Yuen, P.S. (2014) 'Comparison of serum creatinine and serum cystatin C as biomarkers to detect sepsis-induced acute kidney injury and to predict mortality in CD-1 mice', *American journal of physiology.Renal physiology*, 307(8), pp. F939-48.

Lemasters, J. and Nieminen, A. (1997) 'Mitochondrial oxygen radical formation during reductive and oxidative stress to intact hepatocytes', *Bioscience reports*, 17, pp. 281-291.

Leonard, M.O., Cottell, D.C., Godson, C., Brady, H.R. and Taylor, C.T. (2003) 'The role of HIF-1 alpha in transcriptional regulation of the proximal tubular epithelial cell response to hypoxia', *The Journal of biological chemistry*, 278(41), pp. 40296-40304.

Leonard, M.O., Kieran, N.E., Howell, K., Burne, M.J., Varadarajan, R., Dhakshinamoorthy, S., Porter, A.G., O'Farrelly, C., Rabb, H. and Taylor, C.T. (2006) 'Reoxygenation-specific activation of the antioxidant transcription factor Nrf2 mediates cytoprotective gene expression in ischemia-reperfusion injury', *FASEB journal : official publication of the Federation of American Societies for Experimental Biology*, 20(14), pp. 2624-2626.

Leonardo, C.C., Eakin, A.K., Ajmo, J.M. and Gottschall, P.E. (2008) 'Versican and brevican are expressed with distinct pathology in neonatal hypoxic-ischemic injury', *Journal of neuroscience research*, 86(5), pp. 1106-1114.

Leshner, A.M., Zhou, L., Kimura, Y., Sato, S., Gullipalli, D., Herbert, A.P., Barlow, P.N., Eberhardt, H.U., Skerka, C., Zipfel, P.F., Hamano, T., Miwa, T., Tung, K.S. and Song, W.C. (2013) 'Combination of factor H mutation and properdin deficiency causes severe

- C3 glomerulonephritis', *Journal of the American Society of Nephrology : JASN*, 24(1), pp. 53-65.
- Leshner, A. and Song, W.C. (2009) 'New complement regulator exposed', *Blood*, 114(12), pp. 2363-2364.
- Levy, G.G., Nichols, W.C., Lian, E.C., Foroud, T., McClintick, J.N., McGee, B.M., Yang, A.Y., Siemieniak, D.R., Stark, K.R. and Gruppo, R. (2001) 'Mutations in a member of the ADAMTS gene family cause thrombotic thrombocytopenic purpura', *Nature*, 413(6855), pp. 488-494.
- Li, J., Li, Q., Xie, C., Zhou, H., Wang, Y., Zhang, N., Shao, H., Chan, S.C., Peng, X., Lin, S.C. and Han, J. (2004) 'Beta-actin is required for mitochondria clustering and ROS generation in TNF-induced, caspase-independent cell death', *Journal of cell science*, 117(Pt 20), pp. 4673-4680.
- Lieberthal, W., Menza, S.A. and Levine, J.S. (1998) 'Graded ATP depletion can cause necrosis or apoptosis of cultured mouse proximal tubular cells', *The American Journal of Physiology*, 274(2 Pt 2), pp. F315-27.
- Lien, Y.H., Lai, L. and Silva, A.L. (2003) 'Pathogenesis of renal ischemia/reperfusion injury: lessons from knockout mice', *Life Sciences*, 74(5), pp. 543-552.
- Lim, A.I., Tang, S.C., Lai, K.N. and Leung, J.C. (2013) 'Kidney injury molecule-1: More than just an injury marker of tubular epithelial cells?', *Journal of cellular physiology*, 228(5), pp. 917-924.
- Lin, F., Wang, Z.V. and Hill, J.A. (2014) 'Seeing is believing: Dynamic changes in renal epithelial autophagy during injury and repair', *Autophagy*, 10(4), pp. 691-693.
- Lin, M., Li, L., Zhang, Y., Zheng, L., Xu, M., Rong, R. and Zhu, T. (2014) 'Baicalin Ameliorates H₂O₂ Induced Cytotoxicity in HK-2 Cells through the Inhibition of ER Stress and the Activation of Nrf2 Signaling', *International journal of molecular sciences*, 15(7), pp. 12507-12522.
- Lindorfer, M.A., Jinivizian, H.B., Foley, P.L., Kennedy, A.D., Solga, M.D. and Taylor, R.P. (2003) 'B cell complement receptor 2 transfer reaction', *Journal of immunology (Baltimore, Md.: 1950)*, 170(7), pp. 3671-3678.

Linkermann, A., Bräsen, J.H., Himmerkus, N., Liu, S., Huber, T.B., Kunzendorf, U. and Krautwald, S. (2012) 'Rip1 (receptor-interacting protein kinase 1) mediates necroptosis and contributes to renal ischemia/reperfusion injury', *Kidney international*, 81(8), pp. 751-761.

Linkermann, A., Brasen, J.H., Darding, M., Jin, M.K., Sanz, A.B., Heller, J.O., De Zen, F., Weinlich, R., Ortiz, A., Walczak, H., Weinberg, J.M., Green, D.R., Kunzendorf, U. and Krautwald, S. (2013) 'Two independent pathways of regulated necrosis mediate ischemia-reperfusion injury', *Proceedings of the National Academy of Sciences of the United States of America*, 110(29), pp. 12024-12029.

Lip, G.Y. and Blann, A.D. (1995) 'von Willebrand factor and its relevance to cardiovascular disorders', *British heart journal*, 74(6), pp. 580-583.

Liu, S.Q., Roberts, D., Zhang, B., Ren, Y., Zhang, L. and Wu, Y.H. (2013) 'Trefoil factor 3 as an endocrine neuroprotective factor from the liver in experimental cerebral ischemia/reperfusion injury', *PloS one*, 8(10), pp. e77732.

Liu, J., Jha, P., Lyzogubov, V.V., Tytarenko, R.G., Bora, N.S. and Bora, P.S. (2011) 'Relationship between complement membrane attack complex, chemokine (C-C motif) ligand 2 (CCL2) and vascular endothelial growth factor in mouse model of laser-induced choroidal neovascularization', *The Journal of biological chemistry*, 286(23), pp. 20991-21001.

Lloyd, S.G., Wang, P., Zeng, H. and Chatham, J.C. (2004) 'Impact of low-flow ischemia on substrate oxidation and glycolysis in the isolated perfused rat heart', *American journal of physiology.Heart and circulatory physiology*, 287(1), pp. H351-62.

Ma, Z., Wei, Q., Dong, G., Huo, Y. and Dong, Z. (2014) 'DNA damage response in renal ischemia–reperfusion and ATP-depletion injury of renal tubular cells', *Biochimica et Biophysica Acta (BBA)-Molecular Basis of Disease*, 1842(7), pp. 1088-1096.

Madsen, J., Nielsen, O., Tornøe, I., Thim, L. and Holmskov, U. (2007) 'Tissue localization of human trefoil factors 1, 2, and 3', *The journal of histochemistry and cytochemistry : official journal of the Histochemistry Society*, 55(5), pp. 505-513.

Mahmood, T. and Yang, P. (2012) 'Western blot: technique, theory, and trouble shooting', *North American journal of medical sciences*, 4(9), pp. 429.

- Mailand, N., Gibbs-Seymour, I. and Bekker-Jensen, S. (2013) 'Regulation of PCNA–protein interactions for genome stability', *Nature reviews Molecular cell biology*, 14(5), pp. 269-282.
- Malek, M. and Nematbakhsh, M. (2015) 'Renal ischemia/reperfusion injury; from pathophysiology to treatment', *Journal of renal injury prevention*, 4(2), pp. 20.
- Mathern, D.R. and Heeger, P.S. (2015) 'Molecules Great and Small: The Complement System', *Clinical journal of the American Society of Nephrology : CJASN*, 10(9), pp. 1636-1650.
- Matloubian, M., David, A., Engel, S., Ryan, J.E. and Cyster, J.G. (2000) 'A transmembrane CXC chemokine is a ligand for HIV-coreceptor Bonzo', *Nature immunology*, 1(4), pp. 298-304.
- Matsushita, M. and Fujita, T. (2001) 'Ficolins and the lectin complement pathway', *Immunological reviews*, 180(1), pp. 78-85.
- McIlwain, D.R., Berger, T. and Mak, T.W. (2013) 'Caspase functions in cell death and disease', *Cold Spring Harbor perspectives in biology*, 5(4), pp. a008656.
- McTernan, P.G., Fisher, F.M., Valsamakis, G., Chetty, R., Harte, A., McTernan, C.L., Clark, P.M., Smith, S.A., Barnett, A.H. and Kumar, S. (2003) 'Resistin and type 2 diabetes: regulation of resistin expression by insulin and rosiglitazone and the effects of recombinant resistin on lipid and glucose metabolism in human differentiated adipocytes', *The Journal of Clinical Endocrinology & Metabolism*, 88(12), pp. 6098-6106.
- Meldrum, K., Meldrum, D., Hile, K., Burnett, A. and Harken, A. (2001) 'A Novel Model of Ischemia in Renal Tubular Cells Which Closely Parallels *in Vivo* Injury', *Journal of Surgical Research*, 99(2), pp. 288-293.
- Mendolicchio, G.L. & Ruggeri, Z.M. (2005) 'New perspectives on von Willebrand factor functions in hemostasis and thrombosis', *Seminars in hematology* Elsevier, pp. 5.
- Miao, J., Leshner, A.M., Miwa, T., Sato, S., Gullipalli, D. and Song, W. (2014) 'Tissue-specific deletion of Crry from mouse proximal tubular epithelial cells increases susceptibility to renal ischemia–reperfusion injury', *Kidney international*, .

- Michaelson, J.S., Wisniacki, N., Burkly, L.C. and Putterman, C. (2012) 'Role of TWEAK in lupus nephritis: a bench-to-bedside review', *Journal of Autoimmunity*, 39(3), pp. 130-142.
- Michel, F., Ambroisine, M.L., Duriez, M., Delcayre, C., Levy, B.I. and Silvestre, J.S. (2004) 'Aldosterone enhances ischemia-induced neovascularization through angiotensin II-dependent pathway', *Circulation*, 109(16), pp. 1933-1937.
- Milsom, A., Patel, N., Mazzon, E., Tripatara, P., Storey, A., Mota-Filipe, H., Sepodes, B., Webb, A., Cuzzocrea, S. and Hobbs, A. (2010) 'Role for endothelial nitric oxide synthase in nitrite-induced protection against renal ischemia–reperfusion injury in mice', *Nitric Oxide*, 22(2), pp. 141-148.
- Miwa, T., Sato, S., Gullipalli, D., Nangaku, M. and Song, W.C. (2013) 'Blocking properdin, the alternative pathway, and anaphylatoxin receptors ameliorates renal ischemia-reperfusion injury in decay-accelerating factor and CD59 double-knockout mice', *Journal of immunology (Baltimore, Md.: 1950)*, 190(7), pp. 3552-3559.
- Mizushima, N. (2007) 'Autophagy: process and function', *Genes & development*, 21(22), pp. 2861-2873.
- Moon, S., Kim, H., Nho, K., Jang, Y. and Lee, S. (2014) 'Endoplasmic Reticulum Stress Induces Epithelial-Mesenchymal Transition through Autophagy via Activation of c-Src Kinase', *Nephron Experimental Nephrology*, 126(3), pp. 127-140.
- Moore, K.L., Dalley, A.F. and Agur, A.M. (2013) *Clinically oriented anatomy*. Lippincott Williams & Wilkins.
- Morariu, A.M., Schuurs, T.A., Leuvenink, H.G., Van Oeveren, W., Rakhorst, G. and Ploeg, R.J. (2008) 'Early events in kidney donation: progression of endothelial activation, oxidative stress and tubular injury after brain death', *American Journal of Transplantation*, 8(5), pp. 933-941.
- Morris, P. and Knechtle, S.J. (2013) *Kidney transplantation-principles and practice*. Elsevier Health Sciences.
- Mukhopadhyay, S., Panda, P.K., Sinha, N., Das, D.N. and Bhutia, S.K. (2014) 'Autophagy and apoptosis: where do they meet?', *Apoptosis*, 19(4), pp. 555-566.

- Murata, K. and Baldwin III, W.M. (2009) 'Mechanisms of complement activation, C4d deposition, and their contribution to the pathogenesis of antibody-mediated rejection', *Transplantation reviews*, 23(3), pp. 139-150.
- Murphy, K., Travers, P. and Walport, M. (2007) *Janeway's Immunobiology*. 7th edn. Garland Publishing.
- Nabil, K., Rihn, B., Jaurand, M., Vignaud, J., Ripoche, J., Martinet, Y. and Martinet, N. (1997) 'Identification of human complement factor H as a chemotactic protein for monocytes', *Biochem.J*, 326, pp. 377-383.
- Nagamachi, S., Ohsawa, I., Suzuki, H., Sato, N., Inoshita, H., Hisada, A., Honda, D., Shimamoto, M., Shimizu, Y., Horikoshi, S. and Tomino, Y. (2014) 'Properdin has an ascendancy over factor H regulation in complement-mediated renal tubular damage', *BMC nephrology*, 15, pp. 82-2369-15-82.
- Nesargikar, P., Spiller, B. and Chavez, R. (2012) 'The complement system: history, pathways, cascade and inhibitors', *European Journal of Microbiology and Immunology*, 2(2), pp. 103-111.
- Neufeld, G., Cohen, T., Gengrinovitch, S. and Poltorak, Z. (1999) 'Vascular endothelial growth factor (VEGF) and its receptors', *FASEB journal : official publication of the Federation of American Societies for Experimental Biology*, 13(1), pp. 9-22.
- Newstead, C., Bell, D. and Jamieson, N. (2004) 'Guidelines relating to solid organ transplants from non-heart beating donors', *British Transplantation Society Guidelines*, .
- Ni, J., Ma, K., Wang, C., Liu, J., Zhang, Y., Lv, L., Ni, H., Chen, Y., Ruan, X. and Liu, B. (2013) 'Activation of renin-angiotensin system is involved in dyslipidemia-mediated renal injuries in apolipoprotein E knockout mice and HK-2 cells', *Lipids in health and disease*, 12(1), pp. 1.
- Nicholson, M. and Hosgood, S. (2013) 'Renal transplantation after ex vivo normothermic perfusion: the first clinical study', *American Journal of Transplantation*, 13(5), pp. 1246-1252.

- Nickeleit, V., Zeiler, M., Gudat, F., Thiel, G. and Mihatsch, M.J. (2002) 'Detection of the complement degradation product C4d in renal allografts: diagnostic and therapeutic implications', *Journal of the American Society of Nephrology : JASN*, 13(1), pp. 242-251.
- Nielsen, S., Kwon, T., Fenton, R. and Praetorius, J. (2012) 'Anatomy of the kidney', *Brenner and Rector's the Kidney, 9th edn.Elsevier/Saunders, Philadelphia, PA*, , pp. 31-93.
- Nitescu, N., Grimberg, E., Ricksten, S.E., Marcussen, N. and Guron, G. (2007) 'Thrombin inhibition with melagatran does not attenuate renal ischaemia-reperfusion injury in rats', *Nephrology, dialysis, transplantation : official publication of the European Dialysis and Transplant Association - European Renal Association*, 22(8), pp. 2149-2155.
- Noiri, E., Doi, K., Negishi, K., Tanaka, T., Hamasaki, Y., Fujita, T., Portilla, D. and Sugaya, T. (2009) 'Urinary fatty acid-binding protein 1: an early predictive biomarker of kidney injury', *American journal of physiology.Renal physiology*, 296(4), pp. F669-79.
- Noris, M. & Remuzzi, G. (2013) 'Overview of complement activation and regulation', *Seminars in nephrology*Elsevier, pp. 479.
- Odink, K.G., Fey, G., Wiebauer, K. and Diggelmann, H. (1981) 'Mouse complement components C3 and C4. Characterization of their messenger RNA and molecular cloning of complementary DNA for C3', *The Journal of biological chemistry*, 256(3), pp. 1453-1458.
- O'Flynn, J., Dixon, K.O., Faber Krol, M.C., Daha, M.R. and van Kooten, C. (2014) 'Myeloperoxidase directs properdin-mediated complement activation', *Journal of innate immunity*, 6(4), pp. 417-425.
- Oh, J. and Rabb, H. (2013) 'Adiponectin: an enlarging role in acute kidney injury', *Kidney international*, 83(4), pp. 546-548.
- Ohtsuka, H., Imamura, T., Matsushita, M., Tanase, S., Okada, H., Ogawa, M. and Kambara, T. (1993) 'Thrombin generates monocyte chemotactic activity from complement factor H', *Immunology*, 80(1), pp. 140-145.
- Ojo, A.O. (2006) 'Cardiovascular complications after renal transplantation and their prevention', *Transplantation*, 82(5), pp. 603-611.

Ojo, A.O., Hanson, J.A., Meier-Kriesche, H., Okechukwu, C.N., Wolfe, R.A., Leichtman, A.B., Agodoa, L.Y., Kaplan, B. and Port, F.K. (2001) 'Survival in recipients of marginal cadaveric donor kidneys compared with other recipients and wait-listed transplant candidates', *Journal of the American Society of Nephrology : JASN*, 12(3), pp. 589-597.

Oshima, Y., Kinouchi, K., Ichihara, A., Sakoda, M., Kurauchi-Mito, A., Bokuda, K., Narita, T., Kurosawa, H., Sun-Wada, G.H., Wada, Y., Yamada, T., Takemoto, M., Saleem, M.A., Quaggin, S.E. and Itoh, H. (2011) 'Prorenin receptor is essential for normal podocyte structure and function', *Journal of the American Society of Nephrology : JASN*, 22(12), pp. 2203-2212.

Osthoff, M., Brown, K.D., Kong, D.C., Daniell, M. and Eisen, D.P. (2014) 'Activation of the lectin pathway of complement in experimental human keratitis with *Pseudomonas aeruginosa*', *Molecular vision*, 20, pp. 38.

Ota, H., Fox-Talbot, K., Hu, W., Qian, Z., Sanfilippo, F., Hruban, R.H. and Baldwin III, W.M. (2005) 'Terminal complement components mediate release of von Willebrand factor and adhesion of platelets in arteries of allografts', *Transplantation*, 79(3), pp. 276-281.

Owens, D.E. and Peppas, N.A. (2006) 'Opsonization, biodistribution, and pharmacokinetics of polymeric nanoparticles', *International journal of pharmaceutics*, 307(1), pp. 93-102.

Park, H.K., Qatanani, M., Briggs, E.R., Ahima, R.S. and Lazar, M.A. (2011) 'Inflammatory induction of human resistin causes insulin resistance in endotoxemic mice', *Diabetes*, 60(3), pp. 775-783.

Park, P., Haas, M., Cunningham, P.N., Alexander, J.J., Bao, L., Guthridge, J.M., Kraus, D.M., Holers, V.M. and Quigg, R.J. (2001) 'Inhibiting the complement system does not reduce injury in renal ischemia reperfusion', *Journal of the American Society of Nephrology : JASN*, 12(7), pp. 1383-1390.

Pavenstadt, H., Kriz, W. and Kretzler, M. (2003) 'Cell biology of the glomerular podocyte', *Physiological Reviews*, 83(1), pp. 253-307.

Pavlovski, D., Thundyil, J., Monk, P.N., Wetsel, R.A., Taylor, S.M. and Woodruff, T.M. (2012) 'Generation of complement component C5a by ischemic neurons promotes

neuronal apoptosis', *FASEB journal : official publication of the Federation of American Societies for Experimental Biology*, 26(9), pp. 3680-3690.

Peake, P.W., O'Grady, S., Pussell, B.A. and Charlesworth, J.A. (1999) 'C3a is made by proximal tubular HK-2 cells and activates them via the C3a receptor', *Kidney international*, 56(5), pp. 1729-1736.

Peng, Q., Li, K., Smyth, L.A., Xing, G., Wang, N., Meader, L., Lu, B., Sacks, S.H. and Zhou, W. (2012) 'C3a and C5a promote renal ischemia-reperfusion injury', *Journal of the American Society of Nephrology : JASN*, 23(9), pp. 1474-1485.

Perri, A., Vizza, D., Lofaro, D., Gigliotti, P., Leone, F., Brunelli, E., Malivindi, R., De Amicis, F., Romeo, F. and De Stefano, R. (2013) 'Adiponectin is expressed and secreted by renal tubular epithelial cells', *J Nephrol*, 26(6), pp. 1049-1054.

Pillimer, L., Blum, L., Lepow, I., Ross, O., Todd, E. and Wardlaw, A. (1954) 'The properdin system and immunity. I. Demonstration and isolation of a new serum protein, properdin, and its role in immune phenomenon', *Science*, 120, pp. 279.

Pohlmann, A., Hentschel, J., Fechner, M., Hoff, U., Bubalo, G., Arakelyan, K., Cantow, K., Seeliger, E., Flemming, B. and Waiczies, H. (2013) 'High temporal resolution parametric MRI monitoring of the initial ischemia/reperfusion phase in experimental acute kidney injury', *PloS one*, 8(2), pp. e57411.

Porter, A.G. and Janicke, R.U. (1999) 'Emerging roles of caspase-3 in apoptosis', *Cell death and differentiation*, 6(2), pp. 99-104.

Portilla, D. (2003) 'Energy metabolism and cytotoxicity', *Seminars in nephrology* Elsevier, pp. 432.

Poveda, J., Sanchez-Nino, M.D., Glorieux, G., Sanz, A.B., Egido, J., Vanholder, R. and Ortiz, A. (2014) 'P-Cresyl Sulphate has Pro-Inflammatory and Cytotoxic Actions on Human Proximal Tubular Epithelial Cells', *Nephrology, dialysis, transplantation : official publication of the European Dialysis and Transplant Association - European Renal Association*, 29(1), pp. 56-64.

Pratschke, J., Wilhelm, M.J., Laskowski, I., Kusaka, M., Beato, F., Tullius, S.G., Neuhaus, P., Hancock, W.W. and Tilney, N.L. (2001) 'Influence of donor brain death on

chronic rejection of renal transplants in rats', *Journal of the American Society of Nephrology : JASN*, 12(11), pp. 2474-2481.

Pratt, J.R., Basheer, S.A. and Sacks, S.H. (2002) 'Local synthesis of complement component C3 regulates acute renal transplant rejection', *Nature medicine*, 8(6), pp. 582-587.

Pulskens, W.P., Teske, G.J., Butter, L.M., Roelofs, J.J., Van Der Poll, T., Florquin, S. and Leemans, J.C. (2008) 'Toll-like receptor-4 coordinates the innate immune response of the kidney to renal ischemia/reperfusion injury', *PloS one*, 3(10), pp. e3596.

Pushpakumar, S.B., Perez-Abadia, G., Soni, C., Wan, R., Todnem, N., Patibandla, P.K., Fensterer, T., Zhang, Q., Barker, J.H. and Maldonado, C. (2011) 'Enhancing complement control on endothelial barrier reduces renal post-ischemia dysfunction', *Journal of Surgical Research*, 170(2), pp. e263-e270.

Qureshi, M., Callaghan, C., Bradley, J., Watson, C. and Pettigrew, G. (2012) 'Outcomes of simultaneous pancreas–kidney transplantation from brain-dead and controlled circulatory death donors', *British Journal of Surgery*, 99(6), pp. 831-838.

Rabb, H., Daniels, F., O'Donnell, M., Haq, M., Saba, S.R., Keane, W. and Tang, W.W. (2000) 'Pathophysiological role of T lymphocytes in renal ischemia-reperfusion injury in mice', *American journal of physiology. Renal physiology*, 279(3), pp. F525-31.

Racusen, L.C., Colvin, R.B., Solez, K., Mihatsch, M.J., Halloran, P.F., Campbell, P.M., Cecka, M.J., Cosyns, J., Demetris, A.J. and Fishbein, M.C. (2003) 'Antibody-Mediated Rejection Criteria—an Addition to the Banff' 97 Classification of Renal Allograft Rejection', *American Journal of Transplantation*, 3(6), pp. 708-714.

Raeymaekers, L. (2000) 'Basic principles of quantitative PCR', *Molecular biotechnology*, 15(2), pp. 115-122.

Ramos-Vara, J.A. (2011) 'Principles and methods of immunohistochemistry', in Anonymous *Drug Safety Evaluation*. Springer, pp. 83-96.

Rauci, R., Rusolo, F., Sharma, A., Colonna, G., Castello, G. and Costantini, S. (2013) 'Functional and structural features of adipokine family', *Cytokine*, 61(1), pp. 1-14.

- Reinders, M.E., Sho, M., Izawa, A., Wang, P., Mukhopadhyay, D., Koss, K.E., Geehan, C.S., Luster, A.D., Sayegh, M.H. and Briscoe, D.M. (2003) 'Proinflammatory functions of vascular endothelial growth factor in alloimmunity', *The Journal of clinical investigation*, 112(11), pp. 1655-1665.
- Reininger, A.J. (2008) 'VWF attributes–impact on thrombus formation', *Thrombosis research*, 122, pp. S9-S13.
- Remuzzi, G., Cravedi, P., Perna, A., Dimitrov, B.D., Turturro, M., Locatelli, G., Rigotti, P., Baldan, N., Beatini, M. and Valente, U. (2006) 'Long-term outcome of renal transplantation from older donors', *New England Journal of Medicine*, 354(4), pp. 343-352.
- Renner, B., Coleman, K., Goldberg, R., Amura, C., Holland-Neidermyer, A., Pierce, K., Orth, H.N., Molina, H., Ferreira, V.P., Cortes, C., Pangburn, M.K., Holers, V.M. and Thurman, J.M. (2010) 'The complement inhibitors Crry and factor H are critical for preventing autologous complement activation on renal tubular epithelial cells', *Journal of immunology (Baltimore, Md.: 1950)*, 185(5), pp. 3086-3094.
- Ricklin, D., Hajishengallis, G., Yang, K. and Lambris, J.D. (2010) 'Complement: a key system for immune surveillance and homeostasis', *Nature immunology*, 11(9), pp. 785-797.
- Rieger, A.M., Nelson, K.L., Konowalchuk, J.D. and Barreda, D.R. (2011) 'Modified annexin V/propidium iodide apoptosis assay for accurate assessment of cell death', *JoVE (Journal of Visualized Experiments)*, (50), pp. e2597-e2597.
- Rinnert, M., Hinz, M., Buhtz, P., Reiher, F., Lessel, W. and Hoffmann, W. (2010) 'Synthesis and localization of trefoil factor family (TFF) peptides in the human urinary tract and TFF2 excretion into the urine', *Cell and tissue research*, 339(3), pp. 639-647.
- Riss, T.L., Moravec, R.A., Niles, A.L., Benink, H.A., Worzella, T.J., Minor, L., Storts, D. and Reid, Y. (2004) 'Cell Viability Assays', in Sittampalam, G.S., Coussens, N.P., Nelson, H., Arkin, M., Auld, D., Austin, C., Bejcek, B., Glicksman, M., Inglese, J., Iversen, P.W., Li, Z., McGee, J., McManus, O., Minor, L., Napper, A., Peltier, J.M., Riss, T., Trask OJ, J. and Weidner, J. (eds.) *Assay Guidance Manual*. Bethesda (MD): .

- Rizvi, M., Jawad, N., Li, Y., Vizcaychipi, M.P., Maze, M. and Ma, D. (2010) 'Effect of noble gases on oxygen and glucose deprived injury in human tubular kidney cells', *Experimental biology and medicine (Maywood, N.J.)*, 235(7), pp. 886-891.
- Rong, S., Park, J.K., Kirsch, T., Yagita, H., Akiba, H., Boenisch, O., Haller, H., Najafian, N. and Habicht, A. (2011) 'The TIM-1:TIM-4 pathway enhances renal ischemia-reperfusion injury', *Journal of the American Society of Nephrology : JASN*, 22(3), pp. 484-495.
- Rosenbaum, D.M., Rasmussen, S.G. and Kobilka, B.K. (2009) 'The structure and function of G-protein-coupled receptors', *Nature*, 459(7245), pp. 356-363.
- Rosenberg, M.E. and Silkensen, J. (1995) 'Clusterin: physiologic and pathophysiologic considerations', *The international journal of biochemistry & cell biology*, 27(7), pp. 633-645.
- Ross, G.D. (1986) *Immunobiology of the Complement System: An Introduction for Research and Clinical Medicine*. 1st edition edn. Orlando, Florida, USA: Academic Press Inc.
- Rossi, V., Bally, I., Lacroix, M., Arlaud, G.J. and Thielens, N.M. (2014) 'Classical Complement Pathway Components C1r and C1s: Purification from Human Serum and in Recombinant Form and Functional Characterization', in Anonymous *The Complement System*. Springer, pp. 43-60.
- Roumenina, L.T., Loirat, C., Dragon-Durey, M., Halbwachs-Mecarelli, L., Sautes-Fridman, C. and Fremeaux-Bacchi, V. (2011) 'Alternative complement pathway assessment in patients with atypical HUS', *Journal of immunological methods*, 365(1), pp. 8-26.
- Ruggeri, Z.M. (2007) 'The role of von Willebrand factor in thrombus formation', *Thrombosis research*, 120, pp. S5-S9.
- Ruggeri, Z.M., Pareti, F.I., Mannucci, P.M., Ciavarella, N. and Zimmerman, T.S. (1980) 'Heightened interaction between platelets and factor VIII/von Willebrand factor in a new subtype of von Willebrand's disease', *New England Journal of Medicine*, 302(19), pp. 1047-1051.

- Ruggeri, Z.M. and Ruggeri, Z.M. (2004) 'Platelet and von Willebrand factor interactions at the vessel wall', *Hamostaseologie*, 24(1), pp. 1-11.
- Ruseva, M.M., Vernon, K.A., Leshner, A.M., Schwaeble, W.J., Ali, Y.M., Botto, M., Cook, T., Song, W., Stover, C.M. and Pickering, M.C. (2013) 'Loss of properdin exacerbates C3 glomerulopathy resulting from factor H deficiency', *Journal of the American Society of Nephrology : JASN*, 24(1), pp. 43-52.
- Russ, A.L., Haberstroh, K.M. and Rundell, A.E. (2007) 'Experimental strategies to improve in vitro models of renal ischemia', *Experimental and molecular pathology*, 83(2), pp. 143-159.
- Sabbahy, M.E. and Vaidya, V.S. (2011) 'Ischemic kidney injury and mechanisms of tissue repair', *Wiley Interdisciplinary Reviews: Systems Biology and Medicine*, 3(5), pp. 606-618.
- Sade, R.M. (2011) 'Brain death, cardiac death, and the dead donor rule', *Journal of the South Carolina Medical Association (1975)*, 107(4), pp. 146-149.
- Sahin, H. and Wasmuth, H.E. (2013) 'Chemokines in tissue fibrosis', *Biochimica et Biophysica Acta (BBA)-Molecular Basis of Disease*, 1832(7), pp. 1041-1048.
- Sana, T.R., Roark, J.C., Li, X., Waddell, K. and Fischer, S.M. (2008) 'Molecular formula and METLIN Personal Metabolite Database matching applied to the identification of compounds generated by LC/TOF-MS', *J Biomol Tech*, 19(4), pp. 258-266.
- Sandner, P., Wolf, K., Bergmaier, U., Gess, B. and Kurtz, A. (1997) 'Induction of VEGF and VEGF receptor gene expression by hypoxia: divergent regulation in vivo and in vitro', *Kidney international*, 51(2), pp. 448-453.
- Santos, R.A., Ferreira, A.J., Verano-Braga, T. and Bader, M. (2013) 'Angiotensin-converting enzyme 2, angiotensin-(1-7) and Mas: new players of the renin-angiotensin system', *The Journal of endocrinology*, 216(2), pp. R1-R17.
- Sanz, A.B., Sanchez-Nino, M.D., Ramos, A.M., Moreno, J.A., Santamaria, B., Ruiz-Ortega, M., Egido, J. and Ortiz, A. (2010) 'NF-kappaB in renal inflammation', *Journal of the American Society of Nephrology : JASN*, 21(8), pp. 1254-1262.

- Sarma, J.V. and Ward, P.A. (2011) 'The complement system', *Cell and tissue research*, 343(1), pp. 227-235.
- Sasaki, R. (2003) 'Pleiotropic functions of erythropoietin.', *Internal Medicine*, 42(2), pp. 142-149.
- Sauvant, C., Schneider, R., Holzinger, H., Renker, S., Wanner, C. and Gekle, M. (2009) 'Implementation of an in vitro model system for investigation of reperfusion damage after renal ischemia', *Cellular physiology and biochemistry : international journal of experimental cellular physiology, biochemistry, and pharmacology*, 24(5-6), pp. 567-576.
- Schaefer, L. (2010) 'Extracellular matrix molecules: endogenous danger signals as new drug targets in kidney diseases', *Current opinion in pharmacology*, 10(2), pp. 185-190.
- Scherpereel, A., Depontieu, F., Grigoriu, B., Cavestri, B., Tsicopoulos, A., Gentina, T., Jourdain, M., Pugin, J., Tonnel, A. and Lassalle, P. (2006) 'Endocan, a new endothelial marker in human sepsis*', *Critical Care Medicine*, 34(2), pp. 532-537.
- Schiller, M., Heyder, P., Ziegler, S., Niessen, A., Claßen, L., Lauffer, A. and Lorenz, H. (2013) 'During apoptosis HMGB1 is translocated into apoptotic cell-derived membrane vesicles', *Autoimmunity*, 46(5), pp. 342-346.
- Schmittgen, T.D. and Livak, K.J. (2008) 'Analyzing real-time PCR data by the comparative CT method', *Nature protocols*, 3(6), pp. 1101-1108.
- Schramme, A., Abdel-Bakky, M.S., Gutwein, P., Obermüller, N., Baer, P.C., Hauser, I.A., Ludwig, A., Gauer, S., Schäfer, L. and Sobkowiak, E. (2008) 'Characterization of CXCL16 and ADAM10 in the normal and transplanted kidney', *Kidney international*, 74(3), pp. 328-338.
- Schraufstatter, I.U., Discipio, R.G., Zhao, M. and Khaldoyanidi, S.K. (2009) 'C3a and C5a are chemotactic factors for human mesenchymal stem cells, which cause prolonged ERK1/2 phosphorylation', *Journal of immunology (Baltimore, Md.: 1950)*, 182(6), pp. 3827-3836.
- Schumer, M., Colombel, M.C., Sawczuk, I.S., Gobe, G., Connor, J., O'Toole, K.M., Olsson, C.A., Wise, G.J. and Buttyan, R. (1992) 'Morphologic, biochemical, and

molecular evidence of apoptosis during the reperfusion phase after brief periods of renal ischemia', *The American journal of pathology*, 140(4), pp. 831-838.

Schwaeble, W.J. and Reid, K.B. (1999) 'Does properdin crosslink the cellular and the humoral immune response?', *Immunology today*, 20(1), pp. 17-21.

Schwaeble, W.J., Lynch, N.J., Clark, J.E., Marber, M., Samani, N.J., Ali, Y.M., Dudler, T., Parent, B., Lhotta, K., Wallis, R., Farrar, C.A., Sacks, S., Lee, H., Zhang, M., Iwaki, D., Takahashi, M., Fujita, T., Tedford, C.E. and Stover, C.M. (2011) 'Targeting of mannan-binding lectin-associated serine protease-2 confers protection from myocardial and gastrointestinal ischemia/reperfusion injury', *Proceedings of the National Academy of Sciences of the United States of America*, 108(18), pp. 7523-7528.

Scotdir (2015) **Human kidney structures**. Available at: <http://scotdir.com/sciences/anatomy/human-kidney-structures> (Accessed: 2016).

Semenza, G.L. (2000) 'HIF-1: mediator of physiological and pathophysiological responses to hypoxia', *Journal of applied physiology (Bethesda, Md.: 1985)*, 88(4), pp. 1474-1480.

Serinsöz, E., Bock, O., Gwinner, W., Schwarz, A., Haller, H., Kreipe, H. and Mengel, M. (2005) 'Local complement C3 expression is upregulated in humoral and cellular rejection of renal allografts', *American journal of transplantation*, 5(6), pp. 1490-1494.

Shen, L., Lu, G., Dong, N., Jiang, L., Ma, Z. and Ruan, C. (2012) 'Von Willebrand factor, ADAMTS13 activity, TNF- α and their relationships in patients with chronic kidney disease', *Experimental and therapeutic medicine*, 3(3), pp. 530-534.

Shi, Z., Lian, A. and Zhang, F. (2014) 'Nuclear factor- κ B activation inhibitor attenuates ischemia reperfusion injury and inhibits Hmgb1 expression', *Inflammation research : official journal of the European Histamine Research Society ...[et al.]*, 63(11), pp. 919.

Shingu, C., Koga, H., Hagiwara, S., Matsumoto, S., Goto, K., Yokoi, I. and Noguchi, T. (2010) 'Hydrogen-rich saline solution attenuates renal ischemia–reperfusion injury', *Journal of anesthesia*, 24(4), pp. 569-574.

Sierra-Filardi, E., Nieto, C., Dominguez-Soto, A., Barroso, R., Sanchez-Mateos, P., Puig-Kroger, A., Lopez-Bravo, M., Joven, J., Ardavin, C., Rodriguez-Fernandez, J.L.,

- Sanchez-Torres, C., Mellado, M. and Corbi, A.L. (2014) 'CCL2 shapes macrophage polarization by GM-CSF and M-CSF: identification of CCL2/CCR2-dependent gene expression profile', *Journal of immunology (Baltimore, Md.: 1950)*, 192(8), pp. 3858-3867.
- Singh, R.P., Farney, A.C., Rogers, J., Zuckerman, J., Reeves-Daniel, A., Hartmann, E., Iskandar, S., Adams, P. and Stratta, R.J. (2011) 'Kidney transplantation from donation after cardiac death donors: lack of impact of delayed graft function on post-transplant outcomes', *Clinical transplantation*, 25(2), pp. 255-264.
- Slagt, I.K., IJzermans, J.N., Visser, L.J., Weimar, W., Roodnat, J.I. and Terkivatan, T. (2014) 'Independent risk factors for urological complications after deceased donor kidney transplantation', *PloS one*, 9(3), pp. e91211.
- Song, H., Han, I., Kim, Y., Kim, Y.H., Choi, I., Seo, S., Jung, S.Y., Park, S. and Kang, M.S. (2015) 'The NADPH oxidase inhibitor DPI can abolish hypoxia-induced apoptosis of human kidney proximal tubular epithelial cells through Bcl2 up-regulation via ERK activation without ROS reduction', *Life Sciences*, 126, pp. 69-75.
- Sotocinal, S.G., Sorge, R.E., Zaloum, A., Tuttle, A.H., Martin, L.J., Wieskopf, J.S., Mapplebeck, J.C., Wei, P., Zhan, S. and Zhang, S. (2011) 'The Rat Grimace Scale: a partially automated method for quantifying pain in the laboratory rat via facial expressions', *Molecular pain*, 7(1), pp. 1.
- Stadnyk, A.W. (1994) 'Cytokine production by epithelial cells', *FASEB journal : official publication of the Federation of American Societies for Experimental Biology*, 8(13), pp. 1041-1047.
- Steinbrook, R. (2007) 'Organ donation after cardiac death', *New England Journal of Medicine*, 357(3), pp. 209-213.
- Stokman, G., Stroo, I., Claessen, N., Teske, G.J., Weening, J.J., Leemans, J.C. and Florquin, S. (2010) 'Stem cell factor expression after renal ischemia promotes tubular epithelial survival', *PLoS One*, 5(12), pp. e14386.
- Stover, C.M., McDonald, J., Byrne, S., Lambert, D.G. and Thompson, J.P. (2015) 'Properdin levels in human sepsis', *Frontiers in immunology*, 6.

- Stover, C.M., Luckett, J.C., Echtenacher, B., Dupont, A., Figgitt, S.E., Brown, J., Mannel, D.N. and Schwaeble, W.J. (2008) 'Properdin plays a protective role in polymicrobial septic peritonitis', *Journal of immunology (Baltimore, Md.: 1950)*, 180(5), pp. 3313-3318.
- Stroo, I., Claessen, N., Teske, G.J., Butter, L.M., Florquin, S. and Leemans, J.C. (2015) 'Deficiency for the Chemokine Monocyte Chemoattractant Protein-1 Aggravates Tubular Damage after Renal Ischemia/Reperfusion Injury', *PloS one*, 10(4), pp. e0123203.
- Su, G., Wei, Y. and Guo, M. (2011) 'Direct colorimetric detection of hydrogen peroxide using 4-nitrophenyl boronic acid or its pinacol ester', *American Journal of Analytical Chemistry*, 2(08), pp. 879.
- Summers, D.M., Johnson, R.J., Allen, J., Fuggle, S.V., Collett, D., Watson, C.J. and Bradley, J.A. (2010) 'Analysis of factors that affect outcome after transplantation of kidneys donated after cardiac death in the UK: a cohort study', *The Lancet*, 376(9749), pp. 1303-1311.
- Summers, D.M., Johnson, R.J., Hudson, A., Collett, D., Watson, C.J. and Bradley, J.A. (2013) 'Effect of donor age and cold storage time on outcome in recipients of kidneys donated after circulatory death in the UK: a cohort study', *The Lancet*, 381(9868), pp. 727-734.
- Suzuki, C., Isaka, Y., Takabatake, Y., Tanaka, H., Koike, M., Shibata, M., Uchiyama, Y., Takahara, S. and Imai, E. (2008) 'Participation of autophagy in renal ischemia/reperfusion injury', *Biochemical and biophysical research communications*, 368(1), pp. 100-106.
- Sweigard, J.H., Yanai, R., Gaissert, P., Saint-Geniez, M., Kataoka, K., Thanos, A., Stahl, G.L., Lambris, J.D. and Connor, K.M. (2014) 'The alternative complement pathway regulates pathological angiogenesis in the retina', *FASEB journal : official publication of the Federation of American Societies for Experimental Biology*, 28(7), pp. 3171-3182.
- Tadagavadi, R.K., Wang, W. and Ramesh, G. (2010) 'Netrin-1 regulates Th1/Th2/Th17 cytokine production and inflammation through UNC5B receptor and protects kidney against ischemia-reperfusion injury', *Journal of immunology (Baltimore, Md.: 1950)*, 185(6), pp. 3750-3758.

- Terasaki, P.I., Cecka, J.M., Gjertson, D.W. and Takemoto, S. (1995) 'High survival rates of kidney transplants from spousal and living unrelated donors', *New England Journal of Medicine*, 333(6), pp. 333-336.
- Thurman, J.M., Ljubanovic, D., Edelstein, C.L., Gilkeson, G.S. and Holers, V.M. (2003) 'Lack of a functional alternative complement pathway ameliorates ischemic acute renal failure in mice', *Journal of immunology (Baltimore, Md.: 1950)*, 170(3), pp. 1517-1523.
- Thurman, J.M., Royer, P.A., Ljubanovic, D., Dursun, B., Lenderink, A.M., Edelstein, C.L. and Holers, V.M. (2006) 'Treatment with an inhibitory monoclonal antibody to mouse factor B protects mice from induction of apoptosis and renal ischemia/reperfusion injury', *Journal of the American Society of Nephrology : JASN*, 17(3), pp. 707-715.
- Tian, H., Huang, P., Zhao, Z., Tang, W. and Xia, J. (2014) 'HIF-1alpha plays a role in the chemotactic migration of hepatocarcinoma cells through the modulation of CXCL6 expression', *Cellular physiology and biochemistry : international journal of experimental cellular physiology, biochemistry, and pharmacology*, 34(5), pp. 1536-1546.
- Tran, S., Puhar, A., Ngo-Camus, M. and Ramarao, N. (2011) 'Trypan blue dye enters viable cells incubated with the pore-forming toxin HlyII of *Bacillus cereus*', *PLoS One*, 6(9), pp. e22876.
- Turman, M.A. and Rosenfeld, S.L. (1999) 'Heat shock protein 70 overexpression protects LLC-PK1 tubular cells from heat shock but not hypoxia', *Kidney international*, 55(1), pp. 189-197.
- Turner, M.W. (2003) 'The role of mannose-binding lectin in health and disease', *Molecular immunology*, 40(7), pp. 423-429.
- Urbschat, A., Obermüller, N. and Haferkamp, A. (2011) 'Biomarkers of kidney injury', *Biomarkers*, 16(S1), pp. S22-S30.
- Vaidya, V.S., Ramirez, V., Ichimura, T., Bobadilla, N.A. and Bonventre, J.V. (2006) 'Urinary kidney injury molecule-1: a sensitive quantitative biomarker for early detection of kidney tubular injury', *American journal of physiology. Renal physiology*, 290(2), pp. F517-29.

- Valdivia, M.P., Gentil, M., Toro, M., Cabello, M., Rodríguez-Benot, A., Mazuecos, A., Osuna, A. & Alonso, M. (2011) 'Impact of cold ischemia time on initial graft function and survival rates in renal transplants from deceased donors performed in Andalusia', *Transplantation proceedings* Elsevier, pp. 2174.
- van den Elsen, Jean MH, Martin, A., Wong, V., Clemenza, L., Rose, D.R. and Isenman, D.E. (2002) 'X-ray crystal structure of the C4d fragment of human
- van der Pol, P., Schlagwein, N., Van Gijlswijk, D., Berger, S., Roos, A., Bajema, I., de Boer, H., de Fijter, J., Stahl, G. and Daha, M. (2012) 'Mannan-Binding Lectin Mediates Renal Ischemia/Reperfusion Injury Independent of Complement Activation', *American Journal of Transplantation*, 12(4), pp. 877-887.
- van Pelt-Verkuil, E., Van Belkum, A. and Hays, J.P. (2008) *Principles and technical aspects of PCR amplification*. Springer Science & Business Media.
- Vanhove, T., Kuypers, D., Claes, K.J., Evenepoel, P., Meijers, B., Naesens, M., Vanrenterghem, Y., Cornelis, T. and Bammens, B. (2013) 'Reasons for dose reduction of mycophenolate mofetil during the first year after renal transplantation and its impact on graft outcome', *Transplant International*, 26(8), pp. 813-821.
- Vogel, T., Brockmann, J.G., Coussios, C. and Friend, P.J. (2012) 'The role of normothermic extracorporeal perfusion in minimizing ischemia reperfusion injury', *Transplantation reviews*, 26(2), pp. 156-162.
- Volker, D., Bate, M., Gentle, R. and Garg, M. (2000) 'Oral buprenorphine is anti-inflammatory and modulates the pathogenesis of streptococcal cell wall polymer-induced arthritis in the Lew/SSN rat', *Laboratory animals*, 34(4), pp. 423-429.
- Walsh-Reitz, M.M. and Toback, F.G. (1992) 'Phenol red inhibits growth of renal epithelial cells', *Am J Physiol*, 262(4 Pt 2), pp. F687-F691.
- Wang, F., Yu, G., Liu, S., Li, J., Wang, J., Bo, L., Qian, L., Sun, X. and Deng, X. (2011) 'Hydrogen-rich saline protects against renal ischemia/reperfusion injury in rats', *Journal of Surgical Research*, 167(2), pp. e339-e344.

- Wang, W., Tang, T., Zhang, P. and Bu, H. (2010) 'Postconditioning attenuates renal ischemia-reperfusion injury by preventing DAF down-regulation', *The Journal of urology*, 183(6), pp. 2424-2431.
- Wang, P. and Sanders, P.W. (2007) 'Immunoglobulin Light Chains Generate Hydrogen Peroxide', *Journal of the American Society of Nephrology*, 18(4), pp. 1239-1245.
- Wang, Y., Tian, J., Qiao, X., Su, X., Mi, Y., Zhang, R. and Li, R. (2015) 'Intermedin protects against renal ischemia-reperfusion injury by inhibiting endoplasmic reticulum stress', *BMC nephrology*, 16(1), pp. 169-015-0157-7.
- Ward, P.A. (2010) 'The harmful role of c5a on innate immunity in sepsis', *Journal of innate immunity*, 2(5), pp. 439-445.
- Watabe, S., Sakamoto, Y., Morikawa, M., Okada, R., Miura, T. and Ito, E. (2011) 'Highly sensitive determination of hydrogen peroxide and glucose by fluorescence correlation spectroscopy', *Plosone*, 6, pp. 1-5.
- Watschinger, B. and Pascual, M. (2002) 'Capillary C4d deposition as a marker of humoral immunity in renal allograft rejection', *Journal of the American Society of Nephrology : JASN*, 13(9), pp. 2420-2423.
- Watson, C., Wells, A., Roberts, R., Akoh, J., Friend, P., Akyol, M., Calder, F., Allen, J., Jones, M. and Collett, D. (2010) 'Cold machine perfusion versus static cold storage of kidneys donated after cardiac death: a UK multicenter randomized controlled trial', *American Journal of Transplantation*, 10(9), pp. 1991-1999.
- Wei, Q. and Dong, Z. (2012) 'Mouse model of ischemic acute kidney injury: technical notes and tricks', *American journal of physiology. Renal physiology*, 303(11), pp. F1487-94.
- Weinberg, J.M. (2011) 'TWEAK–Fn14 as a mediator of acute kidney injury', *Kidney international*, 79(2), pp. 151-153.
- Westra, D., Wetzels, J., Volokhina, E., Van den Heuvel, L. and Van De Kar, N. (2012) 'A new era in the diagnosis and treatment of atypical haemolytic uraemic syndrome', *Neth J Med*, 70(3), pp. 121-129.

White, S.M., North, L.M., Haines, E., Goldberg, M., Sullivan, L.M., Pressly, J.D., Weber, D.S., Park, F. and Regner, K.R. (2014) 'G-protein betagamma subunit dimers modulate kidney repair after ischemia-reperfusion injury in rats', *Molecular pharmacology*, 86(4), pp. 369-377.

Wiley, S.R. and Winkles, J.A. (2003) 'TWEAK, a member of the TNF superfamily, is a multifunctional cytokine that binds the TweakR/Fn14 receptor', *Cytokine & growth factor reviews*, 14(3), pp. 241-249.

Wilkinson, R., Wang, X., Roper, K.E. and Healy, H. (2011) 'Activated human renal tubular cells inhibit autologous immune responses', *Nephrology, dialysis, transplantation : official publication of the European Dialysis and Transplant Association - European Renal Association*, 26(5), pp. 1483-1492.

Wright, P.A. and Wynford-Thomas, D. (1990) 'The polymerase chain reaction: miracle or mirage? A critical review of its uses and limitations in diagnosis and research', *The Journal of pathology*, 162(2), pp. 99-117.

Wu, Y., Zhang, J., Liu, F., Yang, C., Zhang, Y., Liu, A., Shi, L., Wu, Y., Zhu, T. and Nicholson, M.L. (2013) 'Protective effects of HBSP on ischemia reperfusion and cyclosporine a induced renal injury', *Clinical and Developmental Immunology*, 2013.

Wu, H., Chen, G., Wyburn, K.R., Yin, J., Bertolino, P., Eris, J.M., Alexander, S.I., Sharland, A.F. and Chadban, S.J. (2007) 'TLR4 activation mediates kidney ischemia/reperfusion injury', *The Journal of clinical investigation*, 117(10), pp. 2847-2859.

Wu, H., Ma, J., Wang, P., Corpuz, T.M., Panchapakesan, U., Wyburn, K.R. and Chadban, S.J. (2010) 'HMGB1 contributes to kidney ischemia reperfusion injury', *Journal of the American Society of Nephrology : JASN*, 21(11), pp. 1878-1890.

Xia, Y., Entman, M.L. and Wang, Y. (2013) 'Critical role of CXCL16 in hypertensive kidney injury and fibrosis', *Hypertension*, 62(6), pp. 1129-1137.

Xiang, Y., de Groot, R., Crawley, J.T. and Lane, D.A. (2011) 'Mechanism of von Willebrand factor scissile bond cleavage by a disintegrin and metalloproteinase with a thrombospondin type 1 motif, member 13 (ADAMTS13)', *Proceedings of the National Academy of Sciences of the United States of America*, 108(28), pp. 11602-11607.

Xie, J. and Guo, Q. (2007) 'Par-4 is a novel mediator of renal tubule cell death in models of ischemia-reperfusion injury', *American journal of physiology.Renal physiology*, 292(1), pp. F107-15.

Xie, J. and Guo, Q. (2006) 'Apoptosis antagonizing transcription factor protects renal tubule cells against oxidative damage and apoptosis induced by ischemia-reperfusion', *Journal of the American Society of Nephrology : JASN*, 17(12), pp. 3336-3346.

Xu, W., Berger, S.P., Trouw, L.A., de Boer, H.C., Schlagwein, N., Mutsaers, C., Daha, M.R. and van Kooten, C. (2008) 'Properdin binds to late apoptotic and necrotic cells independently of C3b and regulates alternative pathway complement activation', *Journal of immunology (Baltimore, Md.: 1950)*, 180(11), pp. 7613-7621.

Yabuki, A., Suzuki, S., Matsumoto, M., Kurohmaru, M., Hayashi, Y. and Nishinakagawa, H. (2001) 'Staining pattern of the brush border and detection of cytoplasmic granules in the uriniferous tubules of female DBA/2Cr mouse kidney: comparison among various fixations and stains.', *Journal of veterinary medical science*, 63(12), pp. 1339-1342.

Yamada, K., Miwa, T., Liu, J., Nangaku, M. and Song, W.C. (2004) 'Critical protection from renal ischemia reperfusion injury by CD55 and CD59', *Journal of immunology (Baltimore, Md.: 1950)*, 172(6), pp. 3869-3875.

Yamamoto, T., Noiri, E., Ono, Y., Doi, K., Negishi, K., Kamijo, A., Kimura, K., Fujita, T., Kinukawa, T., Taniguchi, H., Nakamura, K., Goto, M., Shinozaki, N., Ohshima, S. and Sugaya, T. (2007) 'Renal L-type fatty acid-binding protein in acute ischemic injury', *Journal of the American Society of Nephrology : JASN*, 18(11), pp. 2894-2902.

Yan, R., Li, Y., Zhang, L., Xia, N., Liu, Q., Sun, H. and Guo, H. (2015) 'Augmenter of liver regeneration attenuates inflammation of renal ischemia/reperfusion injury through the NF-kappa B pathway in rats', *International urology and nephrology*, 47(5), pp. 861-868.

Yang, B., El Nahas, A.M., Thomas, G.L., Haylor, J.L., Watson, P.F., Wagner, B. and Johnson, T.S. (2001) 'Caspase-3 and apoptosis in experimental chronic renal scarring', *Kidney international*, 60(5), pp. 1765-1776.

Yang, B., Hosgood, S.A., Bagul, A., Waller, H.L. and Nicholson, M.L. (2011) 'Erythropoietin regulates apoptosis, inflammation and tissue remodelling via caspase-3

and IL-1 β in isolated hemoperfused kidneys', *European journal of pharmacology*, 660(2), pp. 420-430.

Yang, B., Hosgood, S.A., Harper, S.J. and Nicholson, M.L. (2010) 'Leucocyte depletion improves renal function in porcine kidney hemoreperfusion through reduction of myeloperoxidase cells, caspase-3, IL-1 β , and tubular apoptosis', *Journal of Surgical Research*, 164(2), pp. e315-e324.

Yang, B., Jain, S., Pawluczyk, I.Z., Imtiaz, S., Bowley, L., Ashra, S.Y. and Nicholson, M.L. (2005) 'Inflammation and caspase activation in long-term renal ischemia/reperfusion injury and immunosuppression in rats', *Kidney international*, 68(5), pp. 2050-2067.

Yang, B., Johnson, T.S., Haylor, J.L., Wagner, B., Watson, P.F., El Kossi, M.M., Furness, P.N. and El Nahas, A.M. (2003) 'Effects of caspase inhibition on the progression of experimental glomerulonephritis', *Kidney international*, 63(6), pp. 2050-2064.

Yang, C., Zhao, T., Zhao, Z., Jia, Y., Li, L., Zhang, Y., Song, M., Rong, R., Xu, M. and Nicholson, M.L. (2014) 'Serum-stabilized naked caspase-3 siRNA protects autotransplant kidneys in a porcine model', *Molecular Therapy*, .

Yang, B., Hosgood, S.A. and Nicholson, M.L. (2011) 'Naked small interfering RNA of caspase-3 in preservation solution and autologous blood perfusate protects isolated ischemic porcine kidneys', *Transplantation*, 91(5), pp. 501-507.

Yang, B., Jain, S., Ashra, S.Y., Furness, P.N. and Nicholson, M.L. (2006) 'Apoptosis and caspase-3 in long-term renal ischemia/reperfusion injury in rats and divergent effects of immunosuppressants', *Transplantation*, 81(10), pp. 1442-1450.

Yang, B., Johnson, T.S., Thomas, G.L., Watson, P.F., Wagner, B. and Nahas, A.M. (2001) 'Apoptosis and caspase-3 in experimental anti-glomerular basement membrane nephritis', *Journal of the American Society of Nephrology : JASN*, 12(3), pp. 485-495.

Yang, C., Zhao, T., Lin, M., Zhao, Z., Hu, L., Jia, Y., Xue, Y., Xu, M., Tang, Q., Yang, B., Rong, R. and Zhu, T. (2013) 'Helix B surface peptide administered after insult of ischemia reperfusion improved renal function, structure and apoptosis through beta common receptor/erythropoietin receptor and PI3K/Akt pathway in a murine model', *Experimental biology and medicine (Maywood, N.J.)*, 238(1), pp. 111-119.

- Yang, H., Wang, H., Czura, C.J. and Tracey, K.J. (2005) 'The cytokine activity of HMGB1', *Journal of leukocyte biology*, 78(1), pp. 1-8.
- Yano, T., Nozaki, Y., Kinoshita, K., Hino, S., Hirooka, Y., Niki, K., Shimazu, H., Kishimoto, K., Funauich, M. and Matsumura, I. (2015) 'The pathological role of IL-18R α in renal ischemia/reperfusion injury', *Laboratory Investigation*, 95(1), pp. 78-91.
- Yilmaz, M.I., Carrero, J.J., Ortiz, A., Martin-Ventura, J.L., Sonmez, A., Saglam, M., Yaman, H., Yenicesu, M., Egido, J. and Blanco-Colio, L.M. (2009) 'Soluble TWEAK plasma levels as a novel biomarker of endothelial function in patients with chronic kidney disease', *Clinical journal of the American Society of Nephrology : CJASN*, 4(11), pp. 1716-1723.
- Ympa, Y.P., Sakr, Y., Reinhart, K. and Vincent, J. (2005) 'Has mortality from acute renal failure decreased? A systematic review of the literature', *The American Journal of Medicine*, 118(8), pp. 827-832.
- Yoshiji, H., Yoshii, J., Ikenaka, Y., Noguchi, R., Yanase, K., Tsujinoue, H., Imazu, H. and Fukui, H. (2002) 'Suppression of the renin-angiotensin system attenuates vascular endothelial growth factor-mediated tumor development and angiogenesis in murine hepatocellular carcinoma cells', *International journal of oncology*, 20(6), pp. 1227-1231.
- Yu, W., Sheng, M., Xu, R., Yu, J., Cui, K., Tong, J., Shi, L., Ren, H. and Du, H. (2013) 'Berberine protects human renal proximal tubular cells from hypoxia/reoxygenation injury via inhibiting endoplasmic reticulum and mitochondrial stress pathways', *Journal of translational medicine*, 11(1), pp. 1.
- Yuan, H., Li, X., Pitera, J.E., Long, D.A. and Woolf, A.S. (2003) 'Peritubular capillary loss after mouse acute nephrotoxicity correlates with down-regulation of vascular endothelial growth factor-A and hypoxia-inducible factor-1 α ', *The American journal of pathology*, 163(6), pp. 2289-2301.
- Zaferani, A., Vives, R.R., van der Pol, P., Hakvoort, J.J., Navis, G.J., van Goor, H., Daha, M.R., Lortat-Jacob, H., Seelen, M.A. and van den Born, J. (2011) 'Identification of tubular heparan sulfate as a docking platform for the alternative complement component properdin in proteinuric renal disease', *The Journal of biological chemistry*, 286(7), pp. 5359-5367.

- Zager, R.A., Johnson, A.C., Lund, S. and Randolph-Habecker, J. (2007) 'Toll-like receptor (TLR4) shedding and depletion: acute proximal tubular cell responses to hypoxic and toxic injury', *American journal of physiology.Renal physiology*, 292(1), pp. F304-12.
- Zezos, P., Papaioannou, G., Nikolaidis, N., Vasiliadis, T., Giouleme, O. and Evgenidis, N. (2005) 'Elevated plasma von Willebrand factor levels in patients with active ulcerative colitis reflect endothelial perturbation due to systemic inflammation', *World journal of gastroenterology*, 11(48), pp. 7639.
- Zhang, Z., Miao, L. and Wang, L. (2012) 'Inflammation amplification by versican: the first mediator', *International journal of molecular sciences*, 13(6), pp. 6873-6882.
- Zhang, W.R., Garg, A.X., Coca, S.G., Devereaux, P.J., Eikelboom, J., Kavsak, P., McArthur, E., Thiessen-Philbrook, H., Shortt, C., Shlipak, M., Whitlock, R., Parikh, C.R. and TRIBE-AKI Consortium (2015) 'Plasma IL-6 and IL-10 Concentrations Predict AKI and Long-Term Mortality in Adults after Cardiac Surgery', *Journal of the American Society of Nephrology : JASN*, 26(12), pp. 3123-3132.
- Zhang, X., Zheng, X., Sun, H., Feng, B., Chen, G., Vladau, C., Li, M., Chen, D., Suzuki, M., Min, L., Liu, W., Garcia, B., Zhong, R. and Min, W.P. (2006) 'Prevention of renal ischemic injury by silencing the expression of renal caspase 3 and caspase 8', *Transplantation*, 82(12), pp. 1728-1732.
- Zhao, G., Wang, S., Wang, Z., Sun, A., Yang, X., Qiu, Z., Wu, C., Zhang, W., Li, H. and Zhang, Y. (2013) 'CXCR6 deficiency ameliorated myocardial ischemia/reperfusion injury by inhibiting infiltration of monocytes and IFN- γ -dependent autophagy', *International journal of cardiology*, 168(2), pp. 853-862.
- Zheng, X., Zhang, X., Sun, H., Feng, B., Li, M., Chen, G., Vladau, C., Chen, D., Suzuki, M., Min, L., Liu, W., Zhong, R., Garcia, B., Jevnikar, A. and Min, W.P. (2006) 'Protection of renal ischemia injury using combination gene silencing of complement 3 and caspase 3 genes', *Transplantation*, 82(12), pp. 1781-1786.
- Zhou, W., Farrar, C.A., Abe, K., Pratt, J.R., Marsh, J.E., Wang, Y., Stahl, G.L. and Sacks, S.H. (2000) 'Predominant role for C5b-9 in renal ischemia/reperfusion injury', *The Journal of clinical investigation*, 105(10), pp. 1363-1371.

Zhu, Y., Zhang, X., Liu, Y., Zhang, S., Liu, J., Ma, Y. and Zhang, J. (2012) 'Antitumor effect of the mTOR inhibitor everolimus in combination with trastuzumab on human breast cancer stem cells in vitro and in vivo', *Tumor Biology*, 33(5), pp. 1349-1362.

Zhuang, S., Yan, Y., Daubert, R.A., Han, J. and Schnellmann, R.G. (2007) 'ERK promotes hydrogen peroxide-induced apoptosis through caspase-3 activation and inhibition of Akt in renal epithelial cells', *American journal of physiology. Renal physiology*, 292(1), pp. F440-7.

Ziello, J.E., Jovin, I.S. and Huang, Y. (2007) 'Hypoxia-Inducible Factor (HIF)-1 regulatory pathway and its potential for therapeutic intervention in malignancy and ischemia', *The Yale journal of biology and medicine*, 80(2), pp. 51-60.

Zipfel, P.F. and Skerka, C. (2009) 'Complement regulators and inhibitory proteins', *Nature Reviews Immunology*, 9(10), pp. 729-740.

zum Büschenfelde, D.M., Hoschützky, H., Tauber, R. and Huber, O. (2004) 'Molecular mechanisms involved in TFF3 peptide-mediated modulation of the E-cadherin/catenin cell adhesion complex', *Peptides*, 25(5), pp. 873-883.

Zwaini, Z., Alammari, D., Byrne, S. and Stover, C. (2016) 'Mode of proximal tubule damage: differential cause for the release of TFF3?', *Frontiers in immunology*, 7